A GLOBAL STUDY ON SPATIO-TEMPORAL VARIABILITY OF AEROSOLS INFERRED FROM SPACE BORNE MEASUREMENTS

BY

MANU MEHTA

(Admission No. 2015DR1141)

THESIS

SUBMITTED TO

INDIAN INSTITUTE OF TECHNOLOGY

(INDIAN SCHOOL OF MINES), DHANBAD

For the award of the Degree of

DOCTOR OF PHILOSOPHY

March, 2019

भारतीय प्रौद्योगिकी संस्थान (भारतीय खनि विद्यापीठ),धनबाद
धनबाद, झारखण्ड, भारत, पिन-826004
INDIAN INSTITUTE OF TECHNOLOGY (INDIAN SCHOOL OF MINES), DHANBAD
DHANBAD, JHARKHAND, INDIA, PIN-826004
(An Autonomous Institute under Ministry of HRD, Govt. of India)

CERTIFICATE

This is to certify that the thesis entitled ***"A GLOBAL STUDY ON SPATIO-TEMPORAL VARIABILITY OF AEROSOLS INFERRED FROM SPACE BORNE MEASUREMENTS"*** being submitted by ***Ms Manu Mehta (2015DR1141)*** to the Indian Institute of Technology (Indian School of Mines), Dhanbad for award of ***Doctor of Philosophy (Ph.D.)*** Degree in ***Environmental Science and Engineering*** is a record of bonafide research work carried out by her under my supervision and guidance. In our opinion, the thesis is worthy of consideration for the award of Doctor of philosophy (Ph.D.) Degree in Environmental Science and Engineering in accordance with the regulation of the Institute. The results presented in this thesis have not been submitted for the award of any other degree.

Dr. Anshumali
(Thesis Supervisor/
Associate professor)

Dr. Narendra Singh
(External Supervisor/
Scientist-E, ARIES)

Date: 27-03-2019
Place: IIT(ISM)

भारतीय प्रौद्योगिकी संस्थान (भारतीय खनि विद्यापीठ),धनबाद
धनबाद, झारखण्ड, भारत, पिन-826004
INDIAN INSTITUTE OF TECHNOLOGY (INDIAN SCHOOL OF MINES), DHANBAD
DHANBAD, JHARKHAND, INDIA, PIN-826004
(An Autonomous Institute under Ministry of HRD, Govt. of India)

CERTIFICATE REGARDING CLASSIFIED DATA

This is to certify that the thesis entitled ***"A GLOBAL STUDY ON SPATIO-TEMPORAL VARIABILITY OF AEROSOLS INFERRED FROM SPACE BORNE MEASUREMENTS"*** being submitted to the Indian Institute of Technology (Indian School of Mines), Dhanbad by ***Ms. MANU MEHTA*** for award of Doctor of Philosophy (Ph.D.) Degree in ***ENVIRONMENTAL SCIENCE AND ENGINEERING*** does not contain any classified information. This work is original and yet not been submitted to any institution or university for the award of any degree.

Manu Mehta
(Adm No. 2015DR1141)

Dr. Anshumali
(Thesis Supervisor/Associate professor)

Dr. Narendra Singh
(External Supervisor/Scientist-E, ARIES)

Date: 27.03.2019

COPYRIGHT AND CONSENT FORM

To ensure uniformity of treatment among all contributors, other forms may not be substituted for this form, nor may any wording of the form be changed. This form is intended for original material submitted to the ISM, Dhanbad and must accompany any such material in order to be published by the ISM. Please read the form carefully and keep a copy for your files.

TITLE OF THESIS: A GLOBAL STUDY ON SPATIO-TEMPORAL VARIABILITY OF AEROSOLS INFERRED FROM SPACE-BORNE MEASUREMENTS

AUTHOR'S NAME & ADDRESS:
Manu Mehta
Admission No:
Department of Environmental Science and Engineering
Indian Institute of Technology (ISM), Dhanbad-826004, Jharkhand, India

COPYRIGHT TRANSFER

1. The undersigned hereby assigns to Indian School of Mines, Dhanbad all rights under copyright that may exist in and to: (a) the above Work, including any revised or expanded derivative works submitted to the ISM by the undersigned based on the work; and (b) any associated written or multimedia components or other enhancements accompanying the work.

CONSENT AND RELEASE

2. In the event the undersigned makes a presentation based upon the work at a conference hosted or sponsored in whole or in part by the ISM, the undersigned, in consideration for his participation in the conference, hereby grants the ISM the unlimited, worldwide, irrevocable permission to use, distribute, publish, license, exhibit, record, digitize, broadcast, reproduce and archive; in any format or medium, whether now known or hereafter developed: (a) his presentation and comments at the conference; (b) any written materials or multimedia files used in connection with his presentation; and (c) any recorded interviews of him (collectively, the "Presentation"). The permission granted includes the transcription and reproduction of the Presentation for inclusion in products sold or distributed by ISM and live or recorded broadcast of the Presentation during or after the conference.

3. In connection with the permission granted in Section 2, the undersigned hereby grants ISM the unlimited, worldwide, irrevocable right to use his name, picture, likeness, voice and biographical information as part of the advertisement, distribution and sale of products incorporating the Work or Presentation, and releases ISM from any claim based on right of privacy or publicity.

4. The undersigned hereby warrants that the Work and Presentation (collectively, the "Materials") are original and that he is the author of the Materials. To the extent the Materials incorporate text passages, figures, data or other material from the works of others, the undersigned has obtained any necessary permissions. Where necessary, the undersigned has obtained all third party permissions and consents to grant the license above and has provided copies of such permissions and consents to ISM.

GENERAL TERMS

* The undersigned represents that he has the power and authority to make and execute this assignment.
* The undersigned agrees to indemnify and hold harmless the ISM from any damage or expense that may arise in the event of a breach of any of the warranties set forth above.
* In the event the above work is not accepted and published by the ISM or is withdrawn by the author(s) before acceptance by the ISM, the foregoing copyright transfer shall become null and void and all materials embodying the Work submitted to the ISM will be destroyed.
* For jointly authored Works, all joint authors should sign, or one of the authors should sign as authorized agent for the others.

Signature of the Author

ACKNOWLEDGEMENT

I express my sincere thanks to my Internal Guide Dr. Anshumali, Associate Professor, Department of Environmental Science and Engineering, Indian Institute of Technology (Indian School of Mines), (IIT(ISM)) Dhanbad, for his guidance and support during the research work.

My profound gratitude to my External Guide, Dr. Narendra Singh, Aryabhatta Research Institute of Observational Sciences (ARIES), Nainital, for his guidance and encouragement to this research work.

I am grateful to Director, Indian Institute of Remote Sensing (IIRS), Dehradun, ISRO, for allowing me to carry out this research as a part of the PHD programme. Special thanks are due to Dean, IIRS, Group Head (GTOPG) and Head (PRSD) for their support. Thanks are also due to the all the IIRS authorities, colleagues and staff members.

I express my deep gratitude to the Director, the Registrar and the Deans of IIT(ISM), Dhanbad and HOD (ESE) for providing all the support at ISM. My sincere thanks are also due to all the IIT(ISM) authorities.

Thanks are also due to Director, ARIES, Nainital for his support to carry out this research programme.

My utmost sincere thanks are due to the MODIS, MISR and CALIPSO Teams for providing access to the satellite data products which have been utilized in this study.

Thanks are also due to Mr. Bijendra Kumar, Dr. Kriti Shukla and Mr. Madavi Venkatesh for providing timely help and support as and when required.

I am indebted to my parents, Mr. Tilak Prakash Mehta and Mrs. Mohini Mehta and my mother-in-law, Mrs. Rama Pant for their constant blessings.

This work would not have been possible without the constant support and unwavering encouragement by my better half, Mr. Jayshreekar Pant. I am indebted to my small kid, Enakshi Pant who has been a source of enthusiasm throughout the work. I am thankful to my sister, Anu and brother, Rajan for their support.

Last but not the least, I thank the Almighty for everything.

Date: 27/3/19

Place: IIT(ISM), Dhanbad

(Manu Mehta)

SYNOPSIS

Introduction

Atmospheric aerosols are the minute liquid or solid suspensions in the atmosphere. Their sizes vary from the range of few nanometres to few hundreds of micrometres (John, 2011). The earth's climate system is affected by the atmospheric aerosols both directly and indirectly (Ackerman et al., 2000; Haywood and Boucher, 2000; Penner et al., 2001). Aerosols may be added in the atmosphere both due to natural process and also due to anthropogenic activities. Their spatio-temporal distribution could be highly variable owing to the meteorological factors, localized sources and transport processes. Their residence times in the atmosphere may variable too. In addition to their strong horizontal variability in space and time, the vertical exchange and uplifts may cause significantly variable vertical distribution as well. Studies like those by Li et al., 2014; Xia, 2011 and Yoon et al., 2012 have provided trends of aerosol properties using data from ground based networks. Similarly, several regional studies have been conducted to understand the vertical structure of the aerosols (Chen et al., 2013; Gadhavi et al., 2006; L'eon et al., 2009; Menzies and Tratt, 2002; Mona et al., 2006; Navas-Guzman et al., 2013; Solanki and Singh, 2014). Here it is notable that while ground based measurements of aerosol properties are precise, but as these are discrete in space, they are insufficient to provide continuous spatial observations. To this end, satellite observations, though associated with certain uncertainties, are able to provide continuous measurements in spatial domain. Several passive and active sensors on board satellite platforms are able to provide the estimates of aerosol optical properties employing different retrieval algorithms. Out of the various aerosol parameters used to study the aerosols' distribution, Aerosol Optical Depth (AOD) is the most widely used optical parameter that provides an estimate of columnar aerosol loading in a vertical column of the atmosphere. Some studies have evaluated global and regional AOD trends using different satellite sensors (de Meij et al., 2010, Mao et al., 2014 and Yoon et al. 2014). Most of them have found negative trends over North America, South America and Europe, but positive trends over South and East Asia. While, most of the passive sensors used for retrieval of aerosol properties provide AOD datasets, an active sensor like LIDAR is able to provide the vertical distribution of aerosols over a footprint. CALIPSO, is the only active space borne

LIDAR that can provide a decadal information of the aerosol properties along the atmospheric vertical column. In this context, several studies have been conducted to understand the global and specific regional variation of aerosol vertical profiles using CALIOP datasets (Koffi et al., 2012, Liu et al. 2008, Winker et al., 2013 and Yu et al., 2010). Despite all these studies, there is need to evaluate and compare the AOD trends from different sensors as the single sensor may provide biased estimates owing to certain uncertainties in the aerosol retrieval, sensor calibration issues etc. Also, there is a research gap in the study of trends of global vertical distribution of aerosols with specific reference to the major aerosol types.

With this motivation, following are the major objectives of this study:

- **Global distribution and trends of total columnar AOD**
  - Comparison of mean annual and seasonal AOD variation from the two sensors - MODIS and MISR
  - Study of changing levels of AOD across the globe
  - Illustration of AOD distribution and trends across the ten most populated countries of the world.
- **Distribution (columnar and vertical) and trends of major aerosol types across the globe**
  - Global columnar distribution of major aerosol types - dust, polluted dust and smoke, using CALIOP datasets
  - Vertical distribution of major aerosol types at various levels of the atmosphere
  - Trends in AOD and vertical profiles of the major aerosol types

Study area

This study is carried out for the entire globe. The major aerosol sources over America include industrial and vehicular emissions, urban activities, and the transported dust particles that are mainly from other continents (Yu et al., 2012). The anthropogenic aerosol sources over Europe include traffic, emissions from industrial and urban activities, and biomass burning (Barnaba, et al., 2011; Karnieli et al., 2009; Marmer et al., 2007). In the Mediterranean basin,

different types of aerosols due to different origins are found i.e. anthropogenic emissions, seasonal transported dust and maritime aerosols from the nearby waters (Hatzianastassiou et al., 2009; Pace et al., 2006; Papadimas et al., 2008). In the Arctic regions, anthropogenic aerosols are transported during winter and spring seasons (mainly from Europe and Russia) (Quinn et al., 2007). In Southern Russia, biomass burning constitutes one of major emission sources during the spring season (Soja et al., 2004). On the other hand, dust is the prominent source of aerosols in countries like Kazakhastan and Mongolia, apart from the anthropogenic emissions (Wang et al., 2008). Over South America, biomass burning activities due to deforestation and agricultural fires are the major emission sources, apart from fossil fuel combustion and urban activities, especially, over the Amazon basin (Evangelista et al., 2007; de Meij et al., 2010; Reddington et al., 2015). Especially notable is the long range transport of dust from North African region which comprises of nearly half of the global emissions (Huneeus et al., 2011; Ridley et al., 2014). Coming to the Middle East countries, desert dust and local pollution due to increasing population, and related shipping activities form the major contributors to the aerosols (Basart et al., 2009; Rashki et al., 2014). The emissions from automobiles, factories, forest fires, dust and sea salt contribute to the type of aerosols over South Africa (Kumar et al., 2014). The sources of aerosols over Asia are both anthropogenic and natural, i.e., vehicular, industrial, urban emissions on the one hand; and, forest fires, crop residue burning, marine aerosols and mineral dust on the other (Alam et al., 2011; Begum et al., 2010; Kaskaoutis et al., 2011; Lawrence and Lelieveld, 2010). The major aerosols over Australia include smoke from biomass burning and desert dust (Luhar et al., 2008; O'Brien and Mitchell, 2003; Tanaka and Chiba, 2006).

Satellite Datasets

The study is based on freely downloadable satellite data products which are available for over a decade.

- **MODIS AOD datasets**

  The Level 3 monthly AOD datasets from MODIS sensor onboard Terra platform were utilized in the study which were available at 1° × 1° spatial resolution. The AOD

retrievals from Dark Target (DT) algorithm were employed in the analysis to account for both oceanic waters and land regimes at the same time (Levy et al., 2010; Remer et al., 2005, 2009).

- **MISR AOD Datasets**

  MISR Level 3 AOD datasets, again from Terra platform were used in the analysis, which were available at 0.5° × 0.5° spatial resolution. In this case, the retrieval of AOD is dependent on surface types, such as vegetated areas, dark water bodies and high contrast terrain (Martonchik et al., 2009).

- **CALIOP Datasets**

  CALIOP, an active LIDAR which is onboard CALIPSO satellite provides vertically distributed properties of aerosols and clouds (Hunt et al, 2009; Omar et al., 2009; Vaughan et al., 2009). The aerosol retrieval process involves identification of features with subsequent determination of feature type and finally the aerosol subtyping. In this study, CALIOP Level 3 night-time global gridded monthly datasets were utilized which were available at spatial resolution of 2º X 5º and vertical resolution of 60 m. It can be noted that before the Level 3 products are created from level 2 products, they are quality screened (Winker et al., 2013). The aerosol parameters used in this study are the AOD and aerosol extinction coefficient (532 nm) for the major aerosol types i.e., dust, polluted dust and smoke.

Methods

In order to make a comparative analysis of AOD variation, changes and trends over different parts of the globe, the averaged spatial distribution over fourteen years was computed using the monthly Level 3 AOD datasets from MODIS and MISR. Seasonal analysis was also carried out over four seasons, December-February, March-May, June-August and September to November. In order to study the changes in AOD variation during the considered time frame, relative changes during the first seven and last seven years were also computed. The AOD trends were computed using weighted least square regression approach wherein each AOD value was weighed by a factor of ($1/\epsilon^2$), where ϵ stands for the expected error

(uncertainty) in AOD (Ramachandran et al., 2012). Student's t-test was performed to test the statistical significance of the results.

Further the AOD variation and trends were reported for the three major aerosol types i.e. dust, polluted dust and smoke using CALIOP datasets. To present the global distribution of vertical aerosol loading, four altitude bins were considered, i.e. 0-1 km, 1-2 km, 2-3 km and 3-4 km above mean sea level (a.m.s.l.). The latitudinal and longitudinal variation of vertical aerosol extinction profiles were also discussed. Again, the trends of vertical aerosol extinction coefficients were computed using the linear regression method.

MAJOR FINDINGS

Global spatial AOD variation from MODIS and MISR datasets (2001-14)

- Over North America, low annual AOD values were found from both the sensors.
- High values were recorded over North America in MAM and JJA seasons which could be due to natural and anthropogenic sources (Andronache, 2004; Dubovik et al., 2001).
- Low mean AOD values were observed annually over European continent but higher values were found over the Mediterranean Sea. AOD values were again higher in MAM and JJA seasons similar to North America.
- Russian landmass also received low mean annual AOD values, especially during DJF and SON seasons.
- Higher AOD values were found over Southern Russia during the MAM and JJA seasons and the adjoining oceanic waters.
- Similar to North America, low annual AOD values were observed over South America.
- Enhanced AOD values were observed over Amazon during SON season which could be manifestation of the seasonal deforestation and sugarcane burning (de Meij et al., 2010; Reddington et al., 2015).
- As MODIS DT algorithm doesn't retrieve AOD over desert areas, we could only take observations from MISR datasets over the African deserts. Moderate to high annual AOD values were observed over these desert lands.

- The dust activities showed a seasonal pattern with highest and lowest AOD values during JJA and DJF seasons respectively.
- A latitudinal shift in AOD values was also observed over the Sahel region during September-February which could be accounted due to the biomass burning activities that spread from North to South Sahel between November and February (Roberts et al., 2009).
- In Southern Africa, high particle loadings were observed during the JJA season due to the seasonal biomass burning practices (Kumar et al., 2014).
- Both the sensors recorded moderate to high AOD values over Eastern China, India (especially in IGP), Middle–East, Pakistan, Bangladesh and adjoining oceanic waters (de Meij et al., 2010; Kaskaoutis et al., 2011; Mehta, 2015).
- A spatially increasing pattern of AOD was found from West to East IGP during DJF which could be associated to the prevailing meteorological conditions. Similarly, high AOD values were also found over East China during DJF period.
- Strikingly increasing values of AOD were observed during MAM season over the entire Asian landmass, and the adjoining waters.
- As the monsoonal shift commenced in JJA, the AOD values maximized with an increasing spatial pattern East to West IGP.
- After the settling of particles to the ground during the rains, particle loading decreased over the Asian mainland and the surrounding waters during SON season.
- Australia received low annual AOD values. However, aerosol loadings were enhanced in the period September-February due to the regional biomass burning, long range transport and marine biogenic emissions as reported in earlier studies (Mitchell et al., 2010; Rosen et al., 2000).

Global AOD trends from MODIS and MISR datasets (2001-14)

- Over North America, negative annual and seasonal AOD trends were found which could be due to the decrease in anthropogenic emissions in North-East America as per Clean Air Act Amendments of 1990 (Pozzer et al., 2015; Hsu et al., 2012; Yoon et al., 2014).

- Over Europe, negative annual and seasonal AOD trends were observed owing to the environmental regularizations (Hsu et al., 2012; Li et al., 2014; Pozzer et al., 2015; Yoon et al., 2014).
- Negative trends were also found over the Mediterranean region which conform to the previous findings (Zhang and Reid, 2010).
- The annual AOD trends over Russia were mostly insignificant. Significant increasing trends were found over the Sea of Okhotsk during MAM season. The negative AOD trends over Russia are in agreement with the previously published work by Plakhina (2012).
- Negative AOD trends were found over South America and the adjoining oceanic regions which are also in agreement with the previous studies (de Meij et al., 2010; Hsu et al., 2012; Li et al., 2014).
- Over Africa, decreasing AOD trends (annual and seasonal) were found. These trends could be due to the lessening of dust activities over the dust source regions (North Africa) (Ridley et al., 2014).
- Negative trends were also observed over South Africa. These decreasing trends could be attributed to the decline in emissions due to environmental regulations (Kumar et al., 2014).
- Negative AOD trends were found over Australia.
- Interestingly, significant positive annual and seasonal (MAM and JJA) trends were found over Middle-East, which are in agreement with earlier studies (Hsu et al., 2012; Pozzer et al., 2015; Yoon et al., 2014).
- Over Asia, negative annual AOD trends were found with the exception of India and surrounding regions. The positive trends over Indian region could be associated with the increase in anthropogenic activities (Hsu et al., 2012; Pozzer et al., 2015). Positive AOD trends were also found over Bay of Bengal and Arabian Sea which could be due to enhanced pollution transport from the adjacent landmasses (de Meij et al., 2010; Kaskaoutis et al., 2011; Zhang and Reid, 2010).

Global columnar and vertical distribution of major aerosol types (2007-16)

Dust

- The Saharan belt constitutes the major dust belt region (as observed using CALIOP) covering parts of Africa, Arabia, India and China; similar to what have been reported earlier by Rashki et al., 2014 and Wang et al., 2008.
- The transport of Saharan dust over the Atlantic Ocean towards American region and also towards the Pacific Ocean were also observed from CALIOP datasets (Hunees et al., 2011; Ridley et al., 2014).
- The extinction signals due to dust gradually decreased in magnitude with increase in altitude.

Polluted dust

- Polluted Dust was found to be distributed over the entire world.
- The maxima were observed over India, East China and Arabian Sea.
- The extinction coefficients were notably high within 0-1 km altitude range and the concentration of polluted dust decreases gradually from lower to higher altitudes.
- The polluted dust particles were more concentrated in the Northern hemisphere, especially in the 0-3 km altitude range.

Smoke

- Smoke, could arise from the anthropogenic emissions and also from biomass burning activities. It was found to be dominant over Southern Africa, Amazonia, Indonesia, South-East China and India as reported in earlier studies also (Evangelista et al., 2007; de Meij et al., 2010; Kumar et al., 2014; Kaskaoutis et al., 2011; Roberts et al., 2009).
- Moderately low amounts of smoke were found over parts of North America, Europe, Russia, and South Atlantics.
- High MAEC values due to smoke particles were observed over the biomass burning regions with maxima in 1-2 km a.m.s.l. and the signals remain high till 4 km a.m.s.l, exhibiting strong vertical mixing.
- High MAEC values were found not just close to ground but at a little higher altitude range over South-East China (due to carbonaceous emissions).

- Moderate to high signals of smoke were found over Amazonia, India and Indonesia with maxima within 1-2 km bin.

Trends of columnar and vertical distribution of major aerosol types (2007-16)

- Globally, negative AOD trends were found for dust and polluted dust particles.
- Columnar AOD values due to smoke emissions have increased during the last decade.
- Statistically significant negative extinction trends due to smoke were recorded over the Eastern US in all the four altitude bins
- Positive AOD trends due to dust were found over North America, particularly over the Central US, also supported by Zhang et al., 2017.
- Positive extinction trends due to dust over Central US were observed within 0-1 km altitude bin.
- Positive AOD trends due to smoke over the Western US were observed which could due to the enhanced wildfires (Westerling et al., 2016).
- Increasing extinction trends due to smoke particles within 1-4 km a.m.s.l. were also observed.
- Negative AOD trends for dust, smoke, polluted dust were found over South America.
- Decreasing trends for aerosol extinction were found over South America for total particle load within 0-3 km a.m.s.l.
- Decreasing AOD trends due to dust over Argentina and Chile could be linked with the dust activities in the Atacama, which needs further investigation.
- Negative AOD trends due to polluted dust were observed along with the negative extinction trends, especially in the 0-1 km altitude range.
- Negative AOD and extinction trends due to smoke were found over Central parts of South America, especially within 1-4 km a.m.s.l.
- Positive trends of AOD and extinction coefficients due to smoke were reported for the Eastern Brazil.
- Negative AOD trends were observed over Europe for polluted dust and smoke.

- Over Africa, on an average, AOD due to dust particles decreased in the last decade but increasing AOD trends due to dust were reported over few places of North Africa and the Greater Horn of Africa.
- Increasing AOD trends for total particle load, smoke and polluted dust were found over Africa similar to those found by de Meij et al. (2010).
- Positive extinction trends for polluted dust within 0-3 km a.m.s.l. were observed over Africa.
- Decreasing AOD and extinction trends due to smoke were found over South Africa, which are in agreement with the study carried out by Kumar et al. (2014).
- Positive extinction trends due to smoke were observed over the biomass burning regions of Africa.
- Positive extinction trends for polluted dust and smoke were found over India.
- AOD and extinction trends were found to be negative over densely populated regions of East China.
- AOD and extinction coefficients due to smoke have increased over Mongolia and sparsely populated regions of China i.e. North-West and North-East.
- Enhanced AOD levels and extinction trends due to smoke were recorded over Siberia due to increased wildfires in the last decade which agree with the previous studies (Ponomarev et al., 2016).
- AOD and extinction trends due to smoke have increased over Indonesia during the last decade.
- Negative trends of extinction coefficients due to polluted dust were observed over Indonesia within 0-1 km bin.
- Columnar and vertically resolved levels of aerosols were found to be increased over the Middle-East which could be due to increasing anthropogenic as previously reported in a study by de Ruyter de Widlt et al. (2012).
- Negative trends of AOD due to dust and polluted dust were found over Australia.
- Increasing levels of AOD due to smoke were found over the North-Western Australian region.

CONCLUSIONS

Aerosols affect the Earth's climate system both directly and indirectly. In order to study their impacts on the changing climatic scenario, it is essential to monitor their spatio-temporal variability both in terms of changing columnar and vertically resolved levels. Satellite remote sensing provides a unique way of continuously monitoring the aerosol properties in space. However, there may be errors associated with the aerosol retrievals of each sensor owing to the sensor calibration issues, algorithm uncertainties etc. Hence, it becomes necessary to assess the changing behavior of aerosols as seen by different sensors. This is the first study of its kind based on space-borne data which not only presents the decadal trends of columnar aerosol loading, but also provides the global scenario of changing aerosol amounts at different altitude levels, with special emphasis on dust, polluted dust and smoke. It was found that during the last fourteen years, total columnar aerosol loading has decreased over North America, South America, South Africa and Europe. These cut offs in the particle loadings could be the manifestations of the strict environmental policies adopted by the respective countries. However, enhanced levels of aerosols were found over India, its surrounding landmasses and adjoining waters. On the other hand, smoke levels (both columnar and vertically resolved) increased across the entire globe during the last decade. Polluted dust levels were found to be decreased over America, Europe and East China. Increased levels of smoke and polluted dust were also found over the developing countries of Africa. Findings from this research work could provide vital inputs to the studies focussed on changing pollution levels and much required mitigation strategies. Of specific concern are the rising smoke levels in context of rising temperatures and wildfires across the globe.

RECOMMENDATIONS

- Future research may focus on the investigation of changing levels of absorption and scattering properties of aerosols along with their size parameters.
- Impacts of changing aerosol levels may be studied on health and some regional studies may be carried out to study the impacts on radiative forcing and snow cover melt.

CONTENTS

Description		*Page No.*
Certificate		
Acknowledgement		
Synopsis		**i-xii**
Contents		**xiii-xv**
List of Tables		**xvi**
List of Figures		**xvii-xxi**
List of Abbreviations		**xxii-xxiv**
CHAPTER I	**INTRODUCTION**	**1-5**
1.1	Background	1
1.2	Objectives	3
1.3	Outline of the thesis	5
CHAPTER 2	**REVIEW OF LITERATURE**	**6-15**
2.1	Earth's atmosphere and atmospheric aerosols	6
2.2	Monitoring of aerosols via ground based measurements	10
2.3	Satellite remote sensing of aerosols	10
2.4	Trends of aerosol columnar distribution across the globe	12
2.5	Present understanding of the aerosol vertical distribution across the globe	13
CHAPTER 3	**STUDY AREA**	**16-25**
3.1	Illustrative study regimes for comparative study of AOD from MODIS and MISR	16
	3.1.1 Zonal description of land use/land cover and climatic conditions	17

	3.1.2 Zonal description of population density, related anthropogenic activities and major aerosol sources	20
3.2	Continental scale study of aerosol types and vertical profiles	24
3.3	Choice of specific regions for illustration of aerosol vertical profiles for major aerosol types	25
CHAPTER 4	**MATERIALS AND METHODS**	**26-35**
4.1	Satellite data products from passive sensors	26
	4.1.1 Terra Platform	26
	4.1.2 MODIS Sensor	26
	4.1.3 MODIS DT Algorithm	27
	4.1.4 MODIS Level 3 AOD Products	29
	4.1.5 MISR Sensor	29
	4.1.6 MISR AOD Retrieval Algorithm	29
	4.1.7 MISR level 3 Products	31
4.2	Satellite data products from active space borne LIDAR	31
	4.2.1 CALIPSO Satellite	31
	4.2.2 CALIOP Sensor	31
	4.2.3 CALIOP Aerosol Retrieval Algorithm	32
	4.2.4 CALIOP Level 3 Aerosol Products	32
4.3	Methods	33
	4.3.1 Spatial correlation between MODIS and MISR AOD	33
	4.3.2 Global spatial AOD variation, relative changes and trends: annual and seasonal analysis of MODIS and MISR AOD datasets	34
	4.3.3 Aerosol vertical distribution using CALIOP datasets	35

CHAPTER 5	**RESULTS AND DISCUSSIONS**	**36-97**
5.1	Global AOD distribution and trends from passive sensors: MODIS and MISR	36
	5.1.1 Spatial correlation between MODIS and MISR AOD	36
	5.1.2 Global spatial AOD variation: annual and seasonal analysis	39
	5.1.3 Global spatial AOD relative changes: annual and seasonal analysis	47
	5.1.4 Global spatial AOD trends: annual and seasonal analysis	54
	5.1.5 AOD distribution over the ten most populous countries of the world	62
	5.1.6 AOD changes and trends over the ten most populous countries of the world	67
5.2	Aerosol type distribution from an active space borne LIDAR	72
5.3	Aerosol vertical distribution across the globe	75
	5.3.1 Distribution of Total particle loading within different altitude bins	75
	5.3.2 Distribution of Dust, Polluted Dust and Smoke within different altitude bins	77
	5.3.3 Latitudinal and longitudinal aerosol distribution across the globe	83
	5.3.4 Trends of AOD and Extinction coefficients at continental scale	87
CHAPTER 6	**SUMMARY AND CONCLUSIONS**	**98-103**
	REFERENCES AND BIBLIOGRAPHY	**104-141**
	ANNEXURES	**142-145**
	List of Publications	

LIST OF TABLES

Table No.	Description	Page No.
Table 2.1	Major satellite sensors used for monitoring of aerosol properties at a global scale	12
Table 3.1	Ten most populous nations of the world in the decreasing order of population (according to World Population Prospects, 2015 Revision, United Nations and World Population Clock, 2015)	24
Table 4.1	Spectral bands used in DT algorithm for AOD retrieval	27
Table 5.1	Annual and seasonal significant trends for ten most populous countries of the world; trends are significant at 95% confidence interval, 'MO': MODIS, 'MI': MISR, '↑': increasing trends, '↓': decreasing trends, '-': no trends, Colors (black/gray) denote agreement in the results from both the sensors	72
Table 5.2	Zonal AOD distribution for total AOD and AOD due to dust, polluted dust and smoke	75
Table 5.3	Zonal AOD trends for total AOD and AOD due to dust, polluted dust and smoke; + indicates significantly increasing trend and – indicates significantly decreasing trend	92

LIST OF FIGURES

Figure No.	Description	Page No.
Figure 2.1	Production, growth and removal of atmospheric aerosols (http://acmg.seas.harvard.edu/)	8
Figure 2.2	Global Mean AOD from MODIS Level 3 data for the period 2000-2011 (*Adapted from Fig. 1(a) Ruiz-Arias et al. 2013*)	9
Figure 3.2	Annually averaged Temperature across the continents (Adapted from https://www.climate-charts.com)	20
Figure 3.3	Annually averaged Rainfall across the continents (Adapted from https://www.climate-charts.com)	20
Figure 3.4	World population density map 2015 (GPWv4) (Adapted from http://sedac.ciesin.columbia.edu/)	22
Figure 3.5	World map showing the countries' boundaries, ten most populous nations highlighted in color. The globe is divided into six regions, namely, North-West, North, North-East, South-West, South and South-East	23
Figure 5.1	Spatial Correlation between MODIS and MISR AOD (1° × 1°) during 2001–2014	38
Figure 5.2	Annual variations of AOD using MODIS (1° × 1°) and MISR (0.5° × 0.5°) datasets	42
Figure 5.3	AOD variations during DJF season using MODIS (1° × 1°) and MISR (0.5° × 0.5°) datasets	43
Figure 5.4	AOD variations during MAM season using MODIS (1° × 1°) and MISR (0.5° × 0.5°) datasets	44
Figure 5.5	AOD variations during JJA season using MODIS (1° × 1°) and MISR (0.5° × 0.5°) datasets	45

Figure 5.6	AOD variations during SON season using MODIS (1° × 1°) and MISR (0.5° × 0.5°) datasets	46
Figure 5.7	Annual relative changes (%) of AOD using MODIS (1° × 1°) and MISR (0.5° × 0.5°) datasets	49
Figure 5.8	Relative changes (%) of AOD during DJF season using MODIS (1° × 1°) and MISR (0.5° × 0.5°) datasets	50
Figure 5.9	Relative changes (%) of AOD during MAM season using MODIS (1° × 1°) and MISR (0.5° × 0.5°) datasets	51
Figure 5.10	Relative changes (%) of AOD during JJA season using MODIS (1° × 1°) and MISR (0.5° × 0.5°) datasets	52
Figure 5.11	Relative changes (%) of AOD during SON season using MODIS (1° × 1°) and MISR (0.5° × 0.5°) datasets	53
Figure 5.12	Annual trends of AOD using MODIS (1° × 1°) and MISR (0.5° × 0.5°) datasets	57
Figure 5.13	AOD trends during DJF season using MODIS (1° × 1°) and MISR (0.5° × 0.5°) datasets	58
Figure 5.14	AOD trends during MAM season using MODIS (1° × 1°) and MISR (0.5° × 0.5°) datasets	59
Figure 5.15	AOD trends during JJA season using MODIS (1° × 1°) and MISR (0.5° × 0.5°) datasets	60
Figure 5.16	AOD trends during SON season using MODIS (1° × 1°) and MISR (0.5° × 0.5°) datasets	61
Figure.5.17	Annual variations of AOD using MODIS and MISR for ten most populous countries of the world, vertical bars represent the standard deviation	64

Figure.5.18	AOD variations during DJF season using MODIS and MISR for ten most populous countries of the world, vertical bars represent the standard deviation	65
Figure.5.19	AOD variations during MAM season using MODIS and MISR for ten most populous countries of the world, vertical bars represent the standard deviation	65
Figure.5.20	AOD variations during JJA season using MODIS and MISR for ten most populous countries of the world, vertical bars represent the standard deviation	66
Figure.5.21	AOD variations during SON season using MODIS and MISR for ten most populous countries of the world, vertical bars represent the standard deviation	66
Figure.5.22	Annual relative changes (%) in AOD using MODIS and MISR for ten most populous countries of the world	69
Figure.5.23	Relative changes (%) in AOD during DJF season using MODIS and MISR for ten most populous countries of the world	70
Figure.5.24	Relative changes (%) in AOD during MAM season using MODIS and MISR for ten most populous countries of the world	70
Figure.5.25	Relative changes (%) in AOD during JJA season using MODIS and MISR for ten most populous countries of the world	71
Figure.5.26	Relative changes (%) in AOD during SON season using MODIS and MISR for ten most populous countries of the world	71

Figure 5.27	Decadal averaged variation of (a) total AOD and AOD due to (b) dust, (c) polluted dust and (d) smoke at a global scale	74
Figure 5.28	Global distribution of MAEC (km^{-1}) for total particle loading within (a) 0-1 km (b) 1-2 km (c) 2-3 km (d) 3-4 km a.m.s.l. during the last decade	76
Figure 5.29	Global distribution of MAEC (km^{-1}) for dust within (a) 0-1 km (b) 1-2 km (c) 2-3 km (d) 3-4 km a.m.s.l. during the last decade	78
Figure 5.30	Global distribution of MAEC (km^{-1}) for polluted dust within (a) 0-1 km (b) 1-2 km (c) 2-3 km (d) 3-4 km a.m.s.l. during the last decade	79
Figure 5.31	Global distribution of MAEC (km^{-1}) for smoke within (a) 0-1 km (b) 1-2 km (c) 2-3 km (d) 3-4 km a.m.s.l. during the last decade	80
Figure 5.32	Different zones depicted over total AOD distribution taken from Figure 5.27	81
Figure. 5.33	Decadal averaged MAEC (km^{-1}) for total particle loading, dust, polluted dust and smoke for dust dominated zones	82
Figure. 5.34	Decadal averaged MAEC (km^{-1}) for total particle loading, dust, polluted dust and smoke for polluted dust dominated zones	82
Figure. 5.35	Decadal averaged MAEC (km^{-1}) for total particle loading, dust, polluted dust and smoke for smoke dominated zones	83

Figure 5.36	Latitudinal variation of mean AOD (Top); and mean MAEC (Bottom) (in km^{-1}) for (a) total particle loading, (b) dust, (c) polluted dust and (d) smoke, across the globe over the last decade	84
Figure 5.37	Longitudinal variation of mean AOD (Top); and MAEC (Bottom) (in km^{-1}) for (a) total particle loading, (b) dust, (c) polluted dust and (d) smoke, across the globe over the last decade	86
Figure.5.38	Statistically significant (≥ 90% confidence level) trends for (a) total AOD and AOD due to (b) dust, (c) polluted dust and (d) smoke at a global scale over the last decade	93
Figure.5.39	Statistically significant aerosol extinction trends (≥90% confidence level) for total particle loading within (a) 0-1 km (b) 1-2 km (c) 2-3 km (d) 3-4 km over the last decade	94
Figure.5.40	Statistically significant aerosol extinction trends (≥90% confidence level) for dust within (a) 0-1 km (b) 1-2 km (c) 2-3 km (d) 3-4 km over the last decade	95
Figure.5.41	Statistically significant aerosol extinction trends (≥90% confidence level) for polluted dust within (a) 0-1 km (b) 1-2 km (c) 2-3 km (d) 3-4 km over the last decade	96
Figure.5.42	Statistically significant aerosol extinction trends (≥90% confidence level) for smoke within (a) 0-1 km (b) 1-2 km (c) 2-3 km (d) 3-4 km over the last decade	97

LIST OF ABBREVIATIONS

(A)ATSR	(Advanced) Along Track Scanning Radiometer
AERONET	Aerosol Robotic Network
A.M.S.L.	Above Mean Sea Level
AMZ	Amazon Zone
AOD	Aerosol Optical Depth
ARFINET	Aerosol Radiative Forcing over India Network
AVHRR	Advanced Very High Resolution Radiometer
CAD	Cloud-Aerosol Discrimination Algorithm
CALIOP	Cloud-Aerosol LIDAR with Orthogonal Polarization
CALIPSO	Cloud-Aerosol LIDAR and Infrared Pathfinder Satellite Observations
CAZ	Central Africa Zone
CL3AP	CALIPSO Level 3 Aerosol Product
DB	Deep Blue
DJF	December-January-February
DT	Dark Target
EARLINET	European Aerosol Research LIDAR Network
ECZ	East China Zone
EOF	Empirical Orthogonal Functions
GAW	Global Atmosphere Watch
GLASS	Geoscience Laser Altimeter System
GOCART	Goddard Chemistry Aerosol Radiation and Transport
GOME	Global Ozone Monitoring Experiment
HERA	Hybrid Extinction Retrieval Algorithm
IGP	Indo-Gangatic Plains
IIR	Imaging Infrared Radiometer
INZ	Indian Zone

IPCC	Intergovernmental Panel on Climate Change
ISRO	Indian Space Research Organization
JJA	June-July-August
LIDAR	Light Detection and Ranging
LULC	Land Use Land Cover
LUT	Look-Up-Table
MAEC	Mean Aerosol Extinction Coefficient
MAM	March-April-May
MERIS	Medium Resolution Imaging Spectrometer
MEZ	Middle-East Zone
MISR	Multi-angle Imaging Spectro-Radiometer
MODIS	Moderate Resolution Imaging Spectro-radiometer
MPLNET	Micro-Pulse LIDAR Network
NASA	National Aeronautics and Space Administration
NAZ	North African Zone
NCEP	National Centers for Environmental Prediction
Nd:YAG	Neodymium-doped Yttrium Aluminum Garnet
NOAA	National Oceanic and Atmospheric Asministration
NPP	National Polar-orbiting Partnership
OMI	Ozone Monitoring Instrument
PCA	Principal Component Analysis
POLDER	Polarisation and Directionality of Earth Reflectances
QAC	Quality Control
REALM	Regional Aerosol Research LIDAR Network
SCA	Scene Classification Algorithm
SCIAMACHY	Scanning Imaging Absorption Spectrometer for Atmospheric Cartography
SeaWiFS	Sea-viewing Wide Field-of-view Sensor
SIBYL	Selective Iterated Boundary Locator

SNR	Signal-to-Noise Ratio
SON	September-October-November
SPM	Suspended Particulate Matter
TOA	Top-Of-Atmosphere
TOMS	Total Ozone Mapping Spectrometer
US	Unites States
VIIRS	Visible Infrared Imaging Radiometer Suite
WFC	Wide Field Camera

Chapter 1

INTRODUCTION

CHAPTER 1

INTRODUCTION

Aerosols are tiny particle suspensions in the atmosphere which are known to affect almost the entire world. These are known to have effects not only over the air quality but also over weather, climate and ecosystems. Not only these minute particles are highly variable over space, but their distribution and properties encounter several changes with time. This Chapter presents a brief background that motivated to carry out the research work. It presents the objectives of the study and also provides an outline of the thesis.

1.1 Background

Aerosols affect the earth's climate system both directly and indirectly (Ackerman et al., 2000; Haywood and Boucher, 2000; Penner et al., 2001). These particles, once released into the atmosphere, undergo several processes that can affect their distribution (regional and global) and properties (physical and chemical) (Levin and Cotton, 2009). Owing to the variable meteorological conditions, local emissions, long range transport and short atmospheric resident times, aerosol concentrations are highly variable in space and time.

Any particular region may have varied aerosols sources e.g., desert dust, smoke from wildfires, along with other anthropogenic emissions that can account for the aerosol characteristics dominant over that area. For instance, African aerosol regime is known to be affected by desert dust, and biomass burning aerosols in addition to the anthropogenic aerosols (Evan et al., 2006; Huneeus et al., 2011; Kumar et al., 2014; Swap et al., 2003). Similarly, the major sources of aerosols affecting Asia are attributed to dust, anthropogenic pollution and smoke from biomass burning activities (Alam et al., 2011; Begum et al., 2010; Dey et al., 2004; Kaskaoutis et al., 2011; Lawrence and Lelieveld, 2010; Ogunjobi et al., 2003). However, in addition to the local sources of aerosols dominating a particular area, the horizontal transport of aerosols from far locations might also be of serious concern in

affecting the aerosol climatology of any region e.g., long range horizontal transport of dust from Africa and Asia is known to affect the aerosol loadings over North America (Gong et al. 2003, 2006; Husar et al., 2001; Prospero, 1999). It is interesting to note that not only it is the horizontal variation but stratosphere-troposphere exchange phenomenon and transport processes that make aerosols variation pronounced in the vertical distribution as well. For example, trans-Pacific and trans-Atlantic transport of pollutants over North America is quite different from each other. If we consider trans-Pacific transport, the maximum concentration in the outflow is found in the 0-2 km levels (i.e., the boundary layer levels) contrary to the strongest outflow fluxes which are found in the lower free troposphere i.e., 2-5 km (Bey et al., 2001; Jacob et al., 1999; Yienger et al., 2000). On the other hand, if trans-Altantic transport is condsidered, the outflow takes place in the lower troposphere almost throughout the year. In addition, during summer season, transport of pollutants in the middle and upper troposphere is also notable (Li et al., 2002). The details on the type of aerosols transported from different locations to specific regions of globe are discussed in Chapter 3. Further, there could be large differences in the columnar properties compared to the surface properties of aerosols owing to the presence of distinct aerosol layers (Ramanathan et al., 2001b). There are, in fact, studies showing the impact of elevated aerosol layers on cloud microphysical properties (Dipu et al., 2013). Ganguly et al., 2009 have shown that the vertical aerosol profiles can be crucial to determine the aerosol compositions and concentrations. Whereas, it is appreciable that the vertical profiles of aerosols is an important factor to characterize the aerosols properties and their interaction mechanisms, there still exists a gap in the comprehensive understanding of their vertical distribution. Infact, there are several uncertainties in the aerosol impact assessment studies as these are based on model simulations of aerosol vertical distribution profiles (Forster et al., 2007; Gadhavi and Jayaraman, 2006; Heitzenberg et al., 1997; Samset et al., 2013; Satheesh et al., 2008; Schulz et al. 2006, Textor et al. 2006; Zarzycki and Bond, 2010).

While ground based measurements of aerosol columnar properties and vertical profiles could provide accurate information but these studies, being point-based, do not provide continuous spatial observations. A global synoptic view, however, is possible to obtain using satellite based sensors. At the same time, the remotely sensed information is based on several

theoretical approaches and assumptions, henceforth, needs to be validated with ground-based measurements. For example, remote sensing satellites could not measure aerosols over the Polar Regions during the dark winter half of the year and beneath the clouds (Barrie, 1986, 1990; Christensen, 1997; Levin and Cotton, 2009). Passive remote sensing sensors like Moderate Resolution Imaging Spectroradiometer (MODIS), Multi-angle Imaging Spectro-Radiometer (MISR) provide the columnar aerosol properties, mostly in cloud-free conditions with little information about the aerosol vertical distribution (Kahn et al., 2005, 2009; Levy et al., 2010; Remer et al., 2005). Out of the many aerosol parameters used to infer columnar aerosol properties using satellite data, aerosol optical depth (AOD) is the most commonly used one (Chapter 2).

However, it should be taken into account that the distribution of AOD alone is not sufficient to describe the distribution of major aerosol parameters, for instance, aerosol mass (the fine aerosols do have stronger mass extinction compared to the larger particles). Nevertheless, the spatio-temporal variation and trends of AOD can provide valuable inputs to study the implications of the changing amounts of aerosol loadings over climate, weather, air quality and precipitation (Levin and Cotton, 2009). Active remote sensing sensors, on the other hand are able to provide the vertically resolved properties of aerosols. Cloud-Aerosol LIDAR with Orthogonal Polarization (CALIOP), onboard Cloud-Aerosol LIDAR and Infrared Pathfinder Satellite Observations (CALIPSO) has been doing so since more than a decade. However, a detailed comprehensive study analyzing the global vertical distribution and changing distribution of aerosols with specific emphasis on dust, polluted dust and smoke needs attention. With the motivation of studying the changing loadings of aerosols over different portions of globe both in the total atmospheric column and at different levels of the atmosphere, this work was attempted with the objectives defined in the next section.

1.2 Objectives

1. Global distribution and trends of total columnar AOD

- Comparison of mean annual and seasonal AOD variation from the two sensors - MODIS and MISR
- Study of changing levels of AOD across the globe

- Illustration of AOD distribution and trends across the ten most populated countries of the world.

The main goals of this objective were to analyze and compare the annual and seasonal (a) spatial AOD distribution (b) relative changes in AOD during the first and last seven years and (c) AOD trends for the time period 2001–2014 at global scale using data from MODIS and MISR, both onboard NASA's Terra platform. The spatial correlations between MODIS and MISR AOD were also reported. In addition, the results for the ten most populated nations of the world were highlighted. Here, it is notable that the findings from a single sensor could be biased or erroneous at some points in time and space, due to the uncertainties involved in the retrieval of aerosol properties by space borne observations (owing to the issues in instrument calibration, data coverage, sampling and algorithm accuracy) (Hsu et al., 2013). In this context, a comparative study of aerosol variations and trends observed with more than one sensor becomes important. Such an analysis could yield reliable results for the locations where findings from multiple sensors match. At the same time, such studies could also reveal the places of mismatch in the results, wherein, more in-depth studies based on remote sensing and/or ground measurements might be required.

2. Distribution (columnar and vertical) and trends of major aerosol types across the globe

- Global columnar distribution of major aerosol types - dust, polluted dust and smoke, using CALIOP datasets
- Vertical distribution of major aerosol types at various levels of the atmosphere
- Trends in AOD and vertical profiles of the major aerosol types

The global distribution of columnar and vertically distributed properties of aerosols using Level 3 CALIOP datasets for the last ten years (September 2006 - August 2016) have been presented. The main goals of this objective were to understand the global spatio-temporal variations and trends in (1) columnar AOD and (2) vertical aerosol extinction profiles, with specific reference to dust, polluted dust and smoke. The results have been discussed in conjugation with those from previously reported studies in literature. In the Objective 1, strong seasonality was observed in the distribution of aerosols across the globe at various locations in space. Hence, for this objective, de-seaonalized linear trends have been

presented, both for columnar and vertically resolved parameters, considering the large amount of data involved.

1.3 Outline of the thesis

Chapter 2 introduces the reader to the advancements in satellite remote sensing of aerosols. It provides a comprehensive literature survey on the present understanding of changing AOD and aerosol vertical distribution through regional and global scale studies. The study was carried out over whole of the globe. To this end, **Chapter 3** describes the aerosol types, distribution and possible sources over different illustrative study regimes considered for columnar and vertically resolved distribution of aerosols. **Chapter 4** provides the description of various satellite data products that were utilized in the study. The methods used for analysis are also discussed therein. **Chapter 5** discusses the spatio-temporal variation of total columnar AOD at a global scale using data from two sensors, MODIS and MISR. Level 3 monthly AOD products at different resolutions were analyzed over different parts of the world during 2001-2014. Relative changes and trends in AOD have been presented at annual and seasonal levels. The chapter also discusses the AOD trends over the ten most populous countries of the world. Further, the chapter presents the global distribution of major aerosol components i.e. dust, polluted dust and smoke. Decadal Level 3 night time standard All-sky data products from CALIOP sensor were analyzed to observe both the columnar and vertical distribution of the major aerosol types. As the data volumes were now much larger considering the different aerosol types and their vertical profiles, de-seasonalized trends of AOD and vertical extinction coefficients have been presented. Finally, **Chapter 6** provides a brief summary of the thesis, highlighting the major findings and the future scope of the work.

Chapter 2

REVIEW OF LITERATURE

CHAPTER 2

REVIEW OF LITERATURE

The impacts of suspended particulate matter (SPM) is known to be significant over the changing climatic scenario and human health. These particles are highly variable in space and time owing to factors like their different origins, characteristics, residence times and meteorological conditions. While in-situ observations provide repeated, accurate and precise data of the aerosol properties, satellite measurements enable irreplaceable and continuous spatio-temporal coverage. This Chapter presents a literature review of the past and present understanding of aerosol columnar and vertical distribution throughout the world.

2.1 Earth's atmosphere and atmospheric aerosols

The thin envelope of gases held by the gravitational force of earth around its surface is known as the Earth's atmosphere. This atmospheric sheath not only supports life on the planet but also protects us from the intense radiations from Sun. The thickness of the atmosphere is around 480 km but most of the concentration lies within first 16 kilometers from the surface of Earth. The composition of the atmosphere is not uniform but is variable in both space and time. This variability is the manifestation of both the natural as well as anthropogenic activities at regional and global scales. Most of the alterations are prominent within the closest altitudes above the Earth's surface. The major gases forming the atmosphere are nitrogen (78%), oxygen (21%) and argon (0.93%). Apart from these, gases like carbon dioxide, neon, helium, methane, krypton, hydrogen, nitrogen dioxide are also present along with water vapor and SPM. Out of these, amounts of carbon dioxide, water vapor, methane, nitrogen dioxide, ozone, SPM and chlorofluorocarbons have strong spatio-temporal variability. SPM refers to the minute liquid or solid particle suspensions in the atmosphere, also known as *atmospheric aerosols*. The size of aerosols may vary from few

nanometers to few hundreds of micrometers (John, 2011). The atmospheric aerosols can be injected directly into the atmosphere (primary aerosols) or they may be formed by aggregation or nucleation from gas-phase molecules (secondary aerosols) (Fuzzi et al., 2006; Levin and Cotton, 2009). Some of the major aerosol types include soil dust, sea salt, carbonaceous aerosols, industrial dust, sulphates, nitrates etc. (Andres et al., 1996; Decesari et al., 2006; Duce, 1995; Kanakidou et al., 2005; Maria et al., 2004; Schulz et al., 2004; Seinfeld and Pandis, 2006). These may vary in terms of their size, size distribution, concentration; and their physiochemical and morphological properties. Further, changes in relative humidity may lead to growth of particles or evaporation which leads to changes in properties of aerosols (Fang et al., 1991; Fitzgerald, 1984). Finally removal of atmospheric aerosols may be due to scavenging by rain or dry deposition to the surface.

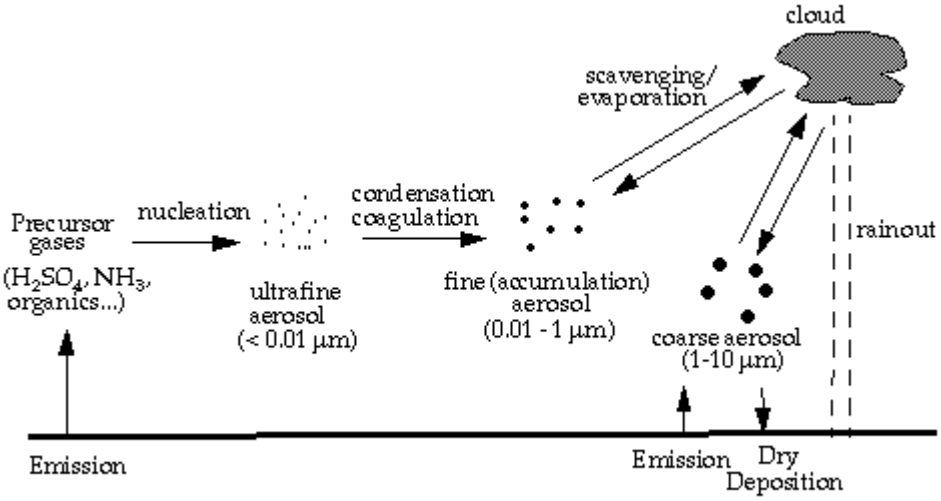

Figure 2.1 Production, growth and removal of atmospheric aerosols (http://acmg.seas.harvard.edu/)

The natural aerosol sources could be dust storms, wildfires, sea salts, biogenic particles and volcanic eruptions. On the other hand, anthropogenic aerosols could arise due to combustion of fuel, industrial emissions, vehicular pollution and biomass burning activities. According to Textor et al., 2006, about 10% of the global aerosol mass is generated anthropogenically, however, is concentrated close to the surface of Earth. Owing to industrial development and increased population, combustion related activities in the commercial, residential and even

in the agricultural domains; atmospheric aerosols have greatly increased in different parts of the globe. The aerosols affect the air quality, especially in the densely populated pockets of the world, and may have detrimental health effects. According to a study by Brauer et al., 2012, high proportions of East and South Asian population intake the air quality with exceeding levels of PM2.5 particles. Due to large heterogeneity in the sources and sinks, short residence times and transport processes in the atmosphere, the amount and properties of aerosols could be highly variable.

One of the most widely used total columnar optical properties used to quantify the amount of aerosols in the atmospheric column is *aerosol optical depth* (AOD). AOD (at a particular wavelength (λ)) is mathematically given by the integral of the aerosol extinction coefficient (β_{ext}) along the length of the vertical column of the atmosphere, (Liou, 2002) i.e.,

$$\boldsymbol{\tau(\lambda) = \int_0^{z_\infty} \beta_{ext}(\lambda, z)\, dz} \qquad \textbf{(2.1)}$$

AOD is a unit less quantity and its range varies from 0 and above. For an illustration, Figure 2.2 gives a glimpse of columnar distribution of 12-year averaged AOD from MODIS Level 3 products (Ruiz-Arias et al., 2013).

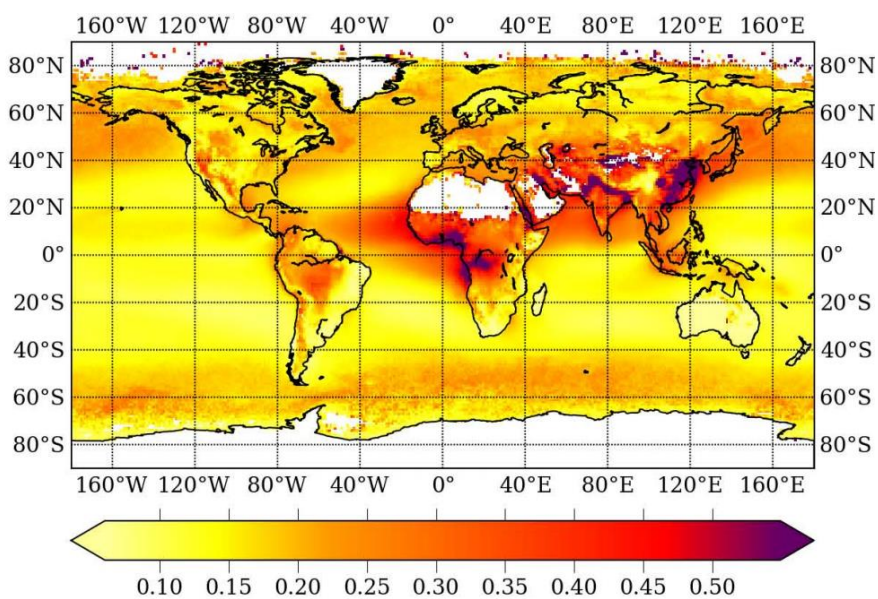

Figure 2.2 Global Mean AOD from MODIS Level 3 data for the period 2000-2011 (Adapted from Fig. 1(a) Ruiz-Arias et al., 2013)

Typically, AOD value of 0 corresponds to a clear sky which is free from aerosols. Lower values (≤ 0.2) correspond to cleaner conditions. The areas having high aerosol loadings usually have AOD greater than 0.5. An AOD value of 1.5 may refer to heavy smoke event/dust event/volcanic eruption. AOD>3 usually means that the solar disc is obscured (Levy et al., 2014).

On the other hand, the aerosol extinction coefficient provides an estimate of the amount of light lost due to absorption and scattering by the aerosols at a particular level (z) in the atmosphere. This parameter provides information on the vertical distribution of the aerosols in the atmosphere. Mathematically, it is a function of the extinction cross section ($\sigma_{ext}(a,\lambda)$) and the height dependent size distribution ($n(z,a)$) of the aerosols, (Liou, 2002) i.e.,

$$\boldsymbol{\beta_{ext}(\lambda,z) = \int_{a_1}^{a_2} \sigma_{ext}(a,\lambda) n(z,a) da} \qquad \textbf{(2.2)}$$

In the proceeding chapters, this term has been used as mean aerosol extinction coefficient (MAEC), where mean refers to the averaged value over a particular time interval (for instance, month, season, year etc.) The units of MAEC are reported in (km^{-1}). Similar to AOD, higher values of MAEC imply larger aerosol amounts at that vertical level of the atmosphere and vice-versa.

Long term spatio-temporal variability in AOD serves as a valuable input for the studies related to climatic change and Earth's radiation budget (Boucher and Haywood, 2001; Boucher and Tanré, 2000; Carslaw et al., 2013; Charlson et al., 1992; Hansen et al., 1997; Miller and Tegen, 1998; Ramanathan et al., 2001a). Direct effects of aerosols include scattering and absorption of radiation whereas their indirect effects are pertinent to the alteration of cloud properties (Ackerman et al., 2000; Gao et al., 2000; Haywood and Boucher, 2000; L'eon et al., 2001; Myhre et al., 2013a,b; Penner et al., 2001; Wang et al., 2009). Evaluation of aerosols' impact over climate requires accurate information of their physical, chemical and optical properties at regional and global scales (Carslaw et al., 2013; Charlson et al., 1992; Menon, 2004; Ramanathan et al. 2001a, b). The longer lifetimes of aerosols in free troposphere allow them to get transported over farther distances, thereby affecting their spatial distribution away from their sources. It should also be noted that not only the precise information of columnar distribution, but also knowledge of the vertical

structure of aerosols is required to correctly understand the aerosol transport and removal processes, emission properties and vertical uplifts (Schulz et al., 2006; Winker at al. 2013). Specifically, the uncertainty in the simulation of transport and removal processes is one of the major factors responsible for the diversity in distribution of aerosols predicted by the global aerosol models (Huneeus et al., 2011; Kinne et al., 2006; Textor et al. 2006). According to the IPCC Report, 2013, aerosols contribute to the largest uncertainty in estimation of radiative forcing estimates. A global perspective of columnar aerosol properties along with the vertically distributed ones, henceforth, is crucial to assess their role in the atmospheric dynamics. In order to study the impacts of aerosols on climate, one of the greatest challenges that is encountered is the large diversity, not only in terms of their origin, size or composition, but also in terms of their spatio-temporal distribution and trends. Various global and regional ground based networks are maintained with an aim to monitor the aerosol properties. The following section provides an overview of ground based measurements intended for the monitoring and characterization of atmospheric aerosols.

2.2 Monitoring of aerosols via ground based measurements

Ground based instruments at a particular location can provide accurate long term trends in the aerosol properties. To this end, worldwide, there are several regional and global aerosols monitoring station networks e.g., Aerosol Robotic Network (AERONET), SKYNET, Global Atmosphere Watch (GAW) Precision Filter radiometer network, Micro-Pulse LIDAR Network of NASA (MPLNET), Aerosol Radiative Forcing over India Network (ARFINET), Regional Aerosol Research LIDAR Network (REALM) and European Aerosol Research LIDAR Network (EARLINET) (Aoki, 2006; Eck et al., 1999; Ganguly et al., 2009; GAW, 2003, Pathak et al., 2016; Wehrli, 2000). As mentioned in Chapter 1, the ground measurements and field campaigns can provide accurate information on aerosol properties, but being point based, are unable to address the continuous spatial variability. Hence, satellite based estimates of aerosols are increasingly being used following the technical and scientific advancements. The next section provides an overview of satellite based aerosol monitoring techniques.

2.3 Satellite remote sensing of aerosols

Previously, the satellite missions with the major intent on other applications were used to provide the estimates of aerosol properties. For instance, Advanced Very High Resolution Radiometer (AVHRR) was launched primarily as a cloud and surface monitoring instrument but contains data in visible and NIR bands which are sensitive to the aerosol properties over the sea surfaces (Stowe et al., 2002). Similarly, satellite sensors like Sea-viewing Wide Field-of-view Sensor (SeaWiFS), Medium Resolution Imaging Spectrometer (MERIS), (Advanced) Along Track Scanning Radiometer ((A) ATSR) were launched with the major objective of retrieving land/sea surface reflectance/temperature, but could be later on used for aerosol retrievals also, though with variable uncertainties (Guanter et al., 2007; Santer et al., 1999; von Hoyningen-Huene et al., 2003). Total Ozone Mapping Spectrometer (TOMS) was originally launched for monitoring of ozone but it contains the UV channels which are sensitive to aerosol absorbing properties and little affected by the land surface reflectance (Hsu et al., 1999; Torres et al., 2002). Other sensors like Global Ozone Monitoring Experiment (GOME), Scanning Imaging Absorption Spectrometer for Atmospheric Cartography (SCIAMACHY) were initially developed for retrieval of trace gases but later on provided aerosol estimates as well. Now-a-days, however, we have satellite sensors that can retrieve the aerosol properties over ocean and land both, in multiple channels, some at even multiple angles and polarization states. Efforts are being made to develop improved cloud screening, retrieval algorithms and ability to estimate aerosol properties over varied land surface features. Some of such passive sensors with improved retrieval algorithms are MODIS, MISR, Ozone Measuring Instrument (OMI), Polarization and Directionality of the Earth's Reflectance (POLDER) (Diner et al., 1998; 2005; King et al., 1999; Levy et al., 2003; Martonchik et al., 2002; Remer et al., 2005; Roujean et al., 1997). Along with the column integrated properties of aerosols, their vertical profiles can also be now studied using the active sensors like CALIOP and Geoscience Laser Altimeter System (GLAS) (Abshire et al., 2005; Winker et al., 2003; 2010). Table 2.1 lists the major satellite sensors used for monitoring of aerosols, along with the aerosol parameters. Though all the satellite retrievals are also subject to uncertainty in their estimates, a combination of studies carried out using multiple sensors can enhance the confidence in the scientific results for the instances where

the findings from different sensors match, while at the same time pave the way for more focused research for the cases where the results do not agree with each other.

Table 2.1 Major satellite sensors used for monitoring of aerosol properties at a global scale

Sensor	**Platform**	**Aerosol properties**
MODIS	Terra/Aqua	Particle Loading, Fine Mode Fraction, Angstrom Exponent, Asymmetry Factor, Effective Radius
MISR	Terra	Particle Loading, Absorbing Optical Depth, Angstrom Exponent; Small, Medium, Large Fractions, Non-Spherical Fraction, Single Scattering Albedo
OMI	Aura	Particle Loading, Absorbing Aerosol Index, Single Scattering Albedo
AVHRR	NOAA series	Particle Loading, Angstrom Exponent
VIIRS	Suomi-NPP	Particle Loading
CALIOP	CALIPSO	Vertically Resolved Particle Loading, Aerosol Extinction and Backscatter Profiles, Color Ratio, Depolarization Ratio

2.4 Trends of aerosol columnar distribution across the globe

AOD trends have been estimated and assessed both worldwide and on regional scales by means of ground based sensors established at various locations over the globe using AERONET (Li et al., 2014; Xia, 2011; Yoon et al., 2012). However, inferences from satellite based sensors are able to provide a global perspective of AOD variation. Several studies focusing on global AOD variations over land and ocean have been performed using satellite retrievals. Some of them have reported decreasing trends of AOD over the oceans except for the regions near industrialized/rapidly developing countries, and those under the influence of Saharan dust and biomass burning (Chylek et al., 2007; Mishchenko et al., 2007; Zhao et al., 2008). Hsu et al. (2012) found weakly positive trend over global ocean, positive trends over

the Arabian Peninsula, and negative trends over the Eastern US and Europe for the period 1997–2010 using data from SeaWiFS. de Meij et al. (2010) evaluated global and regional AOD trends using MODIS, MISR and AERONET AOD datasets, and emission estimates for the period ranging from 2000 to 2009. They found negative trends over North America, South America and Europe, but positive trends over South and East Asia. Recently, global aerosol changes were analyzed using MODIS datasets for the period 2003–2012 and positive AOD changes were reported over Asia (Mao et al., 2014). Yoon et al. (2014), utilizing data from multiple satellite sensors, found decreasing AOD trends over Western Europe and US but increasing trends over the Middle East, Indian subcontinent and parts of China. Region specific studies focusing on the spatio-temporal variation of AOD have also been reported in the recent past. For instance, in contrast to the increasing AOD trends over south Asia during the period 2000–2009, decreasing trends were found over Indo-Gangatic Plains (IGP) during April–September, for the first time using MODIS observations (Kaskaoutis et al., 2011). Specific studies related to spatio-temporal variability of AOD over the regions subjected to frequent dust storms (e.g., North Africa and Sistan region in Iran) have also been reported in literature (Rashki et al., 2014; Shi et al., 2013). Papadimas et al. (2008) presented significant decrease in AOD over the Mediterranean basin during the period 2000–2006. Zhang and Reid (2010) also found a decadal decrease in AOD across Central-North American region and Mediterranean Sea (2000–2009). Decreasing AOD trends were also found over the Sahel and South Africa (Cowie et al., 2013; Kumar et al., 2014). Studies have also focused on the regions with high levels of population and the associated anthropogenic activities. For instance, recent studies have reported significant increasing trends of AOD over Indian region (Dey and Di Girolamo, 2011; Kishcha et al., 2011; Mehta, 2015; Ramachandran et al., 2012, 2015). However, decreasing AOD trends have been observed over other densely populated countries like China, US, Indonesia and Brazil (Panicker et al., 2012; Pozzer et al., 2015; Reddington et al., 2015).

2.5 Present understanding of the aerosol vertical distribution across the globe

In order to understand the vertical structure of the aerosol distribution in the atmosphere, several regional studies have been performed in different parts of the world using ground

based and airborne LIDAR datasets (Cavalieri et al., 2010; Chen et al., 2013; Gadhavi and Jayaraman, 2006; L'eon et al., 2009; Menzies and Tratt, 2002; Mona et al., 2012; Navas-Guzman et al., 2013; Solanki and Singh, 2014). On the other hand, considering the satellite based observations, CALIOP, which is onboard NASA's platform CALIPSO, has been gathering the information of the aerosol vertical distribution over the last ten years. The findings from CALIPSO could compliment the aerosol observations of passive remote sensing systems both in space and time.

Studies have been performed to evaluate regional and global aerosol columnar and vertical properties using CALIOP data. To this end, Liu et al. (2008) presented a height resolved global distribution of dust aerosols using cloud-free nighttime CALIOP measurements. Later, Yu et al. (2010) studied seasonal variations in vertical aerosol profiles obtained from CALIPSO over selected regions in comparison with those from GOCART simulations. In yet another study, regionally averaged monthly aerosol extinction profiles from CALIPSO Level 2 data were employed in Aero Com model inter-comparisons (Koffi et al., 2012). Also, Schuster et al. (2012) provided a climatology for LIDAR ratio of dust over the AERONET sites using CALISPO data. In addition, Winker et al. (2013) reported global 3-D climatology of tropospheric aerosols using 6-year datasets of CALIPSO Level 3 aerosol product (CL3AP). Recently, Papagiannopoulos et al. (2016) have evaluated modified CL3AP over EARLINET locations. They found that the modified product showed an overall 25% deviation from EARLINET observations in extinction coefficients. The comparisons of the modified CL3AP products with respect to other satellite retrievals reveal a bias in CALIOP AOD data compared to other instruments (Kittaka et al., 2011; Redemann et al., 2012). Further, Ma et al. (2013) found that though CL3AP could demonstrate seasonal variability in AOD, however, it was observed that the CALIPSO retrieved AOD was lower over deserts and higher over the biomass burning regions when compared with MODIS AOD datasets. Despite all these studies, a global view of columnar and vertically resolved trends of aerosol properties, in particular for major aerosol types, i.e. smoke, dust and polluted dust, has not been reported so far.

Futher, it is also worth noting that several studies have been conducted to understand the climatology and changing trends in the columnar aerosol properties, especially, AOD at

regional and global scales using data from ground based measurements and satellite sensors as discussed in Section 2.4. However, a comprehensive study investigating the trends in AOD due to major aerosol types is still lacking. In addition, there is no previous literature on the trends of aerosol vertical distribution across the globe, which could serve as important inputs to understand aerosol-induced climate changes. Hence, we are motivated to explore the trends in both, columnar AOD and vertical extinction coefficients, due to major aerosol types.

Chapter 3

STUDY AREA

CHAPTER 3

STUDY AREA

The study was conducted over the entire global region. This Chapter introduces the reader to the major types of aerosols dominant over different regions of the globe. For the sake of illustration, the globe was divided into six regions to study the AOD distribution and trends. Further, the emphasis was also laid on to the ten most populated countries of the world. For studying the vertical distribution and trends, the discussion is done at a continental level. Also, to illustrate the vertically distributed properties of major aerosol types, six representative regions were picked, two each for dust, polluted dust and smoke.

3.1 Illustrative study regimes for comparative study of AOD from MODIS and MISR

The globe was divided into six geographical regions, namely, North-West, North, North-East, South-West, South and South-East (Figure 2.1), but this classification did not follow the geopolitical boundaries and was rather chosen arbitrarily for the purpose of illustration. Nevertheless, this choice allowed to carry out a fair examination of the domains with different atmospheric conditions in terms of aerosol variability. As the study may have important links with the drivers affecting socio-economic development of globe at regional and global scale, the next two sections (Section 3.2.1 and Section 3.2.2) provide an overview of the geographical details along with the description of population density and related anthropogenic activities. Before, the zonal details are presented, it is important to have a glimpse of the climate classification at global scale (Peel et al., 2007). Figure 3.1 presents the land use/land cover map of the world. The figure is adapted and modified from https://phys.org/newman/gfx/news/hires/ 2014/.

Figure 3.2 and 3.3 provide illustration of global mean temperatures and rainfall across the continents (https://www.climate-charts.com). Further, Figure 3.4 provides an estimate of the

Global population density (2015) across the world (http://sedac.ciesin.columbia.edu/). Figure 3.5 depicts the boundaries of the ten most populated countries of the world on the global map and Table 3.1 provides the corresponding geographical boundaries (according to World Population Prospects, 2015 Revision, United Nations and World Population Clock, 2015).

3.1.1 Zonal description of land use/land cover and climatic conditions

North-West

This region comprises of North America along with the adjacent Arctic, Pacific and Atlantic waters. AOD retrieval over the arid/mountainous regions of North-West America is challenging as compared to that over the vegetated regions of North-East America (Levy et al., 2010; Shi et al., 2011). In addition, the sub-arctic pixels are mostly snow covered (with high albedo) and likely to have higher uncertainties in the satellite (especially MODIS) AOD retrievals (Shi et al., 2011; Yoon et al., 2014). Greenland, Canada and US (lying in the Northern hemisphere) have four distinct seasons, namely, spring, summer, autumn and winter. Central Greenland comprises of large ice sheets.

North

Northern region consists of European countries and some parts of Russian landmass, along with the Arctic Ocean regions (Greenland Sea, Norwegian Sea, North Sea, Barents Sea, Black Sea and Mediterranean Sea). Southern Europe has mountainous terrains contrary to the broad Northern Plains (Figure 3.1). European region is mainly affected by Westerlies. Due to Gulf Stream, Europe's climate is warmer and wetter than other areas in the similar latitudes. Most of the European glaciers are located in the Alps, Caucasus and Scandinavian Mountains and Iceland.

North-East

This region includes Russia, Kazakhstan, Kyrgyzstan, Mongolia, Northern China and the surrounding Arctic and Pacific waters. Russia is the largest country in the world in terms of its area, dominated mainly by the humid continental climate. Winters are extremely severe in the inner regions of North-East Siberia. Precipitation is mostly even across seasons in most of the Russian region except for East Siberia and the Far East where winter is drier compared

to summer. The Northern part of this zone consists of several glaciers, ice caps and ice domes (Figure 3.1).

South-West

This region comprises of South America, Mexico along with the surrounding Atlantic and Pacific waters. Most of the South American glaciers lie in the Andes. Winters are milder and summers are warmer if compared to North America. In the tropical regions, winds carry moisture from the Atlantics and result in enormous rainfall (Figure 3.3). The Northern Ecuador and Pacific Coast of Columbia are rainy areas. However, the Atacama Desert is one of the driest regions of the world.

South

The Southern region includes Africa, and the adjoining parts of Indian and Atlantic oceanic regions. The Northern part of Africa is mainly desert land, while Central and Southern areas comprise of Savana plains and rainforest regions (Figure 3.1). The temperatures are on the average the highest across the world (Figure 3.2). The African climate ranges from tropical to subarctic (on its highest peaks).

South-East

This region represents the Indian subcontinent, South China, Australia, Indonesia, Japan along with the parts of Indian and Pacific Oceans. This zone comprises of extremely diverse climates and geographic features and is also dominated by the monsoonal circulation (Figure 3.1 and 3.3). It includes highly undulating topography ranging from huge and widely spread Himalayas to a vast low lying plains. Major desert regions include Gobi desert in Mongolia and Arabian Desert stretching across the Middle East (Figure 3.1).

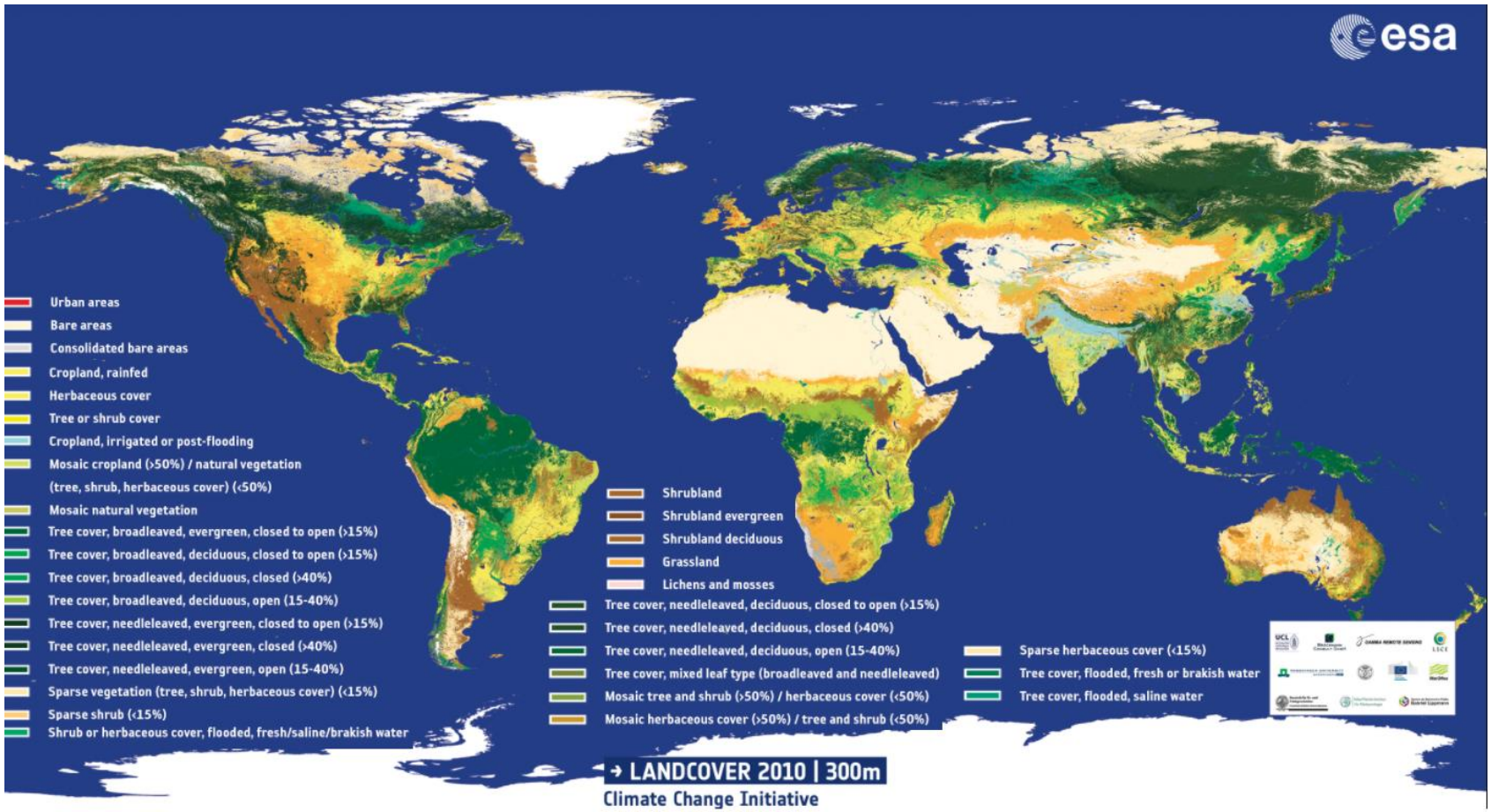

Figure 3.1 Land Use Land Cover (LULC) map

(Adapted form https://phys.org/newman/gfx/news/hires/2014/)

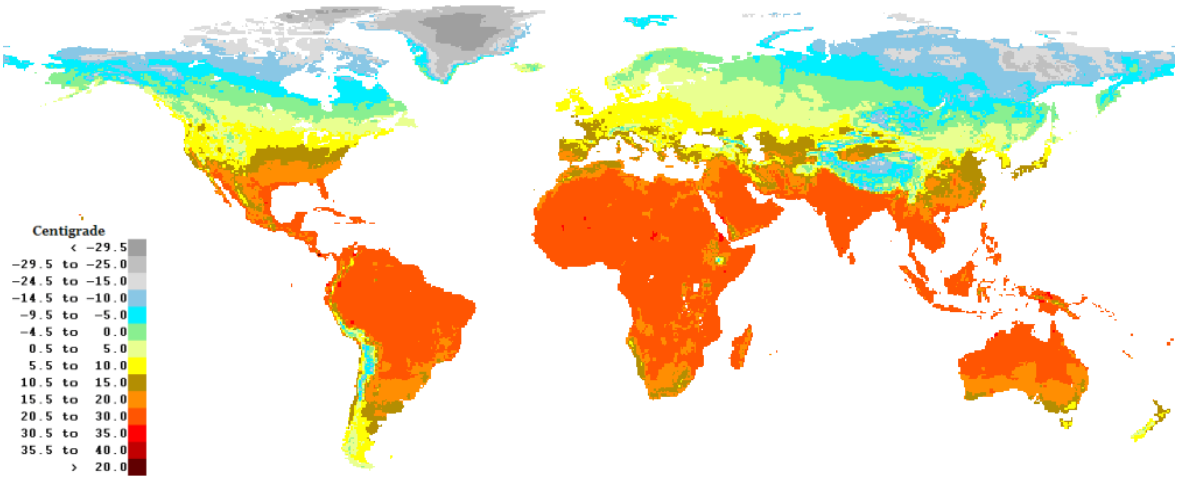

Figure 3.2 Annually averaged Temperature across the continents

(Adapted from https://www.climate-charts.com)

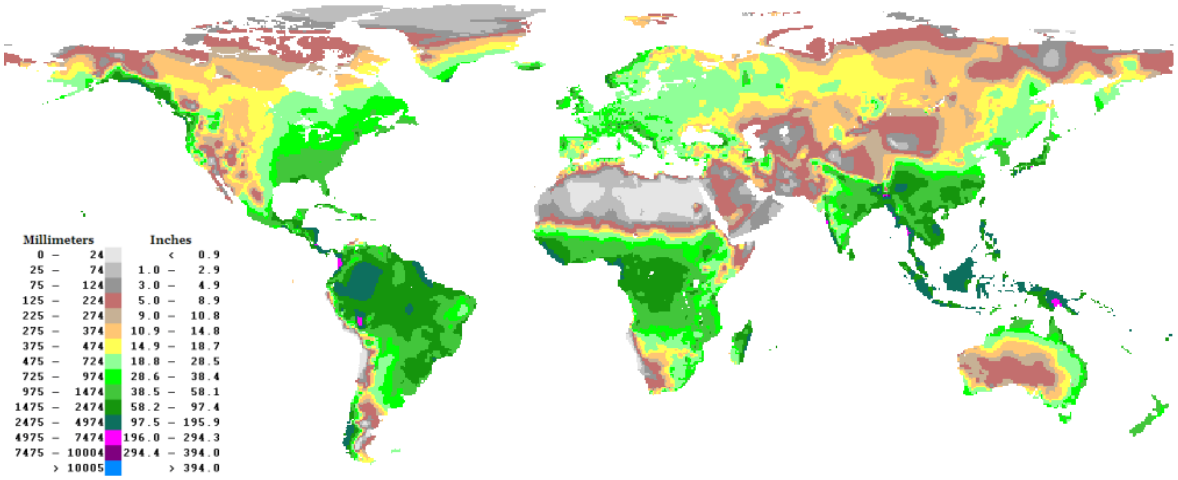

Figure 3.3 Annually averaged Rainfall across the continents

(Adapted from https://www.climate-charts.com)

3.1.2 Zonal description of population density, related anthropogenic activities and major aerosol sources

North-West

The most densely populated pocket of the zone includes the Eastern US. In terms of economic development, US and Canada are amongst the top. The major aerosol sources in the zone

include industrial and vehicular emissions, urban activities, and the dust particles that are mainly imported from Asia, Africa and Middle East (Yu et al., 2012).

North

The anthropogenic aerosol sources include traffic, industrial emissions, urban activities, and biomass burning as a result of forest fires (Barnaba et al., 2011; Benkovitz et al., 1996; Bergamo et al., 2008; Karnieli et al., 2009; Marmer et al., 2007). Over the Mediterranean basin, aerosols of different types and origins are found i.e. anthropogenic emissions from Europe, dust from North Africa (especially in spring-summer) and maritime aerosols from Mediterranean Sea (Hatzianastassiou et al., 2009; Pace et al., 2006; Papadimas et al., 2008; Tafuro et al., 2006).

North-East

Despite the large population, the population density of Russia is low due to its large area. The seasonal atmospheric background, prominent in the Arctic regions and known as Arctic Haze, is observed during winter and spring seasons owing to the transport of anthropogenic aerosols (mainly from Europe and the surrounding Russian landmass) and their slow removal processes (Quinn et al., 2007). Agricultural fires and wildfires are the prominent sources of emission in Southern Russia, contributing mainly in spring season (Soja et al., 2004). In the countries located to the South of this region (Kazakhastan, Mongolia etc.), dust is the major contributor to the aerosols in addition to the anthropogenic emissions (Wang et al., 2008).

South-West

Brazil, Colombia, Mexico, Central America, Argina are amongst the populous countries of this zone. Smoke from biomass burning activities (deforestation and agricultural fires) is a major aerosol type dominant over Amazon basin, Cerrado region and the coastal Atlantic forest (de Meij et al., 2010; Evangelista et al., 2007; Reddington et al., 2015). The other emission sources include fossil fuel combustion and urban activities (Evangelista et al., 2007).

South

Africa is the world's second largest continent in terms of area and second most populated continent (Nigeria being the most populated country). It has been found that the long range transport of dust from North African region contributes to roughly half of the global

emissions (Huneeus et al., 2011; Kaufman et al., 2005; Ridley et al., 2014). The aerosols in the Middle-East countries include desert dust and local pollution due to increasing population, poor regulated vehicular emissions, petroleum industry and related shipping activities (Basart et al., 2009; Rashki et al., 2014; Richter et al., 2004). Over South Africa, aerosols originate due to emissions from automobiles, factories, burning activities (fossil fuel, leaves etc.), forest fires, dust and sea salt (Kumar et al., 2014).

South-East

The highest populated pockets of this zone include the most densely populated countries of the world, i.e., China, India, Indonesia etc. The sources of aerosols in the Asian mainland and the surrounding oceanic regions are both anthropogenic and natural, i.e., emissions due to traffic, industry, urban activities, forest fires, crop residue burning, marine aerosols and mineral dust (Alam et al., 2011; Begum et al., 2010; Dey et al., 2004; Kaskaoutis et al., 2011; Lawrence and Lelieveld, 2010; Ogunjobi et al., 2003). Over Australia and the surrounding waters, the major aerosols include biomass burning emissions (particularly in tropical North) and desert dust (in West and Central Australia) (Luhar et al., 2008; O'Brien and Mitchell, 2003; Tanaka and Chiba, 2006).

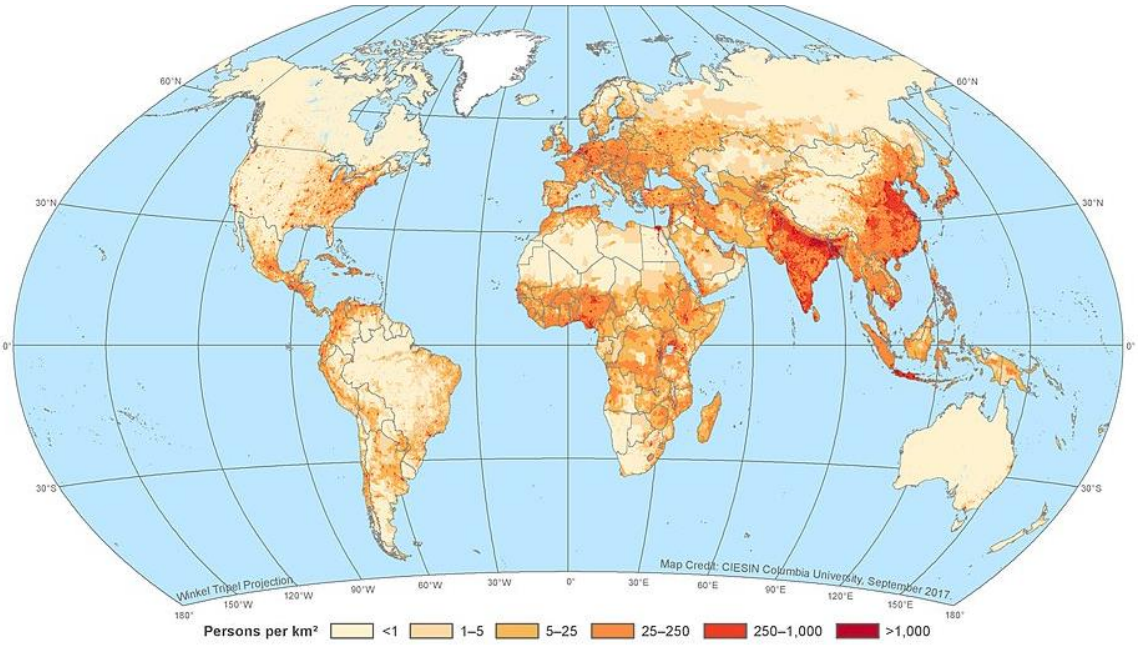

Figure 3.4 World population density map 2015 (GPWv4)

(Adapted from http://sedac.ciesin.columbia.edu/)

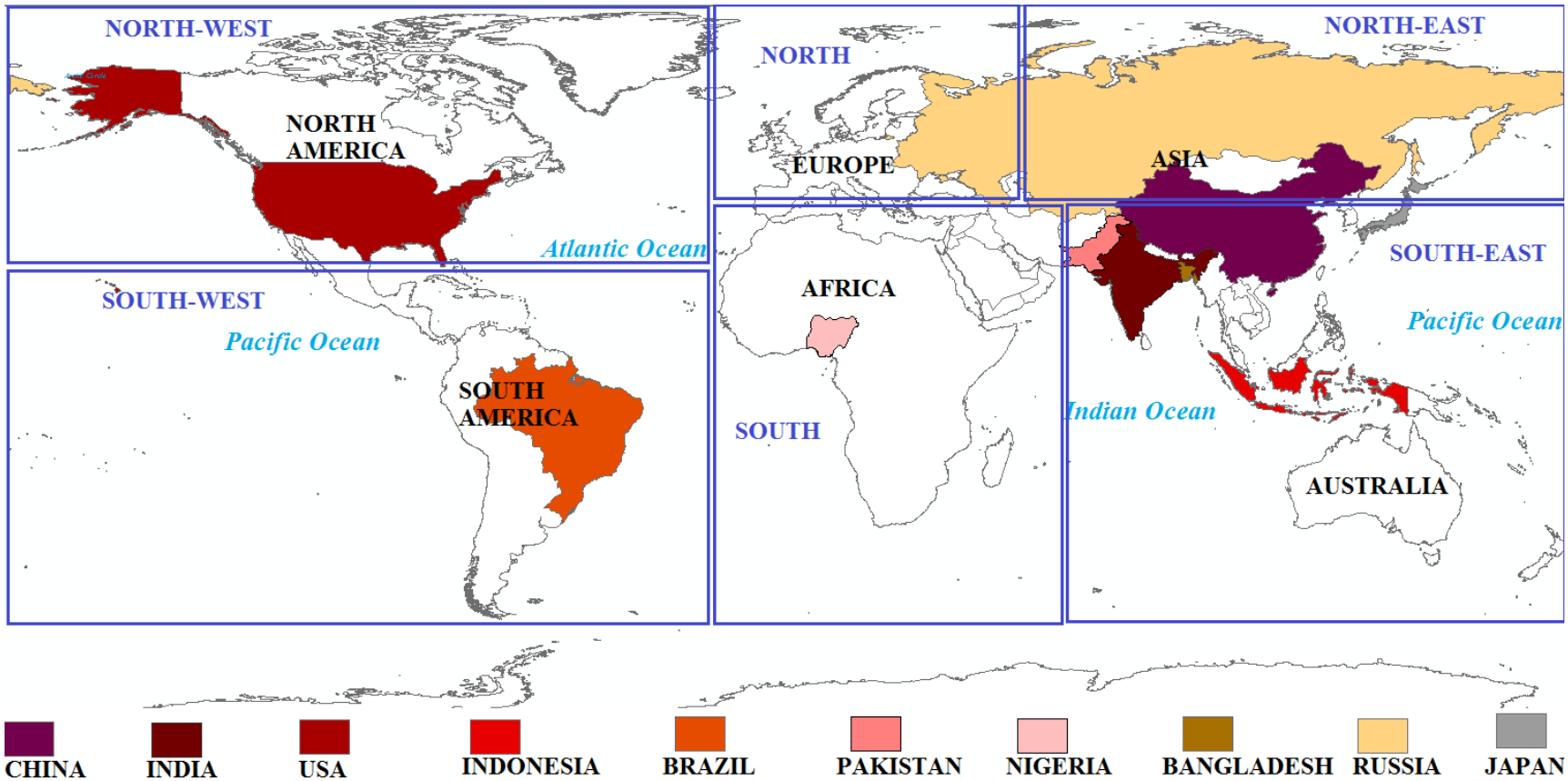

Figure 3.5 World map showing the countries' boundaries, ten most populous nations highlighted in color. The globe is divided into six regions, namely, North-West, North, North-East, South-West, South and South-East.

Table 3.1 Ten most populous nations of the world in the decreasing order of population (according to World Population Prospects, 2015 Revision, United Nations and World Population Clock, 2015)

Country	**Continent**	**Population (10^2 millions)**	**Area (10^4 km^2)**	**Top left coordinates**	**Bottom right coordinates**
China	Asia	13.8	960	(54°N, 74°E)	(19°N, 134°E)
India	Asia	13.1	329	(36°N, 68°E)	(9° N, 97°E)
US	North America	3.2	986	(72°N, 172°W)	(26°N, 67°W)
Indonesia	Asia	2.6	192	(5°N, 95°E)	(10°S, 141°E)
Brazil	South America	2.1	852	(6°N, 73°W)	(33°S, 35°W)
Pakistan	Asia	1.9	80	(38°N, 61°E)	(24°N, 77°E)
Nigeria	Africa	1.8	92	(14°N, 3°E)	(5°N, 14°E)
Bangladesh	Asia	1.6	15	(27° N, 88° E)	(22° N, 92° E)
[#]Russia	Europe and Asia	1.4	1708	(78°N, 20°E)	(36°N, 180°E)
Japan	Asia	1.3	38	(46°N, 129°E)	(32°N, 145°E)

[#] The coordinates of Russia provided in the table correspond to its landmass region lying in Eastern hemisphere. A part of Russian landmass lying in Western Hemisphere with top left coordinates (69°N, 180°W) and bottom right coordinates (65°N, 171°W) was considered in the analysis, corresponding to the shape file (refer to Figure 3.5).

3.2 Continental scale study of aerosol types and vertical profiles

Similar to section 3.1, the distribution of major aerosol types i.e., dust, polluted dust and smoke over different regions of globe was studied across the globe. However, for illustrative purposes, the discussions are carried out at latitudinal and longitudinal levels, along with continental scales in Chapter 5. The details on various types of aerosols and possible sources may be adapted from the Section 3.1.

3.3 Choice of specific regions for illustration of aerosol vertical profiles for major aerosol types

To illustrate the contrasting differences of the various aerosol types over different hotspot regions, the vertical distribution of mean aerosol extinction coefficients (MAEC) was presented over six regions of the world. These regions were, namely, North African Zone (NAZ) [20ºN-12ºN; 17.5ºE-7.5ºW], Middle-East Zone (MEZ) [28ºN-20ºN; 42.5ºE-52.5ºE], Indian Zone (INZ) [28ºN-22ºN; 67.5ºE-82.5ºW], East China Zone (ECZ) [38ºN-30ºN; 102.5ºE-112.5ºE], Amazon Zone (AMZ) [0ºS-6ºN; 62.5ºW-47.5ºW] and Central Africa Zone (CAZ) [2ºS-10ºS; 12.5ºE-32.5ºE]. Two regions were considered, each for dust (NAZ and MEZ), polluted dust (INZ and ECZ) and smoke (AMZ and CAZ) as the major aerosol types.

Chapter 4

MATERIALS AND METHODS

CHAPTER 4

MATERIALS AND METHODS

This Chapter presents details on the datasets used in the study along with the methodology adopted to address the objectives of the thesis. Level 3 satellite data products were utilized which are available in the gridded form. While total columnar AOD datasets were utilized from passive sensors i.e. MODIS and MISR, both from NASA's Terra Platform; the columnar and vertical distribution of different types of aerosols was studied using data from CALIOP sensor which is onboard CALIPSO satellite. These datasets are described in detail in this Chapter. The methodology adopted for computing the distribution of columnar and vertically distributed properties along with their trends is also presented.

4.1 Satellite data products from passive sensors

4.1.1 Terra Platform

The study utilized data from two passive satellite sensors, MODIS and MISR, both onboard NASA's Terra platform. Terra is orbiting at an altitude of 705 km with a 16-days orbital repeat cycle. The orbit of Terra is descending (southward) with an equatorial passing time of around 10:30 am (local solar time).

4.1.2 MODIS Sensor

MODIS has 36 spectral bands with varying spatial resolutions ranging from 250 m to 1 km, spanning over the the wavelength range of 0.41 to 14.24 µm (King et al., 1992; Salomonson et al., 1989). The scanning is possible within an angle of ±55º. As the swath of the sensor is about 2330 km, the sensor is capable of observing the globe almost on a daily basis. The repeat cycle of the sensor is 16 days. The AOD retrieval algorithm over land and water utilizes the data from seven different bands operating in near-UV, visible and near-IR

wavelength regions (Levy et al., 2010; Remer et al., 2005, 2009). The retrieval algorithm is based on Look Up Table (LUT) approach that employs pre-defined set of aerosol types, loadings and geometries. In order to account for both land and ocean, Dark Target (DT) algorithm retrievals were used instead of Deep Blue (DB) algorithm retrievals which were available over land only. The data was archived from ftp://ladsweb.nascom.nasa.gov/data/alldata/51.

4.1.3 MODIS DT Algorithm

Originally, the formulation of DT algorithms for MODIS were proposed by Kaufman et al. (1997) for land and Tanre et al. (1997) over water bodies. The DT algorithm uses the seven wavelength bands which are listed in Table 4.1. These all bands lie in atmospheric window regions wherein the absorption by the atmospheric gases is small. In order to compare the AOD retrievals from the MODIS DT algorithm, studies were made using the data from AERONET observations (Chu et al., 2002; Remer et al., 2002, 2005).

Table 4.1 Spectral bands used in DT algorithm for AOD retrieval

Band No.	Bandwidth (µm)	Spatial resolution (m)	Weighted central wavelength (µm)
1	0.620-0.670	250	0.646
2	0.841-0.876	250	0.855
3	0.459-0.479	500	0.466
4	0.545-0.565	500	0.553
5	1.230-1.250	500	1.243
6	1.628-1.652	500	1.632
7	2.105-2.155	500	2.119

The very first step in the retrieval process is to collect the Level 0 data into five small granules. Then these granules are processed to radiance/reflectance and geo-located datasets. These datasets are corrected for water vapor column and trace gases using NCEP data (MAST, 2006). Further, they are organized into 10 × 10 km boxes followed by separation

into land and ocean pixels. The detailed flowchart showing the basic processing steps is provided in Annexure I (Kokhanovsky and Leeuw, 2009). The uncertainty in the AOD measurements over land and ocean is estimated to be ±0.05 ± 0.20 × AOD and ±0.03 ± 0.15 × AOD respectively (Levy et al., 2010; Remer et al., 2005, 2008).

Over Ocean algorithm

Over ocean algorithm uses the fact that the reflectance over ocean surfaces is close to zero in the red band and bands with longer wavelength regions (Tanre et al., 1997; Levy et al., 2003; Remer et al., 2005; MAST, 2006). Hence, these provide dark background to make observations of aerosols. If all the pixels in the 10 × 10 km box are considered to be water, the ocean algorithm is adopted. Further, the obstructive pixels are removed and good pixels are sorted (Gao et al., 2002; Li et al., 2003; Martins et al., 2002; Platnick et al., 2003). Ocean LUTs are simulated by the vector radiative transfer equations for 2304 sun/surface/satellite geometries (Remer et al., 2005). The LUTs compute the combined spectral reflectance due to molecules, aerosols and ocean surface components. In the inversion procedure, the difference between the observed spectral radiances in the MODIS bands and radiances pre-computed in the LUTs are minimized.

Over land algorithm

Contrary to the ocean surfaces, the surface reflectance over land may vary widely and hence can be an important parameter affecting the retrieval process. If there are well behaved surfaces e.g., a completely dark surface, or a surface whose reflectance can be modeled/assumed; the decoupling process to obtain aerosol signals from top of atmosphere (TOA) signals can be successfully attempted. Over land retrieval algorithm utilizes signals from Band no. 1, 2, 3, 5 and 7 as listed in Table 1. First the good pixels are screened from the data by removing cloudy, snow/ice pixels and those containing sub-pixel water bodies (Gao et al., 2002; Li et al., 2005, Martins et al., 2002; Remer et al., 2005). The later steps include sorting of pixels based on their reflectance in 0.66 µm band and averaging of the spectral reflectance values, followed by the inversion process as illustrated in Annexure I (Kokhanovsky and Leeuw, 2009).

4.1.4 MODIS Level 3 AOD Products

Level 3 AOD gridded products are created from Level 2 AOD swath products. It is worth notable that Level 2 products are derived during the daylight. In 16-day repeat period of MODIS, it is made sure that all parts of the globe are covered during the daylight orbits. In this way, the sampling and geometry of different parts of globe changes from one day to the other. We may have no retrieval at all on certain regions or seasons when the entire Level 2 pixels are cloudy. The level 3 products represent the statistics of Level 2 swath products at regular intervals of time and space. In this study, MODIS Level_3 monthly AOD product over ocean (best) and land (corrected) at 0.55 μm, i.e., MOD_08_M3 (Collection 5.1) was used which was available at 1° × 1° spatial resolution.

4.1.5 MISR Sensor

MISR has nine cameras at nine look-angles with four wavelength bands, i.e., 0.446, 0.558, 0.672 and 0.866 μm (Diner et al., 1998). The cross-track ground spatial resolution is 275 m or 1.1 km. The cameras are kept at fore-aft geometry in a symmetrical arrangement with view angles of 0, 26, 45.6, 60 and 70.5 degrees. The data can be acquired in the two modes, i.e., global and local. In the global mode, which is the nominal operational mode, data is acquired at 275 m resolution in all the nine cameras for red band and nadir cameras in other three bands. For the remaining channels (24), the resolution is fixed at 1.1 km. On the other hand, local mode is the mode in which the prescribed targets are covered at 275 m resolution in all the 36 channels. As the orbit is polar, every nine days, a complete coverage is possible for 82ºN-82ºS latitudes. The AOD retrieval method is also based on LUT approach but the algorithm is dependent on surface types, such as vegetated areas, dark water bodies and high contrast terrain (Martonchik et al., 2009). MISR AOD data was downloaded from ftp://l5eil01.larc.nasa.gov/ pub/misrl2l3/MISR.

4.1.6 MISR AOD Retrieval Algorithm

Once the data is collected in the 36 channels (9 cameras and 4 spectral bands), the data is calibrated radiometerically, geo-rectified and finally, spatially averaged at a resolution of 1.1

km. However, the aerosol retrieval is made at a spatial resolution of 17.6 × 17.6 km. This is done to ensure flexibility in the retrieval methods.

There are some assumptions which are made in order to carry out the retrieval of aerosols from the MISR datasets, which are as follows (Kokhanovsky and Leeuw, 2009):

1. It is assumed that the aerosols are laterally homogeneous over the resolution of 17.6 × 17.6 km surface area.
2. The observed MISR radiances are compared with those obtained from pre-computed model radiances which are calculated for a suite of aerosol compositions and particle size distributions.
3. In order to compare the MISR radiances and pre-computed model radiances, a fit function formalism is adopted. Those models which meet the fit function criterion are accepted as the solutions of the retrieval process.
4. For reflectively heterogeneous land surfaces within 17.6 km region, there are no assumptions on the magnitude or explicit angular shape of the spectral bidirectional reflectance factors.
5. For the regions where surface topography of the land is complex, no retrievals are carried out.

The aerosol retrieval algorithm is based on the Principal Component Analysis (PCA) of the MISR TOA radiances collected in multi-angular multi-channel mode (Preisendorfer et al., 1998). Before the PCA is carried out, the TOA radiances are filtered using cloud screening techniques to provide clear sky conditions (Di Girolamo and Davis, 1994; Di Girolamo and Wilson, 2003; Goodman and Henderson-Sellers, 1988; Kokhanovsky and de Leeuw, 2009; Moroney et al., 2002; Rossow et al., 1985; Rossow, 1989; Yang et al., 2007). The empirical orthogonal functions (EOF) are computed from the PCA analysis to describe the surface directional reflectance properties (Martonchik et al., 1998, 2002). Based on the similarity of the angular shape of the spectral surface directional reflectance properties, the retrieval algorithm selects its own set of acceptable aerosol models (Diner et al., 2005).

4.1.7 MISR Level 3 AOD Products

AOD Level_3 monthly data product, i.e., MISR_AM1_CGAS (collection F15_0031) is created from Level 2 MISR AOD swath products. The gridded Level 3 AOD products are available at a spatial resolution of 0.5° × 0.5°. The validation studies with respect to ground based measurements (AERONET data) have demonstrated that the expected error (over land and ocean) in MISR AOD data is on the order of ±0.05 or ± (0.20 × AOD), whichever is higher (Kahn et al., 2005, 2010).

4.2 Satellite data products from active space borne LIDAR

4.2.1 CALIPSO Satellite

With an aim to improve our understanding of vertically distributed properties of aerosols, CALIPSO mission was launched by NASA in a polar orbit at an altitude of 705 km in 2006 (Hunt et al., 2009; Winker et al., 2003; 2009). The inclination angle is 98.7 degrees and its repeat cycle is of 16 days. CALISPO orbits around the earth 15 times every day. It carries an active LIDAR, CALIOP along with a passive infrared imager i.e., Imaging Infrared Radiometer (IIR) and a visible imager, i.e., Wide Field camera (WFC) in order to study the properties and vertical distribution of aerosols and thin clouds across the globe (Winker et al., 2003).

4.2.2 CALIOP Sensor

CALIOP provides aerosol and cloud vertically distributed properties at two wavelengths, i.e., 532 nm and 1064 nm. In addition, at 532 nm, both parallel and polarized returns are received. This LIDAR is a Mie Rayleigh LIDAR with Nd: YAG laser as the transmitting source. The LIDAR uses a large receiver telescope to provide the best possible measurement sensitivity (Winker et al., 2010). The measure of the footprint diameter is such that it is within the eye safety limits in the atmosphere. The sampling of profiles are done at a vertical resolution of 30 m (below 8.2 km altitude) and 60 m (between 8.2 km and 20.2 km). Its

capabilities include determination of locations of aerosols layers, discrimination of aerosols from clouds, categorization of aerosols into different sub types and estimation of optical depth of each detected aerosol layer (Hunt et al, 2009; Liu et al., 2009; Omar et al., 2009; Vaughan et al., 2009; Young and Vaughan, 2009).

4.2.3 CALIOP Aerosol Retrieval Algorithm

The retrieval of extinction coefficients is achieved by the use of three algorithms, Selective Iterated Boundary Locator (SIBYL), Scene Classification Algorithm (SCA) and Hybrid Extinction Retrieval Algorithm (HERA). Multiple scale spatial averaging is done to improve signal-to-noise ratio (SNR) for aerosol retrieval with better confidence levels.

The retrieval process first initiates with identification of features within the LIDAR signals (aerosol, cloud and surface returns) followed by determination of feature type (Liu et al., 2009; Vaughan et al., 2009). Further, the aerosol subtyping is performed to classify the layers as clean marine, dust, smoke, polluted dust, clean continental and polluted continental particles (Omar et al., 2009). At this stage, cloud phase is also determined, finally followed by retrieval of aerosol extinction profiles (Hu et al., 2007, 2009; Young and Vaughan, 2009). Level 2 CALIOP datasets contain the aerosols retrievals along the track of the satellite. The data comprises of geophysical parameters like aerosol backscatter, extinction, depolarization and aerosol type classification results. Each of the parameter is also supplied with the uncertainty estimates along with a number of quality control flags.

4.2.4 CALIOP Level 3 Aerosol Products

Level 3 data is created at a gridded level utilizing the Level 2 data products. The screening of the Level 2 data is done using several quality control flags before creating the Level 3 product (Winker et al., 2013). A summary of quality control flags is provided in Annexure II (Liu et al., 2009; Young et al., 2013; Young and Vaughan, 2009). The level 3 data is available in four conditions, i.e., daytime all-sky, daytime cloud-free, nighttime all-sky and nighttime cloud-free datasets. In this study, CALIOP Level 3 night-time global gridded monthly datasets, i.e., CAL_LID_L3_APro_AllSky-Standard-V3-00 were used, which were available at spatial resolution of 2º × 5º and vertical resolution of 60 m (from -0.5 to 12 km

above mean sea level (a.m.s.l.)). The major parameters used in this study are the aerosol extinction coefficient (532 nm) and the mean AOD, in particular for dust, polluted dust and smoke.

For more information on clear-sky and all-sky mean aerosol profile inter-comparisons, the reader may refer to work by Winker et al. (2013). Evaluation with respect to other satellite sensors and ground based measurements has not been addressed in this thesis. For details regarding the evaluation of CALIPSO AOD data sets, one may see the works by Kim et al. (2013); Kittaka et al. (2011); Ma et al. (2013); Omar et al. (2013); Redemann et al. (2012) and Schuster et al. (2012). For studies aimed at investigating the aerosol vertical profile products, reader may refer to works by Mamouri et al. (2009); Mona et al. (2006); Papagiannopoulos et al. (2016); Pappalardo et al. (2010); Wandinger et al. (2011); and the references therein. The seasonality of aerosols using CALIPSO data is not the subject of this thesis but has been extensively discussed in the works by Huang et al. (2015) and Winker et al. (2013).

4.3 Methods

4.3.1 Spatial correlation between MODIS and MISR AOD

The spatial correlation between MODIS and MISR AOD was computed using Level 3 monthly data products (Figure 5.1). The MISR datasets at higher spatial resolution (0.5° × 0.5°) were re-sampled to 1° × 1°, in order to compare with those of MODIS data product. For each pixel, the correlation was computed using an equal number of months from both the datasets. This was ensured by excluding those monthly data sets for which null data were recorded by any of the sensors. There were places, where correlation is high (≥0.8) while at other locations, it was found to be moderate (0.5–0.8) to low (≤0.5).

4.3.2 Global spatial AOD variation, relative changes and trends: annual and seasonal analysis of MODIS and MISR AOD datasets

The relative AOD changes were calculated by using the following Equation 4.1

$$\text{Relative AOD change}_{a(s)}\ (\%) = \frac{\text{Average AOD } (2008-14)_{a(s)} - \text{Average AOD } (2001-07)_{a(s)}}{\text{Average AOD } (2001-07)_{a(s)}} * 100 \tag{4.1}$$

where 'a' refers to annual and 's' refers to seasonal AOD values respectively.

The uncertainty in the AOD data was not constant, rather it was heteroskedastic. Hence, the trends were calculated by using weighted least square regression approach instead of the usual least squares fit as illustrated in Ramachandran et al. (2012). While performing the regression analysis, each AOD value was weighed by a factor of ($1/\epsilon^2$), where ϵ is the expected error (uncertainty) in AOD. In this way, the highly uncertain AOD values got lesser weight in the estimated trend and vice versa. The trends were further tested for their statistical significance by using the method of Student's t-test (Eq. (4.2)).

$$t = r\sqrt{\frac{(n-2)}{(1-r^2)}} \tag{4.2}$$

Here, r stands for the correlation coefficient between the original time series and the weighted least squares linear fit and n is the number of observations. Statistically significant trends were reported at 95% confidence level i.e. p-value < 0.05.

For the seasonal analysis, four seasons considered were DJF (December-January- February), MAM (March-April-May), JJA (June-July-August) and SON (September-October-November). It could be noted here that the validation of AOD with respect to the ground based measurements was not addressed in this thesis, which has been extensively reported in other relevant papers (de Meij et al., 2010, Levy et al., 2010, Shi et al., 2011).

For the analysis over ten most populous countries of the world, the corresponding shape files were used to extract the AOD data from MODIS and MISR datasets respectively (see countries depicted in different colors in Figure 3.5 (Chapter 3). As the MODIS and MISR retrievals were at different spatial resolutions, the comparative analysis was subject to uncertainties arising due to differences in computing domains of these countries. This is because some parts of the countries might be falling to those of neighboring countries'

domain and vice versa. It is important to note here that for these countries, only the statistically significant trends were included in the analysis.

4.3.3 Aerosol vertical distribution using CALIOP datasets

In order to study the global distribution of aerosols at different altitude levels, four altitude bins were considered i.e. 0-1 km, 1-2 km, 2-3 km and 3-4 km a.m.s.l. The aerosol extinction profiles were then aggregated and averaged over these altitude bins. For simplicity, the total range of MAEC was categorized as very high (0.4-0.6 km^{-1}), high (0.1-0.2 km^{-1}), moderate (0.05-0.1 km^{-1}) and low (<0.05 km^{-1}). The global latitudinal and longitudinal variation of AOD and vertical distribution of aerosol extinction profiles for total particle loading, dust, polluted dust and smoke, are also presented in Chapter 5.

With an aim to estimate the decadal changes in the aerosol loading across the globe, AOD trends of major aerosol types were computed using the linear regression technique. The monthly datasets were first de-seasonalized by computing the AOD anomalies for each pixel, as illustrated by Hsu et al. (2012). Then for computing trends, the least squares fit was applied following the method by Weatherhead et al. (1998). In order to test the statistical significance, Student's t-test was applied to the estimated trends. In addition, the de-seasonalized trends for extinction due to dust, polluted dust and smoke at different levels of atmosphere are also presented in Chapter 5 which have not been reported till date. Only the pixels with statistically significant trends at greater than or equal to 90% significance level are presented.

Chapter 5

RESULTS AND DISCUSSIONS

CHAPTER 5

RESULTS AND DISCUSSIONS

This Chapter presents the results achieved from the time series analysis of satellite datasets used in the study. First the results on total columnar AOD variation and trends from passive sensors, MODIS and MISR have been discussed followed by those from active space borne LIDAR onboard CALIPSO. Spatial correlation between MODIS and MISR AOD at global scale was first examined before the results were compared from the two sensors. Further, the global spatial variation of AOD has been discussed along with the relative changes and trends in the period 2001-14. In order to have a better understanding of the changing aerosol loadings across different parts of the world,, an illustrative analysis of AOD distribution and trends have also been presented for ten most populous countries of the world. In the later part of the Chapter, a discussion on columnar and vertical distribution of major aerosol types, i.e., dust, polluted dust and smoke is presented. Latitudinal and longitudinal distribution of aerosol types have also been discussed. Finally, the trends of AOD and extinction coefficients for different aerosol types are presented at continental scale. The findings wherever possible, are also augmented and compared with the results from previously published literature.

5.1 Global AOD distribution and trends from passive sensors: MODIS and MISR

5.1.1 Spatial correlation between MODIS and MISR AOD

The spatial correlation between MODIS and MISR AOD was computed using Level 3 monthly data products (Figure 5.1). These findings were in good agreement with the previously reported works by Kahn et al. (2009) and Shi et al. (2011). The correlations were found to be higher for regions with low surface reflectivity, e.g., vegetated regions of South Africa and South America. However, lower correlations were found for the places with high

surface reflectivity, e.g., deserts of Iran, Afghanistan, North-West India, Tibet, and high latitude areas. Over the Atlantic Ocean, Arabian Sea and Bay of Bengal, the AOD measurements were highly correlated as both the sensors capture high aerosol signals over these regions. Correlations were found to be moderate (or low) for the regions with complex surfaces, e.g., East Coast of Brazil, Kazakhstan, Mongolia and East Coast of Africa. Such regions were transition areas of vegetation cover to bare lands or vice versa. For the regions having complex aerosol types, e.g., dark particles and smoke, correlations were again moderate (or low). Such cases were found in regions of Malaysia, Indonesia, Japan and Central Africa for which retrieval algorithms might not accurately represent the microphysical properties of aerosols. Low correlations were recorded for the places where MODIS overestimates AOD, e.g., West coast of US (Shi et al., 2011). Similarly, correlations were found to be low over the regions where MISR underestimates AOD, e.g., the Eastern US and East Asia. Nevertheless, the overall spatial correlation between MODIS and MISR AOD datasets was quite acceptable and no apparent disagreements were found in the annual and seasonal AOD variations during the span of fourteen consecutive years. Hence, AOD datasets from both the sensors could be considered as suitable for comparative study of the spatio-temporal variability of aerosols. For details of the spatial biases between MODIS and MISR AOD products, one may refer to works by Kahn et al. (2009, 2010); Levy et al. (2010) and Shi et al. (2011).

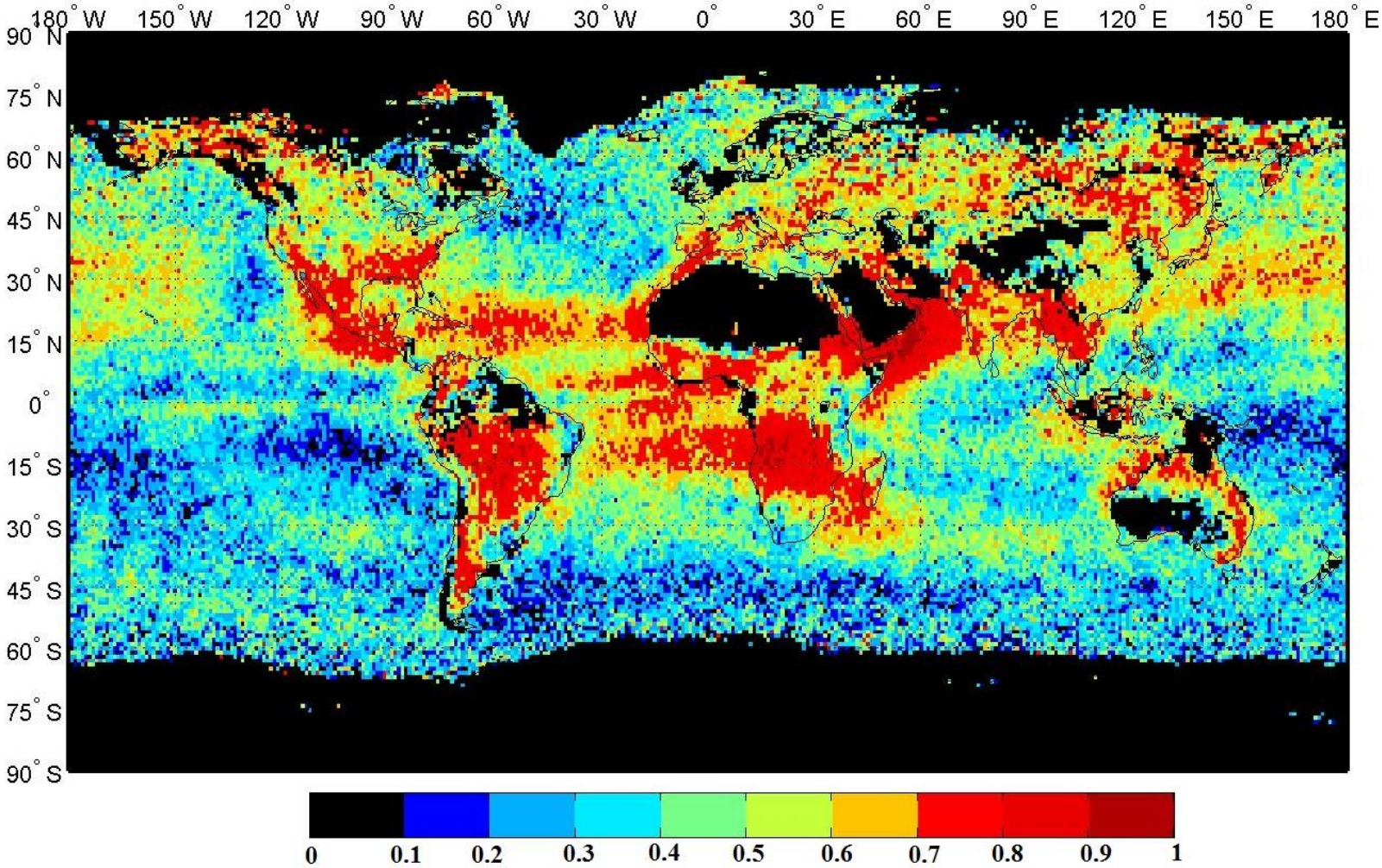

Figure 5.1 Spatial Correlation between MODIS and MISR AOD (1° × 1°) during 2001–2014

5.1.2 Global spatial AOD variation: annual and seasonal analysis

North-West

The annual AOD values remained low (≤0.2), with seasonal high values recorded in MAM and JJA seasons that decreased subsequently in SON and DJF (Figure 5.2-5.6). This seasonality was captured well with both the sensors and could be influenced by natural as well as anthropogenic sources, emission properties, and the modulations induced by precipitation, relative humidity and wind patterns (Andronache, 2004; Dubovik et al., 2001). High AOD values over the Pacific Ocean during MAM season were due to the dust and anthropogenic emissions mainly transported from the Asian mainland (Yu et al., 2012).

North

Over Europe, low annual AOD values were observed. However, comparatively higher aerosol loading was observed over the Mediterranean Sea. AOD values were lower in SON and DJF as compared to the other two seasons. The seasonal high values of AOD during the dry period (MAM and JJA when solar irradiation and boundary layer height increases) could be due to increase in secondary aerosols, biomass burning and dust transport from Sahara (especially in Mediterranean region) (Barnaba et al., 2011; Dayan et al., 2008; de Meij and Lelieveld, 2011; Gonzalez et al., 2000; Hatzianastassiou et al., 2009).

North-East

Mean annual AOD values remained low (≤0.2) over the parts of Russia located in Asian continent. An increasing pattern of aerosol loadings from North to South Russia was observed which could be due to the advection of dry and polluted air masses from Ukraine, Kazakhstan, South-East Asia and China (Plakhina et al., 2007). The aerosol loading remained low during DJF and SON seasons. It could be noted that during the arctic winter, there were lack of observations in the vast majority of the region due to lack of sunshine hours. During MAM and JJA seasons, higher AOD values were found over the southern landmass (countries like Kazakhastan and Mongolia) and the oceanic waters lying along East Russia. The seasonal high AOD values in summer could be due to increase in temperature and

humidity, upwelling of surface particles, photochemical and condensational increase of aerosols, and dust episodes (in and around the nearby desert regions) (Kabanov et al., 2013; Plakhina et al., 2007; Plakhina, 2012).

South-West

Low annual aerosol loadings were recorded over South America. During MAM and JJA seasons, however, higher AOD values were found over Columbia, Venezuela and the surrounding Atlantic waters. High AOD values were recorded over Brazil during SON period due to the seasonal deforestation and sugarcane burning (de Meij et al., 2010; Reddington et al., 2015).

South

MISR reported moderate to high (0.2–0.6) annual aerosol loadings over the African deserts. Over North Africa and the adjoining Atlantic waters (especially surrounding North-West Africa), high annual AOD values (0.3–0.9) were found. A strong seasonal AOD pattern was observed in North Africa owing to the dust activities, with highest and lowest AOD values during JJA and DJF seasons respectively. The mineral dust transport could also be noted across the Atlantic waters towards America (Kaufman et al., 2005; Ridley et al., 2014). A latitudinal shift in AOD pattern was observed over the Sahel during SON and DJF seasons. This could be accounted for the biomass burning activities that spread from North to South Sahel between November and February (Roberts et al., 2009). In Southern Africa, moderate to low annual aerosol loadings were found. However, high AOD signals were recorded during JJA season over the Southern landmass and the surrounding Atlantic waters due to the enormous burning activities that usually take place in dry season (June–October) (Kumar et al., 2014). Over the Middle-East countries and the surrounding Pacific waters, high AOD values were observed during MAM and JJA seasons, due to the increased dust activities in spring summer period (Basart et al., 2009; Rashki et al., 2014).

South-East

Moderate to high (0.3–0.9) AOD values were recorded over Eastern China, India (especially in IGP), Pakistan, Bangladesh, adjoining Arabian Sea and Bay of Bengal. On the contrary, low annual AOD values (≤0.2) were found over Australia, southern parts of the Indian and Pacific Oceans. During DJF season, the aerosols were found to be more concentrated towards the Asian landmass. In particular, aerosol loading exhibited a spatially increasing pattern from West to East IGP during winter owing to the associated meteorological conditions. High AOD values were also recorded over East China during winter season. During MAM season, an overall increase in AOD was recorded over the Asian landmass, and the surrounding oceanic waters (along East China, Arabian Sea and Bay of Bengal). During JJA season, this increase became maximum pertaining to the monsoonal effects, with a shift in increasing AOD pattern from East to West (especially over IGP). Strikingly high AOD values were recorded over Pakistan and Arabian Sea during the monsoon season. During SON season, subsequent to the washout of particles by rains, aerosol loading decreased over the Asian mainland and the surrounding waters. As an exception, high AOD values were found over North-West IGP due to crop residue burning (Sharma et al., 2010). These findings were in order with many of the previously reported studies (de Meij et al., 2010; Kaskaoutis et al., 2011; Mehta, 2015; Prasad and Singh, 2006; Zhang and Reid, 2010). Over Australia and its surroundings, there were lack of significant dust storm activities during JJA season due to low wind speeds. However, during SON and DJF seasons, aerosol loadings were enhanced due to the regional biomass burning, long range transport and marine biogenic emissions. This seasonality was also captured in earlier studies (Mitchell et al., 2010; Rosen et al., 2000).

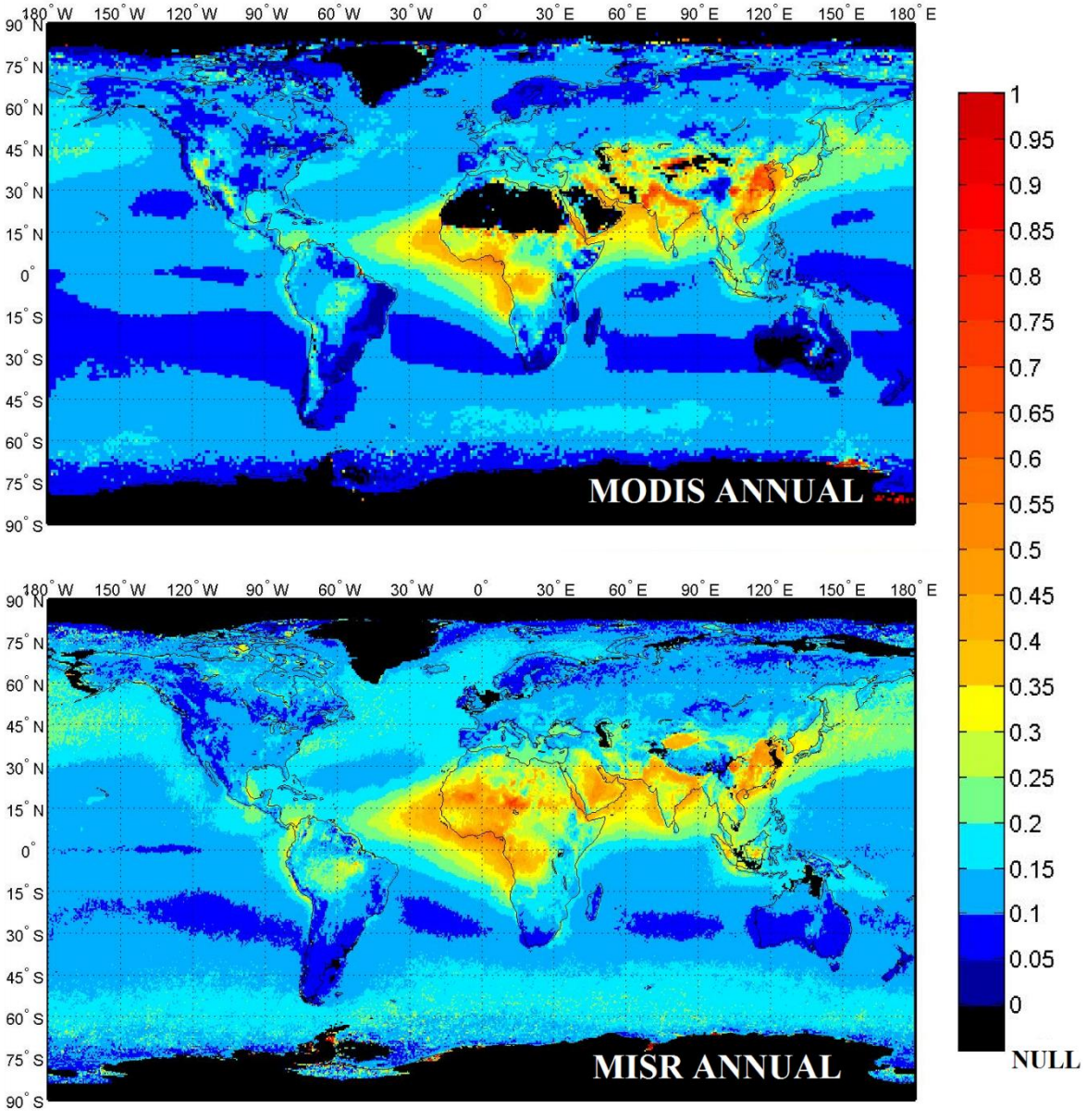

Figure 5.2 Annual variations of AOD using MODIS (1° × 1°) and MISR (0.5° × 0.5°) datasets.

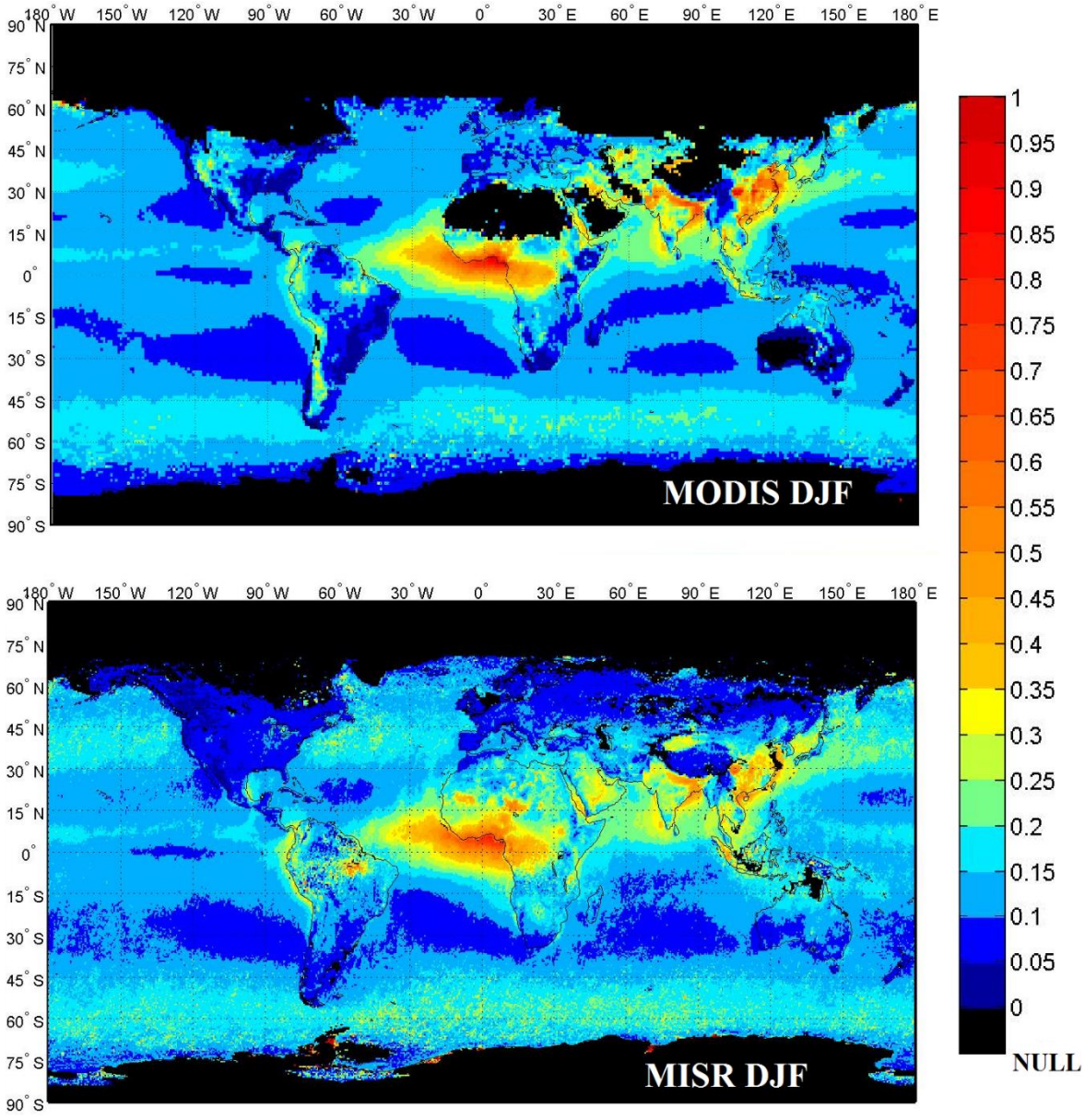

Figure 5.3 AOD variations during DJF season using MODIS (1° × 1°) and MISR (0.5° × 0.5°) datasets.

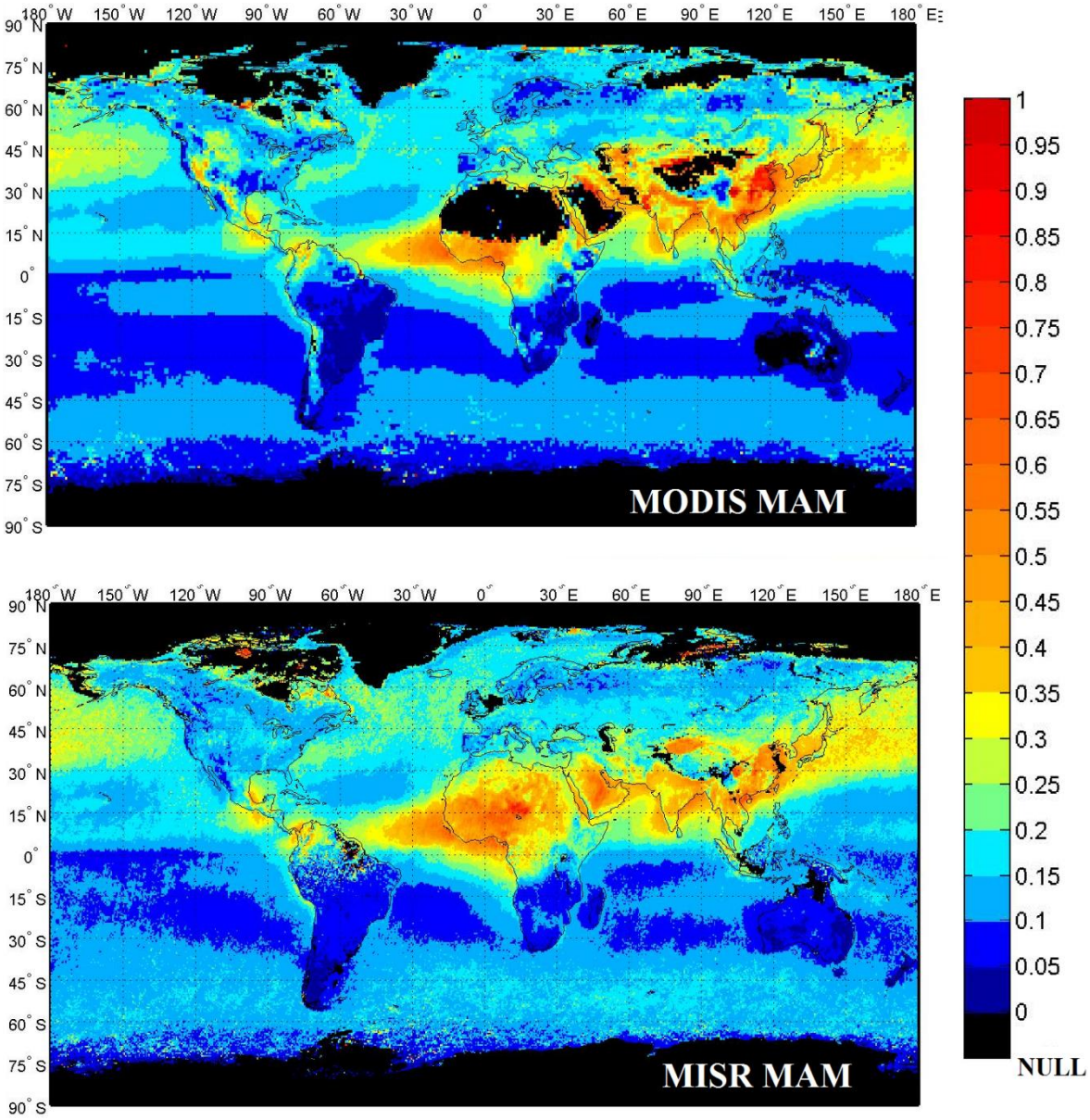

Figure 5.4 AOD variations during MAM season using MODIS (1° × 1°) and MISR (0.5° × 0.5°) datasets.

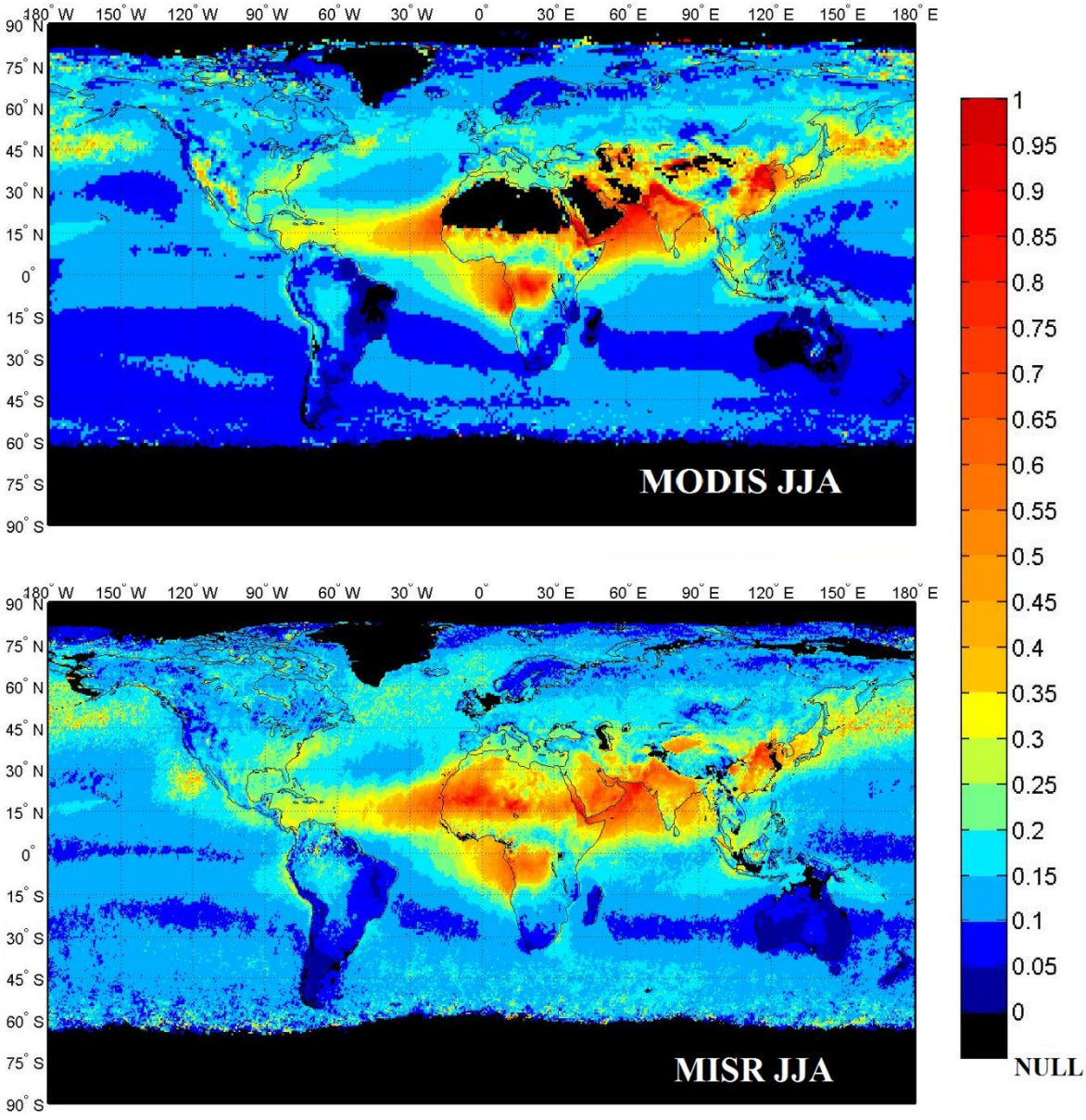

Figure 5.5 AOD variations during JJA season using MODIS (1° × 1°) and MISR (0.5° × 0.5°) datasets.

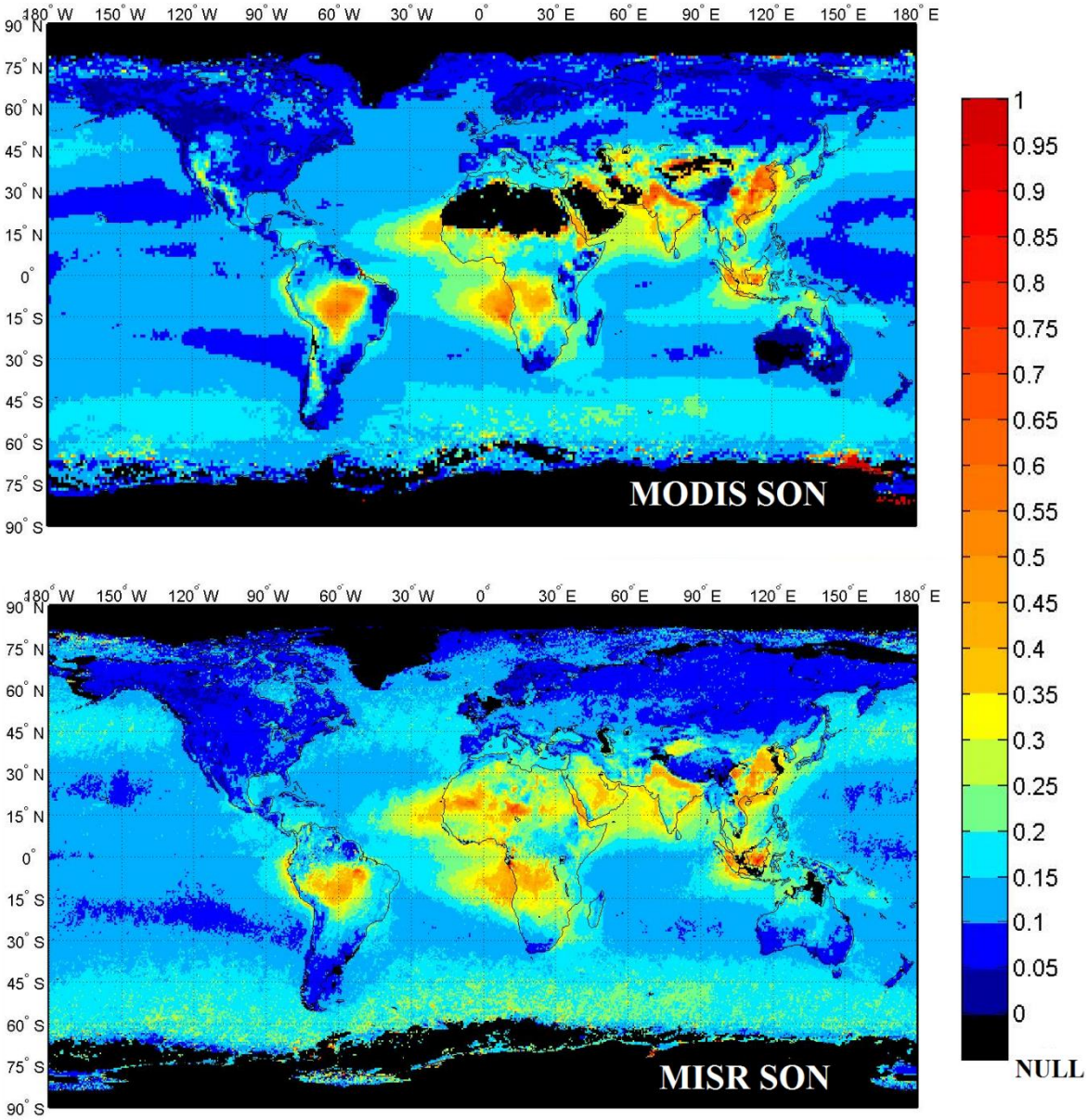

Figure 5.6 AOD variations during SON season using MODIS (1° × 1°) and MISR (0.5° × 0.5°) datasets.

5.1.3 Global spatial AOD relative changes: annual and seasonal analysis

North-West

In the study period of past fourteen years, an overall annual and seasonal decrease in AOD was recorded over the North American landmass (Figure 5.7-5.11). The decrease was especially prominent in the Eastern US as observed from both the sensors. Positive AOD changes were reported over parts of Canada and the adjoining oceanic regions, but the increase in AOD over the sub-arctic pixels could be fake due to the uncertainties in AOD retrievals from satellite data (Shi et al., 2011; Yoon et al., 2014).

North

Negative annual and seasonal AOD changes were reported over the European landmass and the Mediterranean Sea. Though, quantitatively, MODIS reported a higher decrease in AOD as compared to MISR. Increase in AOD over the sub-arctic pixels could be fake.

North-East

The annual and seasonal AOD changes in this region were mostly negative. However, positive changes (especially in JJA season) were found over East Russia and the surrounding oceanic waters. In addition, MISR reported positive AOD changes over Southern region during SON season.

South-West

Negative annual and seasonal AOD changes were found over the region. However, during DJF and MAM seasons, positive AOD changes were observed by MISR over Northern part of this region. In addition, MODIS recorded a distinctive increase in AOD over South Pacific Ocean during JJA season.

South

Negative and positive AOD changes were observed over Africa and the Middle East countries respectively. Over the Atlantic waters surrounding South-West Africa, MODIS specifically reported increase in AOD during MAM, JJA and SON seasons.

South-East

Negative annual changes in AOD were found over parts of Southern China, Australia, Island regions and Southern Indian Ocean. On the contrary, a prominent increase in annual AOD values was recorded over South and East India, Bay of Bengal, Bangladesh and Arabian Sea. During DJF, MAM and SON seasons, aerosol loadings were enhanced over South India, Arabian Sea and Bay of Bengal, but declined over Australia, East China and surrounding Pacific waters. However, negative AOD changes were recorded over the landmass during JJA season.

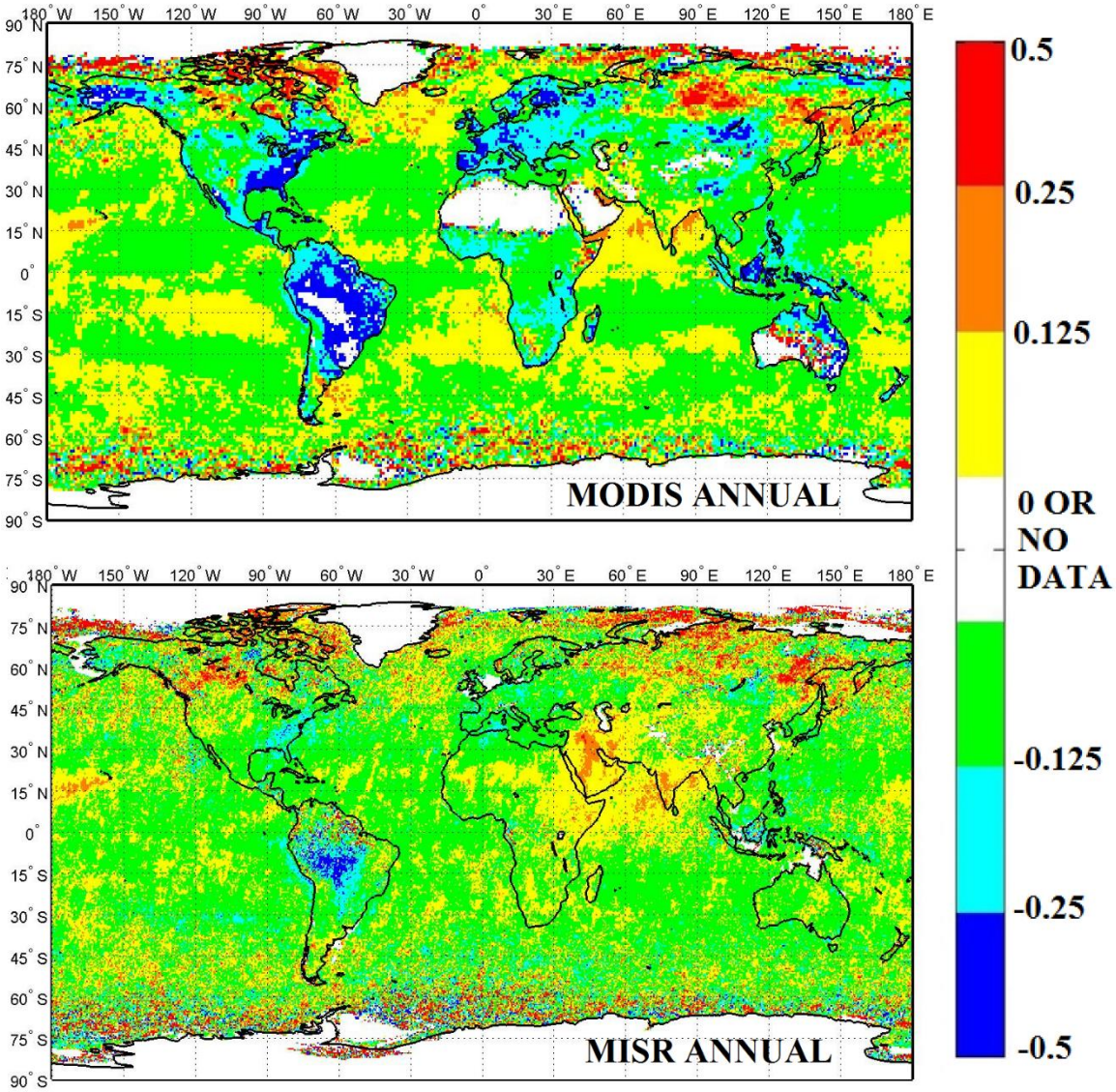

Figure 5.7 Annual relative changes (%) of AOD using MODIS (1° × 1°) and MISR (0.5° × 0.5°) datasets

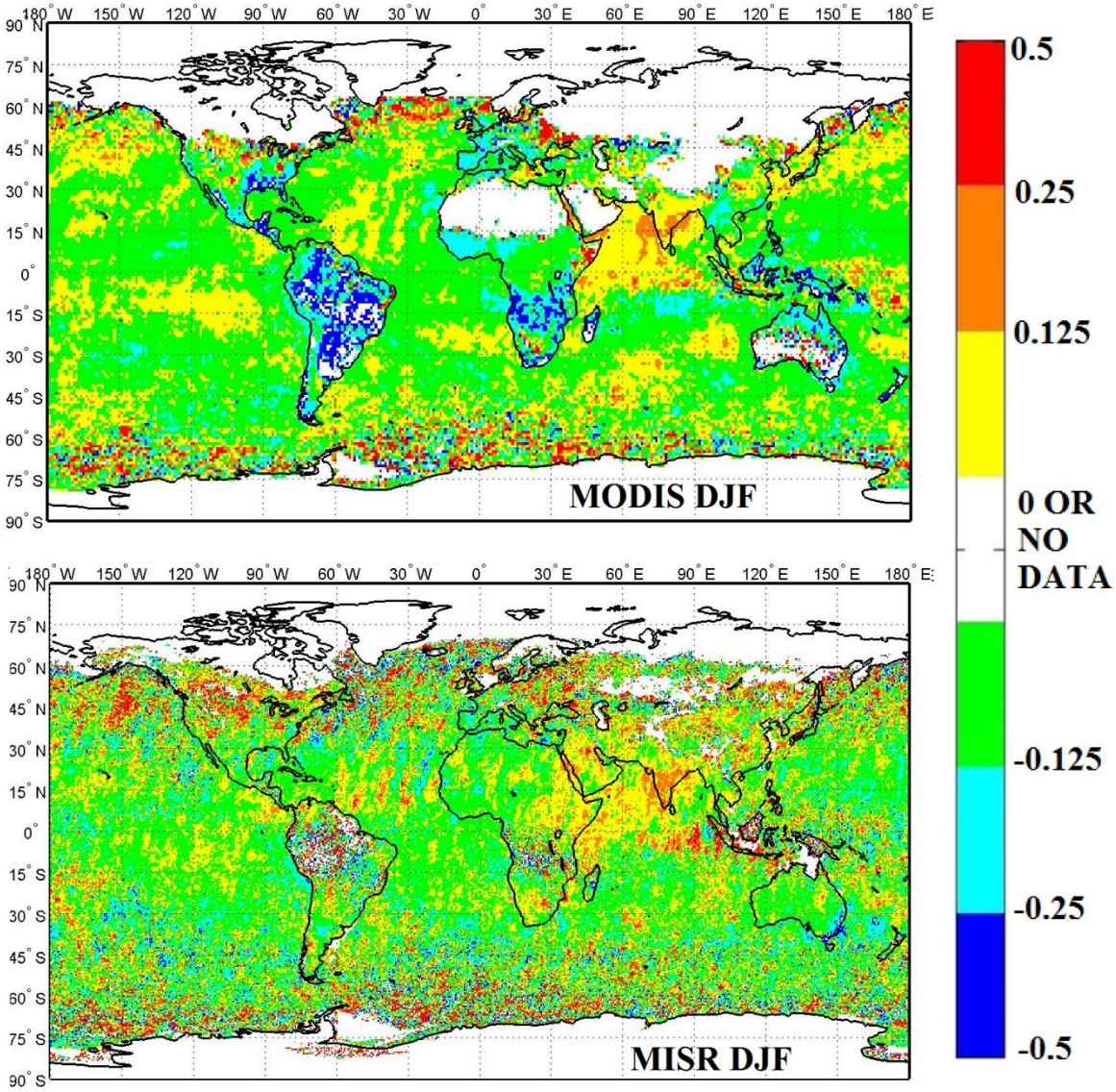

Figure 5.8 Relative changes (%) of AOD during DJF season using MODIS (1° × 1°) and MISR (0.5° × 0.5°) datasets

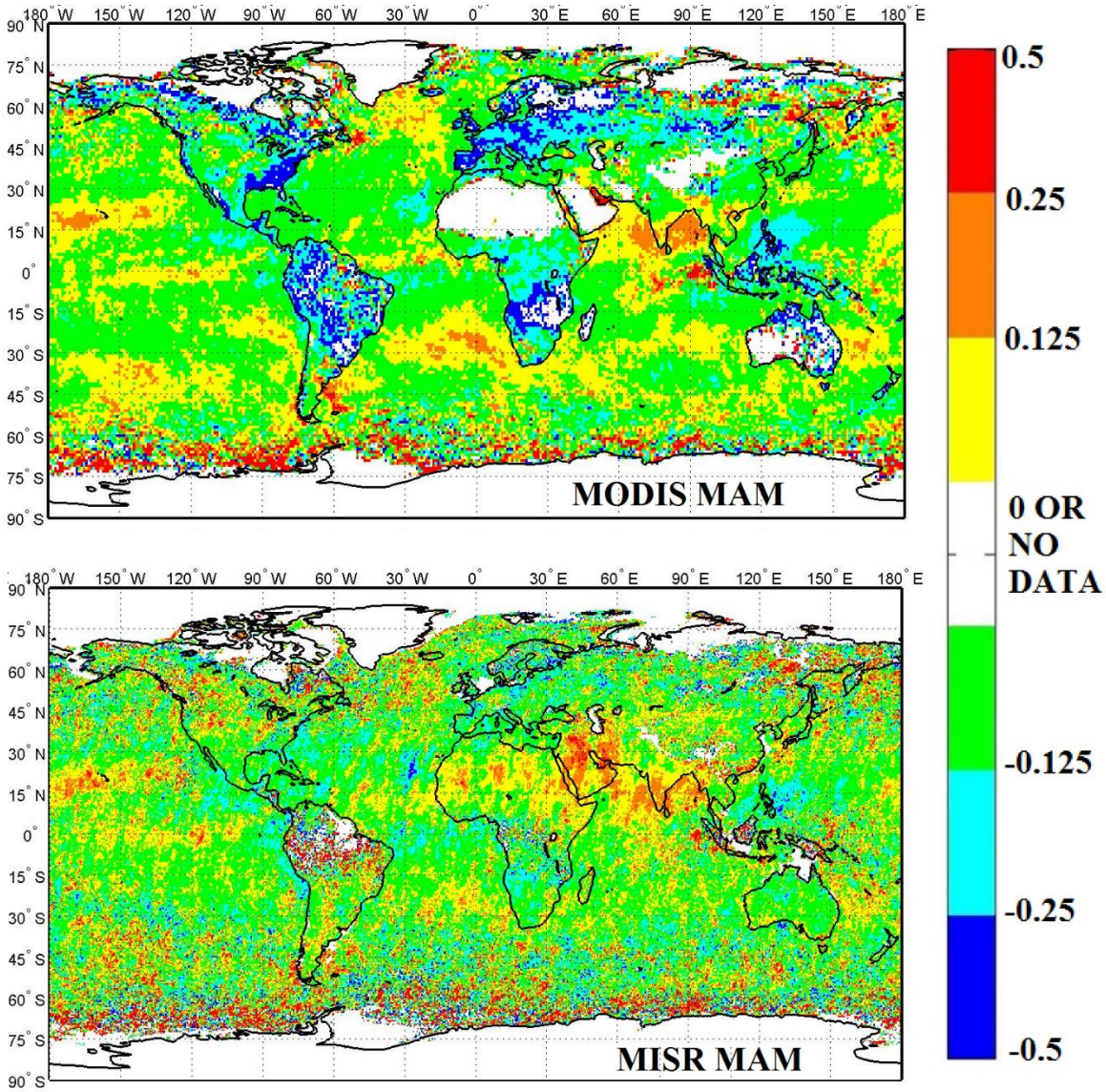

Figure 5.9 Relative changes (%) of AOD during MAM season using MODIS (1° × 1°) and MISR (0.5° × 0.5°) datasets

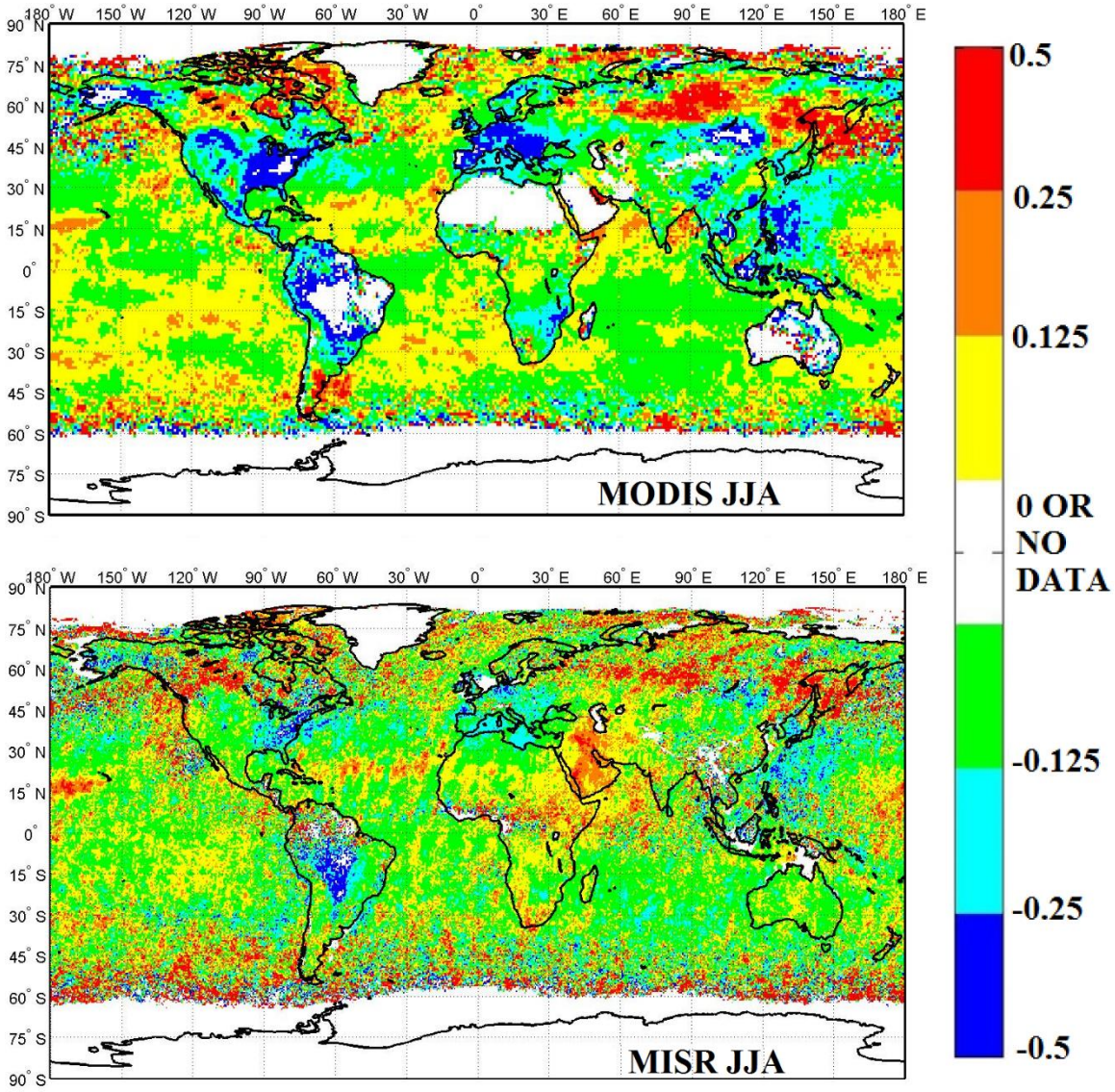

Figure 5.10 Relative changes (%) of AOD during JJA season using MODIS (1° × 1°) and MISR (0.5° × 0.5°) datasets

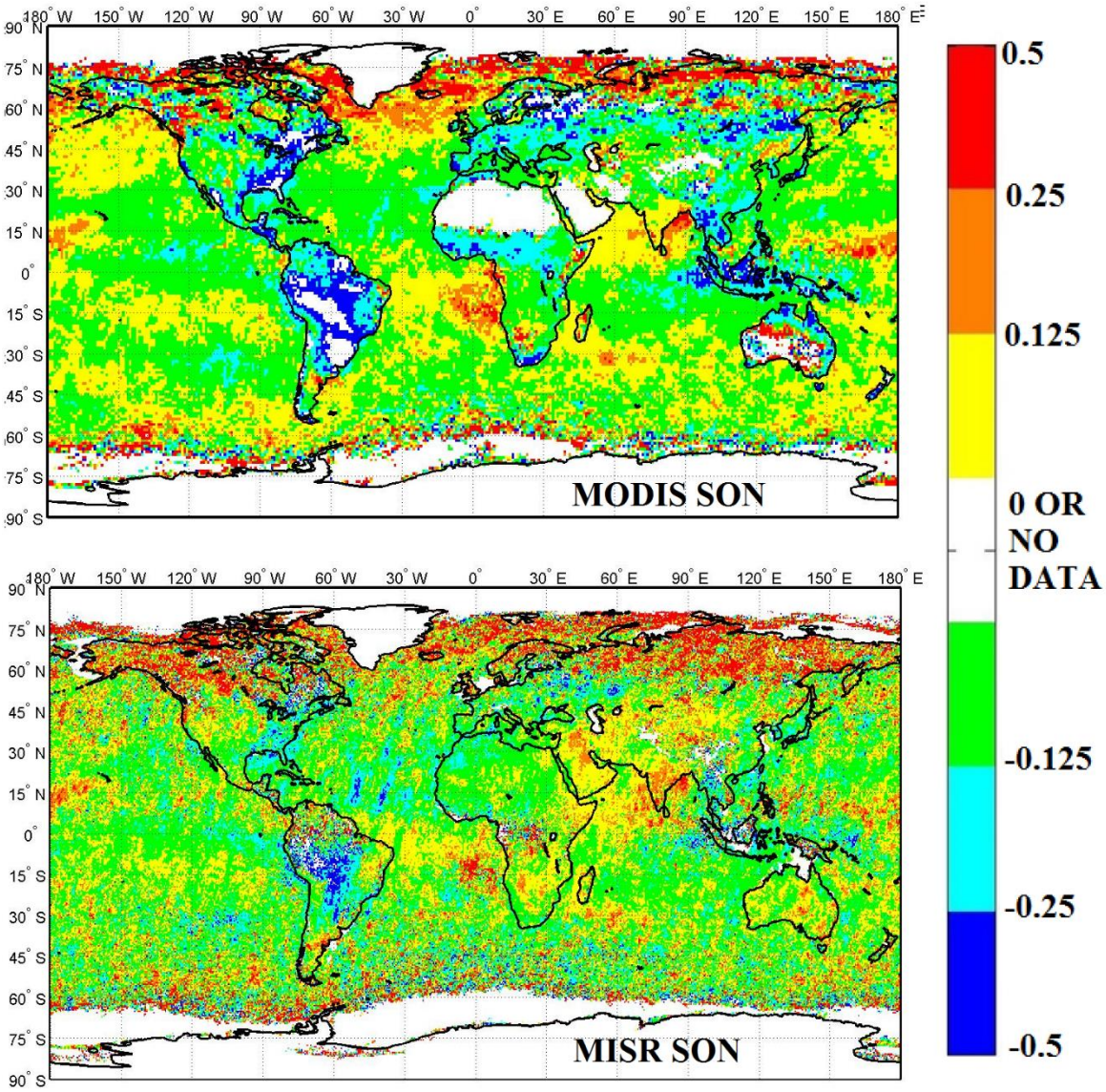

Figure 5.11 Relative changes (%) of AOD during SON season using MODIS (1° × 1°) and MISR (0.5° × 0.5°) datasets

5.1.4 Global spatial AOD trends: annual and seasonal analysis

This sub-section presents the spatio-temporal variability of trends at annual as well as seasonal scales. However, for an illustration on the trends over individual data points (i.e., at pixel level), a graph showing the linear trends of annual AOD using MODIS sensor over five randomly picked locations across different parts of the world has been provided in Annexure III.

North-West

Decreasing annual and seasonal AOD trends were found over this region. MODIS reported significantly decreasing trends over Southern part of North America and North Atlantic Ocean surrounding the Eastern US, whereas the decreasing trends recorded by MISR were mostly insignificant (Figures 5.12-5.16). These trends were indicative of the decrease in anthropogenic emissions in North-East America, especially due to decrease in SO_2 and NO_x emissions (regulated by Clean Air Act Amendments of 1990) (Hsu et al., 2012; Xia, 2011; Pozzer et al., 2015; Zhang and Reid, 2010; Yoon et al., 2014). A recent study based on ground observations reported that the negative AOD trends in North-West America could be due to reduction in natural sources, e.g., dust (Li et al., 2014).

North

Decreasing annual and seasonal AOD trends were found over European landmass region which could be attributed to the strict environmental regularizations leading to decrease in sulphur dioxide and nitrous oxides emissions (de Meij et al., 2010; Hilboll et al., 2013; Hsu et al., 2012; Karnieli et al., 2009; Li et al., 2014; Pozzer et al., 2015; Tørseth et al., 2012; Vestreng et al., 2007; Yoon et al., 2011, 2014; Zhou et al., 2012). The decreasing trends were also found over the Mediterranean region and were in agreement with the earlier findings (Papadimas et al., 2008; Zhang and Reid, 2010).

North-East

The annual AOD trends were mostly insignificant over this region. The trends were positive over Central-North and along the Sea of Okhotsk, and negative over rest of the region.

Statistically significant increasing trends were found (using MODIS data) over the Sea of Okhotsk during spring (MAM) season. In JJA season, significantly decreasing trends were found over the Southern region. The decreasing AOD trends over most of the parts of Russia (mainly due to decreased anthropogenic forcing) and the increasing estimates in Far East Russian region (due to increased industrial emissions and fires) were in agreement with the earlier findings (Plakhina et al., 2007; Plakhina, 2012).

South-West

Significantly decreasing annual and seasonal AOD trends were observed using MODIS data over the landmass and the surrounding Atlantic waters. The decreasing trends found using MISR data were mostly insignificant. Similar trends were also reported in the previous studies (de Meij et al., 2010; Hsu et al., 2012; Li et al., 2014). However, significantly increasing trends were found over South Pacific Ocean (specifically in JJA season) using MODIS data.

South

Negative annual and seasonal AOD trends were found over Africa. These decreasing trends could be linked with the reduction of dust due to stilling of surface winds over the dust source regions in North Africa. This could be attributed mainly to the large scale changes in circulation and greening of the Sahel region (Cowie et al., 2013; Olsson et al., 2005; Ridley et al., 2014). Decreasing AOD trends over South Africa could be mainly due to the reduced emissions owing to the implementation of environmental policies (Kumar et al., 2014). However, increasing AOD trends were found over South Atlantic waters (surrounding South-West Africa) using MODIS data. Statistically significant increasing annual and seasonal (MAM and JJA) trends were found over the Middle-East countries, which were also previously reported in literature (de Meij et al., 2010; de Ruyter de Wildt et al., 2012; Hsu et al., 2012; Pozzer et al., 2015; Yoon et al., 2014).

South-East

Decreasing annual AOD trends were found over this region except for the Indian subcontinent and its surroundings. The increasing annual and seasonal (DJF, MAM, SON) trends over India could be mainly accounted for the increase in anthropogenic emissions (Hsu et al., 2012; Kishcha et al., 2011; Pozzer et al., 2015). However, decreasing AOD trends (especially during JJA season) over IGP could be associated with the lessening of dust activities due to increase in vegetation and precipitation over the Thar Desert region (Kaskaoutis et al., 2011; Pandya et al., 2004). Increasing annual and seasonal (DJF, MAM, SON) trends were also found over Bay of Bengal and Arabian Sea which could be accounted for the increase in pollution transport from the adjacent landmass regions (de Meij et al., 2010; Kaskaoutis et al., 2011; Lelieveld et al., 2001; L'eon et al., 2001; Ramanathan et al., 2001b; Zhang and Reid, 2010). Decreasing annual and seasonal (DJF, MAM, JJA) trends were found over Australia which are also reported by de Meij et al. (2010). The detailed discussion on the AOD seasonality, changes and trends over China, Indonesia, Pakistan, Japan and Bangladesh is given in Section 5.1.5 and 5.1.6.

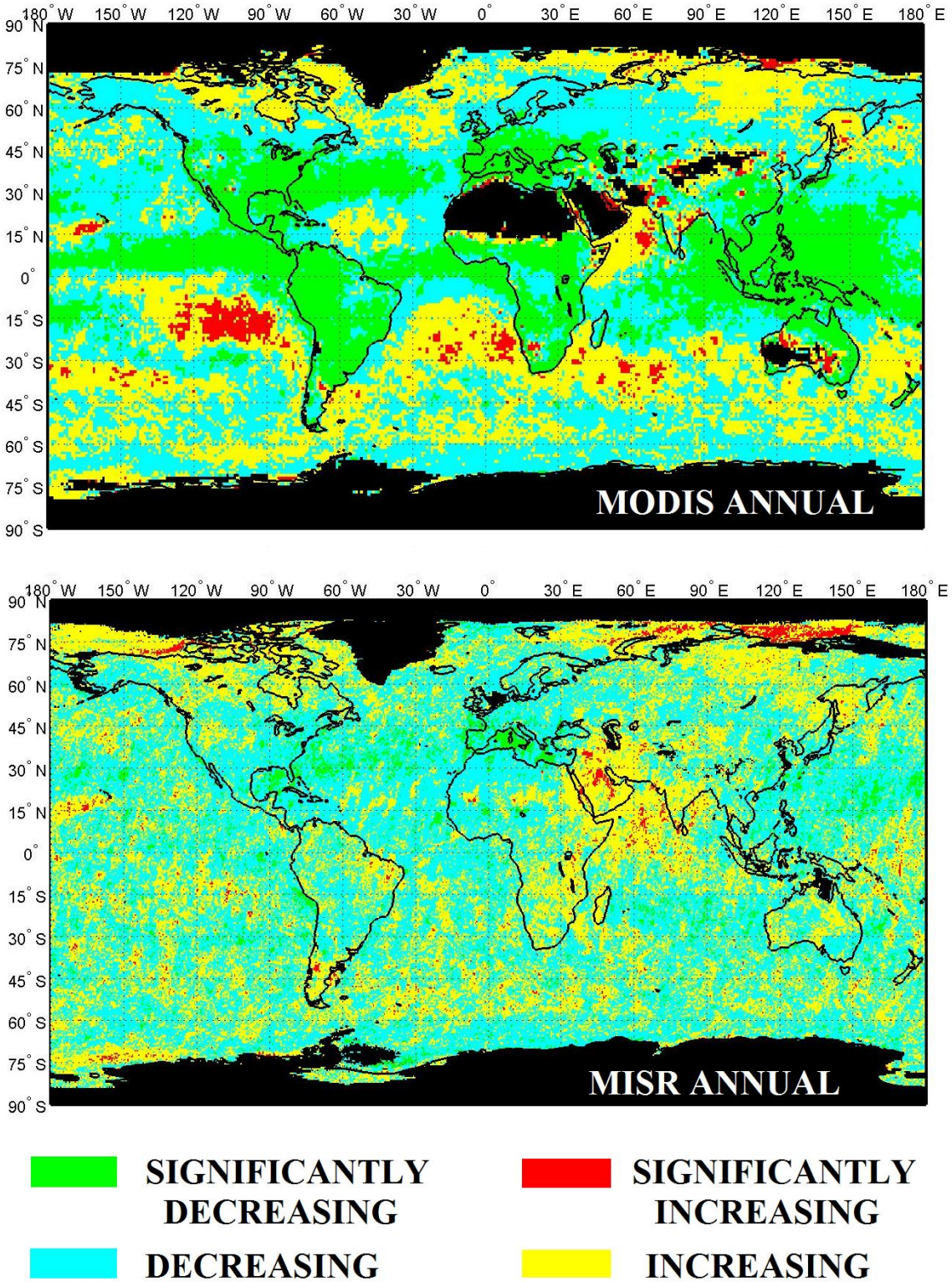

Figure 5.12 Annual trends of AOD using MODIS (1° × 1°) and MISR (0.5° × 0.5°) datasets.

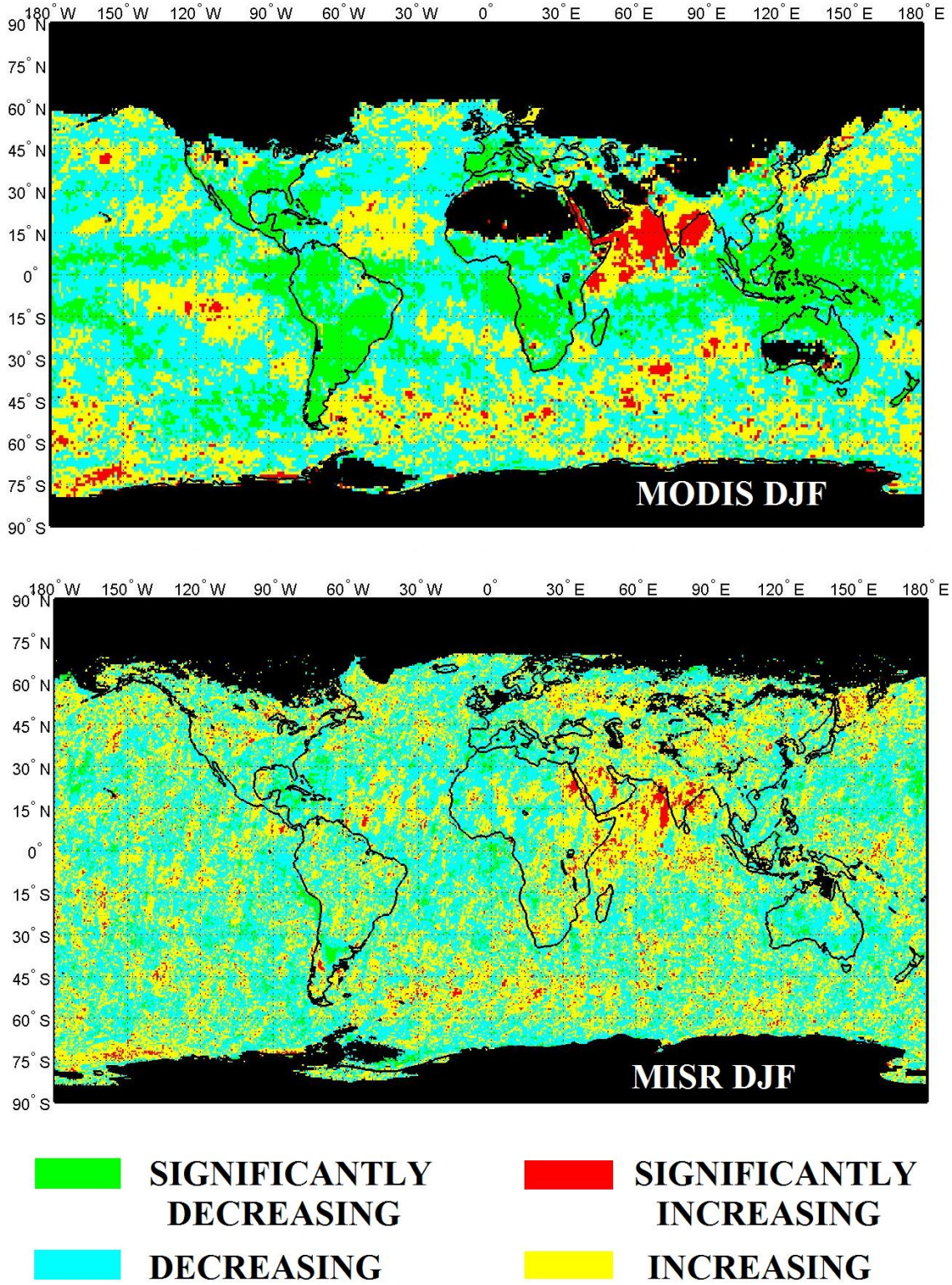

Figure 5.13 AOD trends during DJF season using MODIS (1° × 1°) and MISR (0.5° × 0.5°) datasets.

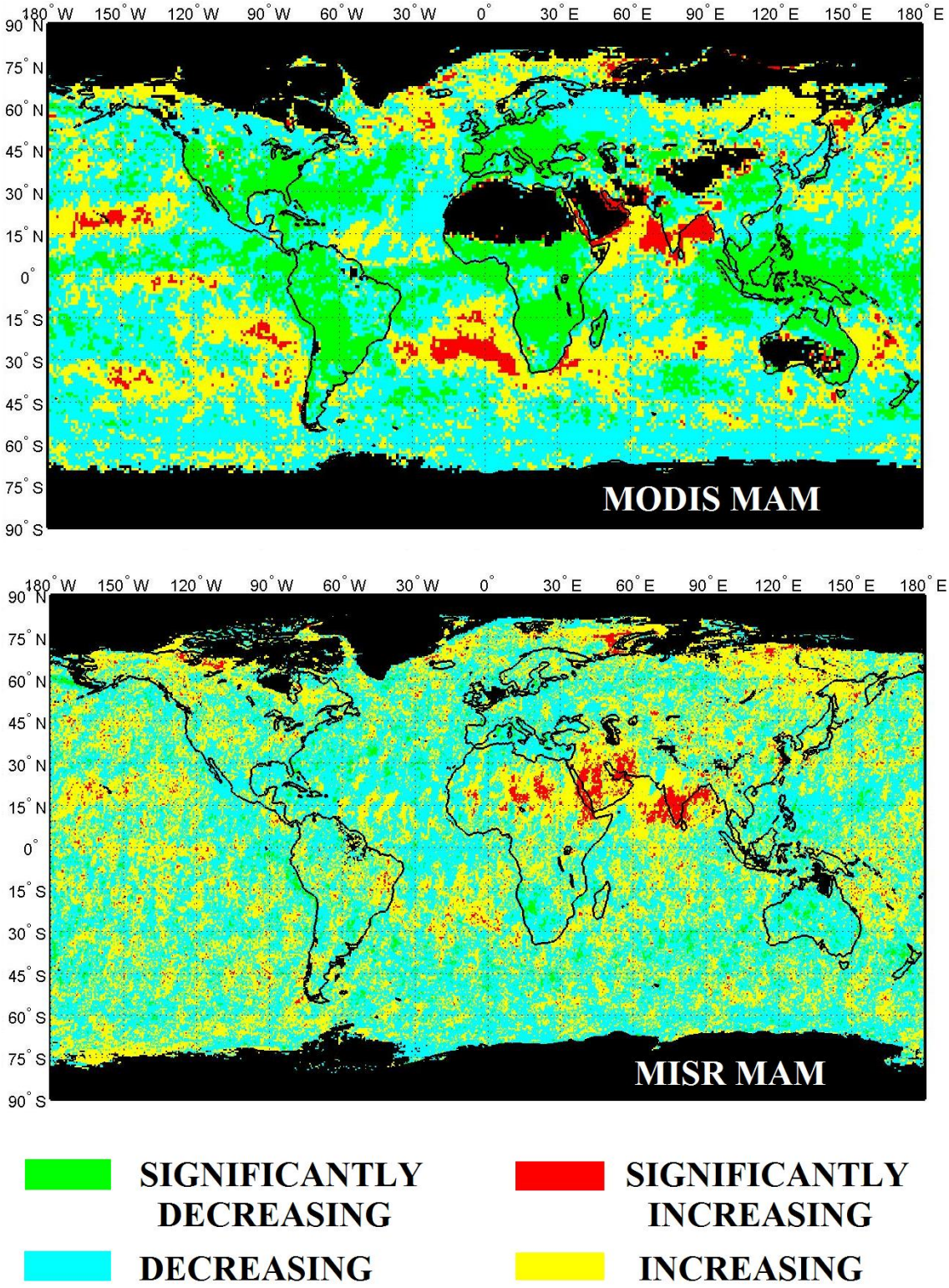

Figure 5.14 AOD trends during MAM season using MODIS (1° × 1°) and MISR (0.5° × 0.5°) datasets.

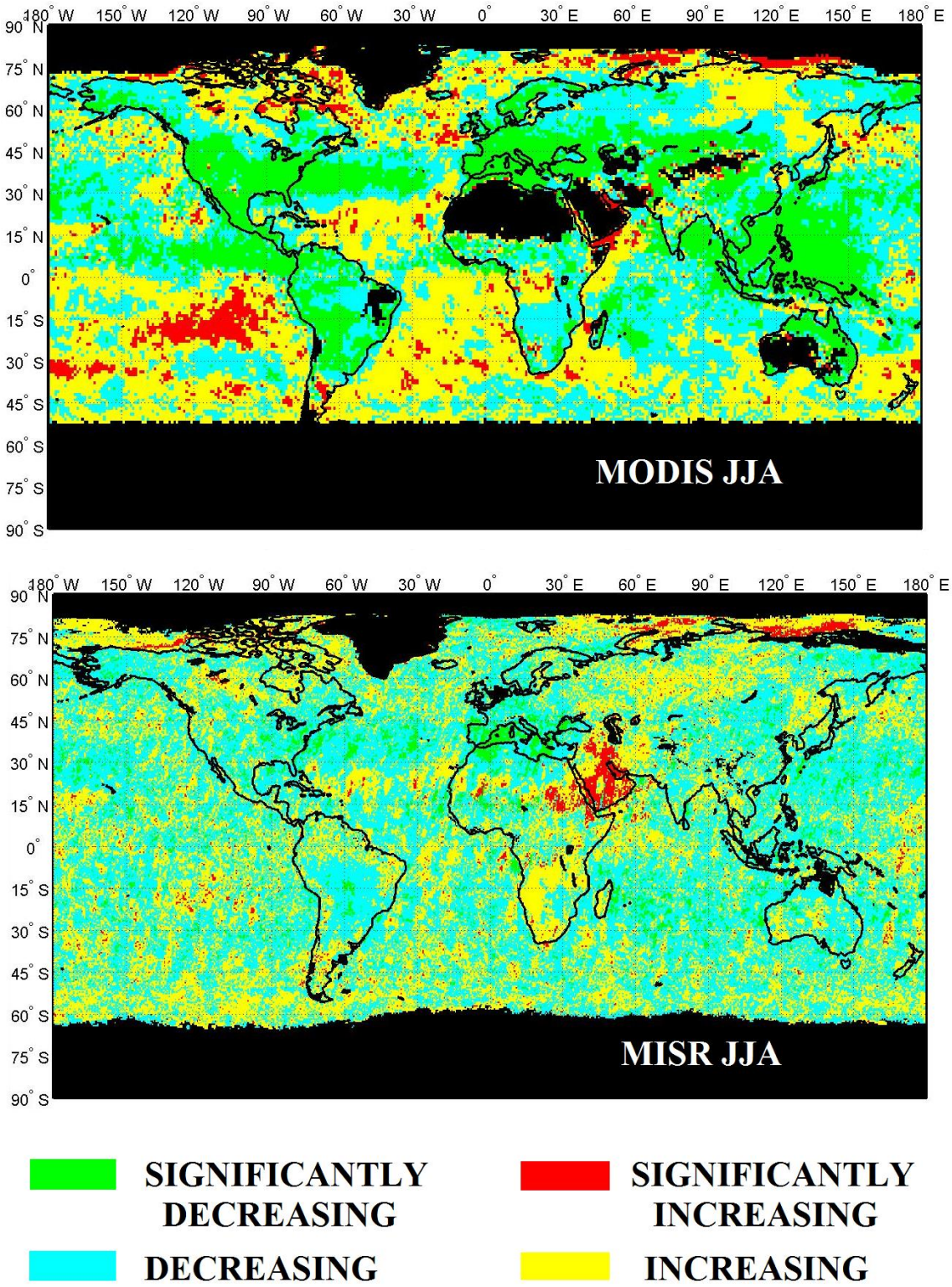

Figure 5.15 AOD trends during JJA season using MODIS (1° × 1°) and MISR (0.5° × 0.5°) datasets.

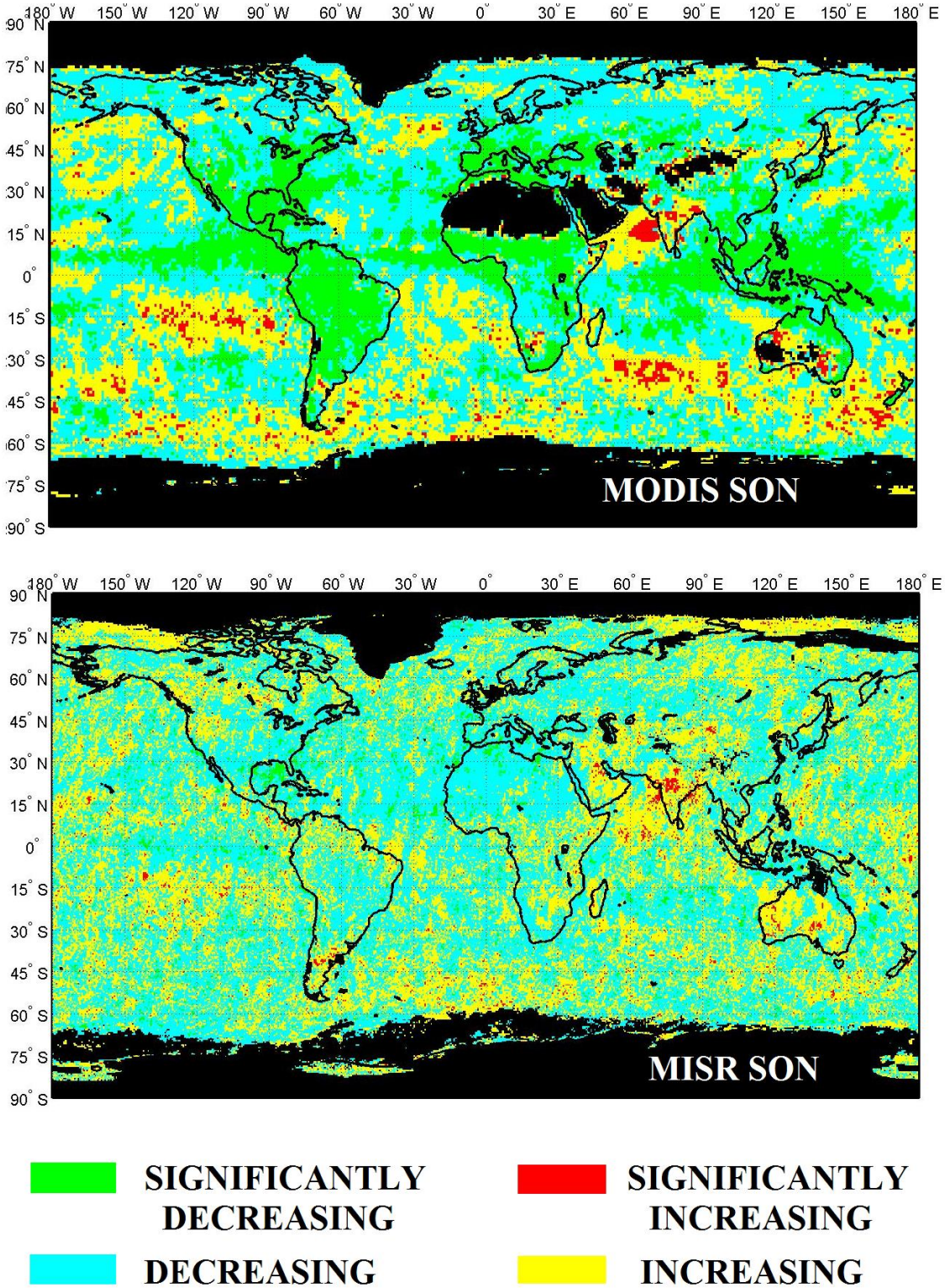

Figure 5.16 AOD trends during SON season using MODIS (1° × 1°) and MISR (0.5° × 0.5°) datasets.

5.1.5 AOD distribution over the ten most populous countries of the world

Annual and seasonal variations of AOD were studied for the ten most populous countries of the world (Figures 5.17-5.21). The vertical bars show the standard deviation in AOD. It can be seen from the Figures that Bangladesh and Pakistan were amongst the most polluted countries in terms of averaged annual aerosol loadings, followed by Nigeria, India and China during the considered study period. During DJF and MAM seasons, Bangladesh and Nigeria witnessed the highest levels of pollution as compared to the other populous countries considered here. In JJA and SON seasons, however, AOD was found to be highest over Pakistan.

China

China, the most populated country, observed a high level of annual aerosol loading. Seasonal high AOD values during MAM and JJA period could be due to the influx of desert dust from China and Mongolia, and the upwelling of surface particles due to high incoming solar radiation (Ogunjobi et al., 2003). The aerosol loading decreased in SON season (due to washout of particles by monsoonal rains) but subsequently increased during winter (DJF) (Park et al., 2011).

India

India, with its rapid economic growth, industrialization and increasing population witnessed high aerosol loading. Aerosol sources in India are of both natural and anthropogenic origins, i.e., mineral dust, sea salts, vehicular emissions, biomass burning and industrial emissions (Kaskaoutis et al., 2011). For details on annual and seasonal AOD variation, one may refer to Section 5.1.2.

US

US, the third most populated country, received lower aerosol loading as compared to its competing counterparts in terms of population. The seasonality in AOD was also observed, with maximum values recorded in MAM season. It is further to be noted that the decrease in AOD from summer to winter (particularly over South-East US) could be associated with the decrease in sulphate and organic aerosols due to shut down of biogenic emissions and UV driven photochemistry (in August–October) (Kim et al., 2015).

Indonesia

The major sources of aerosols in Indonesia include seasonal biomass burning (peat forests, agriculture etc.), urban activities and sea salts (Page et al., 2002). High AOD values were observed during SON season owing to biomass burning during the dry period (Streets et al., 2003).

Brazil

Low values of annual AOD were recorded over Brazil with minimum and maximum values during MAM and SON seasons respectively. One of the major sources of aerosols (apart from other anthropogenic emissions) could be biomass burning due to deforestation, particularly in dry season spanning from August–October (Reddington et al., 2015; Yoon et al., 2014).

Pakistan

High annual aerosol loading was observed over Pakistan and the major aerosol sources could include vehicular and industrial emissions, dust, sea salt and organic carbon (Alam et al., 2011; Bibi et al., 2015). The seasonality in AOD was similar to that found in India (the immediate neighboring country) with highest values during JJA season.

Nigeria

The major sources of aerosols in Nigeria are known to be traffic, industry, oil, sea spray, biomass burning and windblown dust (Efe, 2008). The country observed high annual aerosol loading during the considered study period. Seasonal high AOD values were recorded during the dry period (DJF and MAM), which could be associated with the sand storms and Harmattan dust, especially in Northern Nigeria. The dust particles could be subsequently washed away in rainy season (Ogugbuaja and Barsisa, 2001).

Bangladesh

High annual aerosol loading was observed over Bangladesh and due to its location in the East IGP, the seasonal AOD pattern was similar to that found in the surrounding Indian region (de Meij et al., 2010; Kaskaoutis et al., 2011; Mehta, 2015; Zhang and Reid, 2010). The sources of aerosols could include dust, biomass burning, industry emissions and traffic (Begum et al., 2010). During DJF season, high AOD values could be the manifestations of anthropogenic activities and meteorological conditions that concentrate the aerosol load in

the East IGP. The aerosol loading remained high during MAM and JJA seasons. Minimum AOD values were recorded during SON season when the meteorological conditions favor an increasing AOD pattern towards West IGP.

Russia

Low AOD values were reported over Russia, in general, with the maximum and minimum values during MAM and SON seasons respectively.

Japan

Annual aerosol loading over Japan was found to be moderate and exhibited a seasonal pattern with higher AOD values during MAM and JJA as compared to the other two seasons. This seasonality was also observed by Aoki and Fujiyoshi (2003).

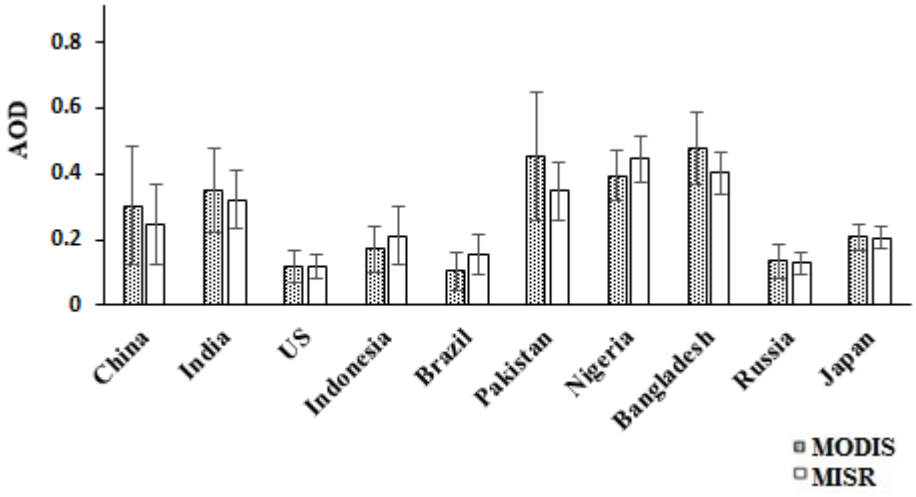

Figure 5.17 Annual variations of AOD using MODIS and MISR for ten most populous countries of the world, vertical bars represent the standard deviation

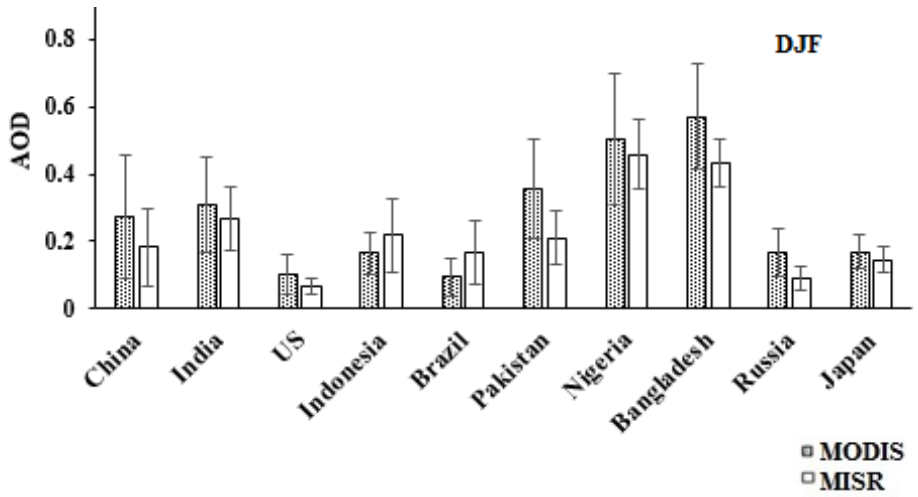

Figure 5.18 AOD variations during DJF season using MODIS and MISR for ten most populous countries of the world, vertical bars represent the standard deviation

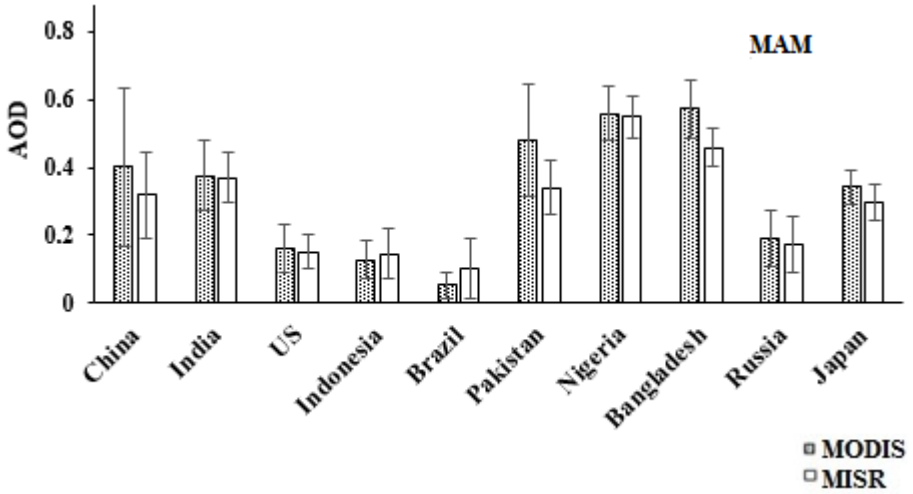

Figure 5.19 AOD variations during MAM season using MODIS and MISR for ten most populous countries of the world, vertical bars represent the standard deviation

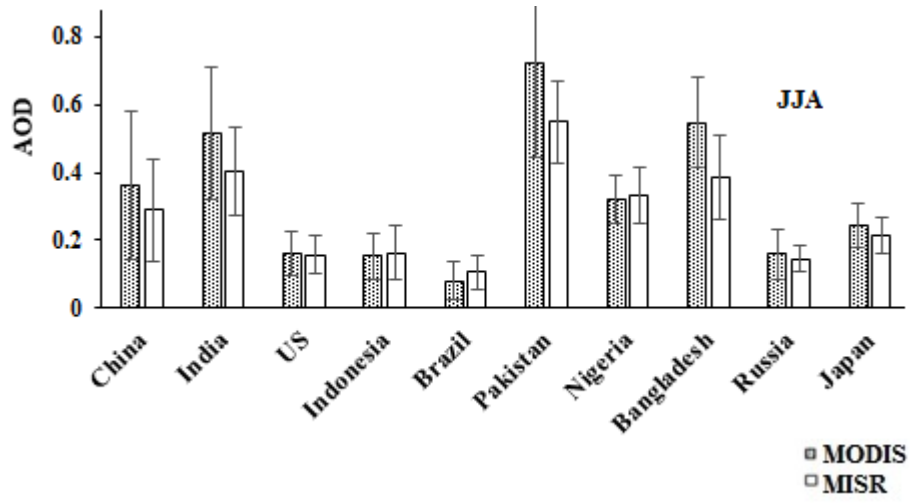

Figure 5.20 AOD variations during JJA season using MODIS and MISR for ten most populous countries of the world, vertical bars represent the standard deviation

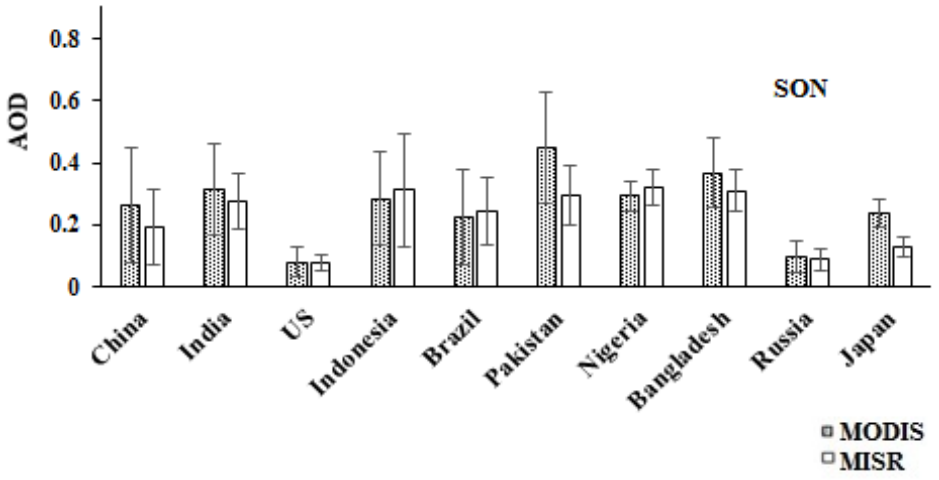

Figure 5.21 AOD variations during SON season using MODIS and MISR for ten most populous countries of the world, vertical bars represent the standard deviation

5.1.6 AOD changes and trends over the ten most populous countries of the world

Figures 5.22-5.26 depict the annual and seasonal relative changes in AOD (%) and Table 5.1 illustrates the AOD trends over the ten countries. The '↑' symbol refers to significantly increasing trend, '↓' symbol represents significantly decreasing trend, '-' represents no significant trend. Colors (black/gray) in the table denote agreement in the results from both the sensors (decreasing/increasing trends).

China

Annual AOD changes estimated using MODIS were found to be negative whereas MISR datasets exhibited the positive variability. However, in JJA season, both the sensors reported negative AOD changes. The annual and seasonal (JJA and SON) trends were found to be significantly decreasing. These decreasing trends could be associated with the reduction in anthropogenic emissions, e.g., implementation of air pollution reduction technologies in the power plants by State Environmental Protection Administration (SEPA) after 2006 (Cao, et al., 2009; Lu et al., 2010; Panicker et al., 2012). These decreasing trends could also be studied in connection with the decrease in frequency of dust events in China (due to change in tropospheric circulation pattern over Asia) (Wang et al., 2008).

India

Annual and seasonal (DJF and SON) trends were found to be significantly increasing, which could be accounted mainly for the anthropogenic factors (Babu et al., 2013; Cofala et al., 2004; de Meij et al., 2010; Dey and Di Girolamo, 2010, 2011; Hsu et al., 2012; Kaskaoutis et al., 2011; Kishcha et al., 2011; Lu et al., 2013; Mehta, 2015; Pozzer et al., 2015; Ramachandran et al., 2012; Zhao et al., 2008). The significantly decreasing AOD trends in JJA season could be associated with the decrease in dust activities in the Thar Desert during the past decade (Kaskaoutis et al., 2011; Pandya et al., 2004).

US

Negative AOD changes were found over the country. Significantly decreasing annual and seasonal trends were reported by both the sensors. These decreasing trends could be linked with the decreasing anthropogenic emissions (mainly sulphur dioxide, ammonia and nitrous oxides) due to environmental regulations in US (EPA, 2011; de Meij et al., 2010; Hsu et al.,

2012; Li et al., 2014; Murphy et al., 2011; Pozzer et al., 2015; Yoon et al., 2012, 2014; Zhao et al., 2008).

Indonesia

Negative annual and seasonal AOD changes were reported. Significantly decreasing annual and seasonal trends were found which could be due to decrease in dust, sea salt transport and biomass burning (Hsu et al., 2012; Pozzer et al., 2015; Yoon and Pozzer, 2014).

Brazil

Negative annual and seasonal AOD changes were found over the country. Significantly decreasing annual and seasonal (DJF, JJA and SON) trends were found, which could be due to decrease in deforestation fires since 2004 as reported by Reddington et al. (2015).

Pakistan

The annual and seasonal AOD changes observed by MISR were positive. On the contrary, negative AOD changes were reported by MODIS except for DJF season. Significantly increasing trends during DJF season were recorded by both the sensors, similar to those observed over India (Dey and Di Girolamo, 2011; Mehta, 2015).

Nigeria

The annual AOD changes were found to be negative, though the recorded decrease with MODIS observations was higher than that with MISR. MODIS demonstrated negative AOD changes in all seasons, while MISR also reported negative changes except for JJA. The annual and seasonal (JJA and SON) trends were found to be significantly decreasing which could be due to the stilling of surface winds in North African deserts (Cowie et al., 2013; Ridley et al., 2014).

Bangladesh

The annual and seasonal AOD changes were positive. However, MODIS reported negative AOD changes during JJA season. Significantly increasing trends were found during SON season, which were similar to those over the surrounding Indian region (Kaskaoutis et al., 2011; Mehta, 2015; Pozzer et al., 2015).

Russia

The annual and seasonal (DJF and SON) AOD changes are the instances of disagreements between the two sensors. Significantly decreasing AOD trends were found during DJF, JJA and SON seasons.

Japan

Negative annual and seasonal AOD changes were reported. However, MISR reported positive AOD changes during DJF season. Significantly decreasing annual and seasonal (JJA and SON) trends were reported by both the sensors. These decreasing trends could be associated with the reduction in anthropogenic emissions and were in agreement with the previously reported studies (Cofala et al., 2004; Hsu et al., 2012; Li et al., 2014; Lu et al., 2010; Nurrohim and Sakugawa, 2004; Xia, 2011; Yoon et al., 2012; Zhang and Reid, 2010).

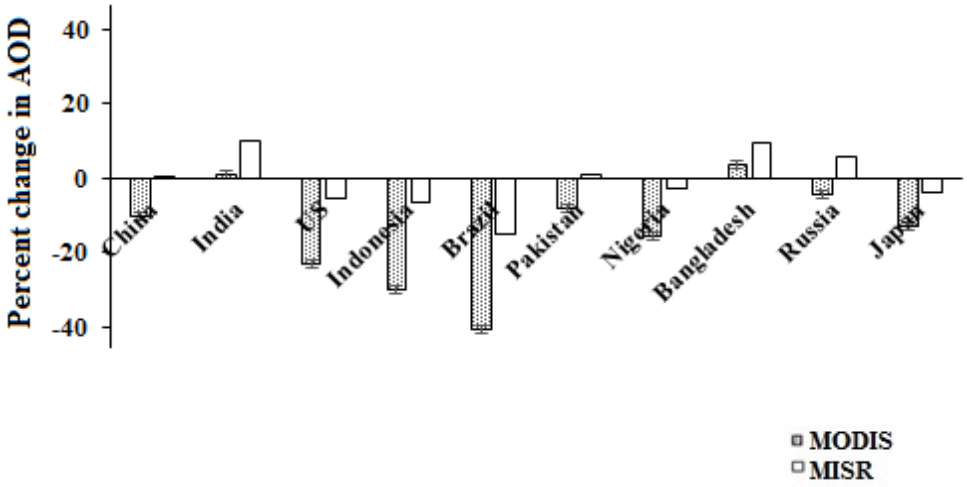

Figure 5.22 Annual relative changes (%) in AOD using MODIS and MISR for ten most populous countries of the world

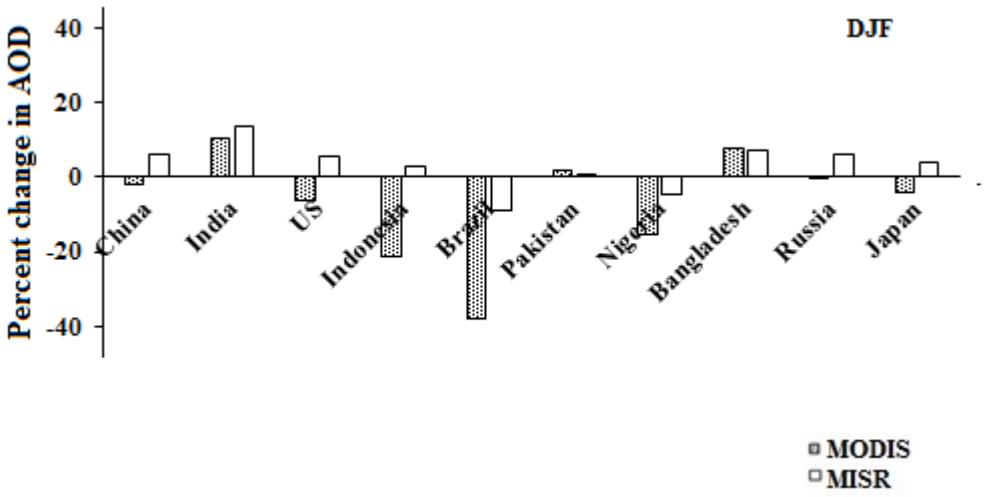

Figure 5.23 Relative changes (%) in AOD during DJF season using MODIS and MISR for ten most populous countries of the world

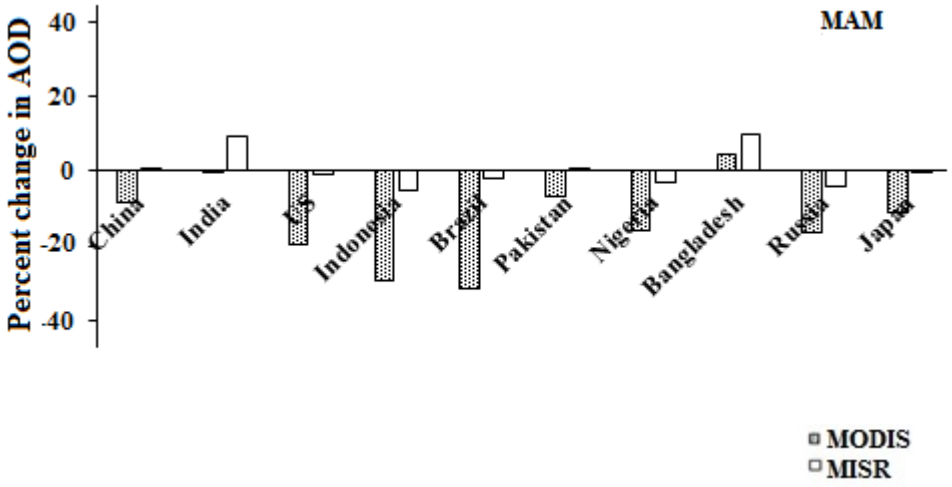

Figure 5.24 Relative changes (%) in AOD during MAM season using MODIS and MISR for ten most populous countries of the world

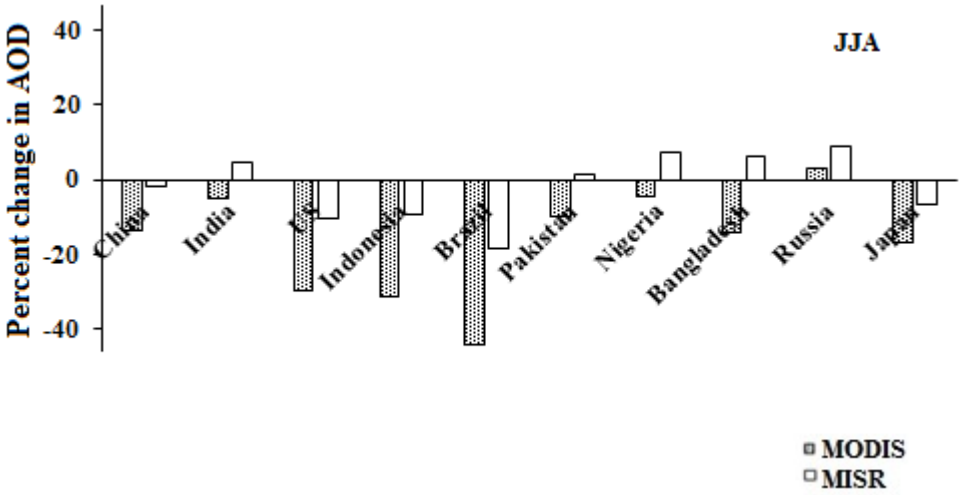

Figure 5.25 Relative changes (%) in AOD during JJA season using MODIS and MISR for ten most populous countries of the world

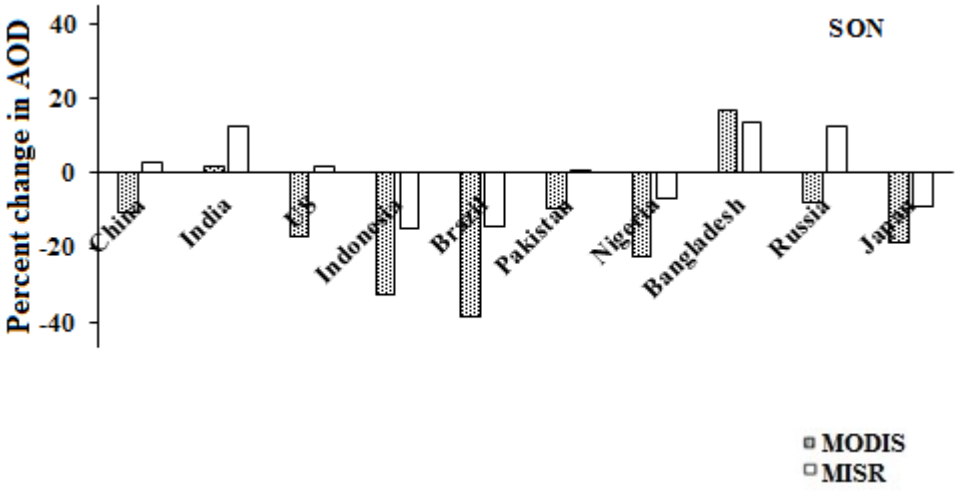

Figure 5.26 Relative changes (%) in AOD during SON season using MODIS and MISR for ten most populous countries of the world

Table 5.1 Annual and seasonal significant trends for ten most populous countries of the world; trends are significant at 95% confidence interval,
'MO': MODIS, 'MI': MISR, '↑'**:** increasing trends, '↓': decreasing trends, '-': no trends,
Colors (black/gray) denote agreement in the results from both the sensors

Countries	Annual		DJF		MAM		JJA		SON	
	MO	MI	MO	MI	MO	MI	MO	MI	MO	MI
China	↓	↓	↓	↑	↓	↑	↓	↓	↓	↓
India	↑	↑	↑	↑	↓	↑	↓	↓	↑	↑
US	↓	↓	↓	↓	↓	↓	↓	↓	↓	↓
Indonesia	↓	↓	↓	↑	↓	↓	↓	↓	↓	↓
Brazil	↓	↓	↓	↓	↓	↑	↓	↓	↓	↓
Pakistan	↓	↑	↑	↑	↓	↑	↓	-	↓	↑
Nigeria	↓	↓	↓	-	↓	↑	↓	↓	↓	↓
Bangladesh	↑	-	-	-	↓	↑	-	↑	↑	↑
Russia	↓	-	↓	↓	↓	↑	↓	↓	↓	↓
Japan	↓	↓	↓	↑	↓	↑	↓	↓	↓	↓

5.2 Aerosol type distribution from an active space borne LIDAR

The distribution of mean AOD due to dust, polluted dust, smoke and total particle loading during the last decade is presented in Figure 5.27. AOD maxima over land (Figure 5.27(a)) were clearly captured over Africa, East China, India, Middle-East and Amazon basin of South America. Similar findings have been reported earlier in Ma et al. (2013) and Winker et al. (2013). Table 5.2 presents the quantitative estimates of decadal mean AOD over different continents. The maximum total columnar AOD was observed over Africa, with competing particle loading over Asia. Over land, the decadal averaged AOD was estimated to be 0.13 compared to that over ocean which was 0.09. Further, the major dust regions

including the Saharan belt were clearly evident over the dust source regions in Africa, Arabia, India and China; similar to what have been reported earlier (Dayan et al., 2008; Dey et al., 2004; Kaufman et al., 2005; Ogunjobi et al., 2003; Rashki et al., 2014; Wang et al., 2008). The transport of dust above the Atlantic waters towards America and also towards the Pacific waters was clearly observed; which was in conformance with the earlier reports (Hunees et al., 2011; Kaufman et al., 2005; Ridley et al., 2014). However, polluted dust, i.e., the dust mixed with smoke from biomass burning (frequently found in regions close to strong sources of both dust and biomass burning) and anthropogenic pollution could be found to be distributed over the whole globe. The polluted dust maxima were observed over India, East China and Arabian Sea. Moderate amounts of polluted dust were also found over Central Africa and South Atlantic Ocean. Smoke, as also reported in earlier findings, was prominently observed over biomass burning regions of Southern Africa, Amazonia, Indonesia; South-East China (mainly due to anthropogenic emissions) and India (Evangelista et al., 2007; de Meij et al., 2010; Kumar et al., 2014; Kaskaoutis et al., 2011; Roberts et al., 2009). Lower AOD values due to smoke were also observed over North America, Europe, Russia, and South Atlantics due to the transported smoke plumes from the hot spot areas and the carbonaceous aerosol emissions from fossil fuel and biofuel combustions.

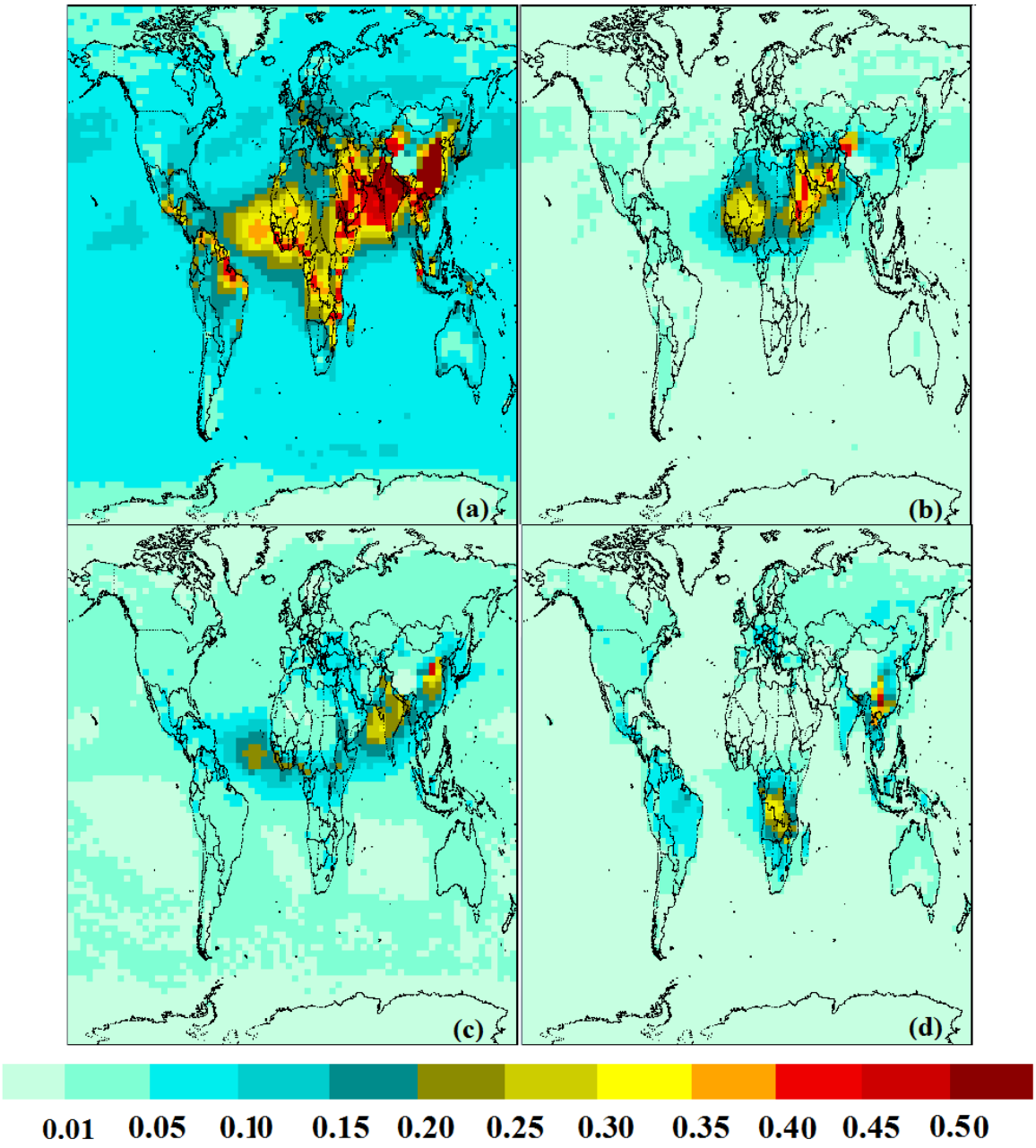

Figure 5.27 Decadal averaged variation of (a) total AOD and AOD due to (b) dust, (c) polluted dust and (d) smoke at a global scale

Table 5.2 Zonal AOD distribution for total AOD and AOD due to dust, polluted dust and smoke

Region	Total AOD	AOD due to Dust	AOD due to Polluted Dust	AOD due to Smoke
North America	0.06	0.02	0.02	0.02
South America	0.16	0.01	0.04	0.06
Europe	0.12	0.01	0.03	0.03
Africa	0.26	0.12	0.06	0.06
Asia	0.20	0.06	0.06	0.04
Australia	0.08	0.01	0.02	0.02
Land	0.13	0.04	0.03	0.03
Ocean	0.09	0.01	0.02	0.004
Global	0.10	0.02	0.03	0.01

5.3 Aerosol vertical distribution across the globe

5.3.1 Distribution of Total particle loading within different altitude bins

If we consider 0-1 km altitude bin, very high MAEC values were observed over India, East China, Middle-East and Arabian Sea (Farahat et al., 2015; Prijith et al., 2016; Tian et al., 2017 and Tiwari et al., 2016) (Figure 5.28). High aerosol signals were found over East coast of Brazil, North Africa; and Atlantic waters between West Africa and America. However, moderate to low MAEC values were observed over the rest of the globe.

Within 1-2 km bin, highest aerosol signals were found over China, whereas high MAEC values were also observed over India, Pakistan, Bangladesh and Middle-East. The aerosol signals remained high over China within 2-3 km bin also, along with values ranging between moderate to high over South Asia, Middle-East, Africa and Brazil. Within 3-4 km bin, moderate values of MAEC were noticed over Africa, India, Middle-East and China. In

general, the aerosols over the oceanic regions were found to be vertically well confined and mixed within 2 km a.m.s.l..

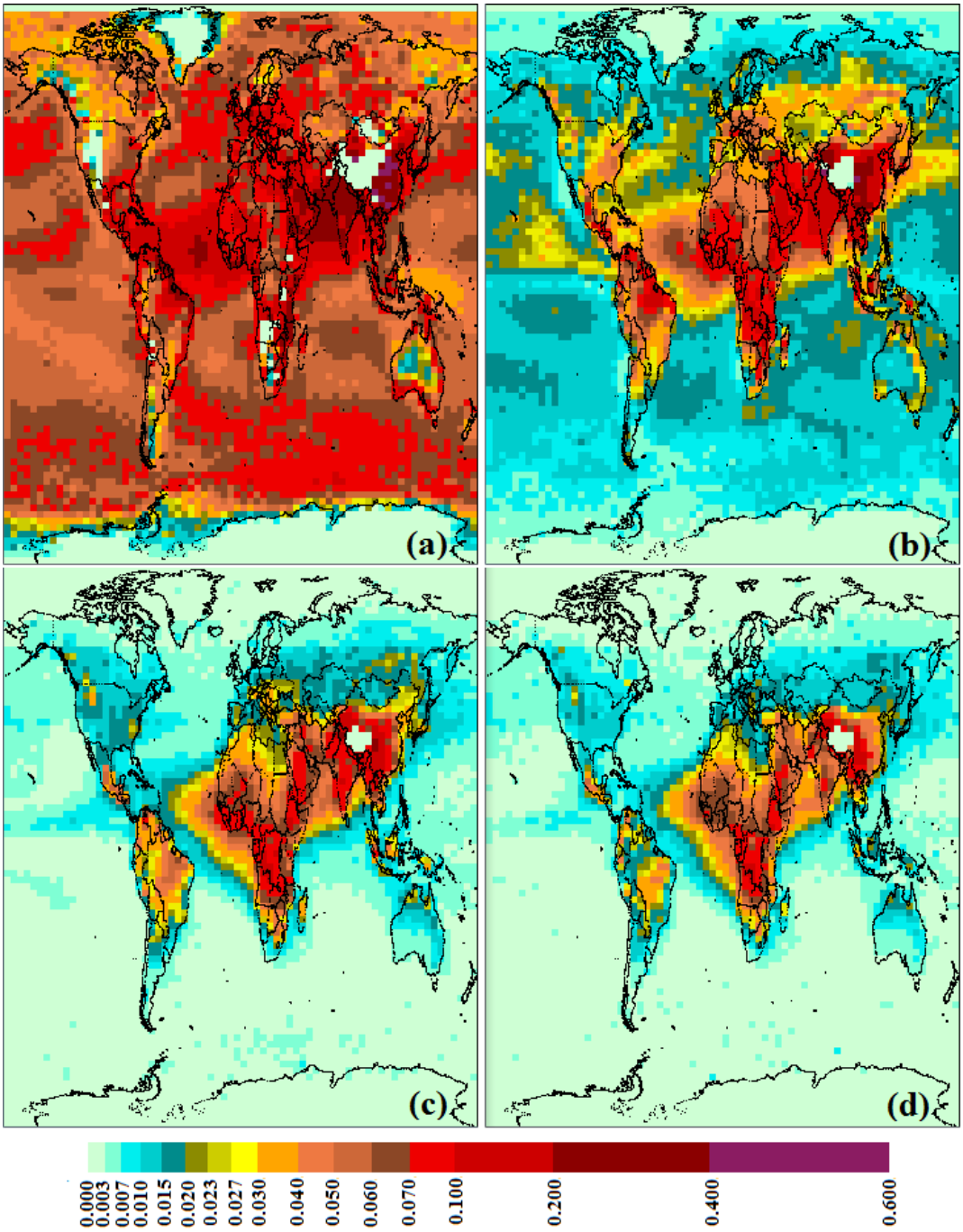

Figure 5.28 Global distribution of MAEC (km^{-1}) for total particle loading within (a) 0-1 km (b) 1-2 km (c) 2-3 km (d) 3-4 km a.m.s.l. during the last decade

5.3.2 Distribution of Dust, Polluted Dust and Smoke within different altitude bins

High values of MAEC due to dust particles were observed over the global dust belt (Figure 5.29). Over the regions where the dust could have been transported from the sources, the aerosol signals gradually decreased in magnitude with increase in altitude. Low values close to the ground were also found over deserts of Australia, North America and South America; which were hardly noticeable at higher altitudes.

In general, the concentration of polluted dust decreased gradually from lower to higher altitudes. These particles were found to be widely spread across the globe with maximum concentrations over India, East China, Arabian Sea; and Atlantic waters between Africa and America, with high MAEC within 0-1 km altitude range. While the MAEC values decreased from moderate to low above 1 km over other regions with high concentration of polluted dust, these remained very high particularly over India and China till 2 km which might have notable climatic implications (Dipu et al., 2013; Ocko et al., 2012; Sarangi et al., 2016; Xu et al., 2017). On comparing the distribution of polluted dust particles across the corresponding Northern and Southern Latitudes, it was seen that the polluted dust particles were comparatively more concentrated in the Northern hemisphere, especially in the 0-3 km altitude range. Similar contrasting differences of the MAEC due to polluted dust particles in the mid-latitude Atlantics between the Northern and Southern hemisphere (Figure 5.30) were also reported earlier by Kanitz et al. (2013).

High MAEC values due to smoke particles were observed over the biomass burning regions of Africa which maximize in 1-2 km a.m.s.l. altitude range (Figure 5.31). However, the signals remained high up to 4 km a.m.s.l. (Das et al., 2017). Similar findings were observed over South-East China where carbonaceous emissions were the major contributors to smoke (Kang et al., 2016; Kumar et al., 2017; Luo et al., 2013 and Tan et al., 2015). Moderate to high signals of smoke were found over Amazonia, India and Indonesia with maxima within 1-2 km bin (Baars et al., 2012; Corrigan et al., 2008; Kaskaoutis et al., 2014; Marenco et al., 2016; Mishra and Shibata, 2012 and Tosca et al., 2011). However, over Russia and Western North America, the MAEC values gradually decreased from 0 to 4 km range of altitudes unlike other places, where maximum signals were observed not just above the ground, but within the next higher altitude bin i.e. 1-2 km a.m.s.l..

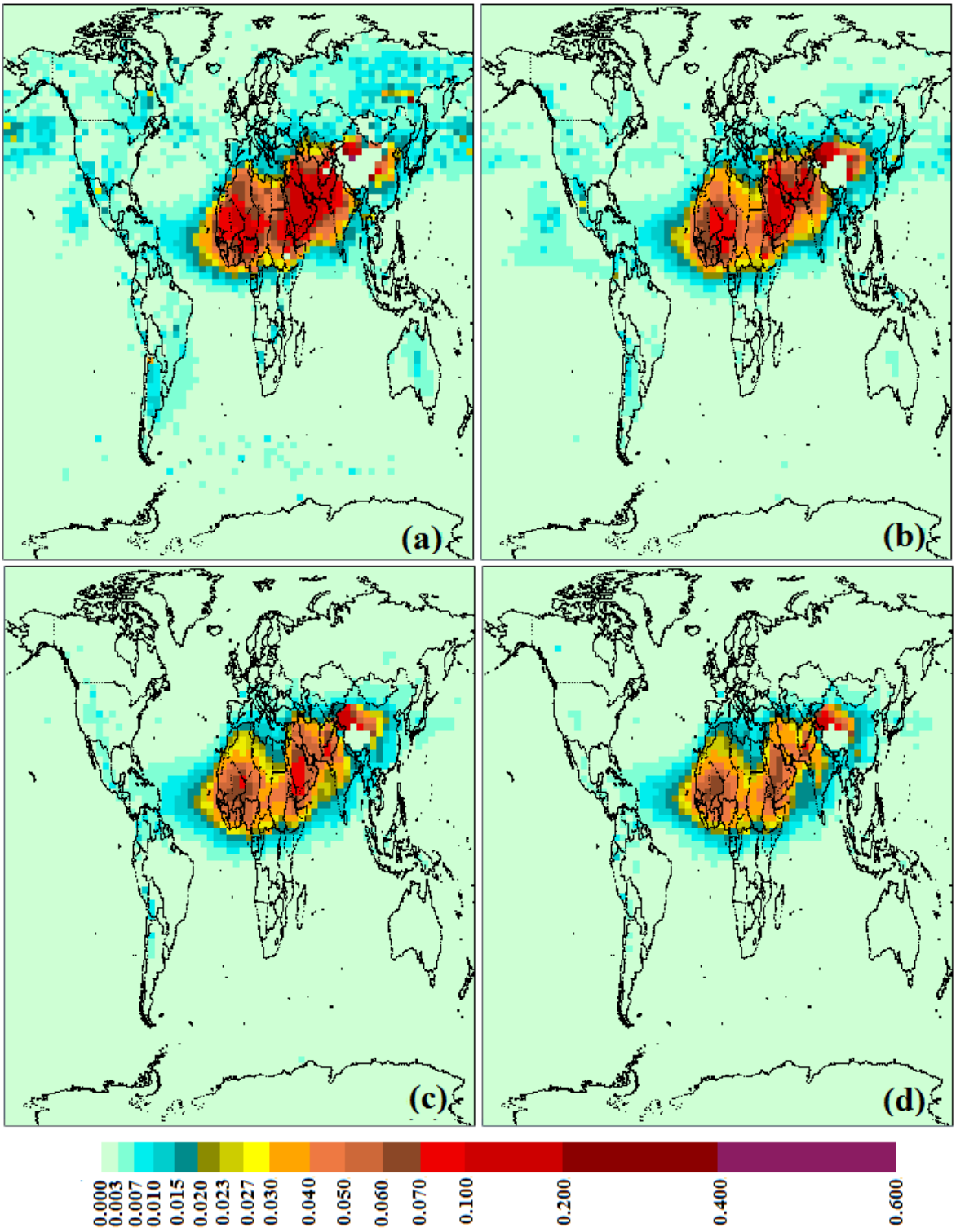

Figure 5.29 Global distribution of MAEC (km^{-1}) for dust within (a) 0-1 km (b) 1-2 km (c) 2-3 km (d) 3-4 km a.m.s.l. during the last decade

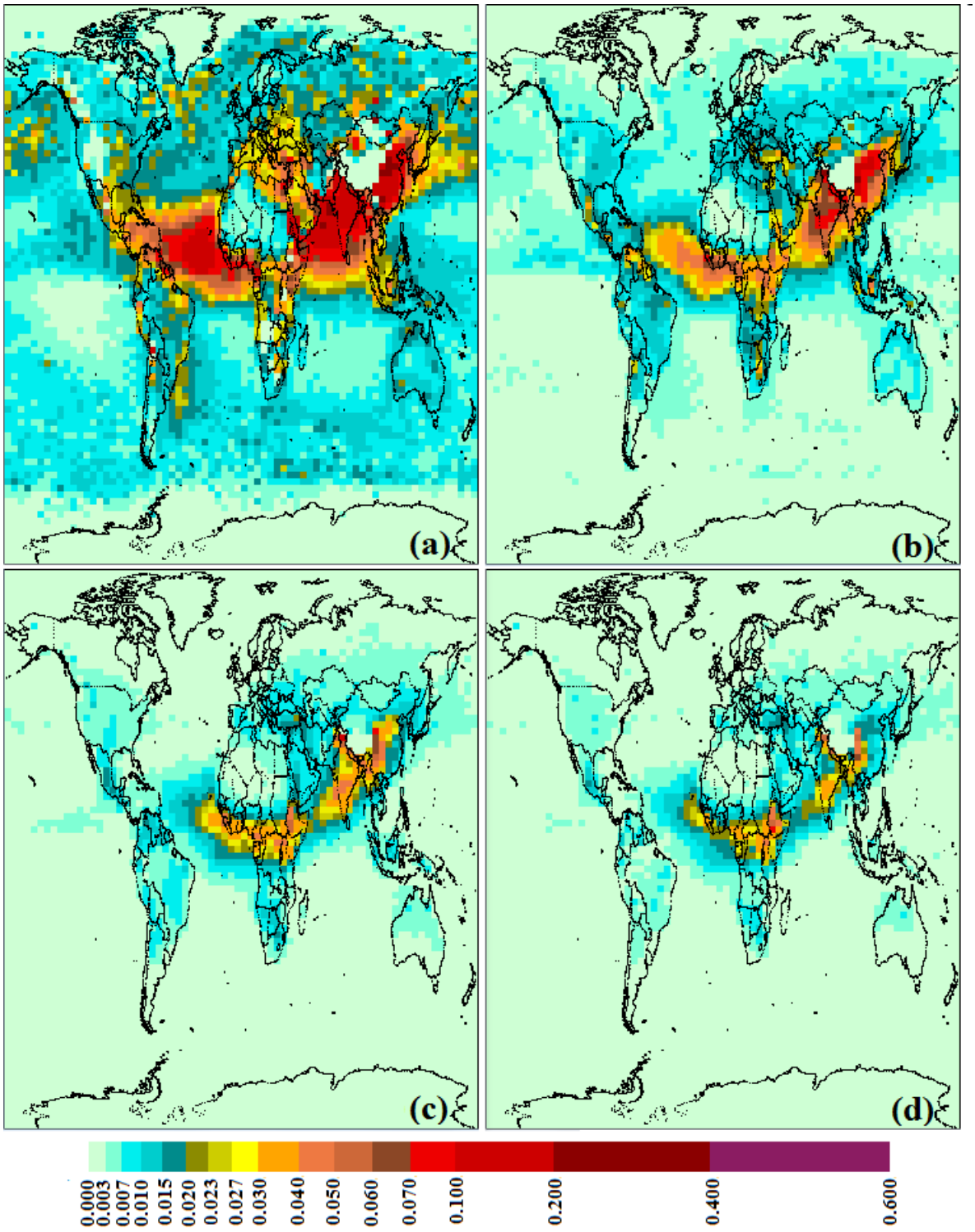

Figure 5.30 Global distribution of MAEC (km^{-1}) for polluted dust within (a) 0-1 km (b) 1-2 km (c) 2-3 km (d) 3-4 km a.m.s.l. during the last decade0

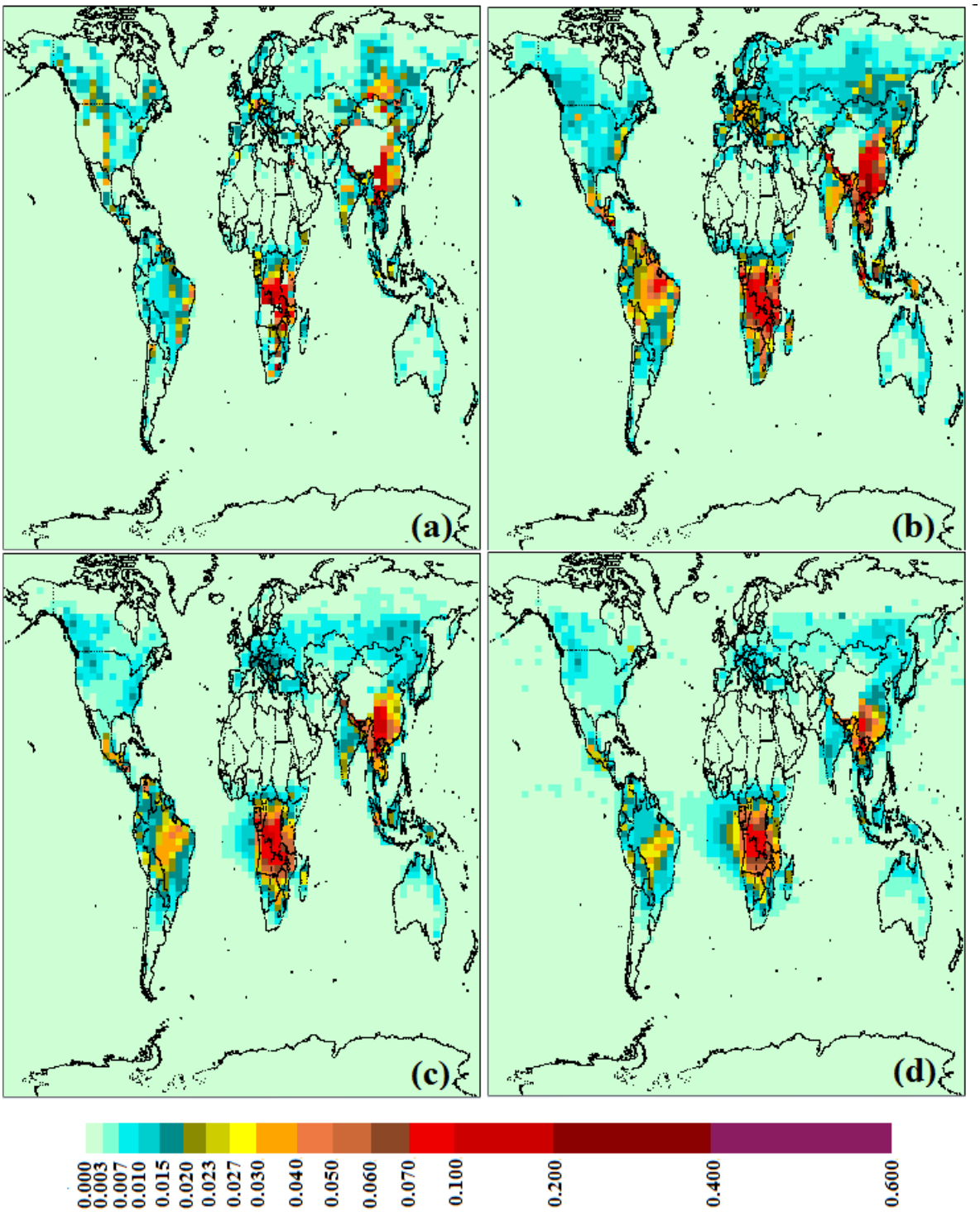

Figure 5.31 Global distribution of MAEC (km^{-1}) for smoke within (a) 0-1 km (b) 1-2 km (c) 2-3 km (d) 3-4 km a.m.s.l. during the last decade

Figure 5.32 presents the vertical distribution of MAEC for each of the six zones (mentioned in Section 3.3) under consideration for the last ten years. It is evident from the Figure that over the dust dominant regions (Figure 5.33); there was a strong vertical mixing of the dust particles at higher altitude regimes, with maxima near the ground and a gradual decrease in particle loading with increase of height. Over INZ and ECZ (Figure 5.34), where polluted dust concentrations were found to be high, maximum particle concentrations were confined at lower altitude regimes. Over the smoke dominated regions (Figure 5.35), it was observed that the smoke particles were concentrated somewhat higher above the ground levels exhibiting strong vertical mixing.

With the above discussion, it is important to mention here, that Figure 5.33-5.35 should be interpreted with caution as these provide information on decadal averaged extinction signals due to aerosols. The actual aerosol vertical distribution might vary seasonally from one location to the other. The specific aerosol events which could be short lived might not also be captured by these images.

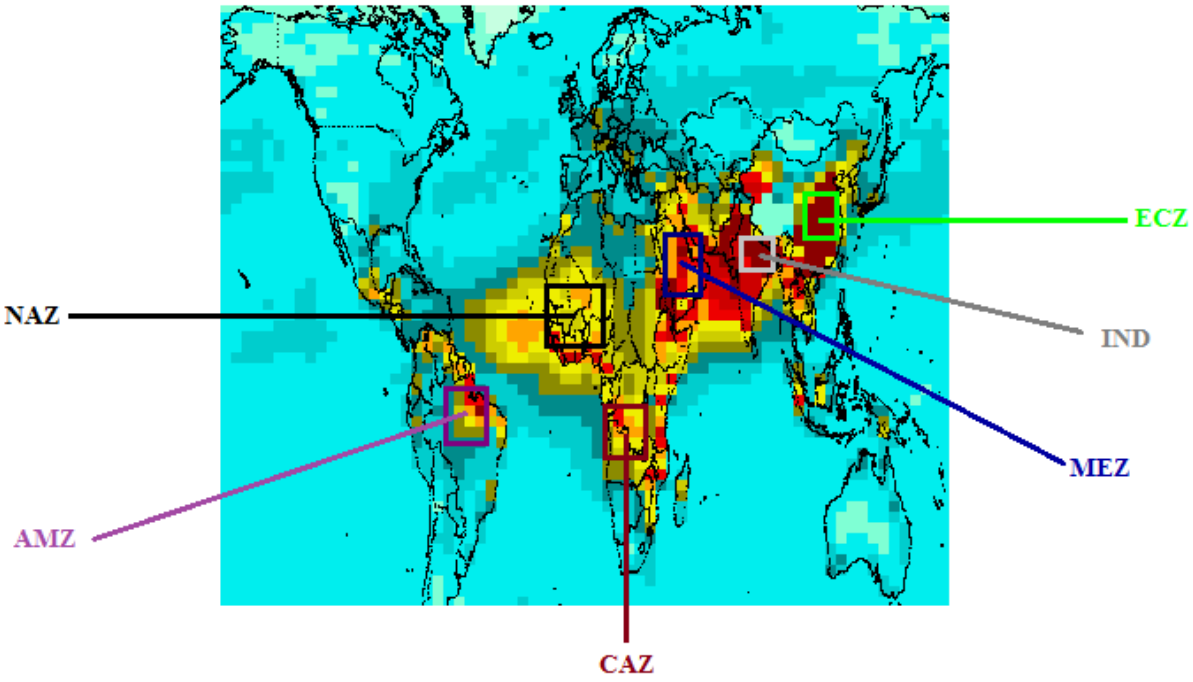

Figure 5.32 Different zones depicted over total AOD distribution taken from Figure 5.27(a)

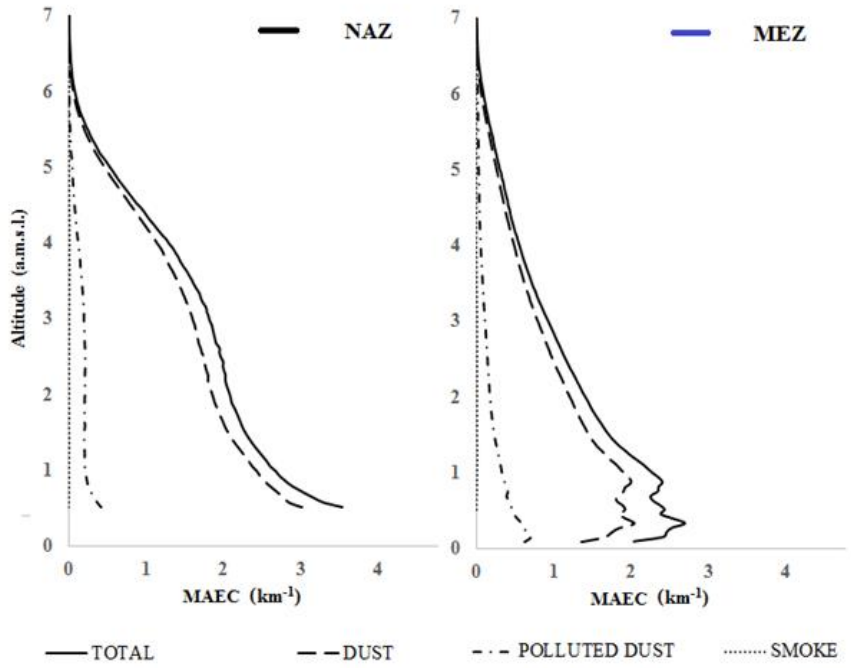

Figure 5.33 Decadal averaged MAEC (km^{-1}) for total particle loading, dust, polluted dust and smoke for dust dominated zones

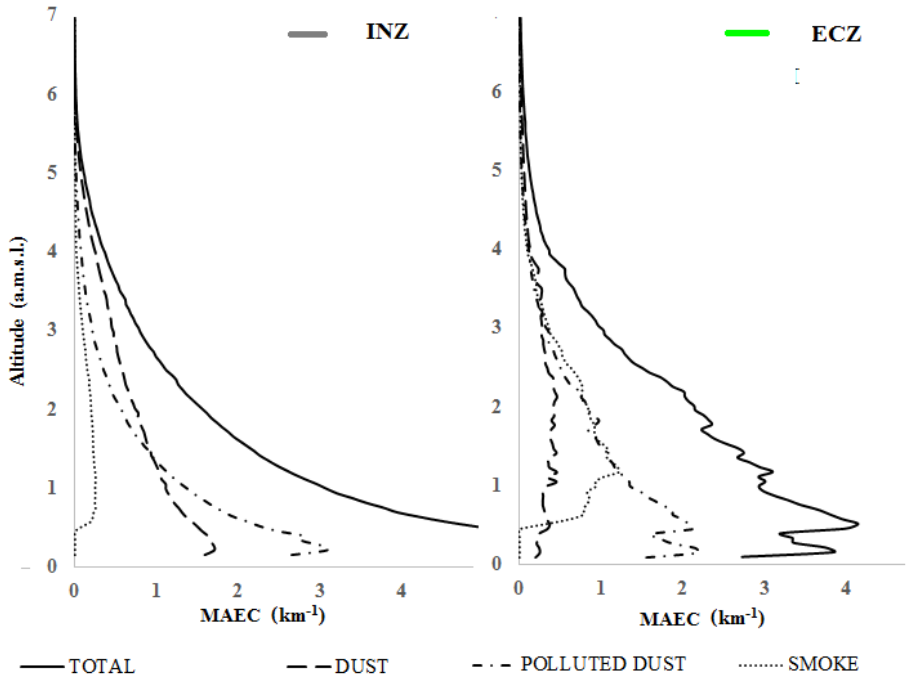

Figure 5.34 Decadal averaged MAEC (km^{-1}) for total particle loading, dust, polluted dust and smoke for polluted dust dominated zones

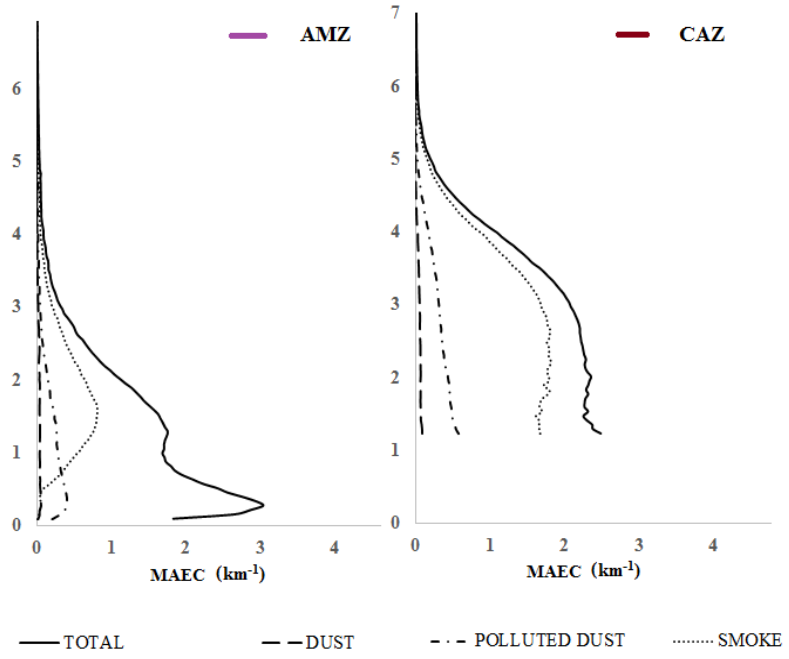

Figure 5.35 Decadal averaged MAEC (km^{-1}) for total particle loading, dust, polluted dust and smoke for smoke dominated zones

5.3.3 Latitudinal and longitudinal aerosol distribution across the globe

Latitudinal variation

The latitudinal variation of AOD and vertical distribution of aerosol extinction profiles for (a) total particle loading, (b) dust, (c) polluted dust and (d) smoke, across the globe is illustrated in Figure 5.36. It can be noted that on an average, it is impractical to find noticeable aerosol concentration in the atmosphere above 6 km a.m.s.l. It is observed that most of the total aerosol load was concentrated between 0-40º N latitudes and the highest MAEC values were found below 2 km a.m.s.l. Elevated aerosol layers with MAEC values ranging between 0.02-0.05 km^{-1} were observed between 2-4 km a.m.s.l. in this latitudinal range. Signatures of aerosols were also evident below 1 km between 40-60º S corresponding to maritime aerosols in Southern oceanic regions, and the aerosols were well mixed and confined within 2 km a.m.s.l. Similar findings were reported by Winker et al. (2013).

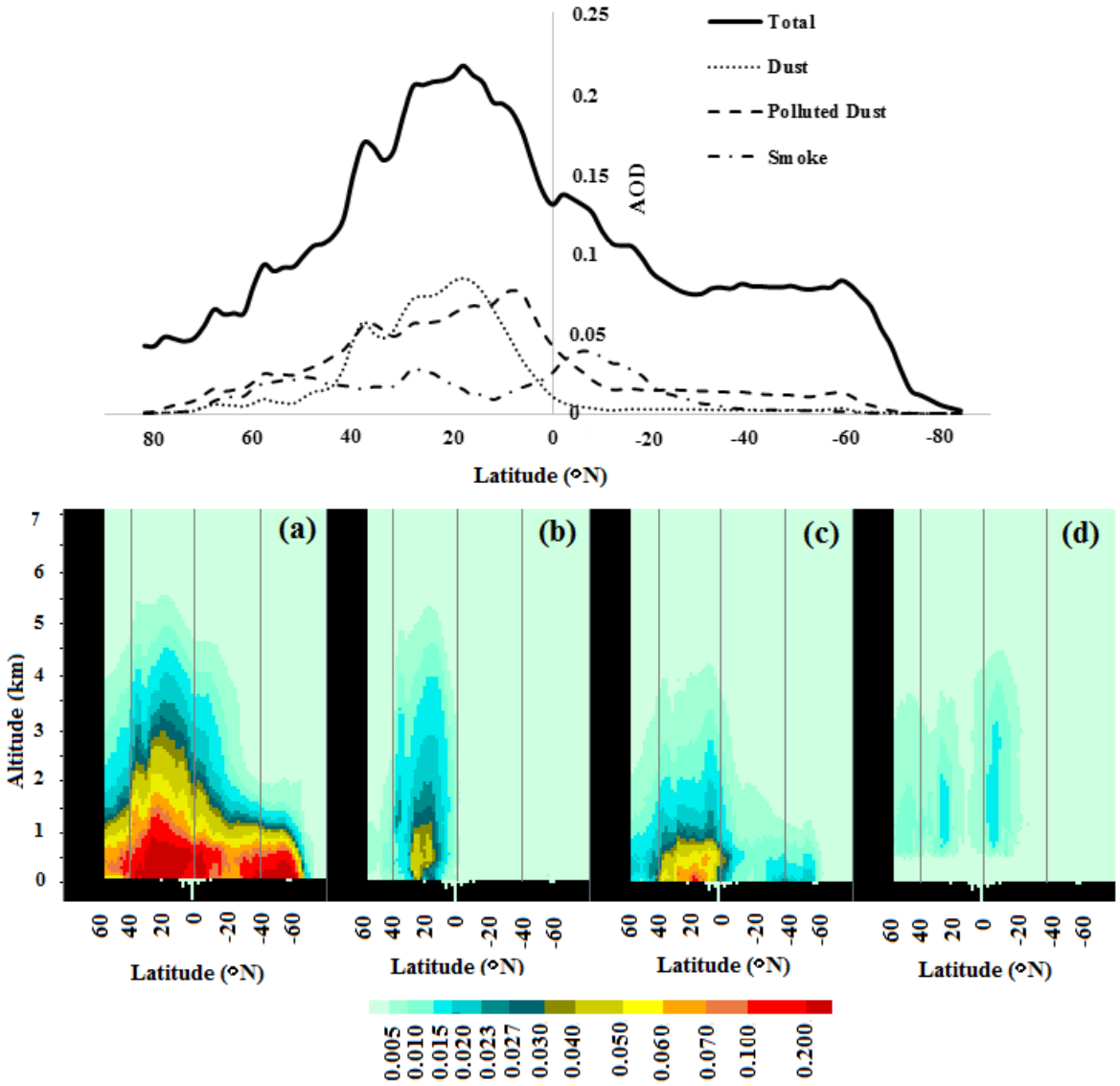

Figure 5.36 Latitudinal variation of mean AOD (Top); and mean MAEC (Bottom) (in km^{-1}) for (a) total particle loading, (b) dust, (c) polluted dust and (d) smoke, across the globe over the last decade

Dust was found to be mostly concentrated within 10-30º N latitudes (Sahara-Middle East-Asia dust belt) with strong vertical transport. Polluted dust, on the other hand, was found to be spread across 0-60º N (and 30-60º S), with higher concentrations close to the ground. It is interesting to note that stronger extinction signals were observed for polluted dust as

compared to dust. Also, the polluted dust particles were found to be well mixed and more confined to lower altitude range when compared with dust particles. The concentration of smoke across the latitudes was found to be lesser as compared to dust and polluted dust, with maxima within 1-10º S (biomass burning in Central Africa and Brazil) and 20-30º N (anthropogenic emission from India, East China) latitudes. Weak averaged signals of smoke from boreal wildfires were also recorded within 40-60º N. It is further interesting to note that the MAEC values for dust and polluted dust were maximum near the surface and gradually decrease with increase in altitudes but, this was partially true for smoke, the maximum signals for which were found not just near the surface but well above that. This ccould be further studied in conjugation with the injection heights of the smoke plumes into the atmosphere as discussed in works by Kahn et al. (2008); Remy et al. (2017) and references therein; but is beyond the scope of the present study.

Longitudinal variation

The longitudinal variation of columnar dust, polluted dust, smoke along with total AOD and the corresponding vertical extinction profiles are depicted in Figure 5.37. The total aerosol load was found to be spread across the globe with strong maxima (≥ 0.10 km^{-1}) within 30-90º E and 10-60º W. Overall, MAEC values ≥ 0.05 km^{-1} were recorded below 1 km a.m.s.l. for all the longitudes. However, between 0-120º E, high extinction returns were also observed within 1-2 km altitude range depending upon the location. MAEC values between 0.02-0.05 km^{-1} were observed within 1-2 km a.m.s.l. for latitudes ranging between 90-180º W and 150-180º E. Between 0-120º E, the strong vertical transport of aerosols was observed with particles reaching as high as 4 km a.m.s.l. Dust particles were mainly observed between 20º W- 90º E latitudes and were confined spatially with larger vertical mixing. Similarly, smoke particles were also confined to narrow longitudinal regimes, between 20-40º E and 100-120º E (regions with biomass burning activities). Signatures of smoke were also observed from the western hemisphere corresponding to the deforestation activities in Amazonia. Polluted dust, on the other hand, was more spatially distributed compared to dust and smoke, especially, over 60-70º E and 110-120º E. Compared to dust and smoke, polluted dust layers were confined to lower altitude domains, mostly below 2 km a.m.s.l. However,

smaller extinction signals were also observed in 3-4 km altitude range depending on the location. In this context, a previous study by Yu et al. (2010) had also shown that the dust and smoke layers were found at higher scale heights near their source regions compared to industrial pollution.

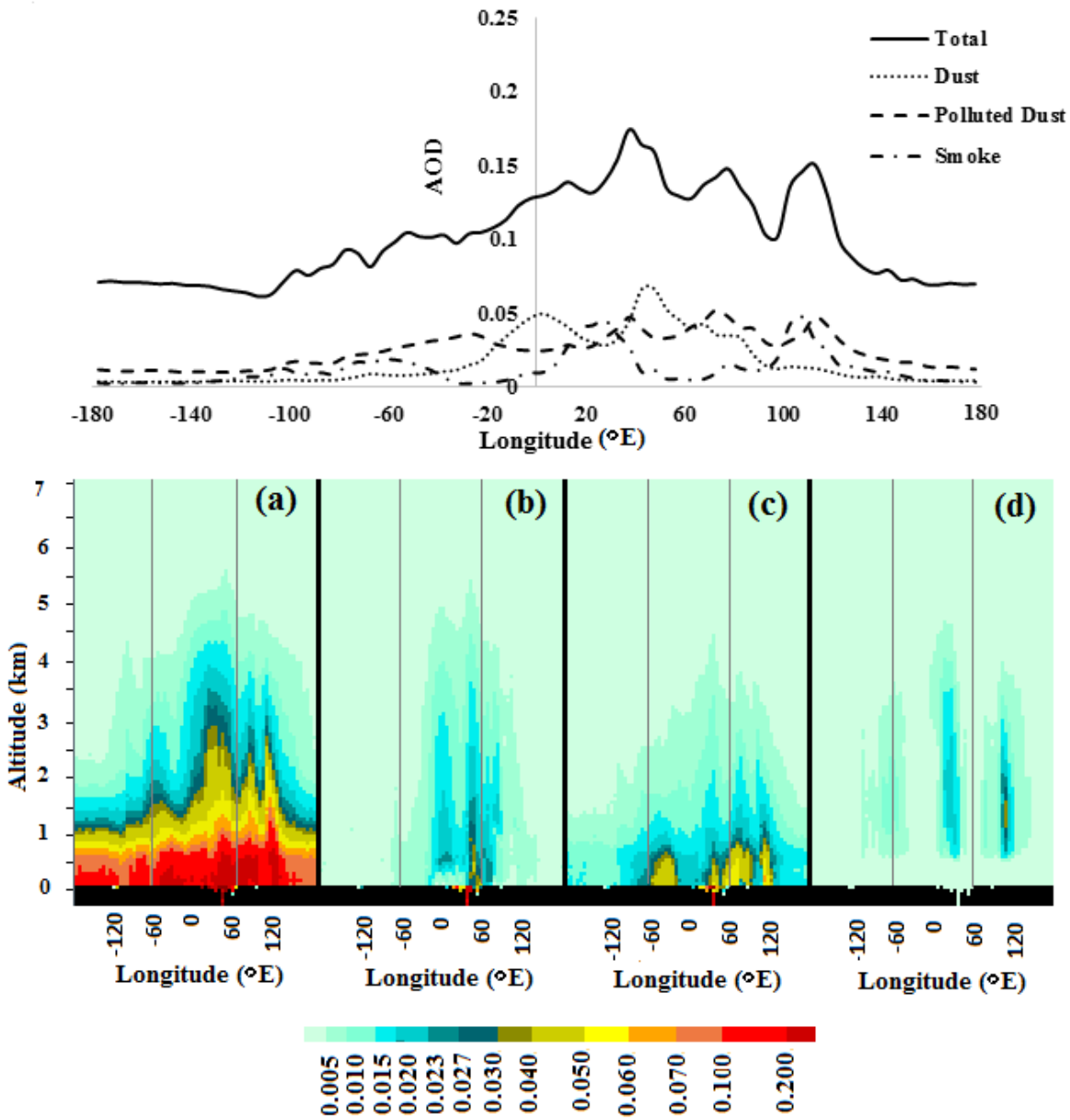

Figure 5.37 Longitudinal variation of mean AOD (Top); and MAEC (Bottom) (in km^{-1}) for (a) total particle loading, (b) dust, (c) polluted dust and (d) smoke, across the globe over the last decade

5.3.4 Trends of AOD and Extinction coefficients at continental scale

Figure 5.38 shows the linear trends for dust, polluted dust, smoke and total AOD. Globally, a decrease in columnar AOD was observed during the past decade with decrease in dust and polluted dust particle loading; and increase in smoke emissions (Table 5.3). Further, with an aim to observe the changes in the aerosol distribution at different vertical levels of the atmosphere in the last decade, aerosol extinction trends were computed within four altitude bins (0-1 km, 1-2 km, 2-3 km and 3-4 km a.m.s.l.) and illustrated in Figures 5.39-5.5.42. It should be noted that increasing (or decreasing) extinction trends in an altitude bin may not necessarily mean increasing (or decreasing) particle loading over that location. Rather, these are indicative of increase (or decrease) in aerosol concentrations within a particular altitude range of atmosphere. Continental level trends are discussed in detail hereinafter.

North America

Trend analysis showed that the total particle loading decreased over North America during the past decade, in particular, over the United States (US). These findings were in agreement with those by Li et al. (2014); Mehta et al. (2016); Pozzer et al. (2015) and Yoon et al. (2014) who examined the AOD trends via various satellite sensors. The decrease in total aerosol load could be attributed to the decrease in anthropogenic emissions owing to the implementation of Clean Air Act Amendments of 1990 over the last ten years (de Gouw et al., 2014; Granier et al., 2011; Xing et al., 2013). Over the Eastern US, statistically significant decreasing extinction trends were recorded for total particle load and smoke in all the four altitude bins (Figure 5.39). However, of particular interest could be the increasing trends in AOD due to dust over North America, particularly over the Central US which were also in accordance with the latest findings by Zhang et al. (2017) using OMI datasets. This was also supported by the extinction trends due to dust over Central US which were found to be positive within 0-1 km altitude bin. An increase in AOD due to smoke over the Western US could be linked with the wildfires which have increased in the last few years (Abatzoglou and Williams, 2016; Dennison et al., 2014; Westerling. 2016; Williams and

Abatzoglou, 2016). Positive extinction trends due to smoke particles within 1-4 km a.ms.l. were also worth notable in this context.

South America

Statistically significant decreasing trends for AOD due to dust, smoke, polluted dust were found over South America. Further, statistically significant decreasing trends for aerosol extinction were found for total particle load within 0-3 km a.m.s.l. The decreasing trends in AOD due to dust over North-Eastern parts of South America could be related to the decreasing concentrations of Saharan dust over Amazon basin transported from Africa in the past decade (Evan et al., 2016). However, the negative AOD trends due to dust over Argentina and Chile could be related with the dust activities in the Atacama, which needs further investigation. However, not much significant extinction trends for dust were observed over South America. Decreasing AOD trends due to polluted dust were also observed together with the negative extinction trends, especially in the 0-1 km altitude range. Similarly, decreasing AOD and extinction trends were also found for smoke over Central parts of South America, especially within 1-4 km a.m.s.l. These negative trends for smoke could be manifestations of decrease in the deforestation and biomass burning activities for agriculture, since 2004 and were in conformance with a recent study by Reddington et al. (2015) as mentioned earlier in Section 5.1.6. However, increasing trends of AOD due to total particle load and smoke were found for the Eastern Brazil which were also supported by the increasing extinction trends within all the four altitude bins. These increasing trends could be due to the increasing wildfires in the Brazilian Amazon during the last decade (especially during 2015 and 2016). In this connection, it is worth to mention the recent study carried out by Silva et al. (2016), using Regional Climate Model, which reported systematic increased fire danger in Brazil throughout the 21st century.

Europe

Over Europe, statistically significant negative AOD trends were observed for polluted dust, smoke and total particle loading. These were augmented by the significant decreasing trends for extinction due to total particle load, polluted dust and smoke, especially up to 2 km

a.m.s.l. However, no significant extinction trends were observed for dust within the altitude bins under consideration. Negative trends for polluted dust and smoke could be due to the environmental regulations in the European countries over the last decade and were similar to those found in the previous studies (Hsu et al, 2012; Pozzer et al, 2015; Yoon et al., 2014).

Africa

Overall negative trends of AOD due to dust particles were found over Africa (Table 2) during the past decade which could be linked with the stilling of surface winds over North African dust source regions and greening of the Sahel (Evan et al., 2016; Cowie et al., 2013; Olsson, et al., 2005; Ridley et al., 2014; Shao et al., 2013). However, interestingly, increasing AOD trends due to dust were reported over few places of North Africa and the Greater Horn of Africa. In this context, a recent study by Boiyo et al. (2017) (using MODIS and OMI datasets) has also reported that AOD levels have increased over East Africa during 2001-2015. The extinction trends over these locations due to dust were also found to be positive, especially within 1-2 km a.m.s.l. However, the increasing trends of dust in these regions need to be further investigated in conjugation with the rising near-surface temperatures (Camberlin, 2017; Engelbrecht et al., 2015). Further, it can be noted that at continental scale, positive AOD trends were observed over Africa for total particle load, smoke and polluted dust. The results were supported by the study carried out by de Meij et al. (2010), which reported positive AOD trends using AERONET data. Also, important to note here is that the extinction due to total particle load over Africa increased especially within 1-4 km a.m.s.l. (except over Southern Africa). Increasing extinction trends were also found for polluted dust within 0-3 km a.m.s.l. On the other hand, the AOD values due to smoke decreased over South Africa, which could be linked with the implementation of environmental regulations during the last decade. These results were in conformance with a previous study carried out by Kumar et al. (2014) utilizing MODIS datasets; and were also further augmented by the negative extinction trends due to smoke over South Africa, especially, within 1-3 km a.m.s.l. Increasing AOD trends (especially for the polluted dust particles) over the Sahel region of Africa were in agreement with those predicted by Hsu et al. (2012) using SeaWiFS data and could be seen in conjugation with the increased local air

pollution over the growing urban areas of West Africa as illustrated by Knippertz et al. (2015). The increase in particle loading (especially smoke) over the developing countries located in Central Africa could be due to anthropogenic emissions (energy consumption, vehicular and domestic emissions) linked with the increasing urban population (CIESIN, 2005, 2012). Over the biomass burning regions of Africa, positive extinction trends of smoke were observed, especially, within 1-4 km a.m.s.l. To this end, one can also refer to the study by Liousse et al. (2014), which provides a quantification of increasing anthropogenic combustion in African continent from 2005 to 2030.

Asia

Statistically significant increasing AOD trends for total particle loading were observed over Indian region which were in accordance with the previously reported studies and could be seen in conjugation with the increasing anthropogenic activities. (Babu et al. 2013; de Meij et al. 2010; Dey and Girolamo 2010, 2011; Hsu et al. 2012; Kaskaoutis et al. 2011; Lu et al. 2013; Mehta, 2015; Mehta et al., 2016; Pozzer et al. 2015). On the other hand, decreasing trends for AOD due to dust over Indian subcontinent could be due lessening of dust activities in the adjoining desert areas (Kasakaoutis et al., 2011). The findings for columnar AOD trends over India were clearly supported by the increasing extinction trends of polluted dust, smoke and total particle loading (except dust) within all the altitude bins. Statistically significant decreasing trends of AOD and extinction coefficients were observed over densely populated regions of East China which were in conformance with the reductions in anthropogenic emissions and decrease in frequency of dust episodes in China over the last decade (Panicker et al., 2012; Wang et al., 2008). Recently, Dong et al. (2017), have also demonstrated the decreasing vertical distribution of particles above 0.3 km a.m.s.l., over Ghuanzhong Plain (one of the most densely populated regions of China) in contrast to increasing particle loading near the surface. However, positive trends of AOD due to smoke were observed over Mongolia and sparsely populated regions of China i.e. North-West (predominantly an arid region) and North-East (mostly vegetated). In this connection, increasing extinction trends due to smoke were recorded over these places within 0-2 km a.m.s.l. Increased AOD due to smoke and the corresponding positive extinction trends were

observed over Siberia due to enhanced wildfires in the last decade (Chubarova et al., 2011; Jolly et al., 2015; Kozlov et al., 2014; Ponomarev et al., 2016; Shvidenko and Schepaschenko, 2013). In general, increasing trends were reported for total columnar AOD over Southern Russia. It is further of interest to note the increasing trends for AOD due to smoke over Indonesia which could be attributed to the increasing fires specifically in the last few years due to the enhanced temperatures (Fernades et al., 2017; Huijnen et al., 2016; Lestari et al., 2014). Further, extinction coefficients due to polluted dust over Indonesia decreased within 0-1 km bin but increased within 1-4 km a.m.s.l., accompanied by positive trends of extinction coefficients due to smoke (1-4 km a.m.s.l.). The decreasing trends of dust (both columnar and vertically resolved) over the Middle-East in the last ten years should be interpreted carefully when compared with the previous studies by Notaro et al. (2015) and Klingmuller et al. (2016), that report positive trends of dust. This is because of the fact that those studies have computed long term trends which include regime shift period 2007-2013 with high dust activities (2008-12) towards the end of the time series, whereas, our study period starts from the active dust period itself. Further, positive trends of polluted dust (both AOD and extinction values) were observed over the Middle-East. In this connection, increasing anthropogenic emissions in and around Middle-East were previously reported in a study by de Ruyter et al. (2012).

Australia

Statistically significant decreasing trends of AOD due to dust, polluted dust and total particle loading were found over Australia. Decrease in AOD during the past decade was also previously reported by de Meij et al. (2010) and Mehta et al. (2016). Negative extinction trends due to total particle loading over Australia were also found upto 2 km a.m.s.l. Decreasing extinction trends were reported for dust and polluted dust within 0-1 km a.m.s.l. On the other hand, positive trends of AOD due to smoke were found, especially in the North-Western region. As Western Australia is mostly of the arid outback, the increase in smoke, could be attributed to the enhanced bushfires in Australia by 40% in the recent years (Dutta et al., 2016). Also, the increase could be linked with the long range transport of smoke from

the Asian countries including Indonesia, where similar increasing trends of smoke were observed using Sun photometer measurements (Mitchell et al., 2010).

Table 5.3 Zonal AOD trends for total AOD and AOD due to dust, polluted dust and smoke;

+ indicates significantly increasing trend and – indicates significantly decreasing trend

Region	Total column	Dust	Polluted Dust	Smoke
North America	-	+	-	-
South America	-	-	-	-
Europe	-	-	-	-
Africa	+	-	+	+
Asia	+	-	+	+
Australia	-	-	-	+
Land	-	-	-	+
Ocean	-	-	-	+
Global	-	-	-	+

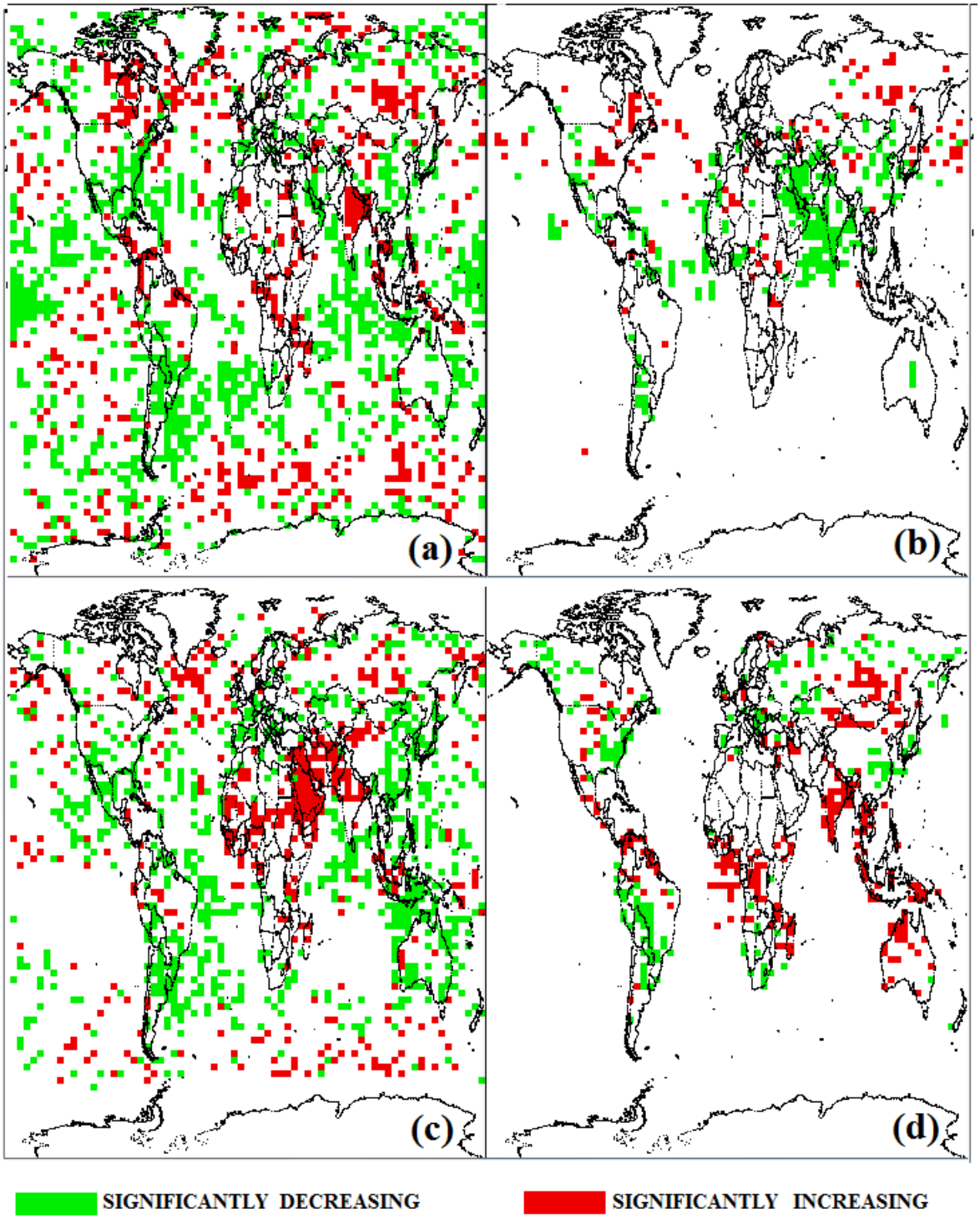

Figure 5.38 Statistically significant (≥ 90% confidence level) trends for (a) total AOD and AOD due to (b) dust, (c) polluted dust and (d) smoke at a global scale over the last decade

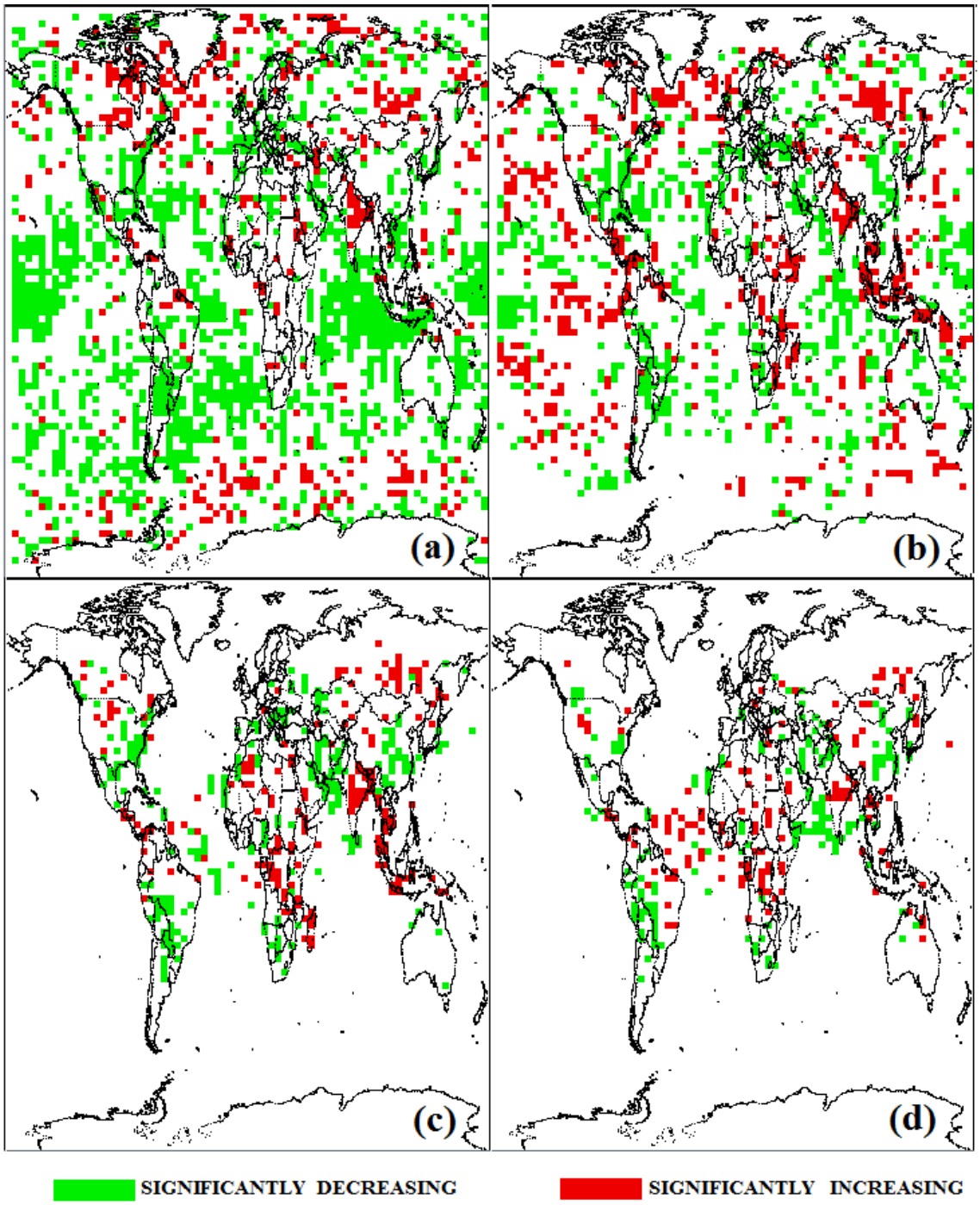

Figure 5.39 Statistically significant aerosol extinction trends (≥90% confidence level) for total particle loading within (a) 0-1 km (b) 1-2 km (c) 2-3 km (d) 3-4 km

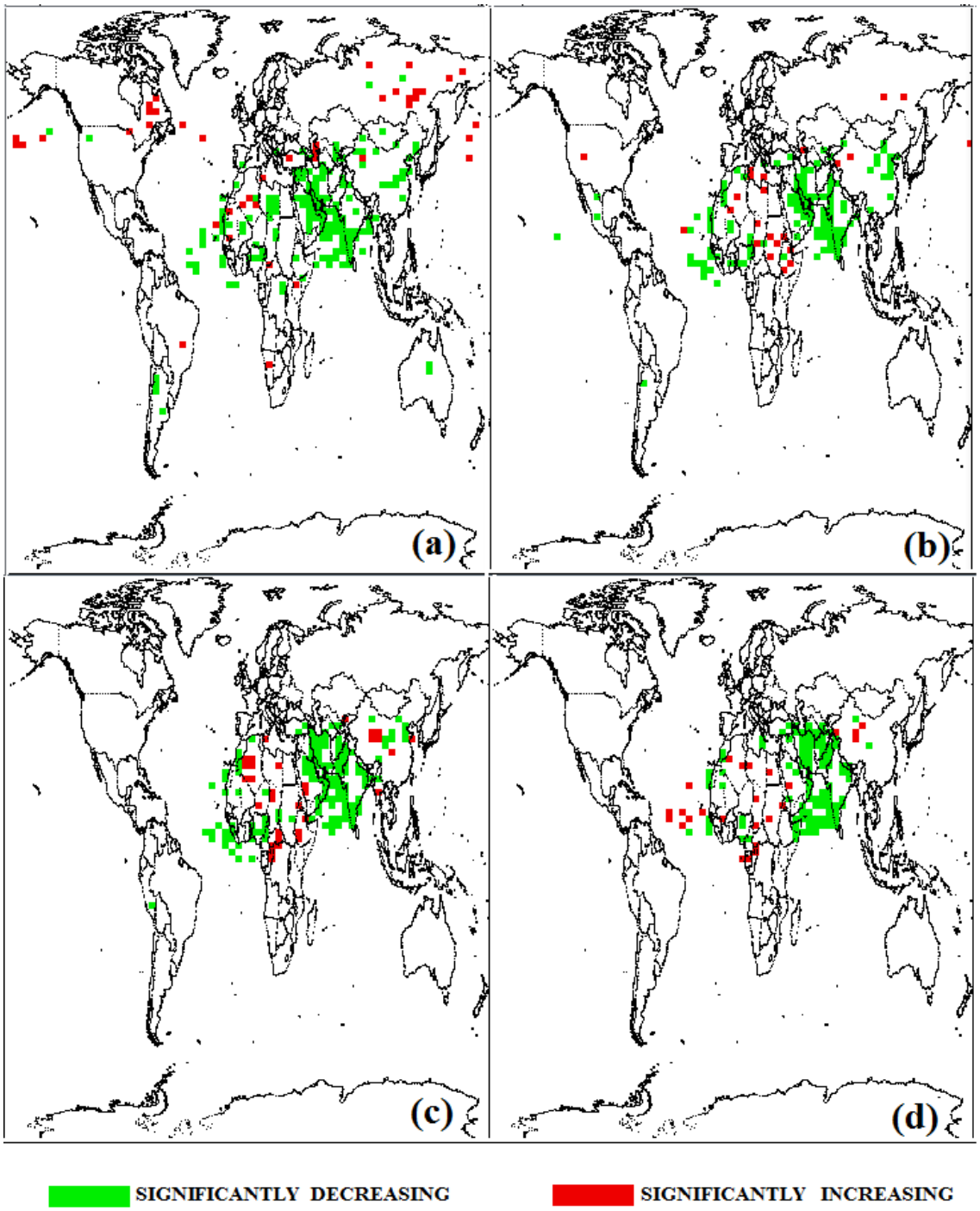

Figure 5.40 Statistically significant aerosol extinction trends (≥90% confidence level) for dust within (a) 0-1 km (b) 1-2 km (c) 2-3 km (d) 3-4 km

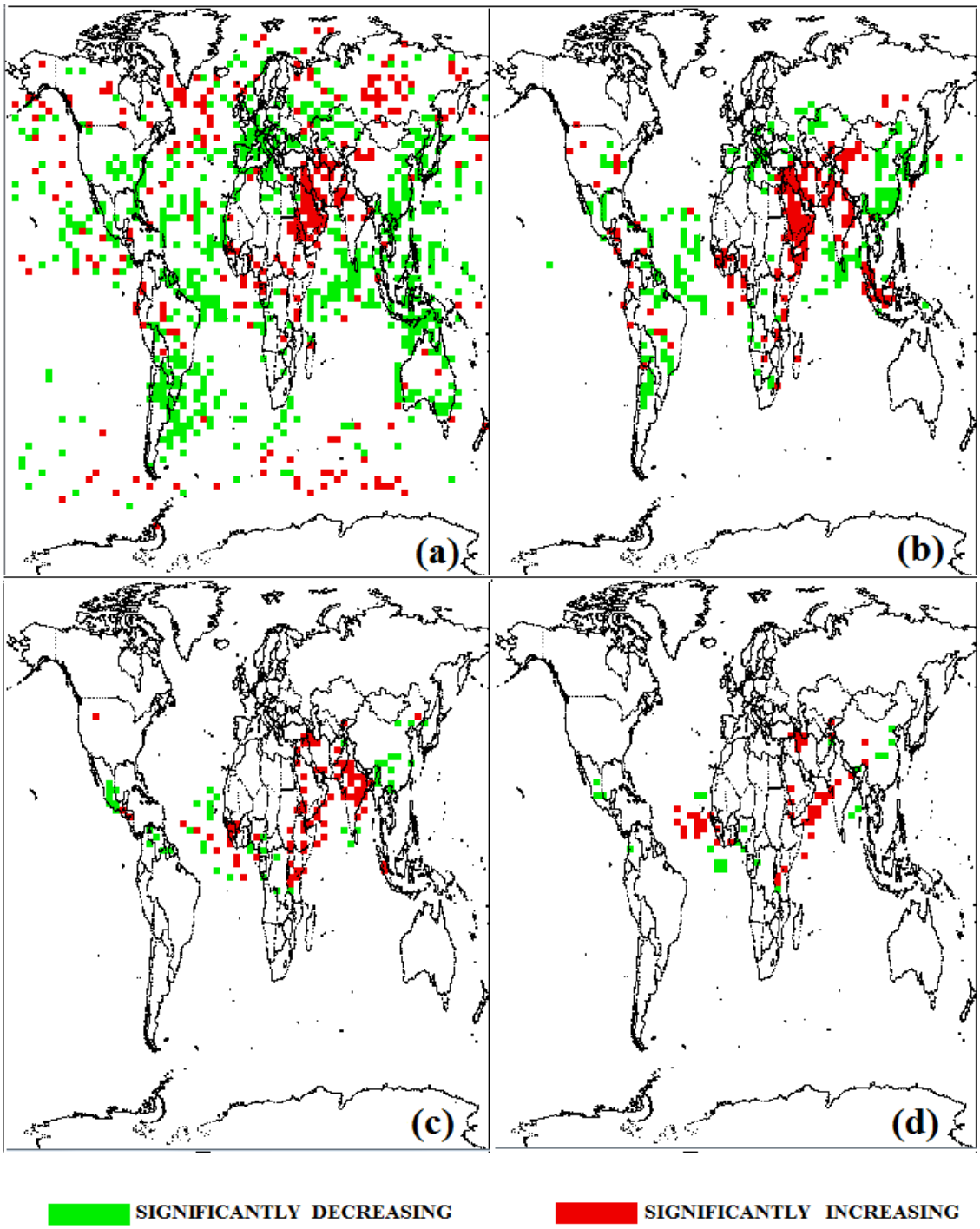

Figure 5.41 Statistically significant aerosol extinction trends (≥90% confidence level) for polluted dust within (a) 0-1 km (b) 1-2 km (c) 2-3 km (d) 3-4 km

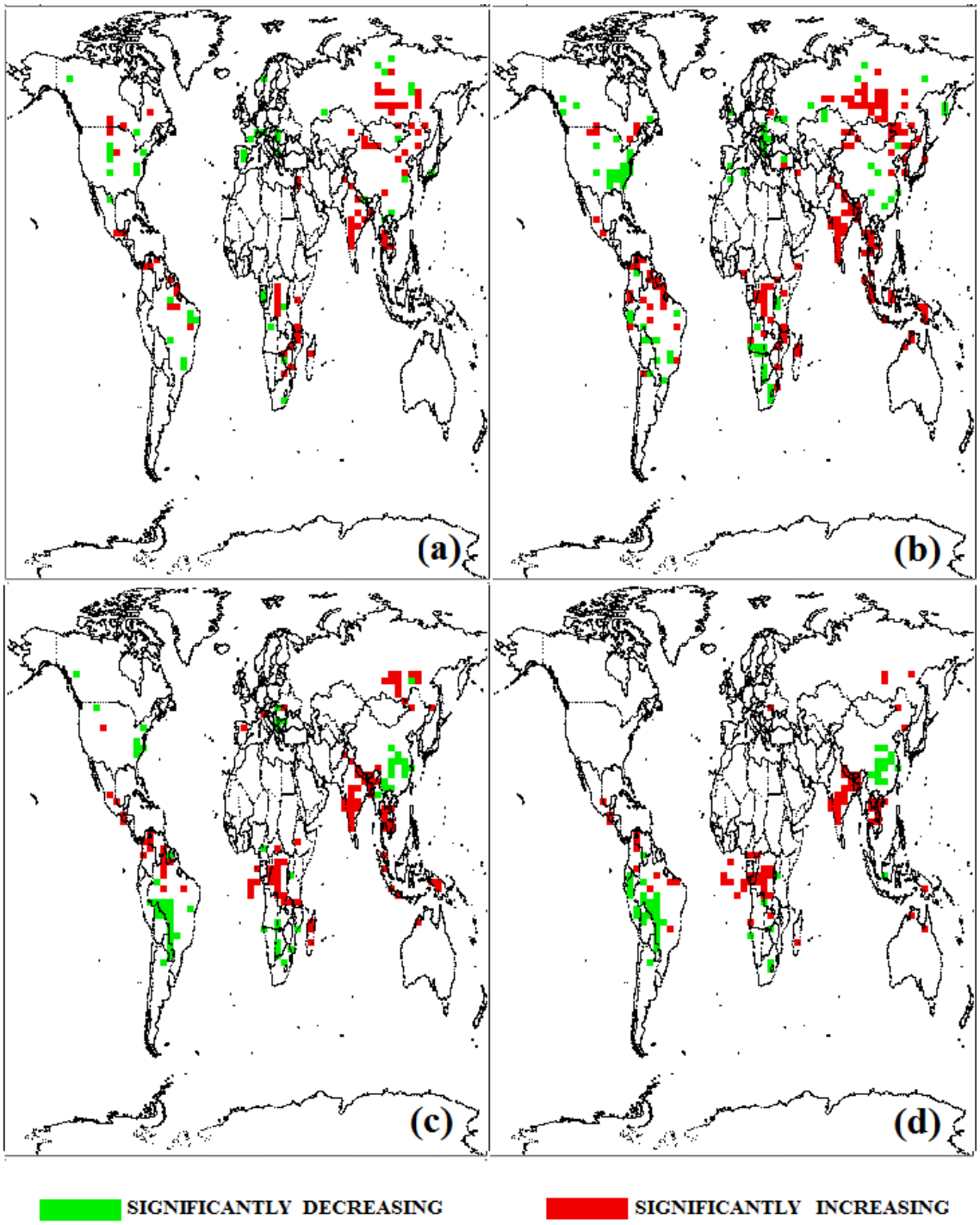

Figure 5.42 Statistically significant aerosol extinction trends (≥90% confidence level) for smoke within (a) 0-1 km (b) 1-2 km (c) 2-3 km (d) 3-4 km

Chapter 6

SUMMRY AND CONCLUSIONS

CHAPTER 6

SUMMARY AND CONCLUSIONS

This Chapter summarizes the major findings obtained from the research. First, the major results from AOD distribution and trends over the entire globe are summarized. Thereafter, the results obtained from the study of vertical distribution of aerosols with special emphasis on major aerosol types have been summed up. Though, there have been continued efforts to observe the trends of aerosols using different ground based and satellite based platforms, however, this is the first ever study that also discusses the aerosol vertical profile trends at a global scale using a space borne instrument. Finally, conclusive remarks are presented followed by the future recommendations.

Aerosol distribution at global and regional scales is one of the crucial parameters for climate change assessment. As aerosols remain one of the largest uncertainties in assessing the atmospheric dynamics and climate change, continued research is required to be carried out to understand how the aerosol properties are evolving over space and time. In order to assess the changing aerosol distribution across the globe, continuous efforts are needed find out the trends from various satellite sensors. This is because the results from one sensor might vary from the other owing to the differences in sensors, specific to their calibration/characterization, sampling (orbital coverage), retrieval algorithms, pixel selection inclusive of the masking/aggregation techniques (Hsu et al., 2013). This study has attempted a comparative study of distribution and trends of total columnar aerosol loading as seen from two different passive satellite sensors. The results are discussed in detail, in light of the previously attempted works at global and regional scales. Later an assessment of changing levels of major types of aerosols, in columnar and vertical levels of atmosphere has been done using data from active space based LIDAR. With an increasing research interest towards the contribution of aerosols to the climate change scenario, this work provides a comprehensive view as how the aerosols have been changing during the last decade, ***not only in the total atmospheric column***

but also within different altitude levels. The information on how the aerosols' vertical structure and spatial distribution have evolved over the last decade can provide vital inputs in the realm of changing pollution levels and atmospheric dynamics.

The thesis presents global spatio-temporal variations in AOD retrieved by MODIS and MISR sensors at spatial resolutions of 1° × 1° and 0.5° × 0.5° respectively. Spatial correlations between MODIS and MISR AOD were reported on annual scale. The entire globe was divided into six sub-regions, i.e., North-West, North, North-East, South-West, South and South-East for illustration. The annual and seasonal mean AOD variations were obtained by analyzing Level 3 monthly datasets for the period 2001–2014. Relative changes (%) in AOD between the first and last seven years (i.e. 2001–2007 and 2008–2014 respectively) were discussed at annual and seasonal levels. AOD trends were calculated using the weighted least squares regression approach and weights were assigned to the AOD values corresponding to the expected errors. Statistically significant trends were reported at 95% confidence level. The results inferred from both the sensors were found to be in quite acceptable agreement. It must be noted that the monthly averaged AOD products are created independently of the data sampling representativeness (Levy et al., 2010; Kahn et al., 2005, 2010; Remer et al., 2005, 2008; Pozzer et al., 2015). There could have been instances, e.g., sub-arctic pixels, when the monthly data could have been created with only a few number of observations due to persistent cloud cover for most of the days of that month. Hence, in such specific cases, the trends could be biased due to insufficient retrievals (Yoon et al., 2014). It is further to be noted that MODIS DT algorithm could not retrieve data over bright surfaces (desert lands and mountainous regions) e.g., Central Australia, Central Asia, Middle East and Sahara, while MISR could do so (Levy et al., 2010; Remer et al., 2005; Shi et al., 2011). Hence, over such areas, comparisons between the findings from the two sensors could not be done. The study also focused on examining the AOD trends over the ten most populous countries of the world.

Further, the columnar and vertical distribution of aerosols across the globe was studied using night time Level 3 Standard All-Sky CALIOP datasets of ten years (September 2006- August 2016). The results were separately reported for dust, polluted dust and smoke. Mean aerosol extinction coefficients were also reported for four altitude bins i.e. 0-1 km, 1-2 km, 2-3 km and 3-4 km above mean sea level (a.m.s.l.). A linear regression

analysis was also carried out using the monthly de-seasonalized datasets in order to observe the decadal trends of AOD and vertical aerosol extinction coefficients.

Major findings of the study

Global total AOD distribution

- High AOD values were found over Africa, India, China and the surrounding oceanic regions.
- AOD values were found to be high over North America during MAM and JJA seasons which could be due to natural and anthropogenic sources.
- Though the annual averaged AOD values remain low over Europe but high aerosol loading was found over the Mediterranean Sea. Further, similar to North America, seasonal high was found in MAM and JJA seasons.
- During DJF and SON seasons, aerosol loadings were low over the Russian landmasses.
- South America observed low annual particle loading during the considered period of fourteen years.
- Peculiar high AOD values were recorded over Amazonia due to seasonal deforestation activities especially in SON season.
- Seasonal biomass burning practices in Southern Africa during JJA could have been responsible for high AOD values encountered during the concerned period.
- During DJF, high AOD values were observed over East China and (spatially increasing AOD pattern) over IGP.
- During the monsoonal shift, the spatially increasing pattern of AOD shifts from East to West IGP.
- Low annual AOD values were reported over Australia with enhanced levels during SON and DJF seasons.

Global total AOD trends

- During the last fourteen years, aerosol loading increased over India and the Arabian Peninsula, whereas, it decreased over Europe, North America, South America and the African deserts.

- The decreasing AOD trends over the mineral dust dominated regions could be indicative of modulations by dust activities and their transport.
- The decreasing trends over Europe and America could be manifestations of strict environmental regulations in the last decade.
- Negative AOD trends were found over Russia (though mostly insignificant).
- Increasing AOD trends were reported over India and Pakistan during the winter season.
- Decreasing particle loading over South Africa could be attributed to imposition of the environmental regulatory measures.
- Increasing AOD trends over Middle-East countries were found during the MAM and JJA seasons.
- Increasing AOD trends were found over India and Bangladesh in post-monsoon season. These increasing trends were reported in stable atmospheric conditions (October–February), which could be indicative of increasing anthropogenic activities.
- In most of the other densely populated countries including China, decreasing AOD trends were reported.
- Bangladesh, Pakistan, Nigeria and India were amongst the most heavily polluted countries

Global aerosol type distribution (columnar and vertical)

Global mean AOD was found to be 0.10, with AOD values of 0.13 and 0.09 for land and ocean respectively, during the last decade.

Dust

- Dust was found to be mainly concentrated along the Saharan belt that constitutes the major dust belt region covering parts of Africa, Arabia, India and China.
- The transport of Saharan dust over the Atlantic Ocean towards American region and also towards the Pacific Ocean was quite notable
- There was a gradual decrease in the aerosol extinction signals due to dust with increase in altitude.

Polluted dust

- Polluted Dust was found to be distributed all across the world. However, the polluted dust particles were more concentrated in the Northern hemisphere, (especially in the 0-3 km altitudes).
- The polluted dust maxima were observed over India, East China and Arabian Sea.
- Within 0-1 km altitude range, the dust extinction signals were found to be higher and the concentration of polluted dust decreases gradually from lower to higher altitudes.

Smoke

- Smoke (due to anthropogenic emissions and biomass burning activities) was found to be dominant over Southern Africa, Amazonia, Indonesia, South-East China and India.
- Over North America, Europe, Russia, and South Atlantics, moderately low amounts of smoke were recorded.
- Over the biomass burning regions, high smoke extinction coefficients were recorded with maxima in 1-2 km a.m.s.l. and the signals showed strong vertical mixing.
- Over South-east China, high smoke loadings due to carbonaceous emissions were observed not just close to ground but at a little higher altitude range.
- Over Amazonia, India and Indonesia, moderate to high signals of smoke were found with maxima within 1-2 km bin.

Global trends of major aerosol types (columnar and vertical)

- An overall decreasing global AOD trend was observed for dust and polluted dust.
- Dust levels increased over North America during the last decade.
- Decreasing polluted dust levels were found over America, Europe and East China.
- Globally, smoke emissions were found to be increased.
- The increasing AOD trends of smoke over Central Africa, Western US, Southern Russia, India, Indonesia and Australia were also supported by the increasing extinction trends of smoke at different altitude levels.

- The decreasing trends of polluted dust and smoke over the Eastern US, South America, South Africa and Europe could be indicative of the environmental regulations imposed in these regions and also were in line with previous findings.
- Over Asia and Africa, there was a substantive increase in the polluted dust and smoke levels (both columnar and vertically distributed), mainly attributable to the anthropogenic activities with rising population levels.

RECOMMENDATIONS

The rising levels of smoke emissions during the recent years can be studied further in conjugation with the rising temperatures and increasing wildfires throughout the globe. Absorption and scattering properties of aerosols may also be investigated at a global scale. As the size of aerosol particles may have a significant impact on health and climate, the global distribution and trends of aerosols characterized by different sized particles may also be studied using satellite datasets. Further, a comparative and comprehensive study of the aerosol parameters measured using ground based instruments may also be attempted w.r.t. the columnar and vertical properties of aerosols. Specifically, regional studies of aerosol types and vertical distribution may be attempted over highly undulating terrains like Himalayas. This may be further studied in terms of their impact on radiative forcing, melting of glaciers etc. using long time series datasets from multiple sensors.

REFERENCES AND BIBLIOGRAPHY

REFERENCES AND BIBILIOGRAPHY

Abatzogloua, J.T. and Williams, A.P., 2016. Impact of anthropogenic climate change on wildfire across western US forests. *PNAS*, 113(42), pp.11770–11775, www.pnas.org/cgi/doi/10.1073/pnas.1607171113.

Abshire, J.B., Sun, X., Riris, H., Sirota, J.M., McGarry, J.F., Palm, S., Yi, D. and Liiva, P., 2005. Geoscience Laser Altimeter System (GLAS) on the ICESat Mission: On-orbit measurement Performance. *Geophysical Research Letters*, 32, L21S02, doi: 10.1029/2005GL024028.

Ackerman, A.S., Toon, O.B., Stevens, D.E., Heymsfield, A.J., Ramanathan, V. and Welton, J., 2000. Reduction of tropical cloudiness by soot. *Science*, 288, pp.1042–1047, http://dx.doi.org/10.1126/science.288.5468.1042.

Alam, K., Qureshi, S. and Blaschke, T., 2011. Monitoring spatio-temporal aerosol patterns over Pakistan based on MODIS, TOMS and MISR satellite data and a HYSPLIT model. *Atmospheric Environment*, 45, pp.4641–4651, http://dx.doi.org/10.1016/j.atmosenv. 2011.05.055.

Andres, R.J., Marland, G., Fung, I. and Matthews, E., 1996. A 1º × 1º distribution of carbon dioxide emissions from fossil fuel consumption and cement manufacture, 1950-1990, *Global Biogeochemical Cycles*, 10, pp.419-429.

Andronache, C., 2004. Estimates of sulfate aerosol wet scavenging coefficient for locations in the Eastern United States. *Atmospheric Environment*, 38, pp.795–804, http://dx. doi.org/10.1016/j.atmosenv.2003.10.035.

Aoki, K., 2006. *Aerosol optical characteristics in Asia from measurements of SKYNET sky radiometers*. In IRS 2004: Current Problems in Atmospheric Radiation (eds. H. Fischer and B.-J. Sohn), pp.311-313, A. Deepak, Hampton, VA.

Aoki, K. and Fujiyoshi, Y., 2003. Sky radiometer measurements of aerosol optical properties over Sapporo, Japan. *Journal of the Meteorological Society of Japan*, 81(3), pp.493–513, http://dx.doi.org/10.2151/jmsj.81.493.

Baars, H., Ansmann, A., Althausen, D., Engelmann, R., Heese, B., Müller, D., Artaxo, P., Paixao, M., Pauliquevis, T. and Souza, R., 2012. Aerosol profiling with LIDAR in the Amazon Basin during the wet and dry season. *Journal of Geophysical Research*, 117, D21201, doi: 10.1029/2012JD018338.

Babu, S.S., Manoj, M.R., Moorthy, K.K., Gogoi, M.M., Nair, V.S., Kompalli, S.K., Satheesh, S.K., Niranjan, K., Ramgopal, K., Bhuyan, P.K., Singh, D., 2013. Trends in aerosol optical depth over Indian region: Potential causes and impact indicators. *Journal of Geophysical Research*, 118, pp.11794–11806, doi: 10.1002/2013JD020507.

Barnaba, F., Angelini, F., Curci, G. and Gobbi, G. P., 2011. An important fingerprint of wildfires on the European aerosol load. *Atmospheric Chemistry and Physics*, 11, pp.10487–10501, http://dx.doi.org/10.5194/acp-11-10487-2011.

Barrie, L.A., 1986. Arctic air pollution: An overview of current knowledge. *Atmospheric Environment*, 20, pp.643-663.

Barrie, L.A., 1990. *Arctic air pollution: A case study of continent-to-ocean-to-continent transport*. In The Long-range Atmospheric Transport of Natural and Contaminant Substances. (eds. A.H. Knap and M.S. Kaiser), pp.137-148, Kluwer Academic Publishers, Dordrecht, Holland.

Basart, S., Pérez, C., Cuevas, E., Baldasano, J.M. and Gobbi, G.P., 2009. Aerosol characterization in Northern Africa, Northeastern Atlantic, Mediterranean Basin and Middle East from direct-sun AERONET observations. *Atmospheric Chemistry and Physics*, 9, pp.8265–8282, http://dx.doi.org/10.5194/acp-9-8265-2009.

Begum, B.A., Biswas, S.K., Markwitz, A. and Hopke, P.K., 2010. Identification of sources of fine and coarse particulate matter in Dhaka, Bangladesh. *Aerosol and Air Quality Research*, 10, pp.345–353, http://dx.doi.org/10.4209/aaqr.2009.12.0082.

Benkovitz, C.M., Scholtz, M.T., Pacyna, J., Tarrason, L., Dignon, J., Voldner, E.C., Spiro, P.A., Logan, J.A. and Graedel, T.E., 1996. Global gridded inventories of anthropogenic emissions of sulphur and nitrogen. *Journal of Geophysical Research*, 101, pp.29239–29253, http://dx.doi.org/10.1029/ 96JD00126.

Bergamo, A., Tafuro, A.M., Kinne, S., de Tomasi, F. and Perrone, M.R., 2008. Monthly averaged anthropogenic aerosol direct radiative forcing over the Mediterranean based on AERONET aerosol properties. *Atmospheric Chemistry and Physics*, 8, pp.6995–7014, http://dx.doi.org/10.5194/acp-8-6995-2008.

Bey, I., Jacob, D.J., Logan, J.A. and Yantosca, R.M., 2001. Asian chemical outflow to the Pacific: Origins, pathways and budgets. *Journal of Geophysical Research*, 106, pp.23097-23114.

Bibi, H., Alam, K., Chishtie, F., Bibi, S., Shahid, I. and Blaschke, T., 2015. Inter comparison of MODIS, MISR, OMI, and CALIPSO aerosol optical depth retrievals for four locations on the Indo-Gangetic plains and validation against AERONET data. *Atmospheric Environment*, 111, pp.113–126, http://dx.doi.org/10.1016/j.atmosenv.2015.04.013.

Boiyo, R., Kumar, K.R., Zhao, T. and Bao, Y., 2017. Climatological Analysis of Aerosol Optical Properties over East Africa Observed from Space-Borne Sensors during 2001-2015. *Atmospheric Environment*, 152, pp.298-313, doi:10.1016/j.atmosenv.2016.12.050.

Boucher, O. and Haywood, J., 2001. On summing the components of radiative forcing of climate change. *Climate Dynamics*, 18, pp.297–302, http://dx.doi.org/10.1007/s003820100185.

Boucher, O. and Tanré, D., 2000. Estimation of the aerosol perturbation to the Earth's radiative budget over oceans using POLDER satellite aerosol retrievals. *Geophysical Research Letters*, 27(8), pp.1103–1106, http://dx.doi.org/10.1029/1999GL010963.

Brauer, M., Amann, M., Burnett, R.T., Cohen, A., Dentener, F., Ezzati, M., Henderson, S.B., Krzyzanowski, M., Martin, R.V., Dingenen, R.V., van Donkelaar, A. and Thurston, G.D. 2012. *Environmental Science & Technology*, 46(2), pp.652-660, doi: 10.1021/es2025752.

Camberlin, P., 2017. Temperature trends and variability in the Greater Horn of Africa: interactions with precipitation. *Climate Dynamics*, 48, pp.477-498.

Cao, J., Garbaccio, R. and Ho, M.S., 2009. China's 11th five-year plan and the environment: Reducing SO_2 emissions. *Review of Environmental Economics and Policy*, 3, pp.231–250, http://dx.doi.org/10.1093/reep/rep006.

Carslaw, K.S., Lee, L.A., Reddington, C.L., Pringle, K.J., Rap, A., Forster, P.M., Mann, G.W., Spracklen, D.V., Woodhouse, M.T., Regayre, L.A. and Pierce, J.R., 2013. Large contribution of natural aerosols to uncertainty in indirect forcing. *Nature*, 503, pp.67–71, http://dx.doi.org/10.1038/nature12674.

Cavalieri, O., Cairo, F., Fierli, F., Di Donfrancesco, G., Snels, M., Viterbini, M., Cardillo, F., Chatenet, B., Formenti, P., Marticorena, B. and Rajot, J.L., 2010. Variability of aerosol vertical distribution in the Sahel. *Atmospheric Chemistry and Physics*. 10, pp.12005–12023, doi: 10.5194/acp-10-12005-2010.

Charlson, R.J., Schwartz, S.E., Hales, J.M., Cess, R.D., Coakley, J.A., Jr., Hansen, J.E., and Hofmann, D.J., 1992. Climate forcing by anthropogenic aerosols. *Science*, 255, pp.423–430, http://dx.doi.org/10.1126/science.255.5043.423.

Chen, B.B., Sverdlik, L.G., Imashev, S.A., Solomon, P.A., Lantz, J., Schauer, J.J., Shafer, M. M., Artamonova, M.S. and Carmichael, G.R., 2013. LIDAR Measurements of the Vertical Distribution of Aerosol Optical and Physical Properties over Central Asia. *International Journal of Atmospheric Sciences*, 261546, http://dx.doi.org/10.1155/2013/261546.

Christensen, J.H., 1997. The Danish Eulerian hemispheric model - a three dimensional model used for the Arctic, *Atmospheric Environment*, 31, pp.4196-4191.

Chu, D.A., Kaufman, Y.J., Ichoku, C., Remer, L.A., Tanre, D. and Holben, B.N., 2002. Validation of MODIS aerosol optical depth retrieval over land. *Geophysical Research Letters*, 29(12), pp.MOD2-1-MOD2-4, https://doi.org/10.1029/2001GL013205.

Chubarova, N., Nezval', Y., Sviridenkov, M., Smirnov, A. and Slutsker, I., 2011. Smoke aerosol and its radiative effects during extreme fire event over Central Russia in summer 2010. *Atmospheric Measurement Techniques Discussions*, 4, pp.6351–6386, doi: 10.5194/amtd-4-6351-2011.

Chylek, P., Lohmann, U., Dubey, M., Mishchenko, M., Kahn, R. and Ohmura, A., 2007. Limits on climate sensitivity derived from recent satellite and surface observations. *Journal of Geophysical Research*, 112, D24S04, doi: 10.1029/2007JD008740.

CIESIN (Center for International Earth Science Information Network) 2005. Socioeconomic Data and Applications Center, United Nations Food and Agriculture Programme, Centro Internacional de Agricultura Tropical, Gridded Population of the World: Future Estimates, available from: http://sedac.ciesin.columbia.edu/gpw/

CIESIN 2012. World population prospects, the 2012 revision, available from http://esa.un.org/unpd/index.htm.

Cofala, J., Amann, M., Gyarfas, F., Schoepp, W., Boudri, J.C., Hordijk, L., Kroeze, C., Li, J.F., Lin, D., Panwar, T.S. and Gupta, S., 2004. Cost effective control of SO_2 emissions in Asia. *Journal of Environmental Management*, 72, pp.149–161, http://dx.doi.org/10.1016/j.jenvman.2004.04.009.

Corrigan, C.E., Roberts, G.C., Ramana, M.V., Kim, D. and Ramanathan, V., 2008. Capturing vertical profiles of aerosols and black carbon over the Indian Ocean using autonomous unmanned aerial vehicles. *Atmospheric Chemistry and Physics*, 8, pp.737–747, www.atmos-chem-phys.net/8/737/2008/.

Cowie, S.M., Knippertz, P., and Marsham, J.H., 2013. Are vegetation related roughness changes the cause of the recent decrease in dust emission from the Sahel? *Geophysical Research Letters*, 40, pp.1868–1872, doi:10.1002/grl.50273.

Das, S., Harshvardhan, H., Bian, H., Chin, M., Curci, G., Protonotariou, A.P., Mielonen, T., Zhang, K., Wang, H. and Liu, X., 2017. Biomass burning aerosol transport and vertical distribution over the South African-Atlantic region. *Journal of Geophysical Research*, 122, pp.6391–6415, doi:10.1002/2016JD026421.

Dayan, U., Ziv, B., Shoop, T. and Enzel, Y., 2008. Suspended dust over South-Eastern Mediterranean and its relation to atmospheric circulations. *International Journal of Climatol*ogy, 28(7), pp.915–924, doi:10.1002/joc.1587.

de Gouw, J.A., Parrish, D.D., Frost, G.J. and Trainer, M., 2014. Reduced emissions of CO_2, NO_X, and SO_2 from U.S. power plants owing to switch from coal to natural gas with combined cycle technology. *Earth's Future,* 2, pp.75–82.

de Meij, A., Pozzer, A. and Lelieveld, J., 2010. Global and regional trends in aerosol optical depth based on remote sensing products and pollutant emission estimates between 2000 and 2009. *Atmospheric Chemistry and Physics Discussions*, 10, pp.30731–30776, doi: 10.5194/acpd-10-30731-2010.

de Meij, A. and Lelieveld, J., 2011. Evaluating aerosol optical properties observed by ground-based and satellite remote sensing over the Mediterranean and the Middle East in 2006. *Atmospheric Research*, 99, pp.415–433, http://dx.doi.org/10.1016/j.atmosres.2010.11.005.

de Ruyter de Wildt, M., Eskes, H., and Boersma, K.F., 2012. The global economic cycle and satellite-derived NO_2 trends over shipping lanes. *Geophysical Research Letters*, 39, L01802, doi: 10.1029/2011GL049541.

Decesari, S., Fuzzi, S., Facchini, M.C., Mircea, M., Emblico, L., Cavalli, F., Maenhaut, W., Chi, X., Schkolnik, G., Falkovich, A., Rudich, Y., Claeys, M., Pashynska, V., Vas, G., Koutchev, I., Vermeylen, Hoffer, A., Andreae, M.O., Tagliavini, E., Moretti, F. and Artaxo, P., 2006. Characterization of the organic composition of aerosols from Rondonia, Brazil, during the LBA-SMOCC 2002 experiment and its representation through model compounds. *Atmospheric Chemistry Physics*, 6, pp.375-402.

Dennison, P., Brewer, S., Arnold, J. and Moritz, M., 2014. Large wildfire trends in the western United States, 1984–2011. *Geophysical Research Letters*, 41, pp.2928–2933.

Dey, S. and Di Girolamo, L., 2010. A climatology of aerosol optical and microphysical properties over the Indian subcontinent from nine years (2000-2008) of Multi angle Imaging Spectro Radiometer (MISR) data. *Journal of Geophysical Research*, 115, D15204, http://dx.doi.org/10.1029/2009JD013395.

Dey, S. and Di Girolamo, L., 2011. A decade of change in aerosol properties over the Indian subcontinent. *Geophysical Research Letters*, 38, L14811, http://dx.doi.org/10.1029/2011GL048153.

Dey, S., Tripathi, S.N., Singh, R.P. and Holben, B.N., 2004. Influence of dust storms on the aerosol optical properties over the Indo-Gangetic plains. *Journal of Geophys*ical *Res*earch, 109, D20211, doi: 10.1029/2004JD004924.

Di Girolamo, L. and Davis, R., 1995. The image navigation cloud mask for the Multi-angle Imaging SpectroRadiometer (MISR). *Journal of Atmospheric and Oceanic Techniques*, 12, pp.1215-1228.

Di Girolamo, L. and Wilson, M.J., 2003. A first look at band-differenced angular singnatures for cloud detection from MISR. *IEEE Transactions on Geosciences and Remote Sensing*, 41, pp.1730-1734.

Diner, D.J., Beckert, J.C., Reilly, T.H., Bruegge, C.J., Conel, J.E., Kahn, R.A. and Martonchik, J.V., 1998. Multiangle Imaging Spectroradiometer (MISR) description and experiment overview. *IEEE Transactions on Geoscience and Remote Sensing*, 36(4), pp.1072–1087, http://dx.doi. org/10.1109/36.700992.

Diner, D.J., Martonchik, J.V., Kahn, R.A., Pinty, B., Gobron, N., Nelson, D.L. and Holben, B.N., 2005. Using angular and spectral shape similarity constraints to improve MISR aerosol and surface retrievals over land. *Remote Sensing of Environment*, 94, pp.155-171.

Dipu, S., Prabha, T.V., Pandithurai, G., Dudhia, J., Pfister, G., Rajesh, K. and Goswami, B.N., 2013. Impact of elevated aerosol layer on the cloud macrophysical properties prior to monsoon onset. *Atmospheric Environment*, 70, pp.454-467, http://dx.doi.org/10.1016/j.atmosenv.2012.12.036.

Dong, Z., Li, Z., Yu, X., Cribb, M., Li, X. and Dai, J., 2017. Opposite long-term trends in aerosols between low and high altitudes: a testimony to the aerosol–PBL feedback. *Atmospheric Chemistry and Phys*ics, 17, pp.7997–8009, https://doi.org/10.5194/acp-17-7997-2017.

Dubovik, O., Holben, B.N., Eck, T.F., Smirnov, A., Kaufman, Y.J., King, M.D. and Tanre, D., 2001. Variability of absorption and optical properties of key aerosol types observed in worldwide locations. *Journal of the Atmospheric Sciences*, 59, pp.590–608.

Duce, R. 1995. *Distributions and fluxes of mineral aerosol*. In Aerosol Forcing of Climate (eds. R.J. Charlson and J. Heintzenberg), pp. 43-72, Wiley, Chichester, UK.

Dutta, R., Das, A. and Aryal, J., 2016. Big data integration shows Australian bush-fire frequency is increasing significantly. *Royal Society Open Sci*ence, 3, 150241. http://dx.doi.org/10.1098/rsos.150241.

Eck, T.F., Holben, B.N., Reid, J.S., Dubovik, O., Smirnov, A., O'Neill, N.T., Slutsker, I. and Kinne, S.1999. Wavelength dependence of the optical depth of biomass burning, urban and desert dust aerosols. *Journal of Geophysical Research*, 104, pp.31333-31350.

Efe, S. I., 2008. Spatial distribution of particulate air pollution in Nigerian cities: Implications for human health. *International Journal of Environmental Health Research*, 7(2), http://www.cieh.org/jehr/jehr2column.aspx?id=14688.

Engelbrecht, F., Adegoke, J., Bopape, M., Naidoo, M., Garland, R., Thatcher, M., McGregor, J., Katzfey, J., Werner, M., Ichoku, C. and Gatebe, C., 2015. Projections of rapidly rising surface temperatures over Africa under low mitigation. *Environmental Research Letters*, 10, 085004, doi:10.1088/1748-9326/10/8/085004

EPA, 2011. Emissions of primary particulate matter and secondary particulate matter precursors, Assessment, http://www.epa.gov/ttn/chief/trends/, CSI 003.

Evan, A.T., Dunion, J., Foley, J.A., Heidinger, A.K. and Velden, C.S., 2006. New evidence for a relationship between Atlantic tropical cyclone activity and African dust outbreaks. *Geophysical research Letters*, 33, L19813, doi: 10.1029/2006GL026408.

Evan, A.T., Flamant, C., Gaetani, M. and Guichard, F., 2016. The past, present and future of African dust. *Nature*, 531, pp.493-495, doi: 10.1038/nature17149.

Evangelista, H., Maldonado, J., Godoi, R.H.M., Pereira, E.B., Koch, D., Tanizaki-Fonseca, K., Grieken, V.R., Sampaio, M., Setzer, A., Alencar, A. and Goncalves, C.S., 2007. Sources and transport of urban and biomass burning aerosol black carbon at the South–West Atlantic Coast. *Journal of Atmospheric Chemistry*, 56(3), pp.225-238, doi: 10.1007/s10874-006-9052-8.

Fang, C.P., McMurry, P.H., Marple, V.A. and Rubow, K.L., 1991. Effect of flow induced relative humidity changes on size cuts for sulfuric acid droplets in the Micro-orifice Uniform Deposit Impactor (MOUDI. *Aerosol Science and Technology*, 14(2), pp.266-277, doi: 10.1080/02786829108959489.

Farahat, A., El-Askary, H. and Al-Shaibani, A., 2015. Study of aerosols' characteristics and dynamics over the Kingdom of Saudi Arabia using a multi sensor approach combined

with ground observations. *Advances in Meteorology*, 247531, http://dx.doi.org/10.1155/2015/247531.

Fernandes, K., Verchot, L., Baethgen, W., Gutierrez-Velez, V., Pinedo-Vasquez, M. and Martius, C., 2017. Heightened fire probability in Indonesia in non-drought conditions: the effect of increasing temperatures. *Environmental Research Letters*, 12, 054002, https://doi.org/10.1088/1748-9326/aa6884.

Fitzgerald, J.W., 1984. Effect of relative humidity on the aerosol backscattering coefficient at 0.694- and 10.6-μm wavelengths. *Applied Optics*, 23, pp.411-418.

Forster, P., Ramaswamy, V., Artaxo, P., Berntsen, T., Betts, R., Fahey, D., Haywood, J., Lean, J., Lowe, D., Myhre, G., Nganga, J., Prinn, R., Raga, G., Schulz, M. and Dorlandet R.V., 2007. *Changes in atmospheric constituents and in radiative forcing*, In Climate Change 2007: The Physical Science Basis. Contribution of Working Group I to the Fourth Assessment Report of the Intergovernmental Panel on Climate Change (eds. S. Solomon et al.), pp.129–234, Cambridge Univ. Press, Cambridge, UK and New York.

Fuzzi, S., Andreae, M.O., Huebert, B.J., Kulmala, M., Bond, T.C., Boy, M., Doherty, S.J., Guenther, A., Kanakodou, M., Kawamura, K., Kerminen, V.M., Lohman, U., Russel, L.M. and Poschl, U. 2006. Critical assessment of the current state of scientific knowledge, terminology, and research needs concerning the role of organic aerosols in the atmosphere, climate, and global change. *Atmospheric Chemistry and Physics*, 6, pp.2017-2038.

Gadhavi, H. and Jayaraman, A., 2006. Airborne LIDAR study of the vertical distribution of aerosols over Hyderabad, an urban site in central India, and its implication for radiative forcing calculations. *Annals of Geophysics*, 24, pp.2461–2470, www.ann-geophys.net/24/2461/2006/.

Ganguly, D., Ginoux, P., Ramaswamy, V., Dubovik, O., Welton, J., Reid, E.A. and Holben, B.N., 2009. Inferring the composition and concentration of aerosols by combining AERONET and MPLNET data: Comparison with other measurements and utilization to evaluate GCM output. *Journal of Geophysical Research*, 114, D16203, doi: 10.1029/2009JD011895.

Gao, B.C., Kaufman, Y.J., Tanre, D., and Li, R.R., 2002. Distinguishing tropospheric aerosols from thin cirrus clouds for improved aerosol retrievals using the ratio of 1.38 µm and 1.24 µm channels. *Geophysical Research Letters*, 29, 1890, doi: 10.1029/2002GL015475.

Gao, Y., Kaufman, Y.J., Tanré, D. and Falkowski, P.G., 2000. Seasonal distribution of Aeolian iron fluxes to the global ocean. *Geophysical Research Letters*, 28, pp.29–33, http://dx.doi.org/10.1029/2000GL011926.

GAW, 2003. *Proceedings of WMO/GAW Aerosol measurement procedures guidelines and recommendations*, GAW Report #153, available at http://www.wmo.ch/web/arep/gaw/gawreports.html.

Gong, S.L., Zhang, X.Y., Zhao, T.L., McKendry, I.G., Jaffe, D.A. and Lu, N.M., 2003. Characterization of soil dust distributions in China and its transport during ACE-ASIA 2. Model simulation and validation. *Journal of Geophysical Research*, 108(D9), 4262, doi: 4210.1029/2002JD002633.

Gong, S.L., Zhang, X.Y., Zhao, T.L., Zang, X.B., Barrie, L.A., McKendry, I.G. and Zhao, C.S., 2006. A simulated climatology of Asian dust aerosol and its trans-pacific transport. 2: Interannual variability and climatic connections. *Journal of Climate*, 19, pp.104-122.

Gonzalez, R.C., Veefkind, J.P. and de Leeuw, G., 2000. Aerosol optical depth over Europe in August 1997 derived from ATSR-2 data. *Geophysical Research Letters*, 27(7), pp.955–958.

Goodman, A.H. and Henderson-Sellers, A., 1988. Cloud detection analysis: a review of recent progress. *Atmospheric Research*, 21, pp.203-228.

Granier, C., Bessagnet, B., Bond, T., d'Angiola, A., van der Gon, H.D., Frost, G., Heil, A., Kaiser, J., Kinne, S., Klimont, Z., Kloster, S., Lamarque, J.-F., Liousse, C., Masui, T., Meleux, F., Mieville, A., Ohara, T., Raut, J.-C., Riahi, K. and Vuuren, D., 2011. Evolution of anthropogenic and biomass burning emissions of air pollutants at global and regional scales during the 1980–2010 period. *Climate Change*, 109, pp.163–190, doi: 10.1007/s10584-011-0154-1.

Guanter, L., Del Carmen Gonzalez-Sanperdo, M. and Moreno, J., 2007. A method for the atmospheric correction of ENVISAT/MERIS data over land targets. *International Journal of Remote Sensing*, 28(3-4), pp.709-728.

Hansen, J., Sato, M. and Ruedy, R., 1997. Radiative forcing and climate response. *Journal of Geophysical Research*, 102, pp.6831–6864, http://dx.doi.org/10.1029/96JD03436.

Hatzianastassiou, N., Gkikas, A., Mihalopoulos, N., Torres, O. and Katsoulis, B.D., 2009. Natural versus anthropogenic aerosols in the Eastern Mediterranean basin derived from multiyear TOMS and MODIS satellite data. *Journal of Geophysical Research*, 114, D24202, http://dx.doi.org/10.1029/2009JD011982.

Haywood, J. and Boucher, O., 2000. Estimates of the direct and indirect radiative forcing due to tropospheric aerosols. *Review of Geophysics*, 38, pp.513–543, http://dx.doi.org/10.1029/1999RG000078.

Heitzenberg, J., Charlson, R.J., Clarke, A.D., Liousse, C., Ramanathan, V., Shine, K.P., Wendisch, M. and Helas, G., 1997. Measurements and modeling of aerosol single scattering albedo: progress, problems and prospects. *Beitraege zur Physik der Atmosphaere*, 70**,** pp.249-263.

Hilboll, A., Richter, A. and Burrows, J.P., 2013. Long-term changes of tropospheric NO_2 over megacities derived from multiple satellite instruments. *Atmospheric Chemistry and Physics*, 13, pp.4145–4169, http://dx.doi.org/10.5194/acp-13-4145-2013.

Hsu, N.C., Gautam, R., Sayer, A.M.M., Bettenhausen, C., Li, C., Jeong, M.J., Tsay, S.-C. and Holben, B.N., 2012. Global and regional trends of aerosol optical depth over land and ocean using SeaWiFS measurements from 1997 to 2010. *Atmospheric Measurement Techniques Discussions*, 12, pp.8465–8501, http://dx.doi.org/10.5194/acpd-12-8465-2012.

Hsu, N.C., Herman, J., Torres, O., Holben, B.N., Tanre, D., Eck, T.F., Smirnov, A., Chatenet, B. and Lavenu, F., 1999. Comparisons of the TOMS aerosol optical thickness: results and applications. *Journal of Geophysical Research*, 104(D6), pp. 6269-6279.

Hsu, N.C., Levy, R.C., Sayer, A.M., Lee, J., Laszlo, I., Bettenhausen, C., Gautam, R., Mattoo, S., Munchak, L.A., and Liu, H. 2013. Suomi NPP VIIRS Aerosol Data Product Assessment Report, NASA, Washington D.C., USA, 77 pp.

Hu, Y., Vaughan, M., Liu, Z., Lin, B., Yang, P., Flittner, D., Hunt, B., Kuehn, R., Huang, J., Wu, D., Rodier, S., Powell, K., Trepte, C. and Winker, D., 2007. The depolarization – attenuated extinction relation: CALIPSO LIDAR measurements vs. theory, *Optics Express*, 9, pp.5327–5332, doi:10.1364/OE.15.005327.

Hu, Y., Winker, D., Vaughan, M., Lin, B., Omar, A., Trepte, C. and Flittner, D., 2009. CALIPSO/CALIOP cloud phase discrimination algorithm. *Journal of Atmospheric and Oceanic Technology*, 26, pp.2293–2309, doi: 10.1175/2009JTECHA1280.1.

Huang, J., Guo, J., Wang, F., Liu, Z., Jeong, M.J., Yu, H. and Zhang Z., 2015. CALIPSO inferred most probable heights of global dust and smoke layers. *Journal of Geophysical Research - Atmos*pheres, 120(10), doi: 10.1002/2014JD022898.

Huijnen, V., Wooster, M.J., Kaiser, J.W., Gaveau, D.L.A., Flemming, J., Parrington, M., Inness, A., Murdiyarso, D., Main, B. and van Weele, M., 2016. Fire carbon emissions over maritime Southeast Asia in 2015 largest since 1997. *Scientific Rep*orts, 6, 26886, doi: 10.1038/srep26886.

Huneeus, N., Schulz, M., Balkanski, Y., Griesfeller, J., Prospero, J., Kinne, S., Bauer, S., Boucher, O., Chin, M., Dentener, F., Diehl, T., Easter, R., Fillmore, D., Ghan, S., Ginoux, P., Grini, A., Horowitz, L., Koch, D., Krol, M.C., Landing, W., Liu, X., Mahowald, N., Miller, R., Morcrette, J.-J., Myhre, G., Penner, J., Perlwitz, J., Stier, P., Takemura, T., and Zender, C.S., 2011. Global dust model inter comparison in AeroCom phase I. *Atmospheric Chemistry and Phys*ics, 11, pp.7781–7816, doi: 10.5194/acp-11-7781-2011.

Hunt, W., Winker, D., Vaughan, M., Powell, K.A., Lucker, P.L. and Weimer, C., 2009. CALIPSO LIDAR description and performance assessment. *Journal of Atmospheric and Oceanic Technol*ogy, 26, pp.1214-1228.

Husar, R.B., Tratt, D.M., Schichtel, B.A., Falke, S.R., Li, F., Jaffe, D., Gasso, S., Gill, T., Laulainen, N.S., Lu, F.,Reheis, M.C., Chun, Y., Westphal, D., Holben, B.N., Gueymard, C., McKendry, I., Kuring, N., Feldman, G.C., McClain, C., Frouin, R.J., Merrill, J.,

DuBois, D.,Vignola, F., Murayama, T., Nickovic, S., Wilson, W.E., Sassen, K., Sugimoto, N. and Malm, W.C., 2001. Asian dust events of April 1998. *Journal of Geophysical Research*, 106, pp.18317-18330.

IPCC, 2013. *Climate Change 2013: The Physical Science Basis. Contribution of Working Group I to the Fifth Assessment Report of the Intergovernmental Panel on Climate Change* [eds. Stocker, T.F., D. Qin, G.-K. Plattner, M. Tignor, S.K. Allen, J. Boschung, A. Nauels, Y. Xia, V. Bex and P.M. Midgley]. 1535 pp., Cambridge University Press, Cambridge, United Kingdom and New York, NY, USA, doi: 10.1017/CBO9781107415324.

Jacob, D.J., Logan, J.A. and Murti, P.P., 1999. Effect of rising Asian emissions on surface ozone in the United States. *Geophysical Research Letters*, 26, pp.2175-2178.

John, W., 2011. *Size Distribution Characteristics of Aerosols*. In Aerosol measurement: principles, Techniques, and Applications (eds. Kulkarni, P., Baron, P.A. and Willeke, K.) pp. 41-54, John Wiley & Sons Inc., New York.

Jolly, W.M., Cochrane, M.A., Freeborn, P.A., Holden, Z.A., Brown, T.J., Williamson, G.J. and Bowman, D.M.J.S., 2015. Climate-induced variations in global wildfire danger from 1979 to 2013. *Nature Communications,* 6, 7537, doi: 10.1038/ncomms8537.

Kabanov, D.M., Beresnev, S. A., Gorda, S.Y., Kornienko, G. I., Nikolashkin, S. V., Sakerin, S. M. and Tashchilin, M.A., 2013. Diurnal behavior of aerosol optical depth of the atmosphere in a few regions of Asian part of Russia. *Atmospheric and Oceanic Optics*, 26(6), pp.466–472, http://dx.doi.org/10.1134/S1024856013060092.

Kahn, R.A., Gaitley, B.J., Garay, M.J., Diner, D.J., Eck, T.F., Smirnov, A. and Holben, B.N. 2010. Multiangle Imaging SpectroRadiometer global aerosol product assessment by comparison with Aerosol Robotic Network. *Journal of Geophysical Research*, 115, D23209, http://dx.doi.org/10.1029/2010JD014601.

Kahn, R.A., Chen, Y., Nelson, D.L., Leung, F., Li, Q., Diner, D.J. and Logan, J.A., 2008. Wildfire smoke injection heights: Two perspectives from space. *Geophysical Research Letters*, 35, L04809, doi: 10.1029/2007GL032165.

Kahn, R.A., Gaitley, A.B., Martonchik, J., Diner, D., Crean, K. and Holben, B.N., 2005. MISR global aerosol optical depth validation based on two years of coincident AERONET observations. *Journal of Geophysical Research*, 110, D10S04, http://dx.doi.org/10.1029/2004JD004706.

Kahn, R., Nelson, D.L., Garay, M., Levy, R.C., Bull, M.A., Martonchik, J.V., Paradise, R.S., Hansen, G.E. and Lorraine, R., 2009. MISR aerosol product attributes and statistical comparisons with MODIS. *IEEE Transactions on Geoscience and Remote Sensing*, 47(12), pp.4095–4114, http://dx.doi.org/10.1109/TGRS.2009.2023115.

Kanakidou, M., Seinfeld, J.H., Pandis, S.N., Barnes, I., Dentener, F.J., Facchini, M.C., Van Dingenen, R., Ervens, B., Nenes, A., Neilsen, C.J., Swietlicki, E., Putaud, J.P., Balkanski, Y., Fuzzi, S., Horth, J., Moorgat, G.K., Winterhalter, R., Myhre, C.E.L.,Tsigaridis, K., Vignati, E., Stephanou, E.G. and Wilson, J., 2005. Organic aerosol and global climate modelling: A review. *Atmospheric Chemistry Physics*, 5, pp.1053-1123.

Kang, N., Kumar, K.R., Hu, K., Yu, X. and Yin, Y., 2016. Long-Term (2002-2014) evolution and trend in Collection 5.1 Level-2 aerosol products derived from the MODIS and MISR sensors over the Chinese Yangtze River Delta. *Atmospheric Research*, 181, pp.29-43, doi:10.1016/j.atmosres.2016.06.008.

Kanitz, T., Ansmann, A., Engelmann, R. and Althausen, D., 2013. North-south cross sections of the vertical aerosol distribution over the Atlantic Ocean from multiwavelength Raman/polarization LIDAR during Polarstern courses. *Journal of Geophysical Research*, 118, pp.2643–2655, doi:10.1002/jgrd.50273.

Karnieli, A., Derimian, Y., Indoitu, R., Panov, N., Levy, R.C., Remer, L.A., Maenhaut, W. and Holben, B.N., 2009. Temporal trend in anthropogenic sulfur aerosol transport from central and Eastern Europe to Israel. *Journal of Geophysical Research*, 114, D00D19, http://dx.doi.org/10.1029/2009JD011870.

Kaskaoutis, D.G., Kharol, S.K., Sinha, P.R., Singh, R.P., Badarinath, K.V.S., Mehdi, W. and Sharma, M., 2011. Contrasting aerosol trends over South Asia during the last decade

based on MODIS observations. *Atmospheric Measurement Techniques Discussions*, 4, pp.5275–5323, http://dx.doi.org/10.5194/amtd-4-5275-2011.

Kaskaoutis, D.G., Kumar, S., Sharma, D., Singh, R.P., Kharol, S.K., Sharma, M., Singh, A.K., Singh, S., Singh, A. and Singh, D., 2014. Effects of crop residue burning on aerosol properties, plume characteristics, and long-range transport over northern India. *Journal of Geophysical Research*, 119, pp.5424–5444, doi: 10.1002/2013JD021357.

Kaufman, Y.J., Koren, I., Remer, L.A., Tanre, D., Ginoux, P., and Fan, S., 2005. Dust transport and deposition observed from the Terra-Moderate Resolution Imaging Spectroradiometer (MODIS) spacecraft over the Atlantic Ocean, *Journal of Geophysical Research*, 110, D10S12, doi: 10.1029/2003JD004436.

Kaufman, Y.J., Tanre, D., Remer, L.A., Vermote, E.F., Chu, A. and Holben, B.N., 1997. Operational remote sensing of tropospheric aerosol over land from EOS moderate resolution imaging spectroradiometer. *Journal of Geophysical Research,* 102(D14), pp.17051-17067, https://doi.org/10.1029/96JD03988

Kim, M.-H., Kim, S.-W., Yoon, S.-C., and Omar, A.H., 2013. Comparison of aerosol optical depth between CALIOP and MODIS-Aqua for CALIOP aerosol subtypes over the ocean. *Journal of Geophysical Research*, 118, pp.13241–13252, doi: 10.1002/2013JD019527.

Kim, P.S., Jacob, D.J., Fisher, J.A., Travis, K., Yu, K., Zhu, L., Yantosca, R.M., Sulprizio, M.P., Jimenez, J.L., Campuzano-Jost, P., Froyd, K.D., Liao, J., Hair, J.W., Fenn, M. A., Butler, C.F., Wagner, N.L., Gordon, T.D., Welti, A., Wennberg, P.O., Crounse, J. D., St. Clair, J.M., Teng, A.P., Millet, D.B., Schwarz, J.P., Markovic, M.Z., and Perring, A.E., 2015. Sources, seasonality, and trends of southeast US aerosol: An integrated analysis of surface, aircraft, and satellite observations with the GEOS-chem chemical transport model. *Atmospheric Chemistry and Physics*, 15, pp.10411–10433, https://doi.org/10.5194/acp-15-10411-2015.

King, M.D., Kaufman, Y.J., Menzel, W.P. and Tanre, D., 1992. Remote sensing of cloud, aerosol, and water vapor from the Moderate Resolution Imaging Spectroradiometer (MODIS). *IEEE Transactions on Geoscience and Remote Sensing*, 30(1), pp.2-27.

King, M.D., Kaufman, Y.J., Tanre, D. and Nakajima, T., 1999. Remote sensing of tropospheric aerosols from space: Past, present and future. *Bulletin of American Meteorological Society*, 80, pp.2229-2259.

Kinne, S., Schulz, M., Textor, C., Guibert, S., Balkanski, Y., Bauer, S.E., Berntsen, T., Berglen, T.F., Boucher, O., Chin, M., Collins, W., Dentener, F., Diehl, T., Easter, R., Feichter, J., Fillmore, D., Ghan, S., Ginoux, P., Gong, S., Grini, A., Hendricks, J., Herzog, M., Horowitz, L., Isaksen, I., Iversen, T., Kirkevåg, A., Kloster, S., Koch, D., Kristjansson, J.E., Krol, M., Lauer, A., Lamarque, J.F., Lesins, G., Liu, X., Lohmann, U., Montanaro, V., Myhre, G., Penner, J., Pitari, G., Reddy, S., Seland, O., Stier, P., Takemura, T. and Tie, X., 2006. An AeroCom initial assessment – optical properties in aerosol component modules of global models. *Atmospheric Chemistry and Physics*, 6, pp.1815-1834, doi: 10.5194/acp-6-1815-2006.

Kishcha, P., Starobinets, B., Kalashnikova, O. and Pinhas, A., 2011. Aerosol optical thickness trends and population growth in the Indian subcontinent. *International Journal of Remote Sensing*, 32(24), pp.9137–9149, http://dx.doi.org/10.1080/01431161.2010.550333.

Kittaka, C., Winker, D.M., Vaughan, M.A., Omar, A., and Remer, L.A., 2011. Inter comparison of column aerosol optical depths from CALIPSO and MODIS-Aqua. *Atmospheric Measurement Techniques*, 4, pp.131–141, doi: 10.5194/amt-4-131-2011.

Klingmüller, K., Pozzer, A., Metzger, S., Stenchikov, G.L. and Lelieveld, J., 2016. Aerosol optical depth trend over the Middle East. *Atmospheric Chemistry and Physics*, 16, pp.5063–5073, doi: 10.5194/acp-16-5063-2016.

Knippertz, P., Evans, M.J., Field, P.R., Fink, A.H., Liousse, C. and Marsham, J.H., 2015. The possible role of local air pollution in climate change in West Africa. *Nature Climate Change*, 5, pp.815-822, https://doi.org/10.1038/nclimate2727.

Koffi, B., Schulz, M., Br´eon, F.-M., Griesfeller, J., Winker, D., Balkanski, Y., Bauer, S., Berntsen, T., Chin, M., Collins, W.D., Dentener, F., Diehl, T., Easter, R., Ghan, S., Ginoux, P., Gong, S., Horowitz, L.W., Iversen, T., Kirkevåg, A., Koch, D., Krol, M., Myhre, G., Stier, P. and Takemura, T., 2012. Application of the CALIOP layer product to evaluate the vertical distribution of aerosols estimated by global models: AeroCom

phase I results. *Journal of Geophysical Research*, 117(10), https://doi.org/10.1029/2011JD016858.

Kokhanovsky, A.A. and de Leeuw, G., 2009. *Satellite Aerosol Remote Sensing over Land*. Springer, Praxis Publishing, Chichester, UK.

Kozlov, V.S., Yausheva, E.P., Terpugova, S.A., Panchenko, M.V., Chernov D.G. and Shmargunov, V.P., 2014. Optical–microphysical properties of smoke haze from Siberian forest fires in summer 2012. *International Journal of Remote Sens*ing, 35(15), pp.5722-5741, http://dx.doi.org/10.1080/01431161.2014.945010.

Kumar, K.R., Kang, N. and Yin, Y., 2017. Classification of key aerosol types and their frequency distributions based on satellite remote sensing data at an industrially polluted city in the Yangtze River Delta, China. *International Journal of Climatology*, 38(1), doi: 10.1002/joc.5178.

Kumar, K.R., Sivakumar, V., Yin, Y., Reddy, R.R., Kang, N., Diao, Y., Joseph, A.A. and Xingna, Y., 2014. Long-term (2003-2013) climatological trends and variations in aerosol optical parameters retrieved from MODIS over three stations in South Africa. *Atmospheric Environment*, 95, pp.400-408, doi:10.1016/j.atmosenv.2014.07.001.

Lawrence, M.G. and Lelieveld, J., 2010. Atmospheric pollutant outflow from Southern Asia: A review. *Atmospheric Chemistry and Physics*, 10, pp.11017–11096, http://dx.doi. org/10.5194/acp-10-11017-2010.

L'eon, J.F., Chazette, P., Dulac, F., Pelon, J., Bonnazola, M., Foret, G., Alfaro, S.C., Cachier, H., Cautenet, S., Hamonou, E., Gaudichet, A., Gomes, L., Rajot, J,-L., Lavenu, F., Inamdar, S.R., Sarode, P.R., Kadadevarmath, J.S., 2001. Large scale advection of continental aerosols during INDOEX. *Journal of Geophysical Research*, 106(D22), pp.28427–28439, http://dx.doi.org/10.1029/2001JD900023.

L'eon, J.F., Derimian, Y., Chiapello, I., Tanr´e, D., Podvin, T., Chatenet, B., Diallo, A. and Deroo, C., 2009. Aerosol vertical distribution and optical properties over M'Bour (16.96º W; 14.39º N), Senegal from 2006 to 2008. *Atmospheric Chemistry and Physics*, 9, pp.9249–9261, www.atmos-chem-phys.net/9/9249/2009/.

Lelieveld, J., Crutzen, P.J., Andreae, M.O., Brenninkmeijer, C.A.M., Campos, T., Cass, G.R., Dickerson, R.R., Fischer, H., de Gouw, J.A., Hansel, A., Jefferson, A., Kley, D., de Laat, A.T., Lal, S., Lawrence, M.G., Lobert, J.M., Mayol-Bracero, O.L., Mitra, A.P., Novakov, T., Oltmans, S.J., Prather, K.A., Reiner, T., Rodhe, H., Scheeren, H.A., Sikka, D. and Williams, J., 2001. The Indian Ocean experiment: Widespread air pollution from South and South-East Asia. *Science*, 291, pp.1031–1036, doi: 10.1126/science.1057103.

Lestari, R.K., Watanabe, M., Imada, Y., Shiogama, H., Field, R.D., Takemura, T. and Kimoto, M., 2014. Increasing potential of biomass burning over Sumatra, Indonesia induced by anthropogenic tropical warming. *Environmental Research Letters*, 9, 104010 (7pp). doi:10.1088/1748-9326/9/10/104010.

Levin, Z. and Cotton, W.R., 2009. *Aerosol Pollution Impact on Precipitation. A Scientific Review*. Springer, ISBN: 978-1-4020-8689-2.

Levy, R., Mattoo, S., Munchak, L., Kleidman, R., Patadia, F. and Gupta, P., 2014. MODIS atmosphere team webinar series #2: Overview of collection 6 dark-target aerosol product, https://aerocenter.gsfc.nasa.gov.

Levy, R.C., Remer, L.A., Kleidman, R.G., Mattoo, S., Ichoku, C., Kahn, R. and Eck, T.F., 2010. Global evaluation of the collection 5 MODIS dark-target aerosol products over land. *Atmospheric Chemistry and Physics*, 10, pp.10399–10420, http://dx.doi.org/10.5194/acp-10-10399-2010.

Levy, R.C., Remer, L.A., Tanre, D., Kaufman, Y.J., Ichoku, C., Holben, B.N., Livingston, J.M., Russel, P.B. and Maring, H., 2003. Evaluation of the MODIS retrievals of dust aerosols over the ocean during PRIDE. *Journal of Geophysical Research*, 108(D14), 8594, doi: 10.1029/2002JD002460.

Li, J., Carlson, B.E., Dubovik, O. and Lacis, A.A., 2014. Recent trends in aerosol optical properties derived from AERONET measurements. *Atmospheric Chemistry and Physics*, 14, pp.12271–12289, https://doi.org/10.5194/acp-14-12271-2014.

Li, R.R., Kaufman, Y.J., Gao, B.C. and Davis, C.O., 2003. Remote sensing of suspended sediments and shallow coastal waters. *IEEE Transactions on Geoscience and Remote Sensing*, 41(3), pp.559-566.

Li, R.R., Remer, L., Kaufman, Y.J., Mattoo, S., Gao, B.-C. and Vermote, E., 2005. Snow an ice mask for the MODIS aerosol products. *IEEE Transactions in Geoscience and Remote Sensing*, 2(3), pp.306-310.

Li, Q.B., Jacob, D.J., Bey, I., Palmer, P.I., Duncan, B.N., Field, B.D., Martin, R.V., Fiore, A.M., Yantosca, R.M., Parrish, D.D., Simmonds, P.G. and Oltmans, S.J., 2002. Transatltantic transport of pollution and its effects on surface ozone in Europe and North America. *Journal of Geophysical Research*, 107(D13), 4166, doi: 10.1029/2001JD001422.

Liou, K.N., 2002. *An Introduction to Atmospheric Radiation*, Second Edition, International Geophysics Series, 84, ISBN 978-0-12-451451-5.

Liousse, C., Assamoi, E., Criqui, P., Granier, C. and Rosset, R., 2014. Explosive growth in African combustion emissions from 2005 to 2030. *Environmental Research Letters*, 9, 035003 (10pp), doi:10.1088/1748-9326/9/3/035003.

Liu, D., Wang, Z., Liu, Z., Winker, D. and Trepte, C., 2008. A height resolved global view of dust aerosols from the first year CALIPSO LIDAR measurements. *Journal of Geophysical Research*, 113, D16214, doi: 10.1029/2007JD009776.

Liu, Z., Vaughan, M.A., Winker, D.M., Kittaka, C., Getzewich, B., Kuehn, R., Omar, A., Powell, K., Trepte, C. and Hostetler, C., 2009. The CALIPSO LIDAR Cloud and Aerosol Discrimination: Version 2 Algorithm and Initial Assessment of Performance. *Journal of Atmospheric and Oceanic Technology*, 26, pp.1198–1213, doi: 10.1175/2009JTECHA1229.1.

Lu, Z., Streets, D.G., de Foy, B. and Krotkov, N.A., 2013. OMI observations of inter annual increase in SO_2 emissions from Indian coal-fired power plants during 2005–2012. *Environmental Science and Technology*, 47, pp.13993–14000, doi: 10.1021/es4039648.

Lu, Z., Streets, D.G., Zhang, Q., Wang, S., Carmichael, G.R., Cheng, Y.F., Wei, C., Chin, M., Diehl, T. and Tan, Q., 2010. Sulfurdioxide emissions in China and sulfur trends in East Asia since 2000. *Atmospheric Chemistry and Physics*, 10, pp.6311–6331. http://dx.doi.org/10.5194/acp-10-6311-2010.

Luhar, A.K., Mitchell, R.M., Meyer, C.P.M., Qin, Y., Campbell, S.K., Gras, J.L. and Parry, D., 2008. Biomass burning emissions over Northern Australia constrained by aerosol measurements: II – Model validation, and impacts on air quality and radiative forcing. *Atmospheric Environment*, 42(7), pp.1647–1664, http://dx.doi.org/10.1016/j.atmosenv.2007.12.040.

Luo, Y., Zheng, X., Zhao, T. and Chen, J., 2013. A climatology of aerosol optical depth over China from recent 10 years of MODIS remote sensing data. *International Journal of Climatology*, 34(3), pp.863-870, doi:10.1002/joc.3728.

Ma, X., Bartlett, K., Harmon, K. and Yu, F., 2013. Comparison of AOD between CALIPSO and MODIS: significant differences over major dust and biomass burning regions. *Atmospheric Measurement Techniques*, 6, pp.2391–2401, doi: 10.5194/amt-6-2391-2013.

Mamouri, R.E., Amiridis, V., Papayannis, A., Giannakaki, E., Tsaknakis, G., and Balis, D.S., 2009. Validation of CALIPSO spaceborne-derived attenuated extinction coefficient profiles using a ground-based LIDAR in Athens, Greece. *Atmospheric Measurement Techniques*, 2, pp.513–522, doi: 10.5194/amt-2-513-2009.

Mao, K.B., Ma, Y., Xia, L., Chen, W.Y., Shen, X.Y., He, T.J. and Xu, T.R., 2014. Global aerosol change in the last decade: An analysis based on MODIS data. *Atmospheric Environment*, 94, pp.680–686, http://dx.doi.org/10.1016/j.atmosenv.2014.04.053.

Marenco, F., Johnson, B., Langridge, J.M., Mulcahy, J., Benedetti, A., Remy, S., Jones, L., Szpek, K., Haywood, J., Longo, K. and Artaxo, P., 2016. On the vertical distribution of smoke in the Amazonian atmosphere during the dry season. *Atmospheric Chemistry and Physics*, 16, pp.2155–2174, doi: 10.5194/acp-16-2155-2016.

Maria, S.F., Russell, L.M., Gilles, M.K. and Myneni, S.C.B., 2004. Organic aerosol growth mechanisms and their climate-forcing implications, *Science*, 306, pp.1921-1924.

Marmer, E., Langmann, B., Fagerli, H. and Vestreng, V., 2007. Direct shortwave radiative forcing of sulphate aerosol over Europe from 1900 to 2000. *Journal of Geophysical Research*, 112(D23), D23S17, http://dx.doi.org/10.1029/2006JD008037.

Martins, J.V., Tanre, D., Remer, L.A., Kaufman, Y.J., Mattoo, S. and Levy, R., 2002. MODIS Cloud screening for remote sensing of aerosol over oceans using spatial variability. *Geophysical Research letters*, 29(12), doi: 10.1029/2001GL013252.

Martonchik, J.V., Diner, D.J., Crean, K.A. and Bull, M.A., 2002. Regional aerosol retrieval results from MISR. *IEEE Transactions on Geoscience and Remote Sensing*, 40, pp.1520-1531, doi: 10.1109/TGRS.2002.801142.

Martonchik, J.V., Diner, D.J., Kahn, R.A., Ackerman, T.P., Verstraete, M.M., Pinty, B. and Gordon, H.R., 1998. Techniques for the retrieval of aerosol properties over land and ocean using multi-angle imagery. *IEEE Transactions on Geoscience and Remote Sensing*, 36, pp.1212-1227, doi: 10.1109/36.701027.

Martonchik, J.V., Kahn, R.A. and Diner, D.J., 2009. *Retrieval of aerosol properties over land using MISR observations*. In Satellite Aerosol Remote Sensing over Land (eds. A.A., Kokhanovsky and G. de Leeuw), Springer, Praxis Publishing, Chichester, UK. http://dx.doi.org/10.1007/978-3-540-69397-0_9.

MAST-MODIS Aerosol Science Team, 2006. Algorithm Theoretical Basis Document (ATBD): algorithm for remote sensing of tropospheric aerosol from MODIS, available from http://modis-atmos.gsfc.nasa.gov/MOD04_L2.

Mehta, M., 2015. A study of aerosol optical depth variations over the Indian region using thirteen years (2001-2013) of MODIS and MISR Level 3 data. *Atmospheric Environment*, 109, pp.161-170, doi: 10.1016/j.atmosenv.2015.03.021.

Mehta, M., Singh, R., Singh, A., Singh, N. and Anshumali, 2016. Recent global aerosol optical depth variations and trends – A comparative study using MODIS and MISR Level 3 datasets. *Remote Sensing of Environment*, 181, pp.137-150, http://dx.doi.org/10.1016/j.rse.2016.04.004.

Menon, S., 2004. Current uncertainties in assessing aerosol effects on climate. *Annual Reviews of Environment and Resources*, 29, pp.1-30, https://doi.org/10.1146/annurev.energy.29.063003.132549.

Menzies, R.T. and Tratt, D.M., 2002. Aerosol layers over the Pacific Ocean: Vertical distributions and optical properties as observed by multi wavelength airborne LIDARs. *Journal of Geophysical Research*, 107(D16), 4292, doi: 10.1029/2001jd001196.

Miller, R.L. and Tegen, I., 1998. Climate response to soil dust aerosols. *Journal of Climatology*, 11, pp.3247–3267.

Mishchenko, M.I., Geogdzhayev, I.V., Rossow, W.B., Cairns, B., Carlson, B.E., Lacis, A.A. and Travis, L.D., 2007. Long-term satellite record reveals likely recent aerosol trend. *Science*, 315(5818), 1543, doi: 10.1126/science.1136709.

Mishra, A.K. and Shibata, T., 2012. Climatological aspects of seasonal variation of aerosol vertical distribution over central Indo-Gangetic belt (IGB) inferred by the space-borne LIDAR CALIOP. *Atmospheric Environment*, 46, pp.365-375, doi: 10.1016/j.atmosenv.2011.09.052

Mitchell, R.M., Campbell, S.K. and Qin, Y., 2010. Recent increase in aerosol loading over the Australian arid zone. *Atmospheric Chemistry and Physics*, 10, pp.1689–1699, doi: 10.5194/acp-10-1689-2010.

Mona, L., Amodeo, A., Pandolfi, M., and Pappalardo, G., 2006. Saharan dust intrusions in the Mediterranean area: three years of Raman LIDAR measurements. *Journal of Geophysical Research*, 111, D16203, doi: 10.1029/2005JD006569.

Mona, L., Liu, Z., Müller, D., Omar, A., Papayannis, A., Pappalardo, G., Sugimoto, N. and Vaughan, M., 2012. LIDAR Measurements for Desert Dust Characterization: An Overview. *Advances in Meteorology*, 356265, doi:10.1155/2012/356265.

Monorey, C., Davis, R. and Muller, J.P., 2002. MISR stereoscopic image matches: techniques and results. *IEEE Transactions on Geoscience and Remote Sensing*, 40, pp.1547-1559.

Murphy, D.M., Chow, J.C., Leibensperger, E.M., Malm, W.C., Pitchford, M., Schichtel, Watson, J.G. and White, W.H., 2011. Decreases in elemental carbon and fine particle mass in the United States. *Atmospheric Chemistry and Physics*, 11, pp.4679–4686, http://dx.doi.org/10.5194/acp-11-4679-2011.

Myhre, G., Samset, B.H., Schulz, M., Balkanski, Y., Bauer, S., Berntsen, T.K., Bian, H., Bellouin, N., Chin, M., Diehl, T., Easter, R.C., Feichter, J., Ghan, S.J., Hauglustaine, D., Iversen, T., Kinne, S., Kirkevåg, A., Lamarque, J.-F., Lin, G., Liu, X., Lund, M.T., Luo, G., Ma, X., van Noije, T., Penner, J.E., Rasch, P. J., Ruiz, A., Seland, Ø., Skeie, R.B., Stier, P., Takemura, T., Tsigaridis, K., Wang, P., Wang, Z., Xu, L., Yu, H., Yu, F., Yoon, J.-H., Zhang, K., Zhang, H. and Zhou, C., 2013a. Radiative forcing of the direct aerosol effect from AeroCom phase II simulations. *Atmospheric Chemistry and Physics*, 13, pp.1853-1877, doi: 10.5194/acp-13-1853-201.

Myhre, G., Shindell, D., Breon, F.-M., Collins, W., Fuglestvedt, J., Huang, J., Koch, D., Lamarque, J.-F., Lee, D., Mendoza, B., Nakajima, T., Robock, A., Stephens, G., Takemura, T., and Zhang, H. 2013b. *Anthropogenic and Natural Radiative Forcing*. In: Climate Change 2013: The Physical Science Basis. Contribution of Working Group I to the Fifth Assessment Report of the Intergovernmental Panel on Climate Change (eds. T.F., Stocker, D., Qin, G.K., Plattner, M., Tignor, S.K., Allen, J., Boschung, A., Nauels, Y., Xia, V., Bex, and P.M., Midgley), pp.659–740, Cambridge University Press, Cambridge, United Kingdom and New York, NY, USA,.

Navas-Guzmán, G., Bravo-Aranda, J.A., Guerrero-Rascado, J.L., Granados-Muñoz, M.J. and Alados-Arboledas, L., 2013. Statistical analysis of aerosol optical properties retrieved by Raman LIDAR over Southeastern Spain. *Tellus B: Chemical and Physical Meteorology*, 65(1), 21234, doi: 10.3402/tellusb.v65i0.21234.

Notaro, M., Yu, Y. and Kalashnikova, O.V., 2015. Regime shift in Arabian dust activity, triggered by persistent Fertile Crescent drought. *Journal of Geophysical Research*, 120, pp.10229–10249, doi: 10.1002/2015JD023855.

Nurrohim, A. and Sakugawa, H., 2004. A fuel-based inventory of NOx and SO_2 emissions from manufacturing industries in Hiroshima Prefecture, Japan. *Applied Energy*, 78(4), pp.355–369, http://dx.doi.org/10.1016/j.apenergy.2003.10.003.

O'Brien, D.M. and Mitchell, R.M., 2003. Atmospheric heating due to carbonaceous aerosol in Northern Australia — Confidence limits based on TOMS aerosol index and sun photometer data. *Atmospheric Research*, 66, pp.21–41, http://dx.doi.org/10.1016/S0169-8095(02)00173-4.

Ocko, I.B., Ramaswamy, V., Ginoux, P., Ming, Y. and Horowitz, L.W., 2012. Sensitivity of scattering and absorbing aerosol direct radiative forcing to physical climate factors. *Journal of Geophysical Research*, 117, D20203, doi: 10.1029/2012JD018019.

Ogugbuaja, V.O. and Barsisa, L.Z., 2001. Atmospheric pollution in north-East Nigeria: Analysis of suspended particulate matter. *Bulletin of the Chemical Society of Ethiopia*, 15(2), pp.109–117, http://dx.doi.org/10.4314/bcse.v15i2.20957.

Ogunjobi, K.O., Kim, Y.J. and He, Z., 2003. Aerosol optical properties during Asian dust storm episodes in South Korea. *Theoretical and Applied Climatology*, 76, pp.65–75, doi: 10.1007/s00704-003-0006-7.

Olsson, L., Eklundh, L., and Ardö, J., 2005. A recent greening of the Sahel–trends, patterns and potential causes. *Journal of Arid Environment*, 63, pp.556–566, doi:10.1016/j.jaridenv.2005.03.008.

Omar, A.H., Winker, D.M., Tackett, J.L., Giles, D.M., Kar, J., Liu, Z., Vaughan, M.A., Powell, K.A., and Trepte, C.R., 2013. CALIOP and AERONET aerosol optical depth comparisons: one size fits none. *Journal of Geophysical Research*, 118, pp.4748–4766, doi:10.1002/jgrd.50330.

Omar, A.H., Winker, D.M., Vaughan, M.A., Hu, Y., Trepte, C.R., Ferrare, R.A., Lee, K.-P. and Hostetler, C.A., 2009. The CALIPSO Automated Aerosol Classification and LIDAR Ratio Selection Algorithm. *Journal of Atmospheric and Oceanic Technology*, 26, pp.1994–2014, doi:10.1175/2009JTECHA1231.1.

Pace, G., di Sarra, A., Meloni, D., Piacentino, S. and Chamard, P., 2006. Aerosol optical properties at Lamped US (Central Mediterranean). 1. Influence of transport and identification of different aerosol types. *Atmospheric Chemistry and Physics*, 6, pp.697–713, http://dx.doi.org/10.5194/acp-6-697-2006.

Page, S.E., Siegert, F., Rieley, J.O., Boehm, H.D.V., Jaya, A. and Limin, S., 2002. The amount of carbon released from peat and forest fires in Indonesia during 1997. *Nature*, 420, pp.61–65, http://dx.doi.org/10.1038/nature01131.

Pandya, M.R., Singh, R.P. and Dadhwal, V.K., 2004. A signal of increased vegetation activity of India from 1981 to 2001 observed using satellite-derived fraction of absorbed photosynthetically active radiation. *Current Science*, 87(8), pp.1122–1126.

Panicker, A.S., Lee, D.I., Kumkar, Y.V., Kim, D., Makie, M. and Uyedaf, H., 2012. Decadal climatological trends of aerosol optical parameters over three different environments in South Korea. *International Journal of Climatology*, 33, pp.1909-1916, doi: 10.1002/joc.3557.

Papadimas, C.D., Hatzianastassiou, N., Mihalopoulos, N., Querol, X. and Vardavas, I., 2008. Spatial and temporal variability in aerosol properties over the Mediterranean basin on 6-year (2000-2006) MODIS data. *Journal of Geophysical Research*, 111, D11205, http://dx.doi.org/10.1029/2007JD009189.

Papagiannopoulos, N., Mona, L., Alados-Arboledas, L., Amiridis, V., Baars, H., Binietoglou, I., Bortoli, D., D'Amico, G., Giunta, A., Guerrero-Rascado, J.L., Schwarz, A., Pereira, S., Spinelli, N., Wandinger, U., Wang, X., and Pappalardo, G., 2016. CALIPSO climatological products: evaluation and suggestions from EARLINET. *Atmospheric Chemistry and Physics*, 16, pp.2341–2357, doi: 10.5194/acp-16-2341-2016.

Pappalardo, G., Wandinger, U., Mona, L., Hiebsch, A., Mattis, I., Amodeo, A., Ansmann, A., Seifert, P., Linné, H., Apituley, A., Arboledas, L.A., Balis, D., Chaikovsky, A., D'Amico, G., De Tomasi, F., Freudenthaler, V., Giannakaki, E., Giunta,A., Grigorov, I., Iarlori, M., Madonna, F., Mamouri, R.-E., Nasti, L., Papayannis, A., Pietruczuk, A., Pujadas, M., Rizi, V., Rocadenbosch, F., Russo, F., Schnell, F., Spinelli, N., Wang, X., Wiegner, M., 2010. EARLINET correlative measurements for CALIPSO: first inter comparison results. *Journal of Geophysical Research*, 115(D4), D00H19, doi: 10.1029/2009JD012147.

Park, S., Panicker, A.S., Lee, D.I., Jung, W.S., Jang, S.M. and Jang, M., 2011. Characterization of aerosol chemical properties over Anmyeon (South Korea), a super site under Global Atmosphere Watch. *Journal of Atmospheric Chemistry*, 67, pp.71–86, http://dx.doi.org/10.1007/s10874-011-9205-2.

Pathak, B., Subba, T., Dahutia, P., Bhuyan, P.K., Moorthy, K.K., Gogoi, M.M., Babu, S.S., Chutia, L., Ajay, P., Biswas, J., Bharali, C., Borgohain, A., Dhar, P., Guha, A., De, B.K., Banik, T., Chakraborty, M., Kundu, S.S., Sudhakar, S. and Singh, S.B., 2016. Aerosol characteristics in north-east India using ARFINET spectral optical depth measurements. *Atmospheric Environment*, 125, pp.461-473, http://dx.doi.org/10.1016/j.atmosenv.2015.07.038.

Peel, M.C., Finlayson, B.L., McMahon, T.A., 2007. Updated world map of the Köppen–Geiger climate classification. *Hydrology and Earth System Sciences*, 11, pp.1633–1644, doi: 10.5194/hess-11-1633-2007.

Penner, J.E., Andreae, M., Annegarn, H., Barrie, L., Feichter, J., Hegg, D., Jayaraman, A., Leaitch, R., Murphy, D., Nganga, J. and Pitari, G., 2001. Aerosols, their direct and indirect effects, in climate change, report to intergovernmental panel on climate change from the scientific assessment working group (WGI). *Cambridge University Press*, pp.289–416, http://hdl.handle.net/11858/00-001M-0000-0014-921E-5.

Plakhina, I.N., 2012. Variations in the aerosol optical depth above Russia from the data obtained at the Russian Actinometeric Network in 1976–2010 years. *Licence Intech*, pp.3–28, http://dx.doi.org/10.5772/48618.

Plakhina, I.N., Makhotkina, E.L. and Pankratova, N.V., 2007. Variations of aerosol optical thickness of the atmosphere in Russia in 1976–2003. *Russian Meteorology and Hydrology*, 32(2), pp.85–92, http://dx.doi.org/10.3103/S1068373907020021.

Platnick, S., King, M.D., Ackerman, S.A., Menzel, W.P., Baum, B.A., Riedi, J.C. and Frey, R.A., 2003. The MODIS cloud products: algorithms and examples from Terra. *IEEE Transactions on Geoscience and Remote Sensing*, 41(2), pp.459-473, doi: 10.1109/TGRS.2002.808301

Ponomarev, E.I., Kharuk, V.I. and Ranson, K.J., 2016. Wildfires Dynamics in Siberian Larch Forests. *Forests*, 7(6), 125, doi: 10.3390/f7060125.

Pozzer, A., de Meij, A., Yoon, J., Tost, H., Georgoulias, A.K. and Astitha, M., 2015. AOD trends during 2001–2010 from observations and model simulations. *Atmospheric Chemistry and Physics*, 15, pp.5521–5535, http://dx.doi.org/10.5194/acp-15-5521-2015.

Prasad, A.K. and Singh, R.P., 2006. Comparison of MISR-MODIS aerosol optical depth over the Indo-Gangetic basin during the DJF and summer seasons (2000–2005). *Remote Sensing of Environment*, 107, pp.109–119, http://dx.doi.org/10.1016/j.rse.2006.09.026.

Preisendorfer, R.W., 1998. *Principal Component Analysis in Meteorology and Oceanography*. Elsevier Science, New York.

Prijith, S.S., Babu, S.S., Lakshmi, N.B., Satheesh, S.K., Moorthy, K.K., 2016. Meridional gradients in aerosol vertical distribution over Indian Mainland: Observations and model simulations, *Atmospheric Environment*, 125, pp.337-345, http://dx.doi.org/10.1016/j.atmosenv.2015.10.066.

Prospero, J.M., 1999. Long-term measurements of the transport of African mineral dust to the southeastern United States: Implications for regional air quality. *Journal of Geophysical Research*, 104(D13), pp.15917-15927, https://doi.org/10.1029/1999JD900072.

Quinn, P.K., Shaw, G., Andrews, E., Dutton, E.G., Ruoho-Airola, T. and Gong, S.L., 2007. Arctic haze: Current trends and knowledge gaps. *Tellus*, 59B, pp.99–114, http://dx.doi.org/10.1111/j.1600-0889.2006.00238.x.

Ramachandran, S., Kedia, S. and Sheel, V., 2015. Spatio temporal characteristics of aerosols in India: Observations and model simulations. *Atmospheric Environment*, 116, pp.225–244, http://dx.doi.org/10.1016/j.atmosenv.2015.06.015.

Ramachandran, S., Kedia, S. and Srivastava, R., 2012. Aerosol optical depth trends over different regions of India. *Atmospheric Environment*, 49, pp.338–347, http://dx.doi.org/10.1016/j.atmosenv.2011.11.017.

Ramanathan, V., Crutzen, P.J., Kiehl, J.T. and Rosenfeld, D., 2001a. Aerosols, climate and the hydrological cycle. *Science*, 294, pp.2119–2124, http://dx.doi.org/10.1126/science.1064034.

Ramanathan, V., Crutzen, P.J., Lelieveld, J., Mitra, A.P., Althausen, D., Anderson, J., Andreae, M.O., Cantrell, W., Cass, G.R., Chung, C.E., Clarke, A.D., Coakley, J.A., Collins, W.D., Conant, W.C., Dulac, F., Heintzenberg, J., Heymsfield, A.J., Holben, B., Howell, S., Hudson, J., Jayaraman, A., Kiehl, J.T., Krishnamurti, T.N., Lubin, D., McFarquhar, G.,

Novakov, T., Ogren, J.A., Podgorny, I.A., Prather, K., Priestley, K., Prospero, J.M., Quinn, P.K., Rajeev, K., Rasch, P., Rupert, S., Sadourny, R.,Satheesh, S.K., Shaw, G.E., Sheridan, P. and Valero, F.P.J., 2001b. The Indian Ocean experiment: An integrated analysis of the climate forcing and effects of the great Indo-Asian haze. *Journal of Geophysical Research*, 106, pp.28371–28398, http://dx.doi.org/10.1029/2001JD900133.

Rashki, A., Kaskaoutis, D.G., Eriksson, P.G., de W. Rautenbach, C.J., Flamant, C., Abdi Vishkaee, F., 2014. Spatio-temporal variability of dust aerosols over the Sistan region in Iran based on satellite observations. *Natural Hazards*, 71, pp.563-585, doi: 10.1007/s11069-013-0927-0.

Reddington, C.L., Butt, E.W., Ridley, D.A., Artaxo, P., Morgan, W.T., Coe, H. and Spracklen, D.V., 2015. Air quality and human health improvements from reductions in deforestation-related fire in Brazil. *Nature Geosciences*, 8, pp.768-771, doi: 10.1038/ngeo2535.

Redemann, J., Vaughan, M.A., Zhang, Q., Shinozuka, Y., Russell, P.B., Livingston, J.M., Kacenelenbogen, M., and Remer, L.A., 2012. The comparison of MODIS-Aqua (C5) and CALIOP (V2 & V3) aerosol optical depth. *Atmospheric Chemistry and Physics*, 12, pp.3025–3043, doi: 10.5194/acp-12-3025-2012.

Remer, L.A., Chin, M., de Cola, P., Feingold, G., Halthore, R., Kahn, R.A., Quinn, P.K., Rind, D., Schwartz, S.E., Streets, D. and Yu, H., 2009. *Executive Summary*, In Atmospheric Aerosol Properties and Climate Impacts. (eds. M. Chin, R.A. Kahn and S.E. Schwartz), A report by the U.S. climate change science program and the subcommittee on global change research, US, National Aeronautics and Space Administration, Washington, D.C..

Remer, L.A., Kaufman, Y.J., Tanre, D., Mattoo, S., Chu, D.A., Martins, J.V., Li, R.-R., Ichoku, C., Levy, R.C., Kleidman, R.G., Eck, T.F., Vermote, E. and Holben, B.N., 2005. The MODIS aerosol algorithm, products and validation. *Journal of the Atmospheric Sciences*, 62, pp.947–973, http://dx.doi.org/10.1175/JAS3385.1.

Remer, L.A., Kleidman, R., Levy, R., Kaufman, Y., Tanré, D., Mattoo, S., Mattoo, S., Martins, J.V., Ichoku, C., Koren, I., Yu, H. and Holben, B.N., 2008. Global aerosol climatology

from the MODIS satellite sensors. *Journal of Geophysical Research*, 113(D14), D14S07, https://dx.doi.org/10.1029/2007JD009661.

Remer, L.A., Tanre, D., Kaufman, Y.J., Ichoku, C., Mattoo, S., Levy, R., Chu, D.A., Chu, Holben, B.N., Dubovik, O., Smirnov, A., Martins, J.V., Li, R.R. and Ahmed, Z., 2002. Validation of MODIS aerosol retrieval over ocean. *Geophysical Research Letters*, 29(12), doi: 10.1029/2001GL013204.

Remy, S., Veira, A., Paugam, R., Sofiev, M., Kaiser, J.W., Marenco, F., Burton, S.P., Benedetti, A., Engelen, R. J., Ferrare, R. and Hair, J.W., 2017. Two global data sets of daily fire emission injection heights since 2003. *Atmospheric Chemistry and Phyics*, 17, pp.2921-2942, doi: 10.5194/acp-17-2921-2017.

Richter, A., Eyring, V., Burrows, J.P., Bovensmann, H., Lauer, A., Sierk, B. and Crutzen, P.J., 2004. Satellite measurements of NO_2 from international shipping emissions. *Geophysical Research Letters*, 31, L23110, http://dx.doi.org/10.1029/2004GL020822.

Ridley, D.A., Heald, C.L. and Prospero, J.M., 2014. What controls the recent changes in African mineral dust aerosol across the Atlantic? *Atmospheric Chemistry and Phys*ics, 14, pp.5735–5747, doi: 10.5194/acp-14-5735-2014.

Roberts, G., Wooster, M.J. and Lagoudakis E., 2009. Annual and diurnal African biomass burning temporal dynamics. *Biogeosciences*, 6, pp.849–866, www.biogeosciences.net/6/849/2009/.

Rosen, J., Young, S.A., Laby, J., Kjome, N. and Gras, J.L., 2000. Springtime aerosol layers in the free troposphere over Australia: Mildura aerosol tropospheric experiment (MATE 98). *Journal of Geophysical Research*, 105, pp.17833–17842, http://dx.doi.org/10.1029/2000JD900208.

Rossow, W.B., 1989. Measuring cloud properties from space: A review. *Journal of Climate*, 2, pp.201-213, doi: 10.1175/1520-0442(1989)002<0201:MCPFSA>2.0.CO;2.

Rossow, W.B., Mosher, F., Kinsella, E., Arking, A., Desbois, M., Harrison, E., Minnis, P., Ruprecht, E., Seze, G., Simmer, C. and Smith, E., 1985. ISCCP cloud algorithm inter

comparison. Journal of Climatology and Applied Meterology, 24(9), pp.887-903, https://doi.org/10.1175/1520-0450(1985)024<0887:ICAI>2.0.CO;2

Roujean, J.-L., Tanre, D., Brecon, F.-M. and Deuze, J.-L., 1997. Retrieval of land surface parameters from airborne POLDER bidirectional reflectance distribution function during HAPEX-Sahel. *Journal of Geophysical Research*, 102(D10), pp.201-218.

Ruiz-Arias, J.A., Dudhia, J., Gueymard, C.A. and Pozo-Vazquez, D., 2013. Assessment of the MODIS daily aerosol optical depth in the context of surface solar radiation and numerical weather modelling. *Atmospheric Chemistry and Physics*, 13, pp.675-692, doi: 10.5194/acp-13-675-2013.

Salomonson, V.V., Barnes, W.L., Maymon, P.W., Montgomery, H.E. and Ostrow, H., 1989. MODIS, advanced facility instrument for studies of the earth as a system. *IEEE Transactions on Geoscience and Remote Sensing*, 27, pp.145-153.

Samset, B.H., Myhre, G., Schluz, M., Balkanski, Y., Bauer, S., Berntsen, T.K., Bian, H., Bellouin, N., Diehl, T., Easter, R.C., Ghan, S.J., Iversen, T., Kinne, S., Kirkevag A., Lamarque, J.-F., Lin, G., Liu, X., Penner, J.E., Seland, O., Skeie, R.B., Stier, P., Takemura, T., Tsigaridis, K. and Zhang, K., 2013. Black carbon vertical profiles strongly affect its radiative forcing uncertainty. *Atmospheric Chemistry and Physics*, 13, pp. 2423–2434, https://doi.org/10.5194/acp-13-1853-2013.

Santer, R., Carrere, V., Dubuisson, P. and Roger, J.C., 1999. Atmospheric correction over land for MERIS. *International Journal of Remote Sensing*, 20, pp.1819-1840.

Sarangi, C., Tripathi, S.N., Mishra, A.K., Goel, A. and Welton, E.J., 2016. Elevated aerosol layers and their radiative impact over Kanpur during monsoon onset period. *Journal of Geophysical Research*, 121, pp.7936–7957, doi: 10.1002/2015JD024711.

Satheesh, S.K., Moorthy, K.K., Babu, S.S., Vinoj, V. and Dutt, C.B.S., 2008. Climate implications of large warming by elevated aerosol over India. *Geophysical Research Letters*, 35, L19809, doi: 10.1029/2008GL034944.

Schulz, M., Leeuw, G. de and Balkanski, Y., 2004. *Sea-salt aerosol source functions and emissions.* In Emissions of Atmospheric Trace compounds (eds. C. Granier, P. Artaxo and C.E. Reeves), pp. 333-359, Springer, Kluwer, Dordrecht.

Schulz, M., Textor, C., Kinne, S., Balkanski, Y., Bauer, S., Berntsen, T., Berglen, T., Boucher, O., Dentener, F., Guibert, S., Isaksen, I.S.A., Iversen, T., Koch, D., Kirkevåg, A., Liu, X., Montanaro, V., Myhre, G., Penner, J.E., Pitari, G., Reddy, S., Seland, Ø., Stier, P., and Takemura, T., 2006. Radiative forcing by aerosols as derived from the AeroCom present-day and pre-industrial simulations. *Atmospheric Chemistry and Phys*ics, 6, pp.5225–5246, doi: 10.5194/acp-6-5225-2006.

Schuster, G.L., Vaughan, M., MacDonnel, D., Su, W., Winker, D., Dubovik, O., Lapyonok, T. and Trepte, C., 2012. Comparison of CALIPSO aerosol optical depth retrievals to AERONET measurements, and a climatology for the LIDAR ratio of dust. *Atmospheric Chemistry and Phys*ics, 12, pp.7431-7452, doi: 10.5194/acp-12-7431-2012.

Seinfeld, J.H. and Pandis, S.N., 2006. *Atmospheric Chemistry and Physics: From Air Pollution to Climate Change*, John Wiley & Sons, New York.

Shao, Y., Klose, M., and Wyrwoll K.H., 2013. Recent global dust trend and connections to climate forcing. *Journal of Geophysical Research*, 118, pp.11107–11118, doi:10.1002/jgrd.50836.

Sharma, A.R., Kharol, S.K., Badarinath, K.V.S. and Singh, D., 2010. Impact of agriculture crop residue burning on atmospheric aerosol loading e a study over Punjab State, India. *Annals of Geophysics*, 28, pp.367–379, http://dx.doi.org/10.5194/angeo-28-367-2010.

Shi, Y., Zhang, J., Reid, J.S., Hyer, E.J., Eck, T.F., Holben, B.N. and Kahn, R.A., 2011. A critical examination of spatial biases between MODIS and MISR aerosol products — Application for potential AERONET deployment. *Atmospheric Measurement Techniques*, 4, pp.2823–2836. http://dx.doi.org/10.5194/amt-4-2823-2011.

Shi, Y., Zhang, J., Reid, J.S., Hyer, E.J. and Hsu, N.C., 2013. Critical evaluation of the MODIS Deep Blue aerosol optical depth product for data assimilation over North Africa. *Atmospheric Measurement Techniques*, 6, pp.949–969, http://dx.doi.org/10.5194/amt-6-949-2013.

Shvidenko, A.Z. and Schepaschenko, D.G., 2013. Climate change and wildfires in Russia. *Contemporary Problems of Ecology,* 6(7), pp.683-692, doi: 10.1134/S199542551307010X.

Silva, P., Bastos, A., DaCamara, C.C. and Libonati, R., 2016. Future projections of fire occurrence in Brazil using EC-Earth Climate Model. *Revista Brasileira de Meteorologia*, 31(3), pp.288-297, doi: http://dx.doi.org/10.1590/0102-778631320150142.

Soja, A.J., Cofer, W.R., Shugart, H.H., Sukhinin, A.I., Stackhouse, P.W., Jr., McRae, D.J. and Conard, S.G., 2004. Estimating fire emissions and disparities in boreal Siberia (1998–2002). *Journal of Geophysical Research*, 109, D14S06, http://dx.doi.org/10.1029/2004JD004570.

Solanki, R. and Singh, N., 2014. LIDAR observations of the vertical distribution of aerosols in free troposphere: Comparison with CALIPSO level-2 data over the central Himalayas. *Atmospheric Environment*, 99, pp.227-238, http://dx.doi.org/10.1016/j.atmosenv.2014.09.083.

Stowe, L.L., Jacobowitz, H., Ohring, G., Knapp, K.R. and Nalli, N.R. 2002. The Advanced very High Resolution Radiometer (AVHRR) Pathfinder Atmosphere (PATMOS) climate dataset: initial analysis and evaluations. *Journal of Climate*, 15, pp.1243-1260.

Streets, D.G., Yarber, K.F., Woo, J.H. and Carmichael, G.R., 2003. Biomass burning in Asia: Annual and seasonal estimates and atmospheric emissions. *Global Biogeochemical Cycles*, 17, 1099, GB002040, http://dx.doi.org/10.1029/2003.

Swap, R.J., Annegarn, H.J., Suttles, J.T., King, M.D., Platnick, S., Privette, J.L. and Scholes, R.J., 2003. Africa burning: A thematic analysis of the Southern African Regional Science Initiative (SAFARI 2000). *Journal of Geophysical Research*, 108, 8465, doi: 8410.1029/2003JD003747.

Tafuro, A.M., Barnaba, F., de Tomasi, F., Perrone, M.R. and Gobbi, G.P., 2006. Saharan dust particle properties over the Central Mediterranean. *Atmospheric Research*, 81, pp.67–93, http://dx.doi.org/10.1016/j.atmosres.2005.11.008.

Tan, C., Zhao, T., Xu, X., Liu, J., Zhang, L. and Tang, L., 2015. Climatic analysis of satellite aerosol data on variations of submicron aerosols over East China. *Atmospheric Environment*, 123, pp.392-398, http://doi.org/10.1016/j.atmosenv.2015.03.054.

Tanaka, T.Y. and Chiba, M., 2006. A numerical study of the contributions of dust source regions to the global dust budget. *Global and Planetary Change*, 52, pp.88–104, http://dx.doi.org/10.1016/j.gloplacha.2006.02.002.

Tanre, D., Kaufman, Y.J., Herman, M. and Mattoo, S., 1997. Remote sensing of aerosol properties over oceans using the MODIS/EOS spectral radiances. *Journal of Geophysical Research*, 102(D14), pp.16971-16988.

Textor , C., Schulz, M., Guibert, S., KInne, S., Balkansk, Y., Bauer, S., Berntsen, T., Berglen, T., Boucher, O., Chin, M., Dentener, F., Diehl, T., Easter, R., Feichter, H., Fillmore, D., Ghan, S., Ginoux, P., Gong, S., Grini, A., Hendricks, J., Horowitz, L., Huang, P., Isaksen, I., Iversen, I., Kloster, S., Koch, D., Kirkevåg, A., Kristjansson, J.E., Krol, M., Lauer, A., Lamarque, J.F., Liu, X., Montanaro, V., Myhre, G., Penner, J., Pitari, G., Reddy, S., Seland, Ø., Stier, P., Takemura, T., and Tie, X., 2006. Analysis and quantification of the diversities of aerosol life cycles within AeroCom. *Atmospheric Chemistry and Physics*, 6, pp.1777-1813, doi: 10.5194/acp-6-1777-2006.

Tian, P., Cao, X., Zhang, L., Sun, N., Sun, L., Logan, T., Shi, J., Wang, Y., Ji, Y., Lin, Y., Huang, Z., Zhou, T., Shi, Y., and Zhang, R., 2017. Aerosol vertical distribution and optical properties over China from long-term satellite and ground-based remote sensing. *Atmospheric Chemistry and Physics*, 17, pp.2509–2523, doi: 10.5194/acp-17-2509-2017.

Tiwari, S., Mishra, A.K. and Singh, A.K., 2016. Aerosol climatology over the Bay of Bengal and Arabian Sea inferred from space-borne Radiometers and LIDAR observations. *Aerosol and Air Quality Research*, 16, pp.2855–2868, doi: 10.4209/aaqr.2015.06.0406.

Torres, O., Decae, R., Veefkind, J.P. and de Leeuw, G., 2002. *OMI aerosol retrieval algorithm*. In OMI Algorithm Theoretical Basis Document, Vol III: Clouds, Aerosols and Surface UV Irradiance (eds. P. Stammes and R. Noordhoek), ATBD-OMI-03, pp.46-71.

Tørseth, K., Aas, W., Breivik, K., Fjæraa, A.M., Fiebig, M., Hjellbrekke, A.G., Myhre, L.C., Solberg, S., and Yttri, K. E., 2012. Introduction to the European Monitoring and

Evaluation Programme (EMEP) and observed atmospheric composition change during 1972–2009. *Atmospheric Chemistry and Physics*, 12, pp.5447–5481, http://dx.doi.org/10.5194/acp-12-5447-2012.

Tosca, M.G., Randerson, J.T., Zender, C.S., Nelson, D.L., Diner, D.J. and Logan, J.A., 2011. Dynamics of fire plumes and smoke clouds associated with peat and deforestation fires in Indonesia. *Journal of Geophysical Research*, 116, D08207, doi: 10.1029/2010JD015148.

Vaughan, M.A., Powell, K.A., Kuehn, R.E., Young, S.A., Winker, D.M., Hostetler, C.A., Hunt, W.H., Liu, Z., McGill, M.J. and Getzewich, B.J., 2009. Fully Automated Detection of Cloud and Aerosol Layers in the CALIPSO LIDAR Measurements. *Journal of Atmospheric and Oceanic Tech*nology, 26, pp.2034–2050.

Vestreng, V., Myhre, G., Fagerli, H., Reis, S. and Tarrasón, L., 2007. Twenty-five years of continuous sulphur dioxide emission reduction in Europe. *Atmospheric Chemistry and Physics*, 7, pp.3663–3681, http://dx.doi.org/10.5194/acp-7-3663-2007.

von Hoyningen-Huene, W., Freitag, M. and Burrows, J.B., 2003. Retrieval of aerosol optical thickness over land surfaces from top-of-atmosphere radiances. *Journal of Geophysical Research*, 108, 4260, doi: 10.1029/2001JD002018.

Wandinger, U., Hiebsch, A., Mattis, I., Pappalardo, G., Mona, L., and Madonna, F., 2011. *Aerosols and clouds: Long-term database from space borne LIDAR measurements*, Technical Report, Final Report, ESTEC Contract 21487/08/NL/HE, ESA Publications Division, Noordwijk, The Netherlands.

Wang, K.C., Dickinson, R.E. and Liang, S.L., 2009. Clear sky visibility has decreased over land globally from 1973 to 2007. *Science*, 323, pp.1468–1470, http://dx.doi.org/10.1126/science.1167549.

Wang, X., Huang, J., Ji, M. and Higuchi, K., 2008. Variability of East Asia dust events and their long-term trend. *Atmospheric Environment*, 42, pp.3156–3165, doi:10.1016/j.atmosenv.2007.07.046.

Weatherhead, E.C., Reinsel, G.C., Tiao, G.C., Meng, X., Choi, D., Cheang, W., Keller, T., DeLuisi, J., Wuebbles, D.J., Kerr, J.B., Miller, A.J., Oltmans, S.J. and Frederick, J.E., 1998. Factors affecting the detection of trends: statistical considerations and applications to environmental data. *Journal of Geophysical Research*, 103(D14), pp.17149-17161.

Wehrli, C., 2000. Calibration of filter radiometers for determination of atmospheric optical depth. *Metrologia*, 37, pp.419-422.

Westerling, A.L.R., 2016. Increasing western US forest wildfire activity: sensitivity to changes in the timing of spring. *Philosophical Transactions of Royal Society B*, 371, 20150178, http://dx.doi.org/10.1098/rstb.2015.0178.

Williams, A.P. and Abatzoglou, J.T., 2016. Recent advances and remaining uncertainties in resolving past and future climate effects on global fire activity. *Current Climate Change Reports*, 2, pp.1–14, doi: 10.1007/s40641-016-0031-0.

Winker, D.M., Couch, R.H. and McCormick, M.P., 2003. The CALIPSO Mission: Spaceborne LIDAR for observation of aerosols and clouds. *Proceedings SPIE*, 4893, pp.1-11.

Winker, D.M., Pelon, J., Coakley Jr., J.A., Ackerman, S.A., Charlson, R.J., Colarco, P.R., Flamant, P., Fu, Q., Hoff, R., Kittaka, C., Kubar, T.L., LeTreut, H., McCormick, M.P., Megie, G., Poole, L., Powell, K., Trepte, C., Vaughan, M.A. and Wielicki, B.A., 2010. The CALIPSO Mission: A global 3D view of aerosols and clouds. *Bulletin of American Meteorological Society*, 91, pp.1211-1229, doi: 10.1175/2010BAMS3009.1.

Winker, D.M., Tackett, J.L., Getzewich, B.J., Liu, Z., Vaughan, M.A. and Rogers, R.R., 2013. The global 3-D distribution of tropospheric aerosols as characterized by CALIOP. *Atmospheric Chemistry and Physics*, 13, pp.3345-3361, doi: 10.5194/acp-13-3345-2013.

Winker, D.M., Vaughan, M.A., Omar, A.H., Hu. Y. and Powell, K.A., 2009. Overview of the CALIPSO Mission and CALIOP data processing algorithms. *Journal of Atmospheric and Oceanic Technology*, 26, pp.2310–2323.

World Population Clock, 2015. US Census Bureau, www.census.gov/popclock/world.

World Population Prospects, 2015. Revision, key findings and advance tables. United Nations, New York: Department of Economic and Social Affairs, Population Division.

Xia, X.G., 2011. Variability of aerosol optical depth and Ångström wavelength exponent derived from AERONET observations in recent decades. *Environmental Research Letters*, 6, 044011, http://dx.doi.org/10.1088/1748- 9326/6/4/044011.

Xing, J., Pleim, J., Mathur, R., Pouliot, G., Hogrefe, C., Gan, C.M. and Wei, C., 2013. Historical gaseous and primary aerosol emissions in the United States from 1990–2010. *Atmospheric Chemistry and Physics*, 13, pp.7531–7549, https://doi.org/10.5194/acp-13-7531-2013.

Xu, H., Guo, J., Wang, Y., Zhao, C., Zhang, Z., Min, M., Miao, Y., Liu, H., He, J., Zhou, S. and Zhai, P., 2017. Warming effect of dust aerosols modulated by overlapping clouds below. *Atmospheric Environment*, 166, pp.393-402, http://dx.doi.org/10.1016/j.atmosenv.2017.07.036.

Yang, Y., Di Girolamo, L. and Mazzoni, D., 2007. Selection of the automated thresholding algorithm for the Multi-angle Imaging Spectroradiometer Camera-by-Camera Cloud Mask over land. *Remote Sensing of Environment*, 107, pp.159-171, doi: 10.1016/j.rse.2006.05.020.

Yienger, J.J., Galanter, M., Holloway, T.A., Phadnis, M.J., Guttikunda, S.K., Carmichael, G.R., Moxim, W.J. and Levi, H.L.II., 2000. The episodic nature of air pollution transport from Asia to North America. *Journal of Geophysical Research*, 105, pp.26931-26945, https://doi.org/10.1029/2000JD900309.

Yoon, J., Burrows, J.P., Vountas, M., von Hoyningen-Huene, W., Chang, D.Y., Richter, A. and Hilbol, A., 2014. Changes in atmospheric aerosol loading retrieved from space-based measurements during the past decade. *Atmospheric Chemistry and Physics*, 14, pp.6881–6902, http://dx.doi.org/10.5194/acp-14-6881-2014.

Yoon, J. and Pozzer, A., 2014. Model-simulated trend of surface carbon monoxide for the 2001–2010 decade. *Atmospheric Chemistry and Physics*, 14, pp.10465–10482, http://dx.doi.org/10.5194/acp-14-10465-2014.

Yoon, J., von Hoyningen-Huene, W., Kokhanovsky, A.A., Vountas, M., and Burrows, J.P., 2012. Trend analysis of aerosol optical thickness and Ångström exponent derived from the

global AERONET spectral observations. *Atmospheric Measurement Techniques*, 5, pp.1271–1299, doi: 10.5194/amt-5-1271-2012.

Yoon, J., von Hoyningen-Huene, W., Vountas, M. and Burrows, J.P., 2011. Analysis of linear long-term trend of aerosol optical thickness derived from SeaWiFS using BAER over Europe and South China. *Atmospheric Chemistry and Physics*, 11, pp.12149–12167, http://dx.doi.org/10.5194/acp-11-12149-2011.

Young, S.A. and Vaughan, M.A., 2009. The retrieval of profiles of particulate extinction from Cloud Aerosol LIDAR Infrared Pathfinder Satellite Observations (CALIPSO) data: Algorithm description. *Journal of Atmospheric and Oceanic Technology*, 26, pp.1105–1119, https://doi.org/10.1175/2008JTECHA1221.1.

Young, S.A., Vaughan, M.A., Kuehn, R.E. and Winker, D.M., 2013. The retrieval of profiles of particulate extinction from Cloud-Aerosol LIDAR Infrared Pathfinder Satellite Observations (CALIPSO) data: Uncertainity and error sensitivity analysis. *Journal of Atmospheric and Oceanic Technology*, 33, doi: 10.1175/JTECH-D-12-00046.1.

Yu, H., Chin, M., Winker, D.M., Omar, A.H., Liu, Z., Kittaka, C., and Diehl, T., 2010. Global view of aerosol vertical distributions from CALIPSO LIDAR measurements and GOCART simulations: Regional and seasonal variations. *Journal of Geophysical Research*, 115, D00H30, pp.395-428, doi: 10.1029/2009JD013364.

Yu, H., Remer, L.A., Chin, M., Bian, H., Tan, Q. and Yuan, T., 2012. Aerosols from overseas rival domestic emissions over North America. *Science*, 337, pp.566–569. http://dx.doi.org/10.1126/science.1217576.

Zarzycki, C.M. and Bond, T.C., 2010. How much can the vertical distribution of black carbon affect its global direct radiative forcing? *Geophysical Research Letters*, 37, L20807, doi: 10.1029/2010GL044555.

Zhang, J. and Reid, J.S., 2010. A decadal regional and global trend analysis of the aerosol optical depth using a data-assimilation grade over-water MODIS and level 2 MISR aerosol products. *Atmospheric Chemistry and Physics*, 10, pp.10949–10963, http://dx.doi.org/10.5194/acp-10-10949-2010.

Zhang, L., Henze, D.K., Grell, G.A., Torres, O., Jethva, H. and Lamsal, L.N., 2017. What factors control the trend of increasing AAOD over the United States in the last decade? *Journal of Geophysical Research*, 122, pp.1797–1810, doi: 10.1002/2016JD025472.

Zhao, T.X.P., Laszlo, I., Guo, W., Heidinger, A., Cao, C., Jelenak, A., Tarpley, D. and Sullivan, J., 2008. Study of long-term trend in aerosol optical thickness observed from operational AVHRR satellite instrument. *Journal of Geophysical Research*, 113, D07201, http://dx.doi.org/10.1029/2007JD009061.

Zhou, Y., Brunner, D., Hueglin, C., Henne, S. and Staehelin, J., 2012. Changes in OMI tropospheric NO_2 columns over Europe from 2004 to 2009 and the influence of meteorological variability. *Atmospheric Environment*, 46, pp.482–495, http://dx.doi.org/10.1016/j. atmosenv.2011.09.024.

ANNEXURE I

Flowchart showing the processing steps required in DT retrieval method for MODIS before chosing the over ocean and land algorithms

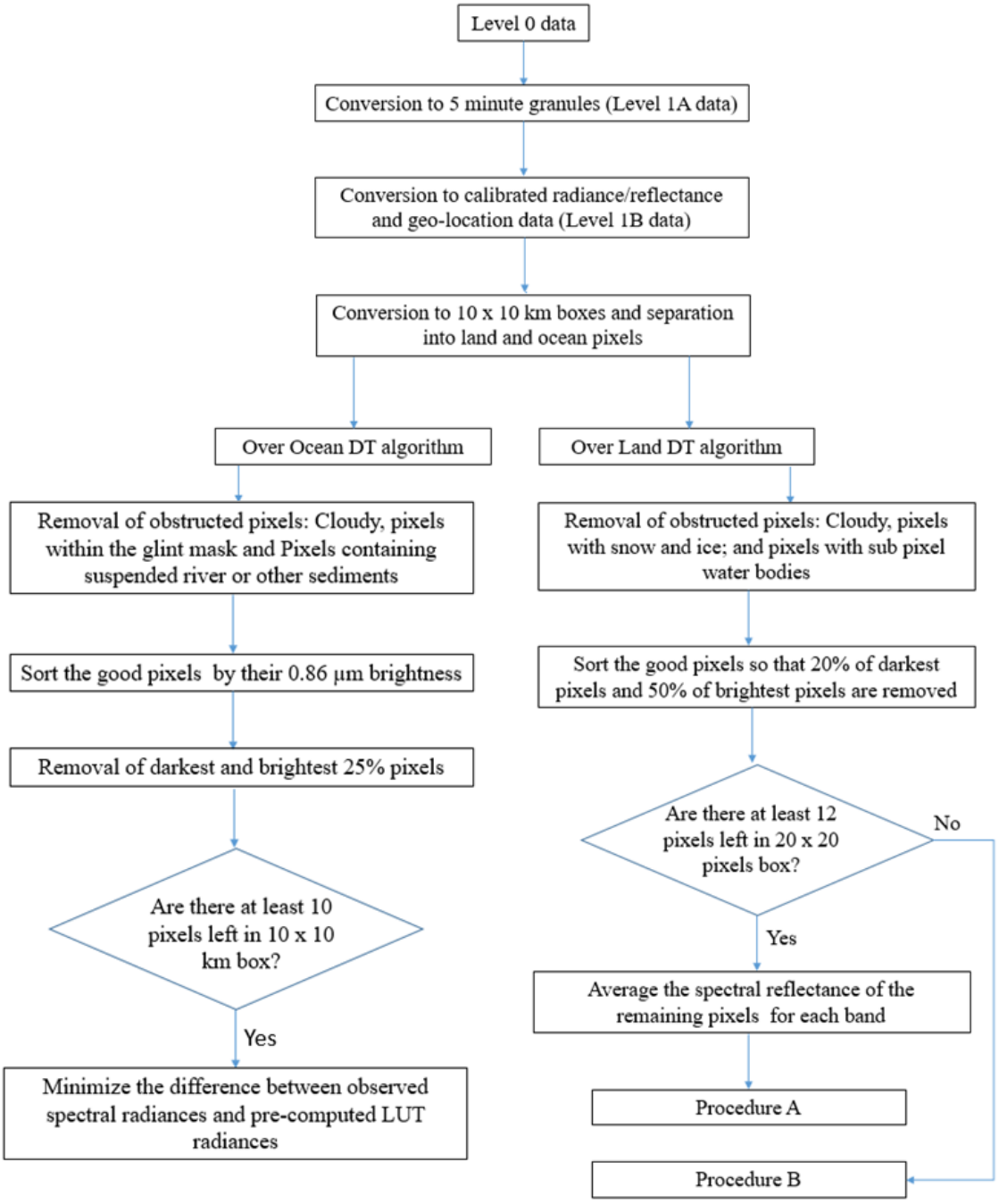

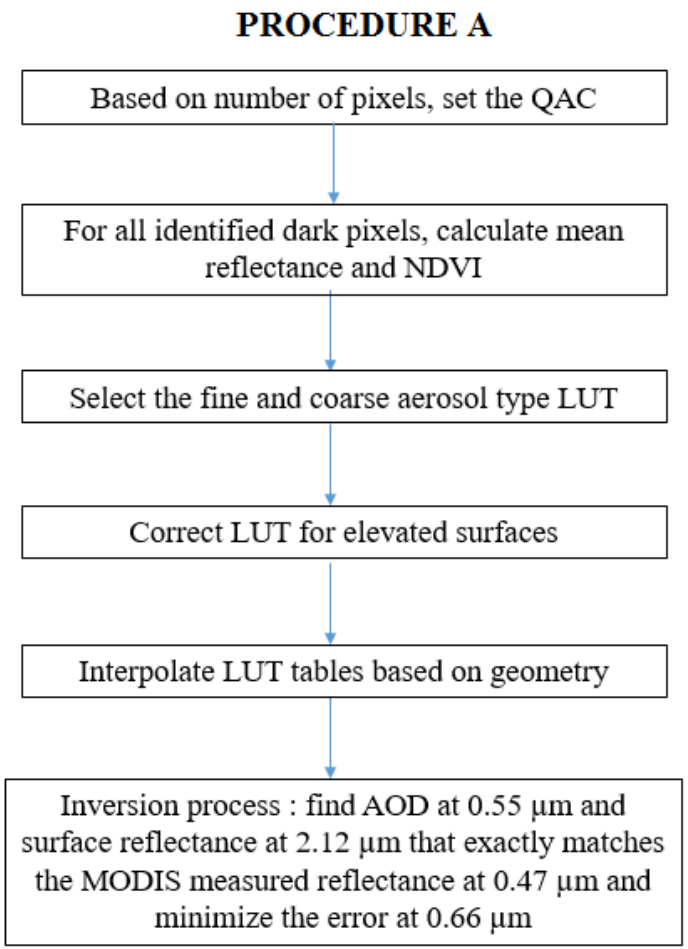
PROCEDURE A
Based on number of pixels, set the QAC
For all identified dark pixels, calculate mean reflectance and NDVI
Select the fine and coarse aerosol type LUT
Correct LUT for elevated surfaces
Interpolate LUT tables based on geometry
Inversion process : find AOD at 0.55 µm and surface reflectance at 2.12 µm that exactly matches the MODIS measured reflectance at 0.47 µm and minimize the error at 0.66 µm

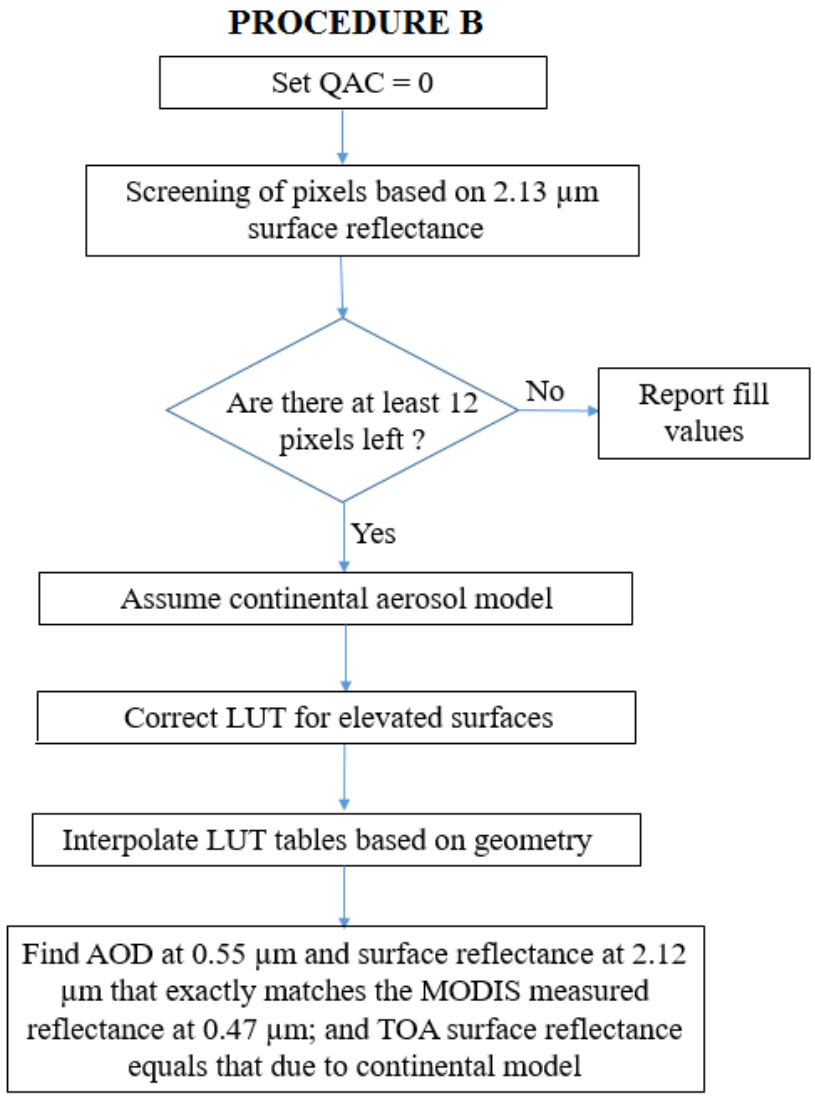
PROCEDURE B
Set QAC = 0
Screening of pixels based on 2.13 µm surface reflectance
Are there at least 12 pixels left ?
No
Report fill values
Yes
Assume continental aerosol model
Correct LUT for elevated surfaces
Interpolate LUT tables based on geometry
Find AOD at 0.55 µm and surface reflectance at 2.12 µm that exactly matches the MODIS measured reflectance at 0.47 µm; and TOA surface reflectance equals that due to continental model

ANNEXURE II

Quality control flags used for screening CALIOP Level 2 datasets

- **CAD Score**

Cloud Aerosol Discrimination (CAD) score indicates the confidence in the layer classification as aerosol or cloud.

- **Extinction Quality Control Flag**

The extinction Quality Control flag provides information on the retrieval type for each layer and indicates the possible problematic retrievals.

- **Uncertainity Flag**

There is always associated an uncertainity to each aerosol extinction value in Level 2 products. An uncertainity value of 99.9 km^{-1} indicates failed retrieval and hence, retrievals with this value of uncertainity flag should be excluded from the analysis.

- **CAD artifacts in the upper troposphere**

This test is applicable to the aerososl layers with bases above 4 km and adjacent to cloud layers only. This is because sometimes, weakly scattering edges of ice clouds may be misclassified as aerosols in the upper troposphere by the CAD algorithm.

- **Noise Spikes**

In the upper troposphere, there may be spurious detection of 80-km aerosol layers due to noise spikes. Though the occurrence is infrequent, but can affect the average profiles in theupper troposphere.

- **Negative Extinction**

Due to noise excursions, there might occur negative extinction coefficients, which could be due to surface contaminationor instrument characteristics.

ANNEXURE III

Graph showing the linear trends of yearly averaged AOD data from MODIS over five randomly chosen locations across the world

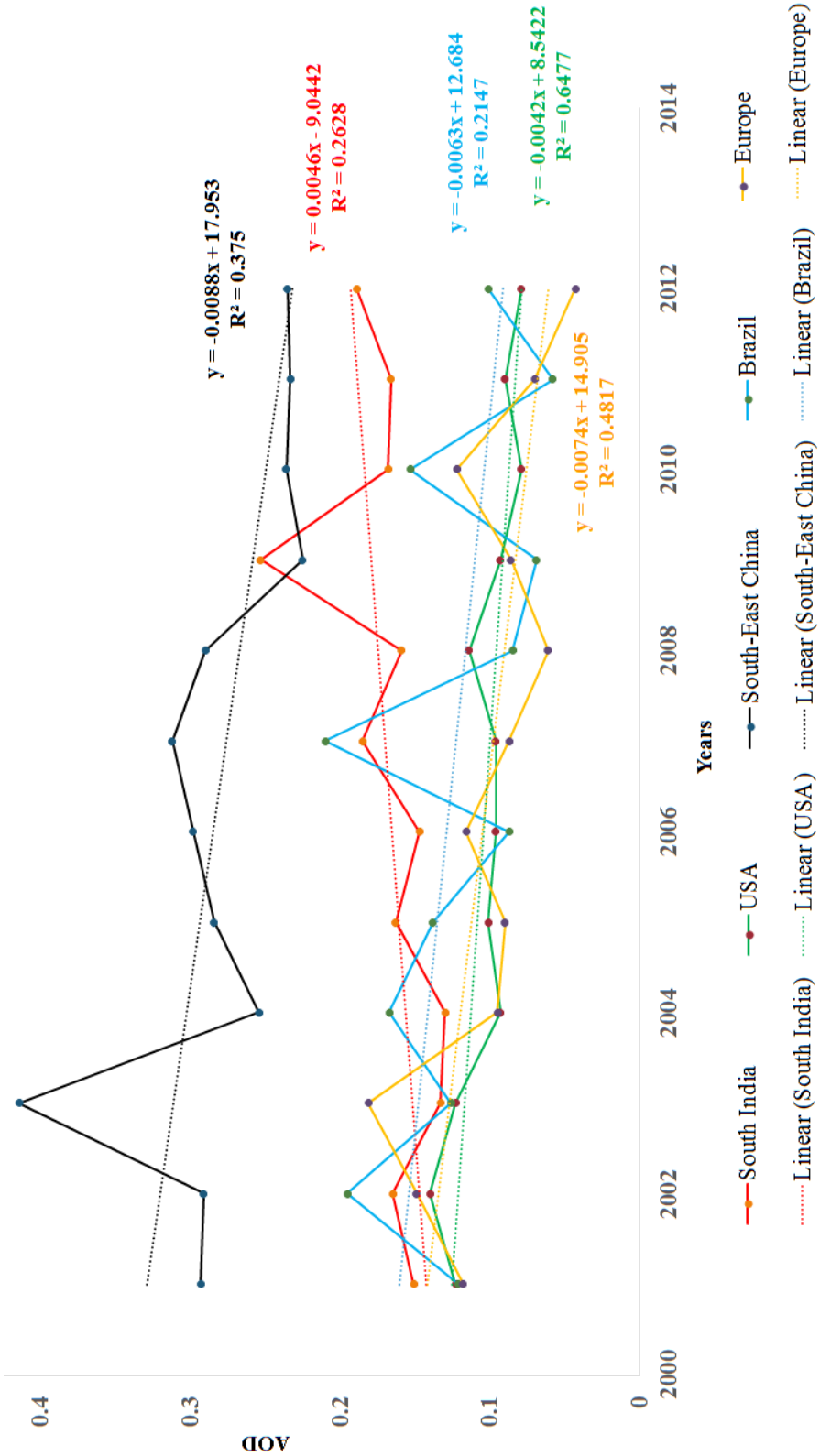

PUBLICATIONS

Remote Sensing of Environment 181 (2016) 137–150

Contents lists available at ScienceDirect

Remote Sensing of Environment

journal homepage: www.elsevier.com/locate/rse

Recent global aerosol optical depth variations and trends — A comparative study using MODIS and MISR level 3 datasets

Manu Mehta [a], Ritu Singh [b], Ankit Singh [b], Narendra Singh [c], Anshumali [d]

[a] Photogrammetry and Remote Sensing Department, Indian Institute of Remote Sensing, Dehradun-248001, India
[b] Department of Computer Science and Engineering, MIET, Meerut, India
[c] Aryabhatta Research Institute of Observational Sciences, Manora Peak, Nainital 263002, India
[d] Deptartment of Environmental Science & Engineering, Indian School of Mines, Dhanbad 826004, India

ARTICLE INFO

Article history:
Received 2 September 2015
Received in revised form 28 March 2016
Accepted 9 April 2016
Available online xxxx

Keywords:
Aerosol optical depth
Global
MODIS
MISR
Annual
Seasonal
Trends

ABSTRACT

Aerosol distribution at global and regional scales is one of the crucial parameters for climate change assessment. The study presents global spatio-temporal variations in aerosol optical depth (AOD) retrieved by Moderate Resolution Imaging Spectroradiometer (MODIS) and Multiangle Imaging Spectroradiometer (MISR) sensors at spatial resolutions of 1° × 1° and 0.5° × 0.5° respectively. Spatial correlations between MODIS and MISR AOD are reported on annual scale. The entire globe is divided into six sub-regions, i.e., North-West, North, North-East, South-West, South and South-East. The annual and seasonal mean AOD variations are obtained by analyzing Level 3 monthly datasets for the period 2001–2014. Relative changes (%) in AOD between the first and last seven years (i.e. 2001–2007 and 2008–2014 respectively) are discussed at annual and seasonal levels. AOD trends are calculated using the weighted least squares regression approach and weights are assigned to the AOD values corresponding to the expected errors. Statistically significant trends are reported at 95% confidence level. The results inferred from both the sensors are found to be in quite acceptable agreement. Increasing trends are found in the economically growing parts of Asian landmass and the surrounding oceanic regions, especially Arabian Sea and Bay of Bengal. On the other hand, decreasing trends are observed over parts of Europe, South America and North America. The study also focuses on examining the AOD trends over the ten most populous nations of the world. In terms of aerosol loadings, Bangladesh, Pakistan and Nigeria turned out to be the most polluted amongst the most populous countries. Significantly increasing trends in AOD are reported over the Indian subcontinent.

© 2016 Elsevier Inc. All rights reserved.

1. Introduction

Long term spatio-temporal variability in aerosol optical depth (AOD) serves as a valuable input for the studies related to climatic change and Earth's radiation budget (Boucher & Haywood, 2001; Boucher & Tanré, 2000; Carslaw et al., 2013; Charlson et al., 1992; Hansen, Sato, & Ruedy, 1997; Miller & Tegen, 1998; Ramanathan, Crutzen, Kiehl, & Rosenfeld, 2001a). Direct effects of aerosols include scattering and absorption of radiation whereas their indirect effects are pertinent to the alteration of cloud properties (Ackerman et al., 2000; Gao, Kaufman, Tanré, & Falkowski, 2000; Haywood & Boucher, 2000; L'eon et al., 2001; Myhre et al., 2013; Penner et al., 2001; Wang, Dickinson, & Liang, 2009). AOD trends have been estimated and assessed both worldwide and on regional scales by means of ground based sensors established at various locations over the globe using Aerosol Robotic Network (AERONET) (Li, Carlson, Dubovik, & Lacis, 2014; Xia, 2011; Yoon, von Hoyningen-Huene, Kokhanovsky, Vountas, & Burrows, 2012). Though ground based instruments provide accurate information about the aerosol optical properties, but being sparsely located and point based, they could not provide continuous spatial measurements. Inferences from satellite based sensors, henceforth, become important to provide a global perspective of AOD variation.

Several studies focusing on global AOD variations over land and ocean have been performed using satellite retrievals. Some of them have reported decreasing trends of AOD over the oceans except for the regions near industrialized/rapidly developing countries, and those under the influence of Saharan dust and biomass burning (Chylek et al., 2007; Mishchenko et al., 2007; Zhao et al., 2008). Hsu et al. (2012) found weakly positive trend over global ocean, positive trends over the Arabian Peninsula, and negative trends over the Eastern United States (US) and Europe for the period 1997–2010 using data from Sea-viewing Wide Field-of-view Sensor (SeaWiFS). de Meij, Pozzer, & Lelieveld (2010) evaluated global and regional AOD trends using Moderate Resolution Imaging Spectroradiometer (MODIS), Multiangle Imaging Spectroradiometer (MISR) and AERONET AOD datasets, and emission estimates for the period ranging from 2000 to 2009. They found negative trends over North America, South America and Europe, but positive trends over South and East Asia. Recently, global aerosol changes were analyzed using MODIS datasets for the period 2003–2012 and positive AOD changes were reported over Asia (Mao

http://dx.doi.org/10.1016/j.rse.2016.04.004
0034-4257/© 2016 Elsevier Inc. All rights reserved.

Remote Sensing of Environment 208 (2018) 120–132

Contents lists available at ScienceDirect

Remote Sensing of Environment

journal homepage: www.elsevier.com/locate/rse

Global trends of columnar and vertically distributed properties of aerosols with emphasis on dust, polluted dust and smoke - inferences from 10-year long CALIOP observations

Manu Mehta[a,c,*], Narendra Singh[b], Anshumali[c]

[a] Photogrammetry and Remote Sensing Department, Indian Institute of Remote Sensing (IIRS), Dehradun, ISRO, India
[b] Aryabhatta Research Institute of Observational Sciences (ARIES), Manora Peak Nainital, India
[c] Indian Institute of Technology (Indian School of Mines) (IIT(ISM)), Dhanbad, India

ARTICLE INFO

Keywords:
CALIPSO
Aerosol properties
Columnar
Vertically distributed
Trends

ABSTRACT

In this paper, the decadal datasets available from the space-borne lidar, Cloud Aerosol Lidar with Orthogonal Polarization (CALIOP) onboard Cloud-Aerosol Lidar and Infrared Pathfinder Satellite Observations (CALIPSO) are analyzed in order to understand the spatial and vertical distributions of aerosols at a global scale. Decadal (September 2006–August 2016) Level 3 night time Standard All-sky data products, created using quality controlled Level 2 datasets are utilized in the study. Columnar aerosol properties are discussed in conjugation with vertical properties of the three major aerosol types i.e. dust, polluted dust and smoke. It is found that the global mean aerosol optical depth (AOD) amounts to 0.10, with AOD values of 0.13 and 0.09 for land and ocean respectively, during the last decade. Mean aerosol extinction coefficients are also reported for four altitude bins i.e. 0–1 km, 1–2 km, 2–3 km and 3–4 km above mean sea level (a.m.s.l.). It is observed that dust and smoke particles have stronger vertical transport compared to polluted dust particles, which are generally found to be confined within the lower altitudes. In order to observe the changes in aerosol loading over different parts of the globe, de-seasonalized trends of AOD and vertical extinction coefficients are computed using linear regression technique. Globally, the total columnar particle load shows a significant negative trend during the last decade. In particular, trends of total particle loading (AOD and extinction) are decreasing over North America, South America, East China and Australia. However, the smoke emissions (columnar and vertically distributed) have increased over India, Russia, North America, Australia and Central Africa. This is of concern in the context of rising temperatures accompanied with increasing wildfires throughout the globe. Additionally, enhanced levels of polluted dust over the developing regions of Africa and Asia are also revealed.

1. Introduction

Evaluation of aerosols' impact over climate requires accurate information of their physical, chemical and optical properties at regional and global scales (Carslaw et al., 2013; Charlson et al., 1992; Menon, 2004; Myhre et al., 2013; Ramanathan et al., 2001a, b). The longer lifetimes of aerosols in free troposphere allow them to get transported over farther distances, thereby affecting their spatial distribution away from their sources. It should also be noted that not only the precise information of columnar distribution, but also knowledge of the vertical structure of aerosols is required to correctly understand the aerosol transport and removal processes, emission properties and vertical uplifts (Schulz et al., 2006; Winker et al., 2013). Specifically, the uncertainty in the simulation of transport and removal processes is one of the major factors responsible for the diversity in distribution of aerosols predicted by the global aerosol models (Huneeus et al., 2011; Kinne et al., 2006; Textor et al., 2006). A global perspective of columnar aerosol properties along with the vertically distributed ones, henceforth, is crucial to assess their role in the atmospheric dynamics. In order to understand the vertical structure of the aerosol distribution in the atmosphere, several regional studies have been performed in different parts of the world using ground based and airborne Lidar datasets (Cavalieri et al., 2010; Chen et al., 2013; Gadhavi and Jayaraman, 2006; L'eon et al., 2009; Menzies and Tratt, 2002; Mona et al., 2006, 2012; Navas-Guzmán et al., 2013; Solanki and Singh, 2014). While in-situ observations provide repeated, accurate and precise data of the aerosol properties, satellite measurements enable irreplaceable and continuous spatio-temporal coverage, though accompanied by retrieval

* Corresponding author at: Photogrammetry and Remote Sensing Department, Indian Institute of Remote Sensing, Dehradun, ISRO, India.
E-mail address: manu@iirs.gov.in (M. Mehta).

https://doi.org/10.1016/j.rse.2018.02.017
Received 16 August 2017; Received in revised form 1 February 2018; Accepted 13 February 2018
0034-4257/ © 2018 Elsevier Inc. All rights reserved.

Journal of Basic and Applied Engineering Research
p-ISSN: 2350-0077; e-ISSN: 2350-0255; Volume 3, Issue 10; July-September, 2016, pp. 906-908
© Krishi Sanskriti Publications
http://www.krishisanskriti.org/Publication.html

Changes in Aerosol Optical Depth in Three Heavily Populated Cities in Indo Gangatic Plains–Delhi, Dhaka and Karachi

Manu Mehta[1], Narendra Singh[2], Ashumali Singh[3], Gopika M[4] and Renuka K[5]

[1]IIRS Dehradun
[2]ARIES, Nainital
[3]ISM Dhanbad
[4,5]NITK, Surathkal
E-mail: [1]manu@iirs.gov.in, [2]narendra@aries.res.in, [3]malijnu@gmail.com,
[4]mgopika1992@gmail.com, [5]renuka9.ce@gmail.com

Abstract—*The study presents decadal changes (2005-2014) in aerosol optical depth (AOD) over three heavily populated and polluted cities lying in Indo-Gangetic Plains (IGP). The cities chosen are namely, Delhi (28.6° N, 77.2° E), Dhaka (23.7° N, 90.4° E) and Karachi (24.9° N, 67.0° E) located in India, Bangladesh and Pakistan respectively. IGP is one of the most populous and polluted regions in Asia. The three locations chosen are representatives of the varied aerosol concentrations and type within IGP. The paper focuses on analyzing decadal satellite data obtained from Multiangle Imaging Spectroradiometer (MISR) sensor onboard NASA'S Terra Platform. The quantified seasonal variations have been presented for the three cities. The average annual AOD values are found to be >0.4 in the three cities. Using MISR Level 3 data, it is observed that the annual average AOD has been increased by 4%, 12% and 6% for Delhi, Dhaka and Karachi respectively.*
Keywords: *Delhi, Dhaka, Karachi, MISR, decadal*

1. INTRODUCTION

Aerosols play important role in altering Earth's radiation budget and cloud properties. The aerosol loading is not only important for observing their climatic impacts but also for human health related studies. This paper discusses the variation of aerosol optical depth, an indicator of aerosol columnar loading over three heavily populated cities of Asia i.e. Delhi, Dhaka and Karachi lying in Indo-Gangetic Plains whereas, Karachi lies in West IGP; Delhi in Central IGP and Bangladesh in East IGP. Thought IGP as a whole, is one of the most polluted and populated regions of world, but due to the varied locations of the three cities within the IGP (also in different countries), the type of aerosols and the amount of aerosol loadings are expected to be different. Previous works in this direction have been attempted at zonal level and for individual locations too. Many works related to spatio-temporal AOD characteristics have been reported over Indian region (Babu et al.,2013; Dey & Di Girolamo,2011; Mehta, 2015). Over Delhi, in particular, similar works have been attempted too. For details, pl. refer to works by Lodhi et al., 2013, Srivastava et al., 2014. Alam et al. 2011 have monitored aerosol patterns over Pakistan using MODIS, TOMS and MISR datasets. Bibi et al. 2015 have compared MODIS, OMI, MISR and CALIPSO AOD for four locations of IGP region and validated the results against AERONET datasets. Begum et al., 2010 identified sources of aerosols (fine and coarse particulate matter) over Dhaka. In this paper, the average AOD at annual and seasonal levels have been presented for the past ten years. Using MISR data, it is observed that the aerosol loading has increased in these cities during the last decade.

2. MISR LEVEL 3 DATA

MISR sensor is onboard NASA's Terra satellite. There are nine cameras at nine look angles in four wavelength regions. The AOD Level 3 data MISR_AM1_CGAS is available at a spatial resolution of 0.5°X0.5°. The data can be downloaded from ftp://l5eil01.larc.nasa.gov/pub/misrl2l3 MISR. The AOD retrieval method utilizes Look up Table approach for different surface targets types. For more details regarding the AOD retrieval techniques employed to generate the data product, pl. refer to Kahn et al., 2009.The location of the three cities have been depicted in Fig. 1.

Seminar on Advances in Remote Sensing and GIS Applications, NESAC, Shillong
May 10-11, 2018,

Vertically resolved de-seasonalized aerosol backscatter trends over a location in Central Himalayas

Manu Mehta[1,3], Narendra Singh[2], Anshumali[3] and Tejaswini[1,4]

[1]Indian Institute of Remote Sensing, Dehradun, ISRO
[2]Aryabhatta Research Institute of Observational Sciences, Nainital
[3]Indian Institute of Technology – Indian School of Mines, Dhanbad
[4]Indian Institute of Information Technology and Management Kerala, Thiruvananthapuram

Abstract

The Himalayan region, owing to its complex topography and location receives a quite different atmospheric dynamics as compared to the planar terrains. Studies have shown that its pristine atmosphere is prone to transport of pollutants from near and far located source regions (Bonasoni et al. 2010; Bucci et al. 2014; Hegde et al. 2009). The study of vertical distribution of aerosols apart from the columnar particle loading is of special concern in such regions. Our study has utilized 10-year long level 2 Cloud-Aerosol Lidar with Orthogonal Polarization (CALIOP) datasets from Cloud–Aerosol Lidar and Infrared Pathfinder Satellite Observation (CALIPSO) platform (Omar et al., 2009; 2013; Winker et al., 2007). The vertically resolved backscatter coefficients are extracted from the datasets and quality screened before analysis. We present a first-time de-seasonalized trend analysis of the aerosol backscatter coefficients at different altitudes in the atmospheric column over a location in Central Himalayan region. Such a study could serve as a crucial input to understand the changing behaviour of particle loading at different levels of atmosphere. Figure 1 presents the backscatter trends of aerosols for the time period 2007-16 over the study area.

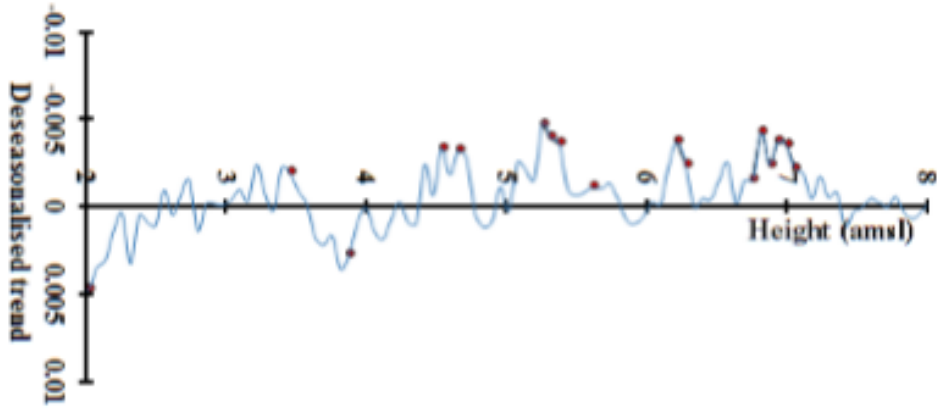

Figure 1 De-seasonlized aerosol backscatter trends during 2007-16 over a location in Central Himalayas

TROPMET-2018, IIT-BHU, Varanasi, Oct 24-27, 2018 (Poster)

VERTICAL DISTRIBUTION OF DUST, POLLUTED DUST AND SMOKE OVER DIFFERENT PARTS OF INDIAN REGION

Manu Mehta*[1,2], Narendra Singh[2], Anshumali[3], Shoubhik Biswas*[4] and Arka Ghosh[4]

[1]Indian Institute of Remote Sensing, Dehradun, ISRO
[2]Aryabhatta Research Institute of Observational Sciences, Nainital
[3]Indian Institute of Technology – Indian School of Mines, Dhanbad
[4]Jadhavpur University

Abstract: *The Indian region experiences the atmospheric loadings of various types of aerosol particles affecting the regional climate as well as the human health. Both the natural as well as anthropogenic emissions, emitted locally as well as affected by long range processes affect the aerosol loading over the Indian region. Whereas, the knowledge of columnar aerosol properties as global and regional scales have greatly improved both due to continuous ground based and satellite based observations; there are still comprehensive studies needed focussing on vertical distribution of aerosol types prevalent over different parts of Indian region. The understanding of columnar as well as vertical distribution of aerosol loadings can improve our knowledge on the aerosol-climate interaction processes. This paper presents the vertical distribution of major aerosol components, i.e., dust, polluted dust and smoke distributed over different parts of Indian region over a decadal period. The data is taken from the space-borne Lidar, i.e., Cloud Aerosol Lidar with Orthogonal Polarisation (CALIOP) on board Cloud-Aerosol Lidar and Infrared Pathfinder Satellite Observations (CALIPSO). The time period of study spans over 2007 to 2016.*

Introduction

Aerosols affect the Earth's climate system both directly as well as indirectly. Though, there have been numerous studies focusing on aerosol columnar properties, however, our understanding of aerosol vertical distribution is still limited. In order to improve our understanding of aerosol induced processes in the atmosphere, we need to know the spatio-temporal variability of aerosol vertical distribution at global and regional scales (Schulz et al., 2006; Winker et al., 2013).

In this work, the satellite retrievals from Cloud Aerosol Lidar with Orthogonal Polarisation (CALIOP) which is a space borne Lidar onboard Cloud-Aerosol Lidar and Infrared Pathfinder Satellite Observations (CALIPSO) platform have been utilized to study the aerosol vertical distribution over Indian region (Hunt et al., 2009; Omar et al., 2009; Winker et al., 2009).

Study region

The study has been carried out for three different regions of India; namely North, Central and South India. The top left and bottom right coordinates for the three regions are respectively {(36°34'N, 69°1'E), (30°38'N, 78°53'E)} for North India, {(30°38'N, 73°57' E), (22°44'N, 83°49'E)} for South India and {(22°44'N, 69°2' E), (12°51'N, 78°53'E)} for Central India.

Datasets used

We have used Level 3 night time monthly aerosol vertical extinction profiles from CALIOP sensor at 2° X 5° spatial resolution for the period 2007-2016. Level 3 data products are created using Level 2 datasets using several quality control flags (Winker et al., 2013).

Results

Global decadal monthly aerosol vertical profiles for the time period 2007-16 have been extracted and averaged from monthly CALIOP Level 3 products. The zonal statistics for the study regions have been computed thereafter.

Figure 1 presents the vertical distribution of the three major aerosol types over North, Central and South Indian regions.

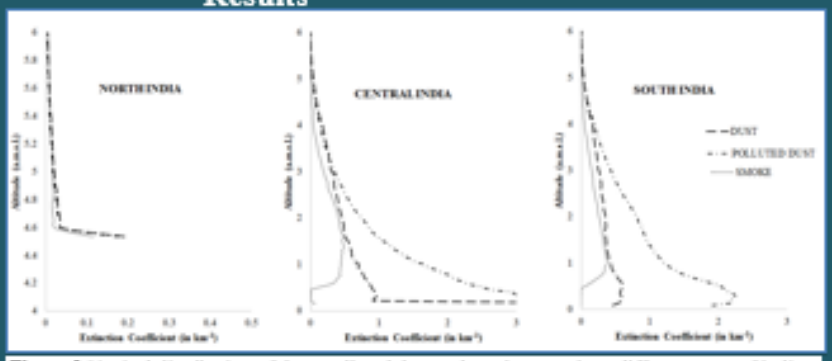

Figure 1 Vertical distribution of dust, polluted dust and smoke over three different parts of India

Conclusions

- In general, concentration of smoke is maximum somewhat above the ground surface, similar to findings by Mehta et al., 2018.
- Over North India, owing to the extent of the study region which is a high mountainous region for the majority of the land, the overall contribution due all the three aerosol types is much smaller compared to the other two regions.
- Over Central India, dust and polluted dust are the most dominating aerosol types, though contribution of smoke is also appreciable at higher altitudes.
- Polluted dust is the most dominant aerosol type over South India, with high concentrations close to ground.

Acknowledgements

We are thankful to the entire CALIOP team for providing the access to the data. Thanks are due to Director, IIRS, Dehradun and Director, IIT-ISM, Dhanbad for allowing to carry out the study.

References

- Hunt, W. et al., 2009. http://dx.doi.org/10.1175/2009JTECHA1223.1.
- Mehta, M. et al., 2018. https://doi.org/10.1016/j.rse.2018.02.017.
- Omar, A. et al., 2009. http://dx.doi.org/10.1175/2009JTECHA1231.1.
- Schulz, M. et. al, 2006. http://dx.doi.org/10.5194/acp-6-5225-2006.
- Winker, D. M. et al., 2009. http://dx.doi.org/10.1175/2009JTECHA1281.1.
- Winker, D. M. Et al., 2013. http://dx.doi.org/10.5194/acp-13-3345-2013.

*manu@iirs.gov.in

The International Archives of the Photogrammetry, Remote Sensing and Spatial Information Sciences, Volume XLII-5, 2018
ISPRS TC V Mid-term Symposium "Geospatial Technology – Pixel to People", 20–23 November 2018, Dehradun, India

ON VERTICAL DISTRIBUTION OF MAJOR AEROSOL TYPES OVER DIFFERENT PARTS OF ASIA

Manu Mehta[1], Narendra Singh[2], Anshumali[3], Meghna Mittal[4] · Mahak Gumber[4, *]

[1]Photogrammetry & Remote Sensing Department, Indian Institute of Remote Sensing, Dehradun, India – manu@iirs.gov.in
[2]Aryabhatta Research Institute of Observational Sciences, Nainital, India - narendra5679@gmail.com
[3]Indian Institute of Technology – Indian School of Mines, Dhanbad, India - malijnu@gmail.com
[4]Banasthali Vidyapith, Tonk, Rajasthan, India – (meghanmittal191997, mehak0197)@gmail.com

Commission V, SS: Atmosphere, Ocean, Weather and Climate

KEY WORDS: CALIOP, dust, polluted dust, smoke, Asia

ABSTRACT:

Asia, being the largest continent, both in its size and population is affected by different types of atmospheric aerosols. Also, owing to different local emissions/sources along with the long range transport mechanisms, there is a large variability in the distribution of different types of aerosols across the continent. Not only the effects are pertinent to the regional and global climate system, but the loadings also affect human health. Though there have been studies in the past focussing on columnar distribution of aerosol types over Asian region at continental and regional scales, studies focussed on regional vertical distribution of major aerosol types over different regions of Asia need attention. This paper presents the decadal (2007-16) vertical distribution of major aerosol components, i.e., dust, polluted dust and smoke over different parts of Asia as seen from the space-borne lidar, i.e., Cloud Aerosol Lidar with Orthogonal Polarisation (CALIOP) onboard Cloud-Aerosol Lidar and Infrared Pathfinder Satellite Observations (CALIPSO). Such a study can be useful in capacity building focussed on aerosol variability through remote sensing techniques.

1. INTRODUCTION

Aerosols are known to have impacts on the Earth's climate system. The spatial distribution of aerosols has helped to understand their contribution to different aspects of climate system as well as human health. However, a comprehensive measurement database of the aerosol vertical structure is still to be established. The knowledge of vertical distribution of aerosols can help to improve the understanding of aerosol induced processes in the atmosphere (Schulz et al., 2006; Winker et al., 2013). One of the major factors behind the diversity in aerosols predicted by modelling approach is the uncertainty in the simulation of transport and removal processes (Huneeus et al., 2011; Kinne et al., 2006; Mehta et al., 2018; Textor et al., 2006).

Though ground based retrievals of aerosol vertical profiles are more accurate but are limited only to point based measurements. In this context, the satellite retrievals can provide continuous mapping of the aerosols though associated with uncertainties. Cloud Aerosol Lidar with Orthogonal Polarisation (CALIOP) is space borne lidar onboard Cloud-Aerosol Lidar and Infrared Pathfinder Satellite Observations (CALIPSO) platform (Hunt et al., 2009; Omar et al., 2009; Winker et al., 2009). It has been providing the vertically resolved aerosol profiles across the globe since 2006.

This work aims to study the decadal variability of aerosol vertical distribution owing to major aerosol types over the three different regions of Asia, dominated by different types of aerosol particles.

2. STUDY REGION

We have considered three different regions of Asia i.e., Indonesia (dominated by forest fires and anthropogenic pollution), India (dominated by anthropogenic pollution and natural factors) and Taklimakan Desert (dominated by desert dust). The regions selected for the present study are dominated by different type of aerosols depending on the local sources and long range transport mechanisms.

3. DATA USED

The satellite data sets used in the study are taken from CALIOP on board CALIPSO, which orbits around the earth 15 times every day. The lidar signals are received at two wavelengths, i.e., 532 nm and 1064 nm. Additionally, the lidar is dual polarised at 532 nm. It is capable to retrieve the aerosol and cloud distribution across the globe.

The aerosol retrieval procedure involves identification of aerosol, cloud and surface returns within the lidar signals. Then, the feature type is determined (Liu et al., 2009). The aerosols are classified as clean marine, dust, smoke, polluted dust, clean continental and polluted continental particles (Omar et al., 2009). Finally, the aerosol vertical extinction profiles are retrieved.

For the present study Level 3 monthly datasets at 2° X 5° spatial resolution have been utilized for the period 2007-2016. Level 3 data products are created using Level 2 datasets using several quality control flags (Winker et al., 2013). In this context, one may refer to evaluation studies by Kim et al. 2013; Kittaka et al. 2011; Ma et al. 2013; Omar et al. 2013. We have analysed the aerosol vertical extinction profiles at 532 nm wavelength region from the satellite datasets.

MEHTA, M.

Department of Environmental Science and Engineering
Indian Institute of Technology (Indian School of Mines)
Dhanbad, 826004, India
Scientist, Photogrammetry and Remote Sensing Department
Indian Institute of Remote Sensing, ISRO, Govt. of India
Email: manu@iirs.gov.in, mehtamanu12@gmail.com
Phone: 0135-2524113

Area of Specialization:
Remote sensing, Time series analysis, Aerosol studies, Digital Image processing

Research Interest:
Natural Resource Management, Climate studies, Aerosol Monitoring

Educational qualification

Qualification	Institute	Percentage/CGPA	Year of passing
Ph.D.*		Thesis submitted	2018
M.Tech. (Optoelectronics & Optical Communication)**	IIT, Delhi	9.8/10 (CGPA)	2009
M.Sc. (Physics)	KUK, Kurukshtera	81 %	2007
B.Sc. (Non-Medical)	MLNC, Yamuna Nagar	89.6 %	2005

***Ph.D. Title: A GLOBAL STUDY ON SPATIO-TEMPORAL VARIABILITY OF AEROSOLS INFERRED FROM SPACE-BORNE MEASUREMENTS**
****M.Tech. Dissertation Title:** Studies on Microstructured Optical Fibres

Awards and scholarships

- 2007-09 M.Tech.(Optoelectonics Optical Communication) Batch Topper
- 2005-07 M.Sc.(Physics) Gold medal
- 2002-05 B.Sc.(Non-Med) Gold Medal
- 2004 Amongst top 1% in National Graduate Physics Examination
- Qualified CSIR-NET 2006 (JRF/LECT) (SPM Qualified)
- Qualified GATE 2007, All India Rank : 41
- Qualified JEST 2007

Membership of professional bodies:
Life Member of ISRS and IMS

Peer Recognition

- **Reviewer:** Remote Sensing of Environment (*Elsevier*), Remote Sensing (*MDPI*), Remote Sensing Letters (*Taylor & Francis Online*), Journal of Atmospheric & Solar-Terrestrial Physics (*Elsevier*), GIScience and Remote Sensing (*Taylor & Francis Online*), Earth Science Research Journal (*ICSA*), Current Science (*IAS*)
- **Section Editor**: Journal of Remote Sensing and GIS, ISSN: 2321–421X
- **Editor:** Recent Trends in Sensor Research & Technology (RTSRT), eISSN: 2393-8765

JOURNAL PUBLICATIONS

International

- **Mehta M., Singh, N. and Anshumali, 2018. Global trends of columnar and vertically distributed properties of aerosols with emphasis on dust, polluted dust and smoke - inferences from 10-year long CALIOP observations. *Remote Sensing of Environment*, 208, pp.120–132, https://doi.org/10.1016/j.rse.2018.02.017.**
- **Mehta, M., Singh, R., Singh, A., Singh N. and Anshumali, 2016. Recent global aerosol optical depth variations and trends — A comparative study using MODIS and MISR level 3 datasets. *Remote Sensing of Environment*, 181, pp.137-150, http://dx.doi.org/10.1016/j.rse.2016.04.004.**
- **Mehta, M., 2015.** A study of aerosol optical depth variations over the Indian region using thirteen years (2001–2013) of MODIS and MISR Level 3 data. *Atmospheric Environment*, 109, pp.161–170, doi:10.1016/j.atmosenv.2015.03.021.
- **Mehta, M.,** Goyal, P. and Nishant, K., 2013. Implementation of simple model for atmospheric radiative transfer code in single scattering approximation for retrieval of aerosol optical depth over Dehradun, India. *Journal of Applied Remote Sensing*, 7 (1), pp.073521 (1-7), doi: 10.1117/1.JRS.7.073521.
- **Mehta, M.**, Anh, Le V., Saha, S.K. and Agrawal, S., 2012. Evaluation of indices and parameters obtained from optical and thermal bands of Landsat 7 ETM+ for mapping of salt-affected soils and water-logged areas. *Asian Journal of Geoinformatics*, 12(4), pp. 9-16.

National

- Ghosh, A., **Mehta, M.** and Biswas, S., 2018. Study of vertical distribution of aerosols during Central Portugal forest fire event using remote sensing data. *Journal of Basic and Applied Engineering Research*, 5(4), pp. 263-267.
- **Mehta, M.**, Rao, R., Doley, G.J., Rajsekhar, A. and Sindhwani, S., 2017. AOD retrieval over different LULC features using AWiFS data — A case study over Dehradun. *Journal of Remote Sensing & GIS*, 8(2), pp.54-57.

- **Mehta, M.**, Gopika, M., Renuka, K., Doley, G.J., Rajshekhar, A. and Sindhwani, S., 2016. On Retrieval of Aerosol Asymmetry Parameter over Dehradun. *Journal of Basic and Applied Engineering Research*, 3(10), pp903-905.
- **Mehta, M., Singh, N., Anshumali, Gopika, M. and Renuka, K. 2016. Changes in aerosol optical depth in three heavily populated cities in Indo Gangatic Plains – Delhi, Dhaka and Karachi. *Journal of Basic and Applied Engineering Research*, 3(10), pp.906-908.**
- **Mehta, M.**, Singh, R., Tyagi, N., Rawat, M., Singh, A., Goel, A. and Singh, S., 2015. Aerosol loadings in association with vegetative properties- A case study over North Indian region. *Journal of Remote Sensing & GIS, 6(3)*, pp. 1-5.
- **Mehta, M.**, Singh, S., Kumar, V., Kumar, A., and Singh, S., 2015. Aerosol optical depth variation over Asian region during the last fourteen years. *Research and Reviews: Journal of Ecology,* 4(2), pp.12-17.
- **Mehta, M.** and Shaw, G., 2015. Analysis of color and particulate depolarization ratio profiles for aerosols using CALIPSO Level 2 data. *Journal of Remote Sensing & GIS,* 6(2), pp.1–5.
- **Mehta, M.**, Naik S.R. and Roshani R., 2015. Anlaysis of aerosol vertical extinction profiles using satellite data - A case study over Dehradun", *Journal of Energy Research and Environmental Management: An Innovative Approach*, pp.94-98
- Rangarajan, S. and **Mehta, M. 2015.** Disaster risk assessment of Tsunami in Indian coast line and mitigation of the same. *Journal of Energy Research and Environmental Management: An Innovative Approach*, pp.90-93.
- **Mehta, M.,** 2014. Study of temporal variation of aerosol optical depth in Dehradun using satellite data. *Journal of Basic and Applied Engineering Research*, 1(9), pp. 47-50.
- **Mehta, M.,** Nishant, K. and Goyal, P., 2013. Retrieval of mid-visible land surface albedo over Dehradun, northern India and its sensitivity to atmospheric parameters. *Current Science,* 105(5), pp.578-579.
- **Mehta, M.** and Agrawal, S., 2012. Cross-calibration of Indian Mini Satellite-1 HySI data using Hyperion: effect on Normalized Difference Vegetation Index. *Current Science,* 103(5), pp.480-481.
- **Mehta, M.** and Agrawal, S., 2011. An approach to address the issues related to cross-calibration and atmospheric correction of IMS-1 HySI data, *Journal of Geomatics,* 5(2), pp. 61-65.
- **Mehta, M.**, Agrawal, S. and Mishra, A.K., 2011. An attempt to estimate vegetation albedo for red and SWIR band of AWiFS data using MODTRAN as Radiative Transfer Code, *National Academy Science Letters,* 34(3 & 4), pp. 143-146.

CONFERENCES/SEMINAR/SYMPOSIA/WORKSHOPS

- Gumber M., **Mehta M**. and Mittal M., 2018. Observation of dust loadings from space-borne measurements (2005–2016). *Int. Arch. Photogramm. Remote Sens. Spatial Inf. Sci. XLII-5*, pp.523-525. https://doi.org/10.5194/isprs-archives-XLII-5-523-2018
- **Mehta M., Singh N. Anshumali Mittal M. and Gumber M., 2018. On vertical distribution of major aerosol types over different parts of Asia. *Int. Arch. Photogramm. Remote Sens. Spatial Inf. Sci. XLII-5*, pp.553-555 https://doi.org/10.5194/isprs-archives-XLII-5-553-2018.**
- Ghosh A., **Mehta M**., Biswas S., Gumber M. and Mittal M., 2018. Absorbing aerosol levels across the Central and Western Himalayan region – A Remote Sensing approach, *Int. Arch. Photogramm. Remote Sens. Spatial Inf. Sci. XLII-5*, pp.519-522 https://doi.org/10.5194/isprs-archives-XLII-5-519-2018.
- Ghosh, A., **Mehta, M.** and Biswas, S., 2018. Absorbing aerosol distribution across the Eastern Himalayan region. *TROPMET-2018*, IIT-BHU, Varanasi, Oct 24-27, 2018.
- **Mehta, M., Singh, N., Anshumali, Biswas, S. and Ghosh, A., 2018. Vertical distribution of dust, polluted dust and smoke over different parts of Indian region. *TROPMET-2018*, IIT-BHU, Varanasi, Oct 24-27, 2018. (Poster)**
- Mittal, M., **Mehta, M.** and Gumber, M., 2018. A case study of respiratory diseases and absorbing aerosol loadings over three densely populated countries of the world. *TROPMET-2018*, IIT-BHU, Varanasi, Oct 24-27, 2018.
- Gumber, M., **Mehta, M.** and Mittal, M., 2018. Study of particle loading over the three major biomass burning regions. *TROPMET-2018*, IIT-BHU, Varanasi, Oct 24-27, 2018.
- Biswas, S., **Mehta, M.** and Ghosh, A., 2018. An analysis of Snow Cover changes in the winter season over the Western and Central Himalayan region (2000 – 2018, *TROPMET-2018*, IIT-BHU, Varanasi, Oct 24-27, 2018.
- Sarma, K. and **Mehta, M.,** 2018. Variation of outgoing longwave radiation with aerosol optical properties as observed over space over India. *TROPMET-2018*, IIT-BHU, Varanasi, Oct 24-27, 2018.
- Ghosh, A., **Mehta, M.** and Biswas, S., 2018. Study of Aerosol Distribution and Properties during Central Portugal Forest Fire Event - A Remote Sensing Approach. *ICCCNT 2018*, IISC Bengaluru, July 10-12, 2018.
- Biswas, S., **Mehta, M.** and Ghosh, A., 2018. Study of aerosol distribution in the vertical column of the atmosphhere during Uttrakhand forest fires 2016. *IEEE International Conference on RTEICT-2018*, Bangaluru, May 18-19, 2018.
- **Mehta, M., Singh, N., Anshumali and Tejaswini. Vertically resolved de-seasonalized aerosol backscatter trends over a location in Central Himalayas. Seminar on Advances in Remote Sensing and GIS Applications, May 10-11, 2018, NESAC, Shillong.**

- **Mehta, M., Singh, N. and Anshumali. On seasonal vertical distribution of aerosols over the Indian Region during the last decade, TS-6D: Aerosol, Radiation and Cloud Physics - 2, p.353, *INTROMET*, November 7-10, 2017, Ahmedabad.**
- Sarma, K. and **Mehta, M.** Assessment of OMI aerosol optical depth over the selected AERONET sites in the Asian region, PS-1: Aerosol and Air Quality-1, p.68, *INTROMET*, November 7-10, 2017, Ahmedabad.
- Srinivas T.S. **Mehta, M.**, P.K. Pal, Amminedu, E. and Kumar, A.S. Inter comparison of HE and IMSRA Rainfall products of INSAT-3D during 2015 ISMR over Indo-Gangetic Plain: A Case Study, PS-3: Atmospheric Process Studies, p.140, *INTROME*T, Nov 7-10, 2017, Ahmedabad.
- Srinivas T.S., **Mehta, M.**, Amminedu, E. and Kumar, A.S. Comparison of Rainfall data from INSAT-3D and IMD over Indo- Gangetic Plain during 2014 and 2015 ISMR, *UPCAR*, June 26-28 2017, Tirupathi.
- Sarma, K. and **Mehta, M.** Spatio-temporal variation of absorption aerosol optical depth in conjugation with air temperature over the Asian region. *ISRS conference*, Decemeber 7-9, 2016, IIRS, Dehradun.
- Srinivas, T.S. and **Mehta, M.** Aerosol-cloud vertical distribution over Indo-Gangetic Plain during 2013 and 2014 Indian Summer Monsoon Rainfall. *ISRS conference*, Decemeber 7-9, 2016, IIRS, Dehradun.
- **Mehta, M.**, Rao, R., Rajsekhar, A. and Doley, G.J. Effect of sensor spectral response on the estimation of aerosol optical depth using SMART model - A case study. *ISRS conference*, Decemeber 7-9, 2016, IIRS, Dehradun.
- Sarma, K. and **Mehta, M.** Global aerosol single scatering albedo characteristics at 388nm. *NGCT*, October 14-16, 2016, UPES Dehradun.
- Dubey, S., **Mehta, M.** and Singh, A. Associative Study of Absorbing Aerosol Index (AAI) and precipitation in India during monsoon season (2005 to 2014). *SPIE Conference*, April 4-7, 2016, New Delhi.
- **Mehta, M.**, Doley, G.J. and Sindhwani, S. AOD estimation over vegetation using AWiFS data: a radiative transfer approach. *AFPCEM*, March 13, 2016, JNU, New Delhi.
- **Mehta, M.**, Sharma, V. and Doley, G.J. Aerosol optical depth variation during a recent dust event in North India. *ICWEES*, March 13-15, 2016, Bhopal.
- **Mehta, M.** and Dubey, S. Spatio-temporal impact of Aerosol Pollution on Precipitation and vegetation in Indian region [2000-2013]. *ICWEES*, 13-15 March 2016, Bhopal.
- Dubey, **S., Mehta, M.** and Prabhashini. Association of UV Aerosol Index and NDVI in monsoon and post-monsoon season – A study over North-western India", *Monsoon Workshop*, 21-22 Feb, 2016, IITM, Pune.

- **Mehta, M.**, Dubey, S., Nithyapriya, B. and Doley, G. Impact of Aerosol pollution on precipitation in Indian region [2000-2013]. *ISG Conference*, December 16-18, 2015, Jaipur.
- **Mehta, M.** and Priya, N. Annual and seasonal variation of Aerosol Index over Indian Region – A study using AURA-OMI Data. *ISG*, December 16-18, 2015, Jaipur.
- **Mehta, M.** and Pradeep S. Post- forest fire change detection for Pauri Garhwal, Uttarakhand using SVM techniques during May 2014 to 2015. *OSGIS*, October 9-10, 2015, IIT BHU, Varanasi.
- **Mehta, M.**, Ankit S., Ritu S., Shefali S. and Vijay K. Aerosol loading in conjugation with rainfall - Inferences from multi-temporal multi-sensor satellite datasets. *NGCT*, IEEE Conf. 36551, September 4-5, 2015, UPES, Dehradun.
- **Mehta, M.**, Vijay K., Shefali S., Ritu S. and Ankit S. Spatial and temporal changes of aerosol optical depth in three most populated countries of Asia over the last decade. *NGCT*, IEEE Conf. 36551, September 4-5, 2015, UPES, Dehradun.
- **Mehta, M.**, Naik S.R. and Roshani R. Analysis of aerosol vertical extinction profiles over Dehradun during a drought year – 2009, Monsoon Workshop, March 2-3, 2015, IITM, Pune.
- **Mehta, M.** Estimation of aerosol optical depth over Dehradun (India) using simple model for atmospheric radiative transfer in multiple scattering approximation, *Int. Arch. Photogramm. Rem. Sens. Spatial Inf. Sci., XL-8, ISPRS Conference*, December 9-12, 2014, pp.271-276, Hyderabad.
- **Mehta, M.** Temporal variation of aerosol optical depth in ten most populous cities of India - a study using MODIS and MISR Level 3 products, *Special Interactive Session, ISPRS Conference*, December 9-12, 2014, Hyderabad.
- **Mehta, M.** 2014.Temporal variation of AOD over Dehradun- A study using MODIS and MISR Level 3 products, *IASTA Proceedings*, pp.207-209, November 11-13, 2014, BHU, Varanasi.
- Anh, Le V., **Mehta, M.**, Saha, S.K., Aggrawal, S. Rule based classification approach for mapping land degradation. *34th Asian Conference of Remote Sensing (ACRS)*, pp. 518-525, Indonesia.

<u>Accepted (Conferences/Seminars/Symposia/Workshops)</u>

- **Mehta, M., Singh, N. and Anshumali. Columnar aerosol optical depth variation over Indian region using CALIPSO Data. *TROPMET*, December 18-21, 2016 Bhubneshwar. (Poster)**
- **Mehta, M.** and Dubey, S. Decadal variations in aerosol index for three major biomass burning regions of the world. *ISPRS Congress, Commission VI, WG VI/4*, July 12-19, 2016, Prague. (Oral)

- **Mehta, M.**, Doley, G.J. and Sindhwani, S. Aerosol optical depth estimation over Resourcesat-AWiFS data using radiative transfer approach. *ISPRS Congress, Commission VI, WG VI/4,* July 12-19, 2016, Prague. (Oral)
- Dubey, S. and **Mehta, M.** Aerosol absorption optical depth trends over Asian Region", *Living Planet Symposium, ESA,* May 9-13, 2016, Prague. (Oral)
- **Mehta, M.** Temporal variation of aerosol optical depth in different altitude locations in Uttarakhand- A satellite perspective. *TROPMET,* February 15-18, 2015, Chandigarh. (Oral)
- **Mehta, M.** AOD trends in two locations of Uttarakhand – A comparative study using MODIS and MISR data. *Workshop on Assessing the Impact of Aerosols & Changing Climate on Monsoon & Extreme Events* 2015, January 12-15, 2015, Gurgaon. (Poster)

Reference:

Dr. Anshumali
Associate Professor
Department of Environmental Science and Engineering
Indian Institute of Technology (ISM), Dhanbad, 826004
Email: malijnu@gmail.com; Tel: +91-9934556176